

Optimizing ethanol yield in *Saccharomyces cerevisiae* fermentations by engineering redox metabolism

Papapetridis, Ioannis

DOI

[10.4233/uuid:36544e23-af5e-45cc-b7ee-b69117df2be6](https://doi.org/10.4233/uuid:36544e23-af5e-45cc-b7ee-b69117df2be6)

Publication date

2018

Document Version

Final published version

Citation (APA)

Papapetridis, I. (2018). *Optimizing ethanol yield in Saccharomyces cerevisiae fermentations by engineering redox metabolism*. [Dissertation (TU Delft), Delft University of Technology].
<https://doi.org/10.4233/uuid:36544e23-af5e-45cc-b7ee-b69117df2be6>

Important note

To cite this publication, please use the final published version (if applicable).
Please check the document version above.

Copyright

Other than for strictly personal use, it is not permitted to download, forward or distribute the text or part of it, without the consent of the author(s) and/or copyright holder(s), unless the work is under an open content license such as Creative Commons.

Takedown policy

Please contact us and provide details if you believe this document breaches copyrights.
We will remove access to the work immediately and investigate your claim.

Optimizing ethanol yield in *Saccharomyces cerevisiae* fermentations by engineering redox metabolism

Dissertation

for the purpose of obtaining the degree of doctor

at Delft University of Technology

by the authority of the Rector Magnificus Prof. dr. ir. T.H.J.J. van der Hagen,

Chair of the Board for Doctorates

to be defended publicly on

Thursday 14 June 2018 at 10:00 o'clock

by

Ioannis PAPAPETRIDIS

Master of Science in Biotechnology,

Wageningen University, The Netherlands,

born in Thessaloniki, Greece

This dissertation has been approved by the promotors Prof. dr. J.T. Pronk and Prof. dr. ir. A.J.A. van Maris.

Composition of the doctoral committee:

Rector Magnificus,	chairperson
Prof. dr. J.T. Pronk,	Delft University of Technology, promotor
Prof. dr. ir. A.J.A. van Maris,	Delft University of Technology, promotor

Independent members:

Prof. dr. P.A.S. Daran-Lapujade,	Delft University of Technology
Prof. Dipl-Ing. dr. D. Mattanovich,	Universität für Bodenkultur Wien
Prof. dr. D. Porro,	Università degli Studi di Milano-Bicocca
Dr. ir. S. Hartmans,	Royal DSM
Dr. ir. J-M.G. Daran	Delft University of Technology

Substitute member:

Prof. dr. ir. M.C.M. van Loosdrecht	Delft University of Technology
-------------------------------------	--------------------------------

The research presented in this thesis was performed at the Industrial Microbiology Section, Department of Biotechnology, Faculty of Applied Sciences, Delft University of Technology, The Netherlands. The project was financed by Royal DSM.

Table of Contents

Summary	1
Samenvatting	6
Chapter 1	13
Introduction: <i>Saccharomyces cerevisiae</i> strains for first- and second-generation ethanol production	
Chapter 2	57
Optimizing anaerobic growth rate and fermentation kinetics in <i>Saccharomyces cerevisiae</i> strains expressing Calvin-cycle enzymes for improved ethanol yield	
Chapter 3	107
Improving ethanol yield in acetate-reducing <i>Saccharomyces cerevisiae</i> by cofactor engineering of 6-phosphogluconate dehydrogenase and deletion of <i>ALD6</i>	
Chapter 4	145
Metabolic engineering strategies for optimizing acetate reduction, ethanol yield and osmotolerance in <i>Saccharomyces cerevisiae</i>	
Chapter 5	185
Laboratory evolution for forced glucose-xylose co-consumption enables identification of mutations that improve mixed-sugar fermentation by xylose-fermenting <i>Saccharomyces cerevisiae</i>	
Outlook	239
Acknowledgements	242
Curriculum vitae	245
List of publications	246

Summary

Mankind's energy requirements, which are currently mainly covered by the combustion of fossil fuels, have been steadily increasing in the past half century. While fossil fuels have a high energy content, their use results in significant emissions of greenhouse gases (mainly CO₂, methane and nitrous oxide). As the industrialization of developing nations continues, the requirement for a paradigm shift is becoming increasingly evident. Microbial fermentation can provide an alternative by enabling the sustainable production of transport fuels that combine a lower carbon footprint with compatibility with current internal combustion engine technology. Bioethanol is, by volume, the biofuel with the highest annual production (ca. 100 billion liters in 2016). Current 'first generation' industrial bioethanol production processes are mainly based on fermentation of hydrolysed corn starch or sugar-cane sucrose by the budding yeast *Saccharomyces cerevisiae* and capitalize on the naturally high sugar-uptake rates and ethanol yield of this microorganism. The first full-scale 'second generation' ethanol production plants that are now coming on line use lignocellulosic hydrolysates, derived from agricultural "waste" such as corn stover or wheat straw, as feedstocks. Second-generation bioethanol production can have a smaller carbon footprint than first-generation processes. Moreover, it uses feedstocks that are not a part of the human food chain. However, yeast-based second-generation bioethanol production poses multiple challenges for scientists. Lignocellulosic hydrolysates contain significant amounts of pentose sugars (mainly D-xylose and L-arabinose) which are not naturally fermentable by *S. cerevisiae*. Further, during biomass pretreatment, inhibitors of yeast performance (phenolics, aldehydes and organic acids) are released into the hydrolysates. To mitigate the negative effects of these inhibitors, yeast strains used in second-generation bioethanol production processes need to maintain high rates of sugar fermentation, both for hexoses and for pentoses. In both first- and second-generation bioethanol production, the price of the hydrolysed feedstock represents the single largest factor in production

costs. Therefore, in an industry that generally operates at low profit margins, maximization of the ethanol yield on fermentable sugars is of paramount importance. **Chapter 1** of this thesis discusses past research and recent advances in strain engineering for improved ethanol production in both first- and second-generation processes.

During industrial bioethanol production, carbon losses occur due to the formation of biomass, CO₂ and fermentation by-products, with glycerol formation accounting for up to 4% of consumed sugars. Glycerol plays multiple roles in yeast metabolism. It forms the backbone of glycerolipids, is a stress protectant (mainly against osmotic stress) and, in anaerobic yeast cultures, its production plays a key role in redox metabolism. Formation of glycerol from dihydroxyacetone-phosphate in the reactions catalysed by glycerol-3-phosphate dehydrogenase and glycerol-3-phosphate phosphatase requires input of NADH. The coenzyme pairs NAD(P)⁺/NAD(P)H play a vital role in mediating >200 cellular redox reactions in *S. cerevisiae*. NAD(P)⁺ and NAD(P)H are conserved moieties; when reduction of NAD(P)⁺ in oxidation reactions is not matched by oxidation of NAD(P)H in reductive reactions, growth rapidly ceases. Anaerobic cultures of *S. cerevisiae* require glycerol formation to reoxidize excess NADH formed in biosynthetic reactions, as glycolysis and alcoholic fermentation already form a redox-neutral pathway. Elimination of glycerol formation by deletion of *GPD1* and *GPD2*, the two genes encoding glycerol-3-phosphate dehydrogenase in *S. cerevisiae*, results in abolishment of anaerobic growth unless an external electron acceptor, such as acetoin that can be reduced to 2,3-butanediol, is provided. However, in industrial processes, such additions would increase operational costs. Recently, functional expression of ribulose-1,5-bisphosphate carboxylase/oxygenase (RuBisCO, *Thiobacillus denitrificans* CbbM) and phosphoribulokinase (*Spinacea oleracea* PRK) in *S. cerevisiae* was shown to enable the use of CO₂ as an alternative electron acceptor. As CO₂ production is stoichiometrically linked to alcoholic fermentation, its external supply to growing cultures is not required. The modified strain displayed a 90% decrease in glycerol yield in anaerobic glucose/galactose-grown chemostat cultures and a

60% decrease in glycerol yield in anaerobic galactose-grown batch cultures, with concomitant increases in the ethanol yield. The use of galactose as an inducer of PRK expression in the proof-of-principle strains, along with the slow anaerobic growth rate and fermentation kinetics remained points of optimization before industrial implementation could be considered. In **Chapter 2** a metabolic engineering strategy for optimization of the RuBisCO/PRK pathway in *S. cerevisiae* is presented and experimentally tested. CRISPR-Cas9 genome-editing technology, with which complicated genetic modifications can be introduced in one or a few steps, was used to modify carbon and redox metabolism in a RuBisCO/PRK-expressing strain. The resulting strain grew at wild-type rate in anaerobic batch cultures on glucose, while displaying a ca. 90% lower glycerol yield and a 15% higher ethanol yield than a non-engineered *S. cerevisiae* strain. As strains engineered in this way do not require specific media compositions or process modifications, this concept may be implemented in industrial yeast strains and used to increase the ethanol yield in bioethanol production processes.

Acetic acid can also be used as an alternative electron acceptor for reoxidizing NADH in anaerobic yeast cultures. Lignocellulosic hydrolysates invariably contain acetic acid, which is released during deconstruction of the hemicellulose fraction during biomass pre-treatment. Lower concentrations of acetic acid have been reported in first-generation feedstocks. Acetic acid is a potent inhibitor of yeast fermentation, as it causes weak-organic acid uncoupling and abolishment of growth at higher concentrations. Expression of a heterologous acetylating-acetaldehyde dehydrogenase (*Escherichia coli* MhpF) in *S. cerevisiae* was previously shown to enable use of acetic acid as an external electron acceptor, by completing an acetate-to-ethanol reduction pathway in combination with the native yeast acetyl-CoA synthetases and alcohol dehydrogenases. This approach not only resulted in higher ethanol yield by replacing glycerol formation with acetate reduction, but also enabled partial *in situ* detoxification of the medium by the engineered strain. As the reduction of acetic acid requires cytosolic NADH, the amount of additional ethanol that can be

produced and the extent of the medium detoxification by the engineered strains is limited by the amount of NADH formed in yeast anabolism. **Chapter 3** explores a redox engineering strategy for increasing cytosolic NADH generation in *S. cerevisiae*. Replacement, in an acetate-reducing strain, of the native, NADP⁺-dependent, 6-phosphogluconate dehydrogenases by a heterologous NAD⁺-dependent enzyme (*Methylobacillus flagellatus* GndA), in combination with deletion of Ald6, resulted in 44 and 3% increases in acetate consumption and ethanol yield, respectively. Replacement of MhpF by the alternative acetylating acetaldehyde dehydrogenase EutE (*Escherichia coli*) significantly improved the specific growth rates of the engineered strains.

The acetate-reducing *S. cerevisiae* strains discussed in **Chapter 3** harboured deletions in *GPD1* and *GPD2*, resulting in the absence of a functional glycerol formation pathway. The inability to produce glycerol could decrease the stress tolerance of engineered strains in industrial media, especially against high osmotic pressure. Metabolic engineering strategies to enable acetate reduction in strains still capable of glycerol formation are discussed in **Chapter 4**. Only expressing EutE was found to be insufficient to enable optimal acetate reduction in the presence of a fully functional glycerol formation pathway. Deletion, in an EutE-expressing strain, of *GPD2*, which is upregulated under anaerobic conditions, resulted in a fourfold lower glycerol production and concomitant increases in acetate consumption and ethanol yield in low-osmolarity media. In high-osmolarity media (1 mol L⁻¹ glucose), acetate reduction and anaerobic growth was enabled by replacement of *GPD1* and *GPD2* by the archaeal, NADP⁺-dependent, glycerol-3-phosphate dehydrogenase GpsA (*Archaeoglobus fulgidus*). Expression, in an EutE-expressing strain, of GpsA, in combination with deletion of Ald6, enabled immediate growth under high-osmolarity conditions. Moreover, the GpsA-expressing strain exhibited equivalent acetate reduction to a Gpd⁻ strain without the associated osmosensitivity, and a 13% higher ethanol yield than observed in a non-acetate reducing *S. cerevisiae*. The metabolic engineering strategies discussed in **Chapters 3** and **4**

should facilitate the transfer of the acetate-reducing pathway to industrial strains and media for testing in process conditions and lignocellulosic hydrolysates.

In addition to the economic importance of increased ethanol yields, second-generation bioethanol production can benefit from decreased fermentation times that can increase overall productivity and process robustness against contaminations. *S. cerevisiae* strains that express functional pentose utilization pathways preferentially consume glucose when media also contain pentoses, resulting in sequential utilization of sugar mixtures and increased overall fermentation times in second-generation bioethanol production processes. **Chapter 5** discusses a combinatorial metabolic and laboratory evolution strategy that was designed and successfully applied towards the identification of genetic mutations that facilitate increased xylose utilization by *S. cerevisiae* in the presence of glucose. Deletion of *PGI1* and *RPE1*, encoding phosphoglucose isomerase and ribulose-5-phosphate epimerase respectively, in xylose-consuming *S. cerevisiae* with a modified pentose-phosphate pathway, forced co-consumption of glucose and xylose in batch cultures. Laboratory evolution in media with increasing glucose concentrations, followed by whole-genome sequencing, identified mutations in *HXK2*, *RSP5* and *GAL83* in evolved strains. Combined introduction of the *HXK2* and *GAL83* mutations in a non-evolved xylose-consuming strain resulted in a 2.5-fold higher xylose consumption rate in the presence of glucose in anaerobic batch cultures on glucose-xylose mixtures. This led to a shorter xylose consumption phase and an overall reduction of the length of anaerobic fermentation experiments of over 24 h. The combinatorial metabolic and evolutionary engineering strategy developed in **Chapter 5** should be applicable to similarly identify relevant beneficial mutations in different yeast strain backgrounds and/or process conditions.

Samenvatting

De energiebehoefte van de mensheid, waarin tegenwoordig vooral wordt voorzien door de verbranding van fossiele brandstoffen, is de laatste 50 jaar gestaag aan het stijgen. Fossiele brandstoffen hebben een hoog energiegehalte, maar hun gebruik resulteert in significante uitstoot van broeikasgassen (vooral CO₂, methaan en stikstofoxide). Nu de industrialisatie van ontwikkelende landen doorgaat, wordt het steeds duidelijker dat een verschuiving in de energievoorziening vereist is. Microbiële fermentatie kan een goed alternatief bieden door de duurzame productie van transportbrandstoffen. Deze moeten dan wel een lage netto CO₂-productie hebben en bovendien compatibel zijn met de huidige technologie voor verbrandingsmotoren. Bio-ethanol is, op basis van volume, de bio-brandstof met de hoogste jaarlijkse productie (wereldwijd ca. 100 miljard liter in 2016). De huidige “eerste generatie” industriële productieprocessen voor bio-ethanol zijn voornamelijk gebaseerd op de fermentatie van gehydrolyseerd maïszetmeel of saccharose uit suikerriet door de gist *Saccharomyces cerevisiae*. Deze processen spelen in op de hoge natuurlijke suikerconsumptiesnelheid en ethanolopbrengst van dit micro-organisme. De eerste “tweede-generatie” ethanolproductieprocessen op industriële schaal die recent van start zijn gegaan, gebruiken lignocellulosische hydrolysaten, die gemaakt worden uit agrarische “afvalstromen” zoals gewasresten van maïs en tarwestro, als grondstoffen. Tweede-generatie bio-ethanolproductie kan een kleinere netto CO₂-uitstoot mogelijk maken dan eerste-generatie processen. Bovendien zijn de gebruikte grondstoffen geen onderdeel van de menselijke voedselketen. Echter, het realiseren van een op gist gebaseerde tweede-generatie bio-ethanolproductie schept meerdere uitdagingen voor wetenschappers. Lignocellulosische hydrolysaten bevatten significante hoeveelheden pentosesuikers (voornamelijk D-xylose en L-arabinose) die niet natuurlijk te fermenteren zijn door *S. cerevisiae*. Verder komen, tijdens de voorbehandeling van plantaardig materiaal, remmers van de giststofwisseling vrij in de hydrolysaten (fenolen, aldehyden en organische zuren). Om de negatieve effecten van deze remmers te verzachten, moeten de

giststammen die worden gebruikt in tweede-generatie bio-ethanolproductieprocessen hoge snelheden van suikerfermentatie behouden, voor zowel hexosesuikers als voor pentosesuikers. In zowel eerste- als tweede-generatie bio-ethanolproductie vertegenwoordigt de prijs van de grondstoffen de grootste factor in de productiekosten. In een industrie die opereert met lage winstmarges, is maximalisatie van de ethanolopbrengst op fermenteerbare suikers zeer belangrijk. **Hoofdstuk 1** van dit proefschrift bespreekt onderzoek uit het verleden en recente vorderingen in de genetisch modificatie van giststammen voor verbeterde ethanolproductie in zowel eerste- als tweede-generatie processen.

Tijdens industriële bio-ethanolproductie gaat koolstof verloren door vorming van biomassa, CO₂ en fermentatiebijproducten, waarbij de productie van glycerol tot wel 4% van de geconsumeerde suikers omvat. Glycerol vervult verschillende functies in de stofwisseling van gist. Glycerol vormt de “ruggengraat” van glycerolipiden en beschermt tegen stress (voornamelijk tegen osmotische stress). In anaërobe gistculturen speelt glycerolproductie bovendien een sleutelrol in de redoxstofwisseling. Vorming van glycerol uit dihydroxyacetonfosfaat, gekatalyseerd door de enzymen glycerol-3-fosfaat dehydrogenase en glycerol-3-fosfaat fosfatase, heeft NADH nodig. De co-enzymen NAD(P)⁺/NAD(P)H spelen een vitale rol in meer dan 200 cellulaire redoxreacties in *S. cerevisiae*. NAD(P)⁺ en NAD(P)H zijn zogenaamde “conserved moieties”; wanneer de snelheid van reductie van NAD(P)⁺ in oxiderende reacties niet overeenkomt met de oxidatiesnelheid van NAD(P)H in reducerende reacties, stopt de groei vrijwel instantaan. Tijdens anaërobe groei van *S. cerevisiae* is vorming van glycerol essentieel voor het reoxideren van de overtollige NADH die wordt gevormd in bio-synthetische reacties, omdat glycolyse en alcoholische fermentatie al een redox-neutrale route vormen. Anaërobe groei is daarom niet meer mogelijk wanneer de glycerolproductie wordt uitgeschakeld door het verwijderen van *GPD1* en *GPD2*, de twee genen die coderen voor glycerol-3-fosfaat dehydrogenase in *S. cerevisiae*. De noodzaak van glycerolproductie in anaërobe cultures kan worden voorkomen door toevoeging van een externe elektronacceptor, zoals acetoïne, dat kan worden gereduceerd tot 2,3-butaandiol. Echter, dit soort toevoegingen is in een industriële

context geen economisch haalbare optie. Recent is aangetoond dat de functionele expressie in *S. cerevisiae* van ribulose-1,5-bisfosfaat carboxylase/oxygenase (RuBisCo, uit de bacterie *Thiobacillus denitrificans* CbbM) en fosforibulokinase (PRK, uit spinazie; *Spinacea oleracea*) het gebruik van CO₂ als een alternatieve elektronacceptor mogelijk maakt. Omdat alcoholische fermentatie stoichiometrisch gekoppeld is aan productie van CO₂, is hiervoor geen externe toevoeging van CO₂ nodig. De gemodificeerde stam liet een 90 % daling van de glycerolopbrengst zien in anaërobe chemostaat-culturen die waren gekweekt op mengsels van glucose en galactose en een 60 % daling van de glycerolopbrengst in anaërobe batch-culturen gekweekt op galactose. Deze verminderde glycerolproductie ging gepaard met een verhoogde ethanolopbrengst. Het gebruik van galactose om de expressie van PRK te induceren in de “proof-of-principle” stam, een lage anaërobe groeisnelheid en fermentatiesnelheid vormden punten die geoptimaliseerd moesten worden voordat implementatie van deze strategie in de industrie kon worden overwogen. In **Hoofdstuk 2** wordt een strategie voor optimalisatie van de RuBisCo/PRK route in *S. cerevisiae* gepresenteerd en experimenteel getest. Gebruik van CRISPR-Cas9 voor modificatie van het gistgenoom, waarmee gecompliceerde genetische modificaties in enkele stappen kunnen worden aangebracht, werd gebruikt om de koolstof- en redox-stofwisseling in een RuBisCo/PRK-expressie stam aan te passen. Deze aanpak resulteerde in een giststam die dezelfde groeisnelheid had als het wildtype in een anaërobe batchcultuur met glucose als koolstofbron. Bovendien resulteerden de aangebrachte modificaties in een ca. 90% lagere opbrengst van glycerol en een 15% hogere opbrengst van ethanol dan in een niet-gemodificeerde *S. cerevisiae*-stam. Wanneer giststammen op deze manier worden gemodificeerd, hebben ze geen specifieke mediumsamenstellingen of procesmodificaties nodig. Dit concept zou geïmplementeerd kunnen worden in industriële giststammen en zo worden gebruikt om de ethanolopbrengst in commerciële bio-ethanol productieprocessen te verhogen.

In plaats van CO₂ kan ook azijnzuur gebruikt worden als alternatieve elektronacceptor voor het reoxideren van NADH in anaërobe gistculturen. Lignocellulosische hydrolysaten bevatten azijnzuur dat tijdens de biomassavorbehandeling vrijkomt bij deconstructie van de

hemicellulosefractie. Azijnzuur komt ook, in lagere concentraties, voor in eerste-generatie bioethanol-grondstoffen. Azijnzuur is een krachtige remmer van de gistfermentatie, want het veroorzaakt ontkoppeling van de pH-gradiënt over het celmembraan en remt bij hogere concentraties de groei zelfs volledig. Eerder was aangetoond dat expressie van een heteroloog acetylerende-aceetaldehyde dehydrogenase (*Escherichia coli* MhpF) in *S. cerevisiae* het gebruik van azijnzuur als externe elektronacceptor mogelijk maakt. Expressie van dit enzym maakt, samen met de van nature in *S. cerevisiae* aanwezige acetyl-CoA synthetases en alcohol dehydrogenases, een acetaat-naar-ethanol route mogelijk. Deze aanpak resulteerde niet alleen in een hogere ethanolopbrengst door het vervangen van glycerolproductie door acetaatreductie tot ethanol, maar maakte tevens en gedeeltelijke *in situ* detoxificatie van het medium mogelijk. Omdat de reductie van azijnzuur cytosolisch NADH verbruikt is de hoeveelheid extra ethanol die geproduceerd kan worden, en daarmee de mate van mediumdetoxificatie door de gemodificeerde stam, gelimiteerd door de hoeveelheid NADH die wordt geproduceerd in het anabolisme van gist. In **Hoofdstuk 3** wordt een strategie onderzocht om het redoxmetabolisme in *S. cerevisiae* zo te veranderen dat de beschikbaarheid van NADH in het cytosol wordt verhoogd. Hiervoor werd het natuurlijke NADP⁺-afhankelijke 6-fosfaatgluconaatdehydrogenase in een acetaat-reducerende stam vervangen door een heteroloog, NAD⁺-afhankelijk enzym (GndA uit *Methylobacillus flagellatus*). Wanneer tegelijkertijd het *ALD6* gen werd uitgeschakeld, leidde deze modificatie tot een 44 % hogere acetaatconsumptie en een verdere toename van de ethanolopbrengst met 3%. De groeisnelheid van de gemodificeerde stam werd significant verbeterd wanneer MhpF werd vervangen door een alternatief acetylerend aceetaldehyde dehydrogenase (EutE uit *Escherichia coli*).

De acetaat-reducerende *S. cerevisiae* stam die wordt besproken in **Hoofdstuk 3** bevatte deleties in *GPD1* en *GPD2*. Deze deleties resulteerden in afwezigheid van een functionele glycerolproductieroute. Het onvermogen om glycerol te produceren zou, in het bijzonder bij een hoge osmotische druk, kunnen leiden tot een verlaagde stresstolerantie van de gemodificeerde stam in industriële media. Strategieën die het mogelijk maken om acetaat te reduceren in

stammen zonder de glycerolproductie volledig uit te schakelen worden besproken in **Hoofdstuk 4**. Alleen expressie van EutE bleek ontoereikend te zijn om optimale acetaatreductie mogelijk te maken in de aanwezigheid van een volledig functionerende glycerolproductieroute. De verwijdering van *GPD2*, waarvan de expressie verhoogd is onder anaërobe condities, in een EutE-expressie stam, resulteerde in een viermaal lagere glycerolproductie en tegelijkertijd een stijging in acetaatconsumptie en ethanolopbrengst in medium met een lage osmolariteit. In medium met een hoge osmolariteit (1 mol L^{-1} glucose), werd acetaatreductie en anaërobe groei mogelijk gemaakt door *GPD1* en *GPD2* te vervangen door een heteroloog, NADP⁺-afhankelijk glycerol-3-fosfaatdehydrogenase (*GpsA* uit *Archaeoglobus fulgidus*). De expressie van *GpsA* in een EutE-expressie stam, in combinatie met een verwijdering van *Ald6*, maakte onmiddellijke groei mogelijk bij hoge osmolariteit. Bovendien vertoonde de *GpsA*-expressiestam een gelijkwaardige acetaatreductie als een *Gpd*- stam, zonder de normaal in *Gpd*-stammen waargenomen gevoeligheid voor hoge osmolariteit, en een 13% hogere ethanolopbrengst dan werd waargenomen in een *S. cerevisiae*-stam die geen acetaat kan reduceren. De strategieën die worden besproken in **Hoofdstuk 3** en **4** kunnen een belangrijke rol spelen bij het implementeren van de acetaat-reductieroute in industriële giststammen, evenals bij tests in industriële kweekmedia en onder industriële procescondities.

Naast het economisch belang van een verhoogde ethanolopbrengst, kan tweede-generatie bio-ethanolproductie het voordeel hebben van een verkorte fermentatieduur, hetgeen de productiviteit en de robuustheid van het proces tegen contaminaties kan verhogen. *S. cerevisiae*-stammen die een functionele route voor pentosefermentatie tot expressie brengen, prefereren consumptie van glucose wanneer deze suiker naast pentoses beschikbaar is. Dit resulteert in het achtereenvolgens benutten van verschillende suikers, wat bijdraagt aan een lange fermentatieduur in tweede-generatie bio-ethanolproductieprocessen. **Hoofdstuk 5** bespreekt hoe een combinatie van gerichte aanpassingen in de stofwisseling en laboratoriumevolucie succesvol werd toegepast om genetische modificaties te identificeren die leiden tot een versneld gebruik van xylose door *S. cerevisiae* in de aanwezigheid van glucose.

Verwijdering van *PGI1* en *RPE1*, twee genen die coderen voor respectievelijk fosfoglucose-isomerase en ribulose-5-fosfaat epimerase, in een xylose-consumerende *S. cerevisiae*-stam met een gemodificeerde pentose-fosfaatroute, forceerde het gelijktijdig gebruik van glucose en xylose in batchculturen. Laboratoriumevolucie in medium met toenemende glucoseconcentraties, gevolgd door het bepalen van de volledige DNA-volgorden van geëvolueerde stammen, leidde tot identificatie van mutaties in *HXK2*, *RSP5* en *GAL83*. De gecombineerde introductie van de gevonden mutaties in *HXK2* en *GAL83* in een niet-geëvolueerde xylose-consumerende stam resulteerde in een 2,5 maal hogere xyloseconsumptiesnelheid in aanwezigheid van glucose in anaërobe batchculturen die werden gekweekt op een mengsel van glucose en xylose. Deze veranderingen leidden tot een kortere xyloseconsumptiefase en een verkorting van de duur van anaërobe fermentatie experimenten met meer dan 24 uur. De combinatie van gerichte modificatie van de stofwisseling en gestuurde evolutie, zoals besproken in **Hoofdstuk 5**, kan in de toekomst worden ingezet voor het vinden van verdere gunstige mutaties in verschillende giststammen en/of onder verschillende procescondities.

CHAPTER 1

Introduction: *Saccharomyces cerevisiae* strains for first- and second-generation ethanol production

Adapted from the publication entitled “*Saccharomyces cerevisiae* strains for second-generation ethanol production: from academic exploration to industrial implementation” by Mickel L.A. Jansen, Jasmine M. Bracher, Ioannis Papapetridis, Maarten D. Verhoeven, Hans de Bruijn, Paul P. de Waal, Antonius J.A. van Maris, Paul Klaassen and Jack T. Pronk in ***FEMS Yeast Research***, Volume 17, Issue 5, August 2017 (<https://doi.org/10.1093/femsyr/fox044>)

1.1 General introduction

Alcoholic fermentation is a key catabolic process in most yeasts and in many fermentative bacteria, which concentrates the heat of combustion of carbohydrates into two thirds of their carbon atoms ($(\text{CH}_2\text{O})_n \rightarrow \frac{1}{3}n \text{ C}_2\text{H}_6\text{O} + \frac{1}{3}n \text{ CO}_2$). Its product, ethanol, has been used as an automotive fuel for over a century [1]. With an estimated annual global production of 100 Mton [2], ethanol is the largest-volume product in industrial biotechnology. Its production is, currently, mainly based on fermentation of sugar cane sucrose or hydrolysed corn starch by the yeast *Saccharomyces cerevisiae*. Such 'first generation' bioethanol processes are characterized by high ethanol yields on fermentable sugars (>90% of the theoretical maximum yield of 0.51 g ethanol (g hexose sugar)⁻¹), ethanol titers of up to 21% (w/w) and volumetric productivities of 2 to 3 kg m⁻³ h⁻¹ [3-5].

Over the past two decades, a large international effort involving researchers in academia, research institutes and industry, aimed to access abundantly available agricultural and forestry residues, as well as fast-growing energy crops, as alternative feedstocks for fuel ethanol production [6]. Incentives for this effort, whose relative impact depends on geographical location and varies over time, include reduction of the carbon footprint of ethanol production [7], prevention of competition with food production for arable land [8, 9], energy security in fossil-fuel importing countries [10] and development of rural economies [11]. Techno-economic forecasts of low-carbon scenarios for global energy supply almost invariably include liquid biofuels as a significant contributor [12]. Moreover, successful implementation of economically and environmentally sustainable 'second generation' bioethanol processes can pave the way for similar processes to produce other biofuels and commodity chemicals [13].

In contrast to starch, a plant storage carbohydrate that can be easily hydrolysed, the major carbohydrate polymers in lignocellulosic plant biomass (cellulose, hemicellulose and, in some cases, pectin) contribute to the structure and durability of stalks, leaves and roots [14]. Consistent with their natural functions, chemical diversity and complexity, mobilization of these

polymers by naturally occurring cellulose-degrading microorganisms requires complex arrays of hydrolytic enzymes [15, 16].

The second-generation ethanol processes that are now coming on line at demonstration and commercial scale (Table 1) are mostly based on fermentation of lignocellulosic biomass hydrolysates by engineered strains of *S. cerevisiae*. While this yeast has a strong track record in first-generation bioethanol production and its amenability to genetic modification is excellent, *S. cerevisiae* cannot hydrolyse cellulose or hemicellulose. Therefore, in conventional process configurations for second-generation bioethanol production, the fermentation step is preceded by chemical/physical pretreatment and enzyme-catalysed hydrolysis by cocktails of fungal hydrolases, which can either be produced on- or off site (Figure 1, [17]). Alternative process configurations, including simultaneous saccharification and fermentation (SSF) and consolidated bioprocessing (CBP) by yeast cells expressing heterologous hydrolases are intensively investigated [18, 19]. However, the high temperature optima of fungal enzymes and low productivity of heterologously expressed hydrolases in *S. cerevisiae* have so far precluded large-scale implementation of these alternative strategies for lignocellulosic ethanol production [18, 20].

Over the past decade, metabolic and evolutionary engineering strategies to increase the ethanol yield and productivity in yeast-based first- and second-generation bioethanol production have been developed. This Chapter provides a review of key advances in the field that contribute to the generation of strain platforms with improved phenotypes.

Table 1. Overview of operational commercial-scale (demonstration) plants for second-generation bioethanol production. Data for US and Canada reflect status in May 2017 [21, 22], data for other countries [21, 22] reflect status in 2016.

Company/Plant	Country (State)	Feedstock	Capacity ML y⁻¹
DuPont Cellulosic Ethanol LLC-Nevada¹	USA (IA)	Corn stover	113.6
Poet-DSM Advanced Biofuels LLC - Project Liberty²	USA (IA)	Corn cobs/corn stover	75.7
Quad County Cellulosic Ethanol Plant	USA (IA)	Corn fiber	7.6
Fiberight Demonstration Plant	US (VA)	Waste stream	1.9
ICM Inc. Pilot integrated Cellulosic Biorefinery	US (MO)	Biomass crops	1.2
American Process Inc. – Thomaston Biorefinery	USA (GA)	Other	1.1
ZeaChem Inc. – Demonstration plant	US (OR)	Biomass crops	1.0
Enerkem Alberta Biofuels LP	Canada (AB)	Sorted municipal solid waste	38
Enerkem Inc.-Westbury	Canada (QC)	Woody biomass	5.0
Iogen Corporation	Canada (ON)	Crop residue	2.0
Woodlands Biofuels Inc. – Demonstration plant	Canada (ON)	Woody biomass	2.0
GranBio	Brazil	Bagasse	82.4
Raizen	Brazil	Sugarcane bagasse/straw	40.3
Longlive Bio-technology Co. Ltd. – commercial demo	China	Corn cobs	63.4
Mussi Chemtex / Beta Renewables	Italy	<i>Arundo donax</i> , rice straw, wheat straw	75
Borregaard Industries AS – ChemCell Ethanol	Norway	Wood pulping residues	20

¹For sale as of January 2018 ²With expansion capacity to 94.6 ML per year

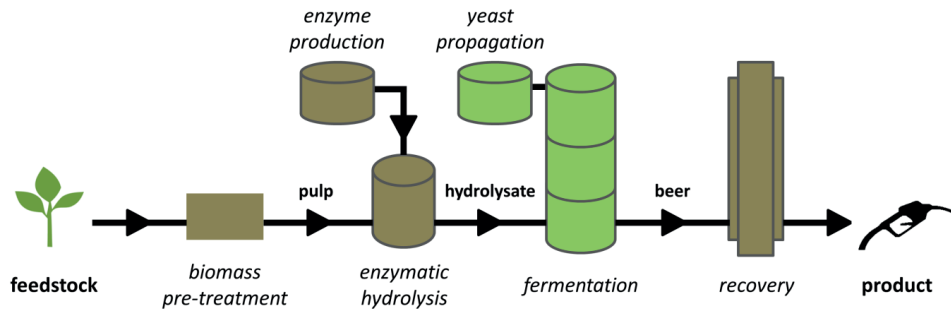


Figure 1. Schematic process-flow diagram for ethanol production from lignocellulose, based on physically separated processes for pretreatment, hydrolysis and fermentation, combined with on-site cultivation of filamentous fungi for production of cellulolytic enzymes and on-site propagation of engineered pentose-fermenting yeast strains.

1.2 Metabolic engineering strategies for maximization of ethanol yield

In both first- and second-generation bioethanol production, the feedstock represents the largest cost contributor [23]. Even small improvements in the product yield on feedstock can therefore substantially improve the economics of industrial processes [24, 25]. Suboptimal ethanol yields during fermentation of industrial substrates occur due to the formation of biomass, CO₂ and by-products, with glycerol accounting for up to 4% of total sugar consumption [24, 26]. The formation of biomass can be minimized by modifications to process unit operations, i.e. by introducing a biomass recycling step in between fermentations [4]. Alternatively, genetic modifications to the sugar assimilation pathways leading to increased ATP expenditure or decreased ATP generation can be made, causing a shift from biomass to ethanol production. Basso *et al.* eliminated extracellular hydrolysis of sucrose to fructose and glucose in *S. cerevisiae* [27]. After laboratory evolution of the engineered strains, in which uptake of sucrose completely relied on proton symport (at a cost of 1 mol ATP per mol sucrose), this modification resulted in a 11% higher ethanol yield in sucrose-limited chemostats [27]. Replacement of the native yeast glyceraldehyde-3-phosphate dehydrogenase by a non-phosphorylating, NADP⁺-linked, bacterial enzyme was shown to lead to an increased carbon flow to ethanol production in multiple strain backgrounds [28-30].

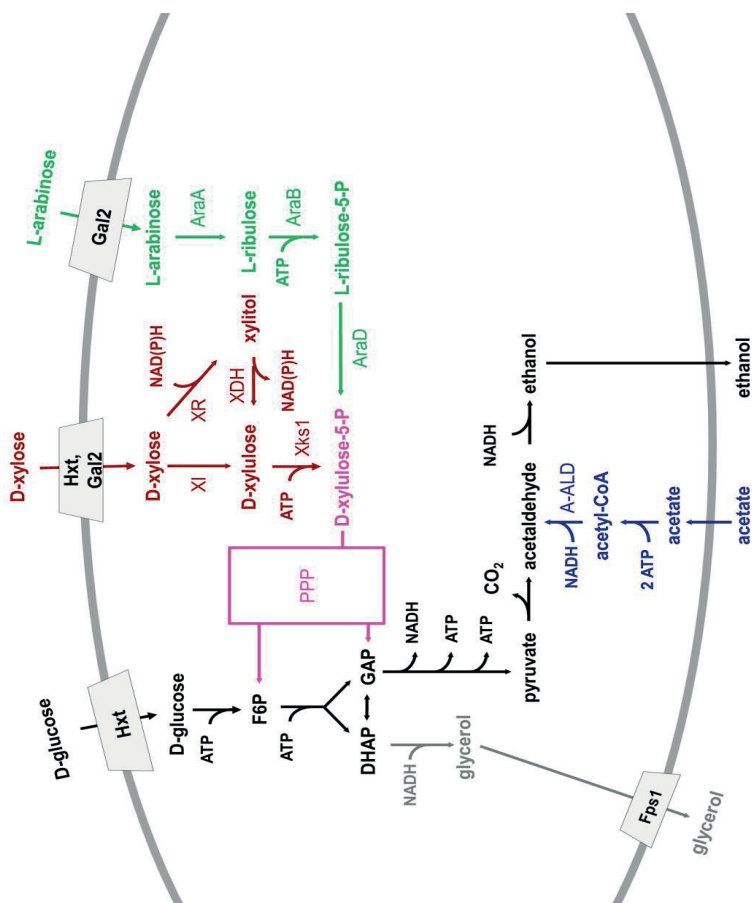
Glycerol formation, catalyzed by the two isoforms of glycerol-3-phosphate dehydrogenase (Gpd1 and Gpd2) and of glycerol-3-phosphate phosphatase (Gpp1 and Gpp2), is required during anaerobic growth of *S. cerevisiae* for reoxidation of NADH generated in biosynthetic reactions [31, 32]. The pathway intermediate glycerol-3P forms the backbone of glycerolipids [33, 34]. Furthermore, glycerol is the main compatible solute in *S. cerevisiae* for adaptation against hyperosmotic stress [35, 36]. Modulation of *GPD1* and *GPD2* expression can decrease glycerol formation at the expense of anaerobic growth rate [37], with deletion of both genes resulting in complete abolishment of anaerobic growth. In *gpd1Δ gpd2Δ* strains, anaerobic growth is restored upon addition of external electron acceptors that can be reduced with NADH as the donor. For example, inclusion of acetoin in fermentation media, which can be reduced to

2,3-butanediol in an NADH-dependent reaction, can restore anaerobic growth of *Gpd*⁻ strains [31]. However, the operational costs resulting from external addition of electron acceptors and subsequent removal of the reduced product from fermentation broths during downstream processing would negate any economic benefits of decreased glycerol production in industrial processes. Alternatively, engineering of redox metabolism to decrease NADH formation during anabolism can result in significant decreases in glycerol formation. In a pioneering study, Nissen *et al.* replaced the NADPH-dependent pathway for glutamate biosynthesis from ammonium and α -ketoglutarate by an alternative route requiring ATP and NADH [38]. Introduction of this additional NADH sink resulted in a 10% higher ethanol yield and 38% low glycerol yield.

Despite the success of strategies such as the above in laboratory conditions, the decrease in available ATP for biomass formation and the requirement for specific medium compositions could limit applicability in industrial processes. Such limitations do not occur when CO₂, which can be reduced to ethanol, is used as an alternative electron acceptor, as its production is stoichiometrically linked to alcoholic fermentation. Reduction of CO₂ to ethanol by *S. cerevisiae* requires the heterologous expression of two key Calvin-cycle enzymes, phosphoribulokinase (PRK) and ribulose-1,5-bisphosphate carboxylase/oxygenase (RuBisCO). Guadalupe-Medina *et al.* successfully co-expressed *Spinacea oleracea* PRK together with *Thiobacillus denitrificans* CbbM and *Escherichia coli* chaperones GroEL/GroES in *S. cerevisiae*, resulting in 90% lower glycerol yield in anaerobic glucose/galactose-grown chemostat cultures and 60% lower glycerol yield in galactose-grown batch cultures, with concomitantly higher ethanol yields [39]. Alternative strategies for eliminating glycerol formation can take advantage of ubiquitous fermentation media constituents. In particular, in second-generation bioethanol production processes, pretreatment of lignocellulosic biomass releases substantial amounts of acetic acid to the hydrolysates, due to the degradation of acetylated hemicellulose [40]. Replacement of *GPD1* and *GPD2* with a heterologous gene (*E. coli* MhpF) encoding an acetylating acetaldehyde dehydrogenase (A-ALD) and supplementation with acetic acid eliminated glycerol formation in anaerobic *S. cerevisiae* cultures on synthetic media [41]. By enabling NADH-dependent reduction

of acetic acid to ethanol (Figure 2), this strategy enabled a significant increase in the final ethanol yield, while decreasing the concentration of the inhibitor acetic acid. This engineering strategy has recently been expanded by altering the redox-cofactor specificity of alcohol dehydrogenase [42], resulting in increased NADH availability for acetate reduction. The A-ALD strategy was also shown to decrease xylitol formation in XR/XDH-based xylose-fermenting engineered strains by reoxidation of excess NADH formed in the XDH reaction [43, 44].

Figure 2. Key strategies for engineering carbon and redox metabolism in *S. cerevisiae* strains for alcoholic fermentation of lignocellulosic feedstocks. Colours indicate the following pathways and processes: Black: native *S. cerevisiae* enzymes of glycolysis and alcoholic fermentation; Magenta: native enzymes of the non-oxidative pentose-phosphate pathway (PPP), overexpressed in pentose-fermenting strains; Red: conversion of D-xylose into D-xylose-5-phosphate by heterologous expression of a xylose isomerase (XI) or combined expression of heterologous xylose reductase (XR) and xylitol dehydrogenase (XDH), together with the overexpression of (native) xylulokinase (Xks1); Green: conversion of L-arabinose into D-xylose-5-phosphate by heterologous expression of a bacteria AraA/AraB/AraD pathway; Blue: expression of a heterologous acetylating acetaldehyde dehydrogenase (A-ALD) for reduction of acetic acid to ethanol; Grey: native glycerol pathway.



1.3 Fermenting lignocellulosic hydrolysates: additional challenges for yeast strain development

A wide range of agricultural and forestry residues, as well as energy crops, are being considered as feedstocks for bioethanol production [45]. Full-scale and demonstration plants using raw materials such as corn stover, sugar-cane bagasse, wheat straw and switchgrass are now in operation (Table 1). These lignocellulosic feedstocks have different chemical compositions, which further depend on factors such as seasonal variation, weather and climate, crop maturity and storage conditions [46]. Despite this variability, common features of feedstock composition and biomass-deconstruction methods generate several generic challenges that have to be addressed in the development of yeast strains for second-generation bioethanol production.

1.3.1 Pentose fermentation

For large-volume products such as ethanol, maximizing the product yield on feedstock and, therefore, efficient conversion of all potentially available substrate molecules in the feedstock is of paramount economic importance [47]. In addition to readily fermentable hexoses such as glucose and mannose, lignocellulosic biomass contains substantial amounts of D-xylose and L-arabinose. These pentoses, derived from hemicellulose and pectin polymers in plant biomass, cannot be fermented by wild-type *S. cerevisiae* strains. D-xylose and L-arabinose typically account for 10 to 25% and 2 to 3%, respectively, of the carbohydrate content of lignocellulosic feedstocks [48]. However, in some feedstocks, such as corn fiber hydrolysates and sugar beet pulp, the arabinose content can be up to ten-fold higher [49, 50]. Early studies already identified metabolic engineering of *S. cerevisiae* for efficient, complete pentose fermentation as key prerequisite for its application in second-generation ethanol production [51-54].

1.3.2 Acetic acid inhibition

In addition to its ubiquitous presence in lignocellulosic hydrolysates, bacterial contamination during biomass storage, pretreatment and/or fermentation may further increase the acetic acid concentrations to which yeasts are exposed in fermentation processes. First-generation

bioethanol processes are typically run at pH values of 4 to 5 to counter contamination with lactic acid bacteria [55]. At these low pH values, undissociated acetic acid ($pK_a = 4.76$) easily diffuses across the yeast plasma membrane. In the near-neutral pH environment of the yeast cytosol, the acid readily dissociates and releases a proton, which forces cells to expend ATP for proton export via the plasma-membrane ATPase to prevent cytosolic acidification [56-58]. The accompanying accumulation of the acetate anion in the cytosol can cause additional toxicity effects [59-61]. Acetic acid concentrations in some lignocellulosic hydrolysates exceed 5 g L^{-1} , which can cause strong inhibition of anaerobic growth and sugar fermentation by *S. cerevisiae* [62]. Acetic acid tolerance at low culture pH is therefore a key target in yeast strain development for second-generation ethanol production. The conversion of acetic acid to ethanol can decrease its extracellular concentration and contribute to process robustness [41].

1.3.3 Inhibitors formed during biomass deconstruction

In biomass deconstruction, a trade-off exists between the key objective to release all fermentable sugars at minimal process costs and the need to minimize generation and release of compounds that compromise yeast performance. Biomass deconstruction generally encompasses three steps: (i) size reduction to increase surface area and reduce degree of polymerization, (ii) thermal pretreatment, often at low pH and high pressure, to disrupt the crystalline structure of cellulose while already (partly) solubilizing hemicellulose and/or lignin and (iii) hydrolysis with cocktails of fungal cellulases and hemicellulases to release fermentable sugars [63-65]. Several inhibitors of yeast performance are generated in chemical reactions that occur during biomass deconstruction and, especially, in high-temperature pretreatment. 5-hydroxymethyl-2-furaldehyde (HMF) and 2-furaldehyde (furfural) are formed when hexoses and pentoses, respectively, are exposed to high temperature and low pH values [59, 66, 67]. These furan derivatives inhibit yeast glycolysis, alcoholic fermentation and TCA cycle [68-70] while, additionally, depleting intracellular pools of NAD(P)H and ATP [71]. Their further degradation, during biomass deconstruction, yields formic acid and levulinic acid [66, 67], whose inhibitory effects overlap with those of acetic acid [59]. Inhibitor profiles of hydrolysates

depend on biomass structure and composition as well as on the type and intensity of the biomass deconstruction method used [71, 72]. During pressurized pretreatment at temperatures above 160 °C, phenolic inhibitors are generated by partial degradation of lignin. This diverse class of inhibitors includes aldehydes, ketones, alcohols and aromatic acids [71]. Ferulic acid, a phenolic compound that is an integral part of the lignin fraction of herbaceous plants [73, 74] is a potent inhibitor of *S. cerevisiae* fermentations [75]. The impact of phenolic inhibitors on membrane integrity and other cellular functions depends on the identity and position of functional groups and carbon-carbon double bonds [76].

Concentrations of inorganic salts in hydrolysates vary depending on the feedstock used [77]. Moreover, pH adjustments during pretreatment can result in high salt concentrations in hydrolysates [78]. Salt- and osmotolerance can therefore be important additional requirements in yeast strain development [79].

The inhibitors in lignocellulosic hydrolysates do not always act independently but can exhibit complex synergistic effects, both with each other and with ethanol [59, 80, 81], while their impact can also be modulated by the presence of water-insoluble solids [82]. Furthermore, their absolute and relative impact can change over time due to variations in feedstock composition, process modifications, or malfunctions in biomass deconstruction. While process adaptations to detoxify hydrolysates have been intensively studied [78, 83-85], the required additional unit operations typically result in a loss of fermentable sugar and are generally considered to be too expensive and complicated. Therefore, as research on optimization of biomass deconstruction processes continues, tolerance to the chemical environments generated by current methods is a key design criterion for yeast strain development.

1.4 Yeast strain development for second-generation ethanol production: key concepts

For almost three decades, yeast metabolic engineers have vigorously explored strategies to address the challenges outlined above. This quest benefited from rapid technological

development in genomics, genome editing, evolutionary engineering and protein engineering. Box 1 lists key technologies and examples of their application in research on yeast strain development for second-generation ethanol production.

1

Box 1. Overview of key technologies used for development of *Saccharomyces cerevisiae* strains for second-generation bioethanol production and examples of their application.

Metabolic engineering

Application of recombinant-DNA techniques for the improvement of catalytic and regulatory processes in living cells, to improve and extend their applications in industry [86].

Metabolic engineering of pentose-fermenting strains commenced with the functional expression of pathways for XR/XDH- [87, 88] or XI-based [89] xylose utilization and pathways for isomerase-based arabinose utilization [90, 91]. Further research focused on improvement of pathway capacity [92, 93], engineering of sugar transport [94, 95], redox engineering to decrease byproduct formation and increase ethanol yield [41-44, 96-98] and expression of alternative pathway enzymes [99, 100]. Expression of heterologous hydrolases provided the first steps towards consolidated bioprocessing [18, 101-103].

Evolutionary engineering

Application of laboratory evolution to select for industrially relevant traits [104]. Also known as adaptive laboratory evolution (ALE).

Evolutionary engineering in repeated-batch and chemostat cultures has been intensively utilized to improve growth and fermentation kinetics on pentoses [105-112] and inhibitor tolerance [113-117].

Whole genome (re)sequencing

Determination of the entire DNA sequence of an organism.

Availability of a high-quality reference genome sequence is essential for experimental design in metabolic engineering. When genomes of strains that have been obtained by non-targeted approaches (e.g. evolutionary engineering or mutagenesis) are (re)sequenced, the relevance of identified mutations can subsequently be tested by their reintroduction in naïve strains, non-evolved strains and/or by classical genetics (reverse engineering: [118]). This approach has been successfully applied to identify mutations contributing to fast pentose fermentation [119-121] and inhibitor tolerance (e.g., [114, 122]).

Quantitative trait loci (QTL) analysis

QTL identifies alleles that contribute to (complex) phenotypes based on their meiotic co-segregation with a trait of interest [123, 124]. In contrast to whole-genome

QTL analysis currently enables resolution to gene or even nucleotide level [125]. QTL analysis has been used to identify alleles contributing to high-temperature tolerance [126], ethanol tolerance [125] and improved ethanol-to-glycerol product ratios [127]. The requirement of QTL analysis for mating limits its applicability in aneuploidy and/or poorly sporulating industrial *S. cerevisiae* strains.

(re)sequencing alone, QTL analysis can identify epistatic interactions.

Protein engineering

Protein engineering has been used to improve the pentose-uptake kinetics, reduce the glucose sensitivity and improve the stability of yeast hexose transporters (e.g., [129-131]; [130, 132-135]). The approach has been utilized to improve the redox cofactor specificity of XR and/or XDH to decrease xylitol formation [97, 136-139]. Directed evolution of xylose isomerase yielded XI variants with increased enzymatic activity [140]. Directed evolution of native yeast dehydrogenases has yielded strains with increased HMF tolerance [141].

Genome editing

The combination of CRISPR-Cas9-based genome editing [143, 144] with *in vivo* assembly of DNA fragments has enabled the one-step introduction of all genetic modifications needed to enable *S. cerevisiae* to ferment xylose [145, 146]; [147]. Recent developments have enabled the application of the system in industrial backgrounds [148]. CRISPR-Cas9 has been used in reverse engineering studies to rapidly introduce multiple single-nucleotide mutations observed in evolutionary engineering experiments in naive strains (e.g., [149]).

1.4.1 Xylose fermentation

Efficiently linking D-xylose metabolism to glycolysis requires two key modifications of the *S. cerevisiae* metabolic network (Figure 2) [150, 151]: introduction of a heterologous pathway that converts D-xylose into D-xylulose and, simultaneously, alleviation of the limited capacity of the native *S. cerevisiae* xylulokinase and non-oxidative pentose-phosphate pathway (PPP). Two strategies for converting D-xylose into D-xylulose have been implemented in *S. cerevisiae*: (i) simultaneous expression of heterologous xylose reductase (XR) and xylitol dehydrogenase (XDH) and (ii) expression of a heterologous xylose isomerase (XI).

The first *S. cerevisiae* strains engineered for xylose utilization were based on expression of XR and XDH from the xylose-metabolising yeast *Scheffersomyces stipitis* [87]. Due to the non-matching redox-cofactor preferences of these enzymes, these strains produced large amounts of the by-product D-xylitol [52, 87, 152]. Modification of these cofactor preferences by protein engineering resulted in reduced xylitol formation under laboratory conditions [153, 154]. A much lower xylitol formation by XR/XDH-based strains in lignocellulosic hydrolysates was attributed to NADH-dependent reduction of furfural, which may contribute to *in situ* detoxification of this inhibitor [155-159]. A potential drawback of XR/XDH-based strains for application in large-scale anaerobic processes is that, even after prolonged laboratory evolution, their anaerobic growth rates are very low [110].

Combined expression of a fungal XI [160] and overexpression of the native *S. cerevisiae* genes encoding xylulokinase and non-oxidative PPP enzymes enabled anaerobic growth of a laboratory strain on xylose. In anaerobic cultures of this strain, in which the aldose-reductase encoding *GRE3* gene was deleted to eliminate xylitol formation, ethanol yields on xylose were the same as on glucose [161]. This metabolic engineering strategy, complemented with laboratory evolution under anaerobic conditions, has been successfully reproduced in different *S. cerevisiae* genetic backgrounds and/or with different XI genes [101, 162-166].

Laboratory evolution (Box 1) for faster xylose fermentation and analysis of evolved strains identified high-level expression of XI as a major contributing factor [112, 121, 167].

Multi-copy introduction of XI expression cassettes, optimization of their codon usage, and mutagenesis of their coding sequences have contributed to higher xylose fermentation rates [140, 162, 168]. Whole-genome sequencing of evolved xylose-fast-fermenting strains expressing *Piromyces* XI identified mutations affecting intracellular homeostasis of Mn^{2+} , a preferred metal ion for this XI [169]. Other mutations affected stress-response regulators and, thereby, increased expression of yeast chaperonins that assisted functional expression of XI [121]. Consistent with this observation, co-expression of the *Escherichia coli* GroEL and GroES chaperones enabled *in vivo* activity of *E. coli* XI in *S. cerevisiae* [170]. A positive effect of mutations in the *PHO13* phosphatase gene on xylose fermentation rates in XI- and XR/XDH-based strains has been attributed to transcriptional upregulation of PPP-related genes by an as yet unknown mechanism [171-174]. Additionally, Pho13 has been implicated in dephosphorylation of the PPP intermediate sedoheptulose-7-phosphate (Xu *et al.* 2016). For other mutations in evolved strains, e.g. in genes involved in iron-sulfur cluster assembly and in the MAP-kinase signaling pathway [175, 176], the mechanisms by which they affect xylose metabolism remain to be identified.

1.4.2 Arabinose fermentation

The metabolic engineering strategy for constructing L-arabinose-fermenting *S. cerevisiae* strains is based on heterologous expression of a bacterial pathway for conversion of L-arabinose into xylulose-5-phosphate, involving L-arabinose isomerase (AraA), L-ribulokinase (AraB) and L-ribulose-5-phosphate-4-epimerase (AraD) [177]. Together with the non-oxidative PPP and glycolysis, these reactions enable redox-cofactor-balanced alcoholic fermentation of arabinose (Figure 2).

Combined expression of *Bacillus subtilis* or *B. licheniformis* *araA* and *E. coli* *araBD* [91, 93, 178] allowed aerobic growth of *S. cerevisiae* on arabinose. Anaerobic growth of *S. cerevisiae* on arabinose was first achieved by expressing the *Lactobacillus plantarum* *araA*, *B* and *D* genes in an XI-based xylose-fermenting strain that already overexpressed the enzymes of the non-oxidative PPP (Figure 2), followed by evolutionary engineering under anaerobic conditions [90].

Increased expression levels of *GAL2*, which encodes a galactose transporter that also transports arabinose [179], was essential for arabinose fermentation [91, 95, 180, 181]. Increased expression of the transaldolase and transketolase isoenzymes Nqm1 and Tkl2 contributed to an increased rate of arabinose fermentation in strains evolved for fast arabinose fermentation [181]. The set of arabinose isomerase genes that can be functionally expressed in *S. cerevisiae* was recently expanded by coexpression of *E. coli araA* with the *groEL* and *groES* chaperones [170].

1.4.3 Engineering of sugar transport and mixed-substrate fermentation

In early *S. cerevisiae* strains engineered for pentose fermentation, uptake of xylose and arabinose exclusively relied on their native hexose transporters. While several of the 18 *S. cerevisiae* Hxt transporters (Hxt1-17 and Gal2) transport xylose, their K_m values for this pentose are one to two orders of magnitude higher than for glucose [130, 182-185]. High-affinity glucose transporters, which are only expressed at low glucose concentrations [186], display a lower K_m for xylose than low-affinity glucose transporters [182, 183]. The galactose transporter Gal2, which also catalyses high-affinity glucose transport [185] also has a much higher K_m for arabinose than for glucose [95, 180].

The higher affinities of Hxt transporters for glucose, combined with the transcriptional repression of Gal2 [187, 188] and other high-affinity Hxt transporters [186, 189] at high glucose concentrations, contribute to a sequential use of glucose and pentoses during mixed-substrate cultivation of engineered strains that depend on Hxt-mediated pentose uptake. Furthermore, the high K_m values of Hxt transporters for pentoses cause a deceleration of sugar fermentation during the pentose-fermentation phase. This 'tailing' effect is augmented by accumulation of ethanol and by the reduced inhibitor tolerance of *S. cerevisiae* at low sugar fermentation rates [190-192]. Intensive efforts have been made to generate yeast strains that can either co-consume hexoses and pentose sugars or sequentially consume all sugars in hydrolysates in an economically acceptable time frame [193, 194].

Evolutionary engineering experiments have played a major role in accelerating mixed-sugar utilization by engineered pentose-fermenting strains [108, 110-112, 195]. Repeated batch cultivation on a sugar mixture can favor selection of mutants that rapidly ferment one of the sugars, while showing deteriorated fermentation kinetics with other sugars in the mixture. In practice, such trade-off scenarios can increase rather than decrease the time required for complete conversion of sugar mixtures [111]. A modified strategy for repeated batch cultivation, designed to equally distribute the number of generations of selective growth on each of the individual substrates in a mixture, enabled acceleration of the anaerobic conversion of glucose-xylose-arabinose mixtures by an engineered *S. cerevisiae* strain [111].

Recently constructed glucose-phosphorylation-negative, pentose-fermenting *S. cerevisiae* strains enabled evolutionary engineering experiments for *in vivo* directed evolution of Hxt variants that supported growth on xylose or arabinose in the presence of high glucose concentrations [119, 130, 196, 197]. Several of the evolved *HXT* alleles were confirmed to encode transporters whose xylose-transport kinetics were substantially less sensitive to glucose inhibition [119, 130, 196, 197]. Remarkably, independent evolutionary engineering studies aimed at selecting glucose-insensitive xylose and arabinose Hxt transporters yielded single-amino-acid substitutions at the exact corresponding positions in Hxt7(N370), Gal2 (N376), and in a chimera of Hxt3 and Hxt6 (N367) [119, 130, 197]. Additional Hxt variants with improved relative affinities for pentoses and glucose were obtained by *in vitro* directed evolution and knowledge-based protein engineering [130, 198] (Box 1).

Low-, moderate- and high-affinity pentose transporters from pentose-metabolizing filamentous fungi or non-*Saccharomyces* yeasts, have been functionally expressed in *S. cerevisiae* [95, 199-209]. Expression and/or activity of several of these transporters were further improved by directed evolution [129, 201, 208] or evolutionary engineering [194, 210]. Such high-affinity transporters may be suited to 'mop up' low concentrations of pentoses towards the end of a fermentation process. Since high-affinity sugar transporters are typically proton symporters, care should be taken to avoid scenarios in which their simultaneous expression

with Hxt-like transporters, which mediate facilitated diffusion, causes futile cycles and negatively affects inhibitor tolerance.

1.4.4 Inhibitor tolerance

Yeast enzymes involved in detoxification of specific inhibitors provide logical targets for metabolic engineering. For example, overexpression of native NAD(P)⁺-dependent alcohol dehydrogenases stimulates conversion of furfural and HMF to the less toxic alcohols furanmethanol and furan-2,5-dimethanol, respectively [211-213]. Similarly, combined overexpression of the aldehyde dehydrogenase Ald5, the decarboxylase Pad1 and the alcohol acetyltransferases Atf1 and Atf2 increased resistance to several phenolic inhibitors [214].

Genome-wide expression studies have revealed intricate, strain- and context-dependent stress-response networks as major key contributors to inhibitor tolerance [61, 71, 215-219]. An in-depth transcriptome analysis implicated *SFP1* and *ACE2*, which encode transcriptional regulators involved in ribosomal biogenesis and septum destruction after cytokinesis, respectively, in the phenotype of an acetic-acid and furfural-tolerant strain. Indeed, overexpression of these transcriptional regulators significantly enhanced ethanol productivity in the presence of these inhibitors [220].

Whole-genome resequencing of tolerant strains derived from evolutionary engineering, mutagenesis and/or genome shuffling has yielded strains with increased tolerance whose causal mutations could be identified [105, 113, 122, 221, 222]. Physiological and evolutionary engineering experiments demonstrated the importance of high sugar fermentation rates for acetic acid tolerance [192, 223]. When the acetic-acid concentration in anaerobic, xylose-grown continuous cultures was continually increased over time, evolving cultures acquired the ability to grow at acetic-acid concentrations that prevented growth of the non-evolved *S. cerevisiae* strain. However, after growth in the absence of acetic acid, full expression of their increased tolerance required pre-exposure to a lower acetic-acid concentration. This observation indicated that the acquired tolerance was inducible rather than constitutive [223]. Constitutive tolerance to acetic acid was shown to reflect the fraction of yeast populations able to initiate growth upon

exposure to acetic acid stress [224]. Based on this observation, an evolutionary engineering strategy that involved alternating batch cultivation cycles in the presence and absence of acetic acid was successfully applied to select for constitutive acetic acid tolerance [221].

Exploration of the natural diversity of inhibitor tolerance among *S. cerevisiae* strains [225-227] is increasingly used to identify genes and alleles that contribute to tolerance. In particular, combination of whole genome sequencing and classical genetics is a powerful approach to identify relevant genomic loci, genes and even nucleotides [123] (Quantitative Trait Loci (QTL) analysis, see Box 1). For example, Meijnen *et al.* (2016) used whole-genome sequencing of pooled tolerant and sensitive segregants from crosses between a highly acetic-acid tolerant *S. cerevisiae* strain and a reference strain to identify mutations in five genes that contributed to tolerance.

1.5. Development of industrial yeast strains and processes

Much of the research discussed in the preceding paragraphs was based on laboratory yeast strains, grown in synthetic media whose composition can be different from that of industrial lignocellulosic hydrolysates. Table 2 provides examples of ethanol yields and biomass-specific conversion rates that have been obtained with engineered *S. cerevisiae* strains in synthetic media.

While data on the performance of current industrial strains on industrial feedstocks are proprietary, many scientific publications describe the fermentation of hydrolysates by xylose-fermenting strains (either XI or XR-XDH-based, but so far without arabinose pathways). These studies cover a wide variety of feedstocks, biomass deconstruction and fermentation strategies (batch, fed-batch, SSF), aeration regimes and nutritional supplementations (e.g. yeast extract, peptone, low-cost industrial supplements, trace elements, nitrogen sources). However, with few exceptions, these data are restricted to final ethanol yields and titers, and do not include quantitative information of the biomass-specific conversion rates (q_{xylose} , q_{ethanol} , expressed in $\text{g} (\text{g biomass})^{-1} \text{h}^{-1}$) that are essential for strain comparison and process design. Table 3 summarizes

results of studies on fermentation of biomass hydrolysates that include or enable calculation of biomass-specific conversion rates and ethanol yields.

Table 2. Ethanol yields ($Y_{E/S}$, g ethanol (g sugar) $^{-1}$) and biomass-specific rates of xylose and/or arabinose consumption and ethanol production (q_{xylose} , $q_{arabinose}$ and $q_{ethanol}$, respectively, g (g biomass) $^{-1}$ h $^{-1}$) in cultures of *S. cerevisiae* strains engineered for pentose fermentation, grown in synthetic media. Asterisks (*) indicate values estimated from graphs in the cited reference.

<i>S. cerevisiae</i> strain	Pentose fermentation strategy	Key genetic modifications	Fermentation conditions	$Y_{E/S}$ g g $^{-1}$	$q_{ethanol}$ g g $^{-1}$ h $^{-1}$	q_{xylose} g g $^{-1}$ h $^{-1}$	$q_{arabinos}$ g g $^{-1}$ h $^{-1}$	Reference
TMB3400	XR/XDH (<i>S. stipitidis</i> XYL1, XYL2)	<i>SsXYL1</i> , <i>SsXYL2</i> + <i>XKS1</i> ↑, random mutagenesis	Anaerobic batch (bioreactor), 5% xylose	0.33	0.04	0.13	-	[159]
GLBRCY87	XR/XDH (<i>S. stipitidis</i> XYL1, XYL2)	<i>SsXYL1</i> , <i>SsXYL2</i> , <i>SsXYL3</i> , evolved on xylose and hydrolysate inhibitors	Semi-anaerobic batch (flask) 5% glucose and 5% xylose	0.34*	0.036*	0.13	-	[175]
SR8	XR/XDH (<i>S. stipitidis</i> XYL1, XYL2)	<i>SsXYL1</i> , <i>SsXYL2</i> , <i>SsXYL3</i> , <i>ald6</i> Δ, evolved on xylose	Anaerobic batch (reactor), 4% xylose	0.39	0.25	0.64	-	[43]
TMB3421	XR/XDH (<i>S. stipitidis</i> XYL1, XYL2)	<i>S. stipitidis</i> XYL1 ^{N272D/P275Q} , XYL2 + XKS1↑ TALI↑ TKL1↑ RPE1↑ RKI1↑ <i>gre3</i> Δ, evolved on xylose	Anaerobic batch (reactor), 6% xylose	0.35	0.20	0.57	-	[153]
RWB 217	XI (<i>Piromyces</i> XylA)	<i>Piromyces</i> XylA + XKS1↑ TALI↑ TKL1↑ RPE1↑ RKI1↑, <i>gre3</i> Δ	Anaerobic batch (reactor), 2% xylose	0.43	0.46	1.06	-	[92]
RWB 218	XI (<i>Piromyces</i> XylA)	Derived from RWB 217 after evolution on glucose/xylose mixtures	Anaerobic batch (reactor) 2% xylose	0.41	0.49	1.2	-	[108]
HI31-A3-ALS	XI (<i>Piromyces</i> XylA)	XylA, XylB, XKS1↑ TALI↑ TKL1↑ RPE1↑ RKI1↑, <i>gre3</i> Δ, evolved on xylose	Anaerobic batch (reactor), 4% xylose	0.43	0.76	1.9	-	[112]
IMS0010	XI/AraABD (<i>Piromyces</i> XylA, <i>L. plantarum</i> AraA, B, D)	XylA; XKS1↑ TALI↑ TKL1↑ RPE1↑ RKI1↑ AraT, AraA, AraB, AraD, evolved on glucose, xylose, arabinose mixtures	Anaerobic batch (reactor), 3% glucose, 1.5% xylose and 1.5% arabinose	0.43	-	0.35	0.53	[228]
GS11.11-26	XI/AraABD (<i>Piromyces</i> XylA, <i>L. plantarum</i> AraA, B, D, <i>K. lactis</i> ARAT)	XylA, XKS1↑ TALI↑ TKL1↑ RPE1↑ RKI1↑ XylA HX77↑ K1AraT, AraA, AraB, AraD, TAL2↑ TKL2↑, several rounds of mutagenesis and evolution on xylose	Semi-anaerobic batch (flask), synthetic medium, 3.5% xylose	0.46	0.48	1.1	-	[105]

Table 3. Ethanol yields on consumed sugar ($Y_{E/S}$, g ethanol (g sugar)⁻¹) and biomass-specific rates of glucose and xylose consumption and ethanol production (q_{glucose} , q_{xylose} and q_{ethanol} , respectively, g (g biomass)⁻¹ h⁻¹) in cultures of *S. cerevisiae* strains engineered for pentose fermentation, grown in lignocellulosic hydrolysates. Asterisks (*) indicate specific conversion rates estimated from graphs in the cited reference; daggers (†) indicate crude estimates of biomass-specific rates calculated based on the assumption that biomass concentrations did not change after inoculation, these estimates probably overestimate actual biomass-specific conversion rates.

<i>S. cerevisiae</i> strain	Description	Feedstock, pretreatment conditions, hydrolysate sugar composition ³	Fermentation conditions, added nutrients ¹	$Y_{E/S}$ g g ⁻¹	q_{glucose} g g h ⁻¹	q_{ethanol} g g h ⁻¹	q_{xylose} g g h ⁻¹	Ref
TMB3400	XR/XDH <i>S. stipitis</i> XYL1 and XYL2; XKS1†	Spruce, two-step dilute acid hydrolysis, 1.6% glucose, 0.4% xylose, 1% mannose, 1% galactose,	Anaerobic batch (flasks), (NH ₄) ₂ HPO ₄ NaH ₂ PO ₄ MgSO ₄ , YE	0.41	0.021	0.005	0.005	[159]
GLBRCY87	XR/XDH <i>S. stipitis</i> XYL1, XYL2 and XYL3 evolved on xylose and hydrolysate inhibitors	Corn Stover, ammonia fiber expansion, 8% glucose, 3.8% xylose.	Semi-anaerobic batch (flasks), pH 5.5, Urea, YNB	0.28	1.4*	0.27*	0.04	[175]
GLBRCY87	XR/XDH <i>S. stipitis</i> XYL1, XYL2 and XYL3 evolved on xylose and hydrolysate inhibitors	Switchgrass, ammonia fiber expansion, 6.1% glucose, 3.9% xylose.	Semi-anaerobic batch (flasks), Urea, YNB	0.35	1.65*	0.28*	0.07	[175]
MEC1122	XR/XDH, industrial host strain <i>S. stipitis</i> XYL1 ^(NZ720/P275-0) and XYL2, XKS1† TALI†	Corn cobs, autohydrolysis (202 °C), liquid fraction acid-treated, 0.3% glucose, 2.6% xylose.	Oxygen limited batch (flasks), cheese whey, urea, YE, K ₂ O ₅ S ₂	0.3	-	0.12†*	0.25†	[229]
RWB 218	XI <i>Piromyces</i> Xy1A, XKS1† TALI† TKL1† RPE1† RKI1†, gre3Δ, evolved on glucose/xylose mixed substrate	Wheat straw hydrolysate, steam explosion, 5% glucose, 2% xylose	Anaerobic batch (reactor), (NH ₄) ₂ PO ₄	0.47	1.58†	1.0†	0.32†	[151]
GSI.11-26	XI, AraABD <i>Piromyces</i> Xy1A, XKS1† TALI† TKL1† RPE1† RKI1† HXT7† AraT, Ara4, AraB, AraD, TALZ† TKLZ†, several rounds of mutagenesis and evolution on xylose	Spruce (no hydrolysis), acid pre-treated, 6.2% glucose, 1.8% xylose, 1% mannose	Semi-anaerobic batch (flasks), YNB, (NH ₄) ₂ SO ₄ , amino acids added,	0.43	2.46†	0.3†	0.11†	[105]
XH7	Multiple integrations of <i>RuXy1A</i> ; XKS1† TALI† TKL1† RPE1† RKI1† <i>pho13Δ gre3Δ</i> , evolved on xylose	Corn stover, steam explosion, 6.2% glucose, 1.8% xylose	Semi-anaerobic batch (flasks), urea	0.39	0.14	0.080	0.096	[230]
LF1	Selection mutant of XH7 further evolved on xylose and hydrolysates with MGT transporter introduced	Corn stover, steam explosion, 8.7% glucose, 3.9% xylose	Semi-anaerobic batch (flasks), urea	0.41	0.57	0.34	0.23	[230]

¹Abbreviations of supplements: YE, yeast extract; YP, yeast extract and peptone; YNB, Yeast Nitrogen Base.

Despite the heterogeneity of the studies included in Tables 2 and 3, the available data clearly illustrate that, while even ‘academic’ strain platforms can exhibit high ethanol yields in hydrolysates, conversion rates under these conditions are much lower than in synthetic media. Improving kinetics and robustness in industrial hydrolysates is therefore the single most important objective in industrial yeast strain development platforms.

Due to the complex, multigene nature of inhibitor tolerance, screening of natural and industrial *S. cerevisiae* strains is a logical first step in the development of industrial strain platforms. The power of this approach is illustrated by the Brazilian first-generation bioethanol strain PE-2. Stable maintenance of this strain in non-aseptically operated industrial reactors, over many production campaigns [231], was attributed to its innate tolerance to the sulfuric-acid washing steps that are employed between fermentation cycles to combat bacterial contamination [232]. In contrast to most laboratory strains, robust industrial strains of *S. cerevisiae* are heterozygous diploids or polyploids which, additionally, are prone to whole-chromosome or segmental aneuploidy [233, 234]. Acquiring high-quality, well annotated genome sequences (Box 1) of these complex genomes is an important prerequisite for interpreting the results of strain improvement campaigns and for targeted genetic modification.

Episomal expression vectors carrying auxotrophic marker genes, which are commonly used in academic research, do not allow for stable replication and selection, respectively, in complex industrial media [235-237]. Instead, industrial strain development requires chromosomal integration of expression cassettes. Even basic academic designs of xylose- and arabinose-fermenting strains encompass the introduction of 10-12 different expression cassettes [90, 181], some of which need to be present in multiple copies (e.g. for high-level expression of XI genes [112, 167, 169, 238]). Additional genetic modifications, on multiple chromosomes in the case of diploid or polyploid strains, are required to reduce by-product formation, improve inhibitor tolerance and/or improve product yields. Genetic modification of complex industrial yeast genomes has now been strongly accelerated by novel, CRISPR-based genome editing tools (Box 1).

Non-targeted strategies for strain improvement (Box 1) including mutagenesis with chemical mutagens or irradiation, evolutionary engineering, recursive breeding and/or genome shuffling remain essential for industrial strain improvement. Down-scaling, automation and integration with high-throughput screening of the resulting strains in hydrolysates strongly increases the success rates of these approaches (e.g. for ethanol tolerance, [239]). In non-targeted strain improvement campaigns, it is important to maintain selective pressure on all relevant aspects of strain performance, to avoid trade-offs between, for example, fermentation kinetics with different sugars (glucose, xylose and arabinose), and/or inhibitor tolerance [105, 111, 116].

Even when kinetics of yeast growth and fermentation in hydrolysates are suboptimal (Table 2) due to the impact of inhibitors and/or strain characteristics, industrial fermentation processes need to achieve complete sugar conversion within acceptable time limits (typically 72 h or less). This can be accomplished by increasing the initial yeast biomass densities, which, in second generation processes, are typically 2- to 8-fold higher than the initial concentrations of 0.125-0.25 g L⁻¹ that are used in first-generation processes without biomass recycling [240]. Several second-generation bioethanol plants therefore include on-site bioreactors for cost-effective generation of the required yeast biomass. Precultivation in the presence of mild concentrations of inhibitors can prime yeast cells for improved performance upon exposure to stressful conditions [241-243]. Especially when biomass propagation uses non-lignocellulosic feedstocks [244, 245] and/or is operated aerobically to maximize biomass yields, yeast strain development must take into account the need to maintain pentose- fermentation kinetics and inhibitor tolerance during biomass propagation.

Metabolic engineering strategies to further improve yeast performance in second generation bioethanol processes are already being explored. For example, the option is investigated to implement the strategies discussed above in non-*Saccharomyces* yeasts with industrially interesting properties, such as high-temperature and low-pH tolerance strains [246-249]. Other research focuses on the improvement of these characteristics in *S. cerevisiae* [250,

251]. Furthermore, as production volumes increase, the economic relevance of the conversion of minor, potentially fermentable substrates such as uronic acids and deoxysugars into ethanol [252] will increase. Co-feeding of additional, low-value carbon sources can be explored as a strategy to further increase ethanol yield. For example, glycerol, derived from fermentation stills or biodiesel manufacturing [253] is considered as a potential co-substrate. Significant rates of glycerol utilization have already been achieved in *S. cerevisiae* strains by simultaneously (over-) expressing glycerol dehydrogenase (*GCY1*), dihydroxyacetone kinase (*DAK1*) and a heterologous glycerol transporter [98]. These glycerol conversion pathways can be combined with the engineered pathways for acetic acid reduction discussed above to further optimize ethanol yields and process robustness [254, 255].

Consolidated bio-processing (CBP), i.e., the full integration of pretreatment, hydrolysis and fermentation towards ethanol in a single microbial process step, remains a 'holy grail' in lignocellulosic ethanol production. Engineered starch-hydrolysing *S. cerevisiae* strains are already applied in first-generation processes [256]. The first important steps towards efficient cellulose and xylan hydrolysis by *S. cerevisiae* have been made by functional expression of heterologous polysaccharide hydrolases [18, 19]. The resulting engineered strains often produce significant amounts of di- and/or trisaccharides [257-259]. The ability to ferment cellobiose has been successfully introduced into *S. cerevisiae* by combined expression of a heterologous cellobiose transporter and β -glucosidase (Galazka *et al.* 2010, Hu *et al.* 2016).

1.6 Scope of this thesis

The main objective of this thesis was maximizing ethanol yield in anaerobic *Saccharomyces cerevisiae* cultures, with an emphasis on designing, implementing and testing strategies with potential for industrial implementation. To this end, redox engineering strategies for minimization of glycerol formation that did not require additional or modified unit operations in industrial fermentation processes were implemented by genetic modification and tested in lab-scale bioreactor experiments.

The use of CO₂ as electron acceptor for oxidation of excess NADH formed in biosynthesis can significantly decrease glycerol formation in anaerobic *S. cerevisiae* cultures. The goal of **Chapter 2** was to investigate the genetic requirements for developing fast-growing yeast strains that rely on CO₂ reduction via the RuBisCO/PRK pathway for redox cofactor balancing. CRISPR-Cas9 genome editing was used to construct strains with differentially regulated PRK expression. Their physiology was quantitatively analysed in anaerobic batch and chemostat cultures. Additional modifications in glycerol metabolism and pentose phosphate pathway genes enabled the generation of strains that showed an almost complete elimination of glycerol formation and improved ethanol yield in anaerobic batch cultures, while growing at wild-type rates.

Reduction of acetic acid to ethanol can replace glycerol formation as a redox sink in anaerobic *S. cerevisiae* cultures, thereby enhancing ethanol yields while simultaneously contributing to detoxification of fermentation media. The goal of **Chapter 3** was to develop a redox engineering strategy for increasing cytosolic NADH formation in *S. cerevisiae*, with the aim of enhancing anaerobic acetic acid utilization by engineered strains. The strategy was based on replacement of the native, NADP⁺-dependent, 6-phosphogluconate dehydrogenase by a heterologous NAD⁺-dependent enzyme, with combined deletion of the NADP⁺-dependent acetaldehyde dehydrogenase Ald6, in an acetate-reducing strain. The engineered strains showed significant increases in acetate reduction in anaerobic bioreactor batch cultures.

Abolishment of glycerol production increases the osmosensitivity of *S. cerevisiae* mutants. Therefore, optimization of acetate reduction in strains still capable of glycerol formation can be beneficial for industrial implementation. The goal of **Chapter 4** was to develop metabolic engineering strategies to optimize acetate reduction in low- and high-osmolarity anaerobic cultures of *S. cerevisiae*. To this end, modifications of the native glycerol production pathway were performed using CRISPR-Cas9 genome editing. Deletion of *GPD2* significantly enhanced acetate reduction in low-osmolarity anaerobic batch cultures. Replacement of *GPD1* and *GPD2* by a NADP⁺-dependent heterologous glycerol-3-phosphate dehydrogenase, combined with deletion of *ALD6*, enabled optimal acetate reduction in both low- and high-osmolarity

anaerobic batch cultures, while maintaining a substantial osmotolerance of the engineered strains.

In second-generation bioethanol production processes, increased rates of sugar consumption not only directly improve volumetric productivity but can also contribute to inhibitor tolerance. The introduction of a NAD⁺-dependent 6-phosphogluconate dehydrogenase discussed in **Chapter 3** can enable increased fluxes through the oxidative pentose-phosphate pathway by decreasing NADPH overflow. In **Chapter 5** this modification was used as part of a novel laboratory evolution approach to select for mutants in which xylose metabolism occurred simultaneously with glucose fermentation. Deletion of phosphoglucose-isomerase and ribulose-5-phosphate epimerase in a xylose-consuming strain with a modified oxidative pentose-phosphate pathway forced the resulting yeast cells to co-consume xylose and glucose. Laboratory evolution for faster growth was followed by whole genome sequencing for identifying potential causal mutations in the evolved strains. Introduction of several of these mutations in non-evolved, xylose-fermenting *S. cerevisiae* strains enabled significant increases in xylose utilization in the presence of glucose in anaerobic batch cultures.

1.7 References

1. Bernton H, Kovarik B, Sklar S. The forbidden fuel: Power alcohol in the twentieth century. New York: Caroline House Pubns; 1982.
2. Renewable Fuels Association. World fuel ethanol production report. 2016. <http://ethanolrfa.org/resources/industry/statistics/>. Accessed 24 March 2017.
3. Lopes ML, de Lima Paulillo SCdL, Godoy A, Cherubin RA, Lorenzi MS, Giometti FHC, Bernardino CD, Amorim Neto HBd, Amorim HVd. Ethanol production in Brazil: a bridge between science and industry. *Braz J Microbiol.* 2016;47:64-76.
4. Della-Bianca BE, Basso TO, Stambuk BU, Basso LC, Gombert AK. What do we know about the yeast strains from the Brazilian fuel ethanol industry? *Appl Microbiol Biotechnol.* 2013;97:979-91.
5. Thomas K, Ingledew W. Production of 21% (v/v) ethanol by fermentation of very high gravity (VHG) wheat mashes. *J Ind Microbiol Biotechnol.* 1992;10:61-68.
6. Rude MA, Schirmer A. New microbial fuels: a biotech perspective. *Curr Opin Microbiol.* 2009;12:274-81.
7. Otero JM, Panagiotou G, Olsson L: Fueling industrial biotechnology growth with bioethanol. In *Biofuels*. Edited by Olsson L. Springer Berlin Heidelberg; 2007: 1-40.
8. Nordhoff S. Editorial: Food vs fuel – the role of biotechnology. *Biotechnol J.* 2007;2:1451.
9. Tenenbaum DJ. Food vs. fuel: Diversion of crops could cause more hunger. *Environ Health Perspect.* 2008;116:A254-A57.
10. Farrell AE, Plevin RJ, Turner BT, Jones AD, Hare M, Kammen DM. Ethanol can contribute to energy and environmental goals. *Science.* 2006;311:506.
11. Kleinschmidt J. Biofueling rural development: making the case for linking biofuel production to rural revitalization. In *The Carsey School of Public Policy at the Scholars' Repository.* Durham NHTCI, University of New Hampshire. 2007. <http://scholars.unh.edu/cgi/viewcontent.cgi?article=1019&context=carsey>. Accessed 24 March 2017.
12. Yan X, Inderwildi OR, King DA. Biofuels and synthetic fuels in the US and China: A review of Well-to-Wheel energy use and greenhouse gas emissions with the impact of land-use change. *Energy Environ Sci.* 2010;3:190-97.
13. Pereira LG, Dias MOS, Mariano AP, Maciel Filho R, Bonomi A. Economic and environmental assessment of n-butanol production in an integrated first and second generation sugarcane biorefinery: Fermentative versus catalytic routes. *Appl Energy.* 2015;160:120-31.
14. Hahn-Hägerdal B, Galbe M, Gorwa-Grauslund MF, Lidén G, Zacchi G. Bio-ethanol – the fuel of tomorrow from the residues of today. *Trends Biotechnol.* 2006;24:549-56.
15. Van den Brink J, de Vries RP. Fungal enzyme sets for plant polysaccharide degradation. *Appl Microbiol Biotechnol.* 2011;91:1477.
16. Lynd LR, Weimer PJ, van Zyl WH, Pretorius IS. Microbial cellulose utilization: fundamentals and biotechnology. *Microbiol Mol Biol Rev.* 2002;66:506-77.
17. Sims-Borre P: The economics of enzyme production. In *Ethanol Producer Magazine.* 2010. <http://www.ethanolproducer.com/articles/7048>. Accessed 24 March 2017.
18. Den Haan R, Van Rensburg E, Rose SH, Görgens JF, van Zyl WH. Progress and challenges in the engineering of non-cellulolytic microorganisms for consolidated bioprocessing. *Curr Opin Biotechnol.* 2015;33:32-38.
19. Olson DG, McBride JE, Joe Shaw A, Lynd LR. Recent progress in consolidated bioprocessing. *Curr Opin Biotechnol.* 2012;23:396-405.
20. Vohra M, Manwar J, Manmode R, Padgilwar S, Patil S. Bioethanol production: Feedstock and current technologies. *J Environ Chem Eng.* 2014;2:573-84.
21. Ethanol Producer Magazine: U.S. Ethanol Plants. 2017. <http://www.ethanolproducer.com/plants/listplants/US/All/Cellulosic>. Accessed 14 February 2017.

22. UNCTAD. Second generation biofuel markets: state of play, trade and developing country perspectives. United Nations Conference on Trade and Development. 2016.
23. Maiorella BL, Blanch HW, Wilke CR, Charles E. Wyman Ib. Economic evaluation of alternative ethanol fermentation processes. *Biotechnol Bioeng.* 2009;104:419-43.
24. Nielsen J, Larsson C, van Maris AJA, Pronk JT. Metabolic engineering of yeast for production of fuels and chemicals. *Curr Opin Biotechnol.* 2013;24:398-404.
25. Van Maris AJA, Abbott DA, Bellissimi E, van den Brink J, Kuyper M, Luttik MA, Wisselink HW, Scheffers WA, van Dijken JP, Pronk JT. Alcoholic fermentation of carbon sources in biomass hydrolysates by *Saccharomyces cerevisiae*: current status. *Antonie Van Leeuwenhoek.* 2006;90:391-418.
26. Gombert AK, van Maris AJA. Improving conversion yield of fermentable sugars into fuel ethanol in 1st generation yeast-based production processes. *Curr Opin Biotechnol.* 2015;33:81-86.
27. Basso TO, de Kok S, Dario M, do Espirito-Santo JCA, Müller G, Schlögl PS, Silva CP, Tonso A, Daran J-MG, Gombert AK, et al. Engineering topology and kinetics of sucrose metabolism in *Saccharomyces cerevisiae* for improved ethanol yield. *Metab Eng.* 2011;13:694-703.
28. Guo Z, Zhang L, Ding Z, Shi G. Minimization of glycerol synthesis in industrial ethanol yeast without influencing its fermentation performance. *Metab Eng.* 2011;13:49-59.
29. Zhang L, Tang Y, Guo Z-P, Ding Z-Y, Shi G-Y. Improving the ethanol yield by reducing glycerol formation using cofactor regulation in *Saccharomyces cerevisiae*. *Biotechnol Lett.* 2011;33:1375-80.
30. Bro C, Regenber B, Förster J, Nielsen J. *In silico* aided metabolic engineering of *Saccharomyces cerevisiae* for improved bioethanol production. *Metab Eng.* 2006;8:102-11.
31. Björkqvist S, Ansell R, Adler L, Lidén G. Physiological response to anaerobicity of glycerol-3-phosphate dehydrogenase mutants of *Saccharomyces cerevisiae*. *Appl Environ Microbiol.* 1997;63:128-32.
32. Van Dijken JP, Scheffers WA. Redox balances in the metabolism of sugars by yeasts. *FEMS Microbiol Lett.* 1986;32:199-224.
33. Bishop WR, Bell RM. Assembly of phospholipids into cellular membranes: biosynthesis, transmembrane movement and intracellular translocation. *Annu Rev Cell Biol.* 1988;4:579-606.
34. Athenstaedt K, Daum G. 1-acyldihydroxyacetone-phosphate reductase (Ayr1p) of the yeast *Saccharomyces cerevisiae* encoded by the open reading frame *YIL124w* is a major component of lipid particles. *J Biol Chem.* 2000;275:235-40.
35. Hohmann S. Osmotic stress signaling and osmoadaptation in yeasts. *Microbiol Mol Biol Rev.* 2002;66:300-72.
36. Nevoigt E, Stahl U. Osmoregulation and glycerol metabolism in the yeast *Saccharomyces cerevisiae*. *FEMS Microbiol Rev.* 1997;21:231-41.
37. Hubmann G, Guillouet S, Nevoigt E. Gpd1 and Gpd2 fine-tuning for sustainable reduction of glycerol formation in *Saccharomyces cerevisiae*. *Appl Environ Microbiol.* 2011;77:5857-67.
38. Nissen TL, Kielland-Brandt MC, Nielsen J, Villadsen J. Optimization of ethanol production in *Saccharomyces cerevisiae* by metabolic engineering of the ammonium assimilation. *Metab Eng.* 2000;2:69-77.
39. Guadalupe-Medina V, Wisselink HW, Luttik MA, de Hulster E, Daran J-MG, Pronk JT, van Maris AJA. Carbon dioxide fixation by Calvin-Cycle enzymes improves ethanol yield in yeast. *Biotechnol Biofuels.* 2013;6:125.
40. Van Hazendonk JM, Reinerik EJM, de Waard P, Van Dam JEG. Structural analysis of acetylated hemicellulose polysaccharides from fibre flax (*Linum usitatissimum L.*). *Carbohydr Res.* 1996;291:141-54.

41. Guadalupe-Medina V, Almering MJH, van Maris AJA, Pronk JT. Elimination of glycerol production in anaerobic cultures of a *Saccharomyces cerevisiae* strain engineered to use acetic acid as an electron acceptor. *Appl Environ Microbiol.* 2010;76:190-95.
42. Henningsen BM, Hon S, Covalla SF, Sonu C, Argyros DA, Barrett TF, Wiswall E, Froehlich AC, Zelle RM. Increasing anaerobic acetate consumption and ethanol yields in *Saccharomyces cerevisiae* with NADPH-specific alcohol dehydrogenase. *Appl Environ Microbiol.* 2015;81:8108-17.
43. Wei N, Quarterman J, Kim SR, Cate JHD, Jin YS. Enhanced biofuel production through coupled acetic acid and xylose consumption by engineered yeast. *Nat Commun.* 2013;4.
44. Zhang GC, Kong II, Wei N, Peng D, Turner TL, Sung BH, Sohn JH, Jin YS. Optimization of an acetate reduction pathway for producing cellulosic ethanol by engineered yeast. *Biotechnol Bioeng.* 2016;113:2587-96.
45. Khoo HH. Review of bio-conversion pathways of lignocellulose-to-ethanol: Sustainability assessment based on land footprint projections. *Renew Sust Energy Rev.* 2015;46:100-19.
46. Kenney KL, Smith WA, Gresham GL, Westover TL. Understanding biomass feedstock variability. *Biofuels.* 2013;4:111-27.
47. Lin Y, Tanaka S. Ethanol fermentation from biomass resources: current state and prospects. *Appl Microbiol Biotechnol.* 2006;69:627-42.
48. Lynd LR. Overview and evaluation of fuel ethanol from cellulosic biomass: technology, economics, the environment, and policy. *Annu Rev Energy Env.* 1996;21:403-65.
49. Grohmann K, Bothast R. Pectin-rich residues generated by processing of citrus fruits, apples, and sugar beets. In *Enzymatic Conversion of Biomass for Fuels Production. Volume 566*: ACS Publications; 1994:372-90.
50. Grohmann K, Bothast RJ. Saccharification of corn fibre by combined treatment with dilute sulphuric acid and enzymes. *Process Biochem.* 1997;32:405-15.
51. Bruinenberg PM, Bot PH, van Dijken JP, Scheffers WA. The role of redox balances in the anaerobic fermentation of xylose by yeasts. *Appl Microbiol Biotechnol.* 1983;18:287-92.
52. Hahn-Hägerdal B, Wahlbom CF, Gárdonyi M, van Zyl WH, Otero RRC, Jönsson LJ: Metabolic engineering of *Saccharomyces cerevisiae* for xylose utilization. *Adv Biochem Eng Biotechnol.* 2001;73:53-84.
53. Kötter P, Amore R, Hollenberg CP, Ciriacy M. Isolation and characterization of the *Pichia stipitis* xylitol dehydrogenase gene, *XYL2*, and construction of a xylose-utilizing *Saccharomyces cerevisiae* transformant. *Curr Genet.* 1990;18:493-500.
54. Sedlak M, Ho NW. Expression of *E. coli* *araBAD* operon encoding enzymes for metabolizing L-arabinose in *Saccharomyces cerevisiae*. *Enzyme Microb Technol.* 2001;28:16-24.
55. Beckner M, Ivey ML, Phister TG. Microbial contamination of fuel ethanol fermentations. *Lett Appl Microbiol.* 2011;53:387-94.
56. Axe DD, Bailey JE. Transport of lactate and acetate through the energized cytoplasmic membrane of *Escherichia coli*. *Biotechnol Bioeng.* 1995;47:8-19.
57. Pampulha ME, Loureiro-Dias MC. Energetics of the effect of acetic acid on growth of *Saccharomyces cerevisiae*. *FEMS Microbiol Lett.* 2000;184:69-72.
58. Verduyn C, Postma E, Scheffers WA, van Dijken JP. Effect of benzoic acid on metabolic fluxes in yeasts: A continuous-culture study on the regulation of respiration and alcoholic fermentation. *Yeast.* 1992;8:501-17.
59. Palmqvist E, Hahn-Hägerdal B. Fermentation of lignocellulosic hydrolysates. II: inhibitors and mechanisms of inhibition. *Bioresour Technol.* 2000;74:25-33.
60. Russel JB. Another explanation for the toxicity of fermentation acids at low pH: anion accumulation versus uncoupling. *J Appl Microbiol.* 1992;73:363-70.
61. Ullah A, Chandrasekaran G, Brul S, Smits G. Yeast adaptation to weak acids prevents futile energy expenditure. *Front Microbiol.* 2013;4.

62. Taherzadeh MJ, Eklund R, Gustafsson L, Niklasson C, Lidén G. Characterization and fermentation of dilute-acid hydrolyzates from wood. *Ind Eng Chem Res.* 1997;36:4659-65.
63. Hendriks ATWM, Zeeman G. Pretreatments to enhance the digestibility of lignocellulosic biomass. *Bioresour Technol.* 2009;100:10-18.
64. Narron RH, Kim H, Chang HM, Jameel H, Park S. Biomass pretreatments capable of enabling lignin valorization in a biorefinery process. *Curr Opin Biotechnol.* 2016;38:39-46.
65. Silveira MHL, Morais ARC, Da Costa Lopes AM, Oleksyszzen DN, Bogel-Łukasik R, Andreus J, Pereira Ramos L. Current pretreatment technologies for the development of cellulosic ethanol and biorefineries. *ChemSusChem.* 2015;8:3366-90.
66. Ulbricht R, Northup S, Thomas J. A review of 5-hydroxymethylfurfural (HMF) in parenteral solutions. *Fundam Appl Toxicol.* 1984;4:843-53.
67. Dunlop AP. Furfural Formation and Behavior. *Ind Eng Chem.* 1948;40:204-09.
68. Modig T, Lidén G, Taherzadeh MJ. Inhibition effects of furfural on alcohol dehydrogenase, aldehyde dehydrogenase and pyruvate dehydrogenase. *Biochem J.* 2002;363:769-76.
69. Banerjee N, Bhatnagar R, Viswanathan L. Inhibition of glycolysis by furfural in *Saccharomyces cerevisiae*. *Appl Microbiol Biotechnol.* 1981;11:226-28.
70. Sárvári Horváth I, Franzén CJ, Taherzadeh MJ, Niklasson C, Lidén G. Effects of furfural on the respiratory metabolism of *Saccharomyces cerevisiae* in glucose-limited chemostats. *Appl Environ Microbiol.* 2003;69:4076-86.
71. Almeida JRM, Modig T, Petersson A, Hähn-Hägerdal B, Lidén G, Gorwa-Grauslund MF. Increased tolerance and conversion of inhibitors in lignocellulosic hydrolysates by *Saccharomyces cerevisiae*. *J Chem Technol Biotechnol.* 2007;82:340-49.
72. Kumar R, Mago G, Balan V, Wyman CE. Physical and chemical characterizations of corn stover and poplar solids resulting from leading pretreatment technologies. *Bioresour Technol.* 2009;100:3948-62.
73. Lawther JM, Sun R, Banks WB. Fractional characterization of alkali-labile lignin and alkali-insoluble lignin from wheat straw. *Ind Crops Prod.* 1996;5:291-300.
74. Klinké HB, Ahring BK, Schmidt AS, Thomsen AB. Characterization of degradation products from alkaline wet oxidation of wheat straw. *Bioresour Technol.* 2002;82:15-26.
75. Larsson S, Quintana-Sainz A, Reimann A, Nilvebrant NO, Jonsson LJ. Influence of lignocellulose-derived aromatic compounds on oxygen-limited growth and ethanolic fermentation by *Saccharomyces cerevisiae*. *Appl Biochem Biotechnol.* 2000;84-86:617-32.
76. Adeboye PT, Bettiga M, Olsson L. The chemical nature of phenolic compounds determines their toxicity and induces distinct physiological responses in *Saccharomyces cerevisiae* in lignocellulose hydrolysates. *AMB Express.* 2014;4:46.
77. Klinké HB, Thomsen AB, Ahring BK. Inhibition of ethanol-producing yeast and bacteria by degradation products produced during pre-treatment of biomass. *Appl Microbiol Biotechnol.* 2004;66:10-26.
78. Jönsson LJ, Alriksson B, Nilvebrant NO. Bioconversion of lignocellulose: inhibitors and detoxification. *Biotechnol Biofuels.* 2013;6:16.
79. Casey E, Mosier NS, Adamec J, Stockdale Z, Ho N, Sedlak M. Effect of salts on the co-fermentation of glucose and xylose by a genetically engineered strain of *Saccharomyces cerevisiae*. *Biotechnol Biofuels.* 2013;6:83.
80. Taherzadeh MJ, Gustafsson L, Niklasson C, Lidén G. Conversion of furfural in aerobic and anaerobic batch fermentation of glucose by *Saccharomyces cerevisiae*. *J Biosci Bioeng.* 1999;87:169-74.
81. Liu ZL, Slininger PJ, Dien BS, Berhow MA, Kurtzman CP, Gorsich SW. Adaptive response of yeasts to furfural and 5-hydroxymethylfurfural and new chemical evidence for HMF conversion to 2,5-bis-hydroxymethylfuran. *J Ind Microbiol Biotechnol.* 2004;31:345-52.

82. Koppram R, Mapelli V, Albers E, Olsson L. The presence of pretreated lignocellulosic solids from birch during *Saccharomyces cerevisiae* fermentations leads to increased tolerance to inhibitors – a proteomic study of the effects. *PLoS ONE*. 2016;11:e0148635.
83. Sivers MV, Zacchi G, Olsson L, Hähn-Hägerdal B. Cost analysis of ethanol production from willow using recombinant *Escherichia coli*. *Biotechnol Prog*. 1994;10:555-60.
84. Palmqvist E, Hahn-Hägerdal B. Fermentation of lignocellulosic hydrolysates. I: inhibition and detoxification. *Bioresour Technol*. 2000;74:17-24.
85. Canilha L, Chandel AK, Suzane Dos Santos Milessi T, Antunes FAF, Luiz Da Costa Freitas W, Das Graças Almeida Felipe M, Da Silva SS. Bioconversion of sugarcane biomass into ethanol: An overview about composition, pretreatment methods, detoxification of hydrolysates, enzymatic saccharification, and ethanol fermentation. *J Biomed Biotechnol*. 2012.
86. Bailey J. Toward a science of metabolic engineering. *Science*. 1991;252:1668-75.
87. Kötter P, Ciriacy M. Xylose fermentation by *Saccharomyces cerevisiae*. *Appl Microbiol Biotechnol*. 1993;38:776-83.
88. Tantirungkij M, Nakashima N, Seki T, Yoshida T. Construction of xylose-assimilating *Saccharomyces cerevisiae*. *J Ferment Bioeng*. 1993;75:83-88.
89. Kuyper M, Winkler AA, van Dijken JP, Pronk JT. Minimal metabolic engineering of *Saccharomyces cerevisiae* for efficient anaerobic xylose fermentation: a proof of principle. *FEMS Yeast Res*. 2006;4:655-64.
90. Wisselink HW, Toirkens MJ, del Rosario Franco Berriel M, Winkler AA, van Dijken JP, Pronk JT, van Maris AJA. Engineering of *Saccharomyces cerevisiae* for efficient anaerobic alcoholic fermentation of L-arabinose. *Appl Environ Microbiol*. 2007;73:4881-91.
91. Becker J, Boles E. A modified *Saccharomyces cerevisiae* strain that consumes L-arabinose and produces ethanol. *Appl Environ Microbiol*. 2003;69:4144-50.
92. Kuyper M, Hartog MM, Toirkens MJ, Almering MJ, Winkler AA, van Dijken JP, Pronk JT. Metabolic engineering of a xylose-isomerase-expressing *Saccharomyces cerevisiae* strain for rapid anaerobic xylose fermentation. *FEMS Yeast Res*. 2005;5:399-409.
93. Wiedemann B, Boles E. Codon-optimized bacterial genes improve L-arabinose fermentation in recombinant *Saccharomyces cerevisiae*. *Appl Environ Microbiol*. 2008;74:2043-50.
94. Fonseca C, Olofsson K, Ferreira C, Runquist D, Fonseca LL, Hahn-Hägerdal B, Lidén G. The glucose/xylose facilitator Gxf1 from *Candida intermedia* expressed in a xylose-fermenting industrial strain of *Saccharomyces cerevisiae* increases xylose uptake in SSCF of wheat straw. *Enzyme Microb Technol*. 2011;48:518-25.
95. Subtil T, Boles E. Improving L-arabinose utilization of pentose fermenting *Saccharomyces cerevisiae* cells by heterologous expression of L-arabinose transporting sugar transporters. *Biotechnol Biofuels*. 2011;4:38.
96. Roca C, Nielsen J, Olsson L. Metabolic engineering of ammonium assimilation in xylose-fermenting *Saccharomyces cerevisiae* improves ethanol production. *Appl Environ Microbiol*. 2003;69:4732-36.
97. Watanabe S, Kodaki T, Makino K. Complete reversal of coenzyme specificity of xylitol dehydrogenase and increase of thermostability by the introduction of structural zinc. *J Biol Chem*. 2005;280:10340-49.
98. Yu KO, Kim SW, Han SO. Engineering of glycerol utilization pathway for ethanol production by *Saccharomyces cerevisiae*. *Bioresour Technol*. 2010;101:4157-61.
99. Ota M, Sakuragi H, Morisaka H, Kuroda K, Miyake H, Tamaru Y, Ueda M. Display of *Clostridium cellulovorans* xylose isomerase on the cell surface of *Saccharomyces cerevisiae* and its direct application to xylose fermentation. *Biotechnol Prog*. 2013;29:346-51.
100. Brat D, Boles E, Wiedemann B. Functional expression of a bacterial xylose isomerase in *Saccharomyces cerevisiae*. *Appl Environ Microbiol*. 2009;75:2304-11.

101. Ha S, Galazka JM, Rin Kim S, Choi J, Yang X, Seo J, Louise Glass N, Cate JHD, Jin Y-S. Engineered *Saccharomyces cerevisiae* capable of simultaneous cellobiose and xylose fermentation. *Proc Natl Acad Sci USA*. 2011;108:504-09.
102. Ilmén M, den Haan R, Brevnova E, McBride J, Wiswall E, Froehlich A, Koivula A, Voutilainen SP, Siika-aho M, la Grange DC, et al. High level secretion of cellobiohydrolases by *Saccharomyces cerevisiae*. *Biotechnol Biofuels*. 2011;4:30.
103. Sadie CJ, Rose SH, den Haan R, van Zyl WH. Co-expression of a cellobiose phosphorylase and lactose permease enables intracellular cellobiose utilisation by *Saccharomyces cerevisiae*. *Appl Microbiol Biotechnol*. 2011;90:1373-80.
104. Sauer U. Evolutionary engineering of industrially important microbial phenotypes. *Adv Biochem Eng Biotechnol*. 2001;73:129-69.
105. Demeke MM, Dietz H, Li Y, Foulquié-Moreno MR, Mutturi S, Deprez S, Den Abt T, Bonini BM, Liden G, Dumortier F. Development of a D-xylose fermenting and inhibitor tolerant industrial *Saccharomyces cerevisiae* strain with high performance in lignocellulose hydrolysates using metabolic and evolutionary engineering. *Biotechnol Biofuels*. 2013;6:89.
106. Garcia Sanchez R, Karhumaa K, Fonseca C, Sánchez Nogué V, Almeida JR, Larsson CU, Bengtsson O, Bettiga M, Hahn-Hägerdal B, Gorwa-Grauslund MF. Improved xylose and arabinose utilization by an industrial recombinant *Saccharomyces cerevisiae* strain using evolutionary engineering. *Biotechnol Biofuels*. 2010;3:13.
107. Kim SR, Skerker JM, Kang W, Lesmana A, Wei N, Arkin AP, Jin Y-S. Rational and evolutionary engineering approaches uncover a small set of genetic changes efficient for rapid xylose fermentation in *Saccharomyces cerevisiae*. *PLOS ONE*. 2013;8:e57048.
108. Kuyper M, Toirkens MJ, Diderich JA, Winkler AA, van Dijken JP, Pronk JT. Evolutionary engineering of mixed-sugar utilization by a xylose-fermenting *Saccharomyces cerevisiae* strain. *FEMS Yeast Res*. 2005;5:925-34.
109. Lee SM, Jellison T, Alper HS. Systematic and evolutionary engineering of a xylose isomerase-based pathway in *Saccharomyces cerevisiae* for efficient conversion yields. *Biotechnol Biofuels*. 2014;7:122.
110. Sonderegger M, Sauer U. Evolutionary engineering of *Saccharomyces cerevisiae* for anaerobic growth on xylose. *Appl Environ Microbiol*. 2003;69:1990-98.
111. Wisselink HW, Toirkens MJ, Wu Q, Pronk JT, van Maris AJA. Novel evolutionary engineering approach for accelerated utilization of glucose, xylose, and arabinose mixtures by engineered *Saccharomyces cerevisiae* strains. *Appl Environ Microbiol*. 2009;75:907-14.
112. Zhou H, Cheng J-S, Wang BL, Fink GR, Stephanopoulos G. Xylose isomerase overexpression along with engineering of the pentose phosphate pathway and evolutionary engineering enable rapid xylose utilization and ethanol production by *Saccharomyces cerevisiae*. *Metab Eng*. 2012;14:611-22.
113. Almario MP, Reyes LH, Kao KC. Evolutionary engineering of *Saccharomyces cerevisiae* for enhanced tolerance to hydrolysates of lignocellulosic biomass. *Biotechnol Bioeng*. 2013;110:2616-23.
114. González-Ramos D, Gorter De Vries AR, Grijseels SS, van Berkum MC, Swinnen S, van den Broek M, Nevoigt E, Daran J-MG, Pronk JT, van Maris AJA. A new laboratory evolution approach to select for constitutive acetic acid tolerance in *Saccharomyces cerevisiae* and identification of causal mutations. *Biotechnol Biofuels*. 2016;9.
115. Koppram R, Albers E, Olsson L. Evolutionary engineering strategies to enhance tolerance of xylose utilizing recombinant yeast to inhibitors derived from spruce biomass. *Biotechnol Biofuels*. 2012;5:32.
116. Smith J, van Rensburg E, Görgens JF. Simultaneously improving xylose fermentation and tolerance to lignocellulosic inhibitors through evolutionary engineering of recombinant *Saccharomyces cerevisiae* harbouring xylose isomerase. *BMC Biotechnol*. 2014;14:41.

117. Wright J, Bellissimi E, de Hulster E, Wagner A, Pronk JT, van Maris AJA. Batch and continuous culture-based selection strategies for acetic acid tolerance in xylose-fermenting *Saccharomyces cerevisiae*. *FEMS Yeast Res.* 2011;11:299-306.
118. Oud B, van Maris AJA, Daran J-MG, Pronk JT. Genome-wide analytical approaches for reverse metabolic engineering of industrially relevant phenotypes in yeast. *FEMS Yeast Res.* 2012;12:183-96.
119. Nijland JG, Shin HY, de Jong RM, De Waal PP, Klaassen P, Driessen AJ. Engineering of an endogenous hexose transporter into a specific D-xylose transporter facilitates glucose-xylose co-consumption in *Saccharomyces cerevisiae*. *Biotechnol Biofuels.* 2014;7:168.
120. Dos Santos LV, Carazzolle MF, Nagamatsu ST, Sampaio NMV, Almeida LD, Pirolla RAS, Borelli G, Corrêa TLR, Argueso JL, Pereira GAG. Unraveling the genetic basis of xylose consumption in engineered *Saccharomyces cerevisiae* strains. *Sci Rep.* 2016;6:38676.
121. Hou J, Jiao C, Peng B, Shen Y, Bao X. Mutation of a regulator Ask10p improves xylose isomerase activity through up-regulation of molecular chaperones in *Saccharomyces cerevisiae*. *Metab Eng.* 2016.
122. Pinel D, Colatrisano D, Jiang H, Lee H, Martin VJ. Deconstructing the genetic basis of spent sulphite liquor tolerance using deep sequencing of genome-shuffled yeast. *Biotechnol Biofuels.* 2015;8:53.
123. Liti G, Louis EJ. Advances in quantitative trait analysis in yeast. *PLoS Genet.* 2012;8:e1002912.
124. Wilkening S, Lin G, Fritsch ES, Tekkedil MM, Anders S, Kuehn R, Nguyen M, Aiyar RS, Proctor M, Sakhanenko NA, et al. An evaluation of high-throughput approaches to QTL mapping in *Saccharomyces cerevisiae*. *Genetics.* 2014;196:853-65.
125. Swinnen S, Schaerlaekens K, Pais T, Claesen J, Hubmann G, Yang Y, Demeke M, Foulquié-Moreno MR, Goovaerts A, Souvereyns K, et al. Identification of novel causative genes determining the complex trait of high ethanol tolerance in yeast using pooled-segregant whole-genome sequence analysis. *Genome Res.* 2012;22:975-84.
126. Sinha H, Nicholson BP, Steinmetz LM, McCusker JH. Complex genetic interactions in a quantitative trait locus. *PLOS Genet.* 2006;2:e13.
127. Hubmann G, Mathé L, Foulquié-Moreno MR, Duitama J, Nevoigt E, Thevelein JM. Identification of multiple interacting alleles conferring low glycerol and high ethanol yield in *Saccharomyces cerevisiae* ethanolic fermentation. *Biotechnol Biofuels.* 2013;6:87.
128. Marcheschi RJ, Gronenberg LS, Liao JC. Protein engineering for metabolic engineering: current and next-generation tools. *Biotechnol J.* 2013;8:545-55.
129. Li H, Schmitz O, Alper HS. Enabling glucose/xylose co-transport in yeast through the directed evolution of a sugar transporter. *Appl Microbiol Biotechnol.* 2016;100:10215-23.
130. Farwick A, Bruder S, Schadeweg V, Oreb M, Boles E. Engineering of yeast hexose transporters to transport D-xylose without inhibition by D-glucose. *Proc Natl Acad Sci USA.* 2014;111:5159-64.
131. Wang C, Bao X, Li Y, Jiao C, Hou J, Zhang Q, Zhang W, Liu W, Shen Y. Cloning and characterization of heterologous transporters in *Saccharomyces cerevisiae* and identification of important amino acids for xylose utilization. *Metab Eng.* 2015;30:79-88.
132. Reznicek O, Facey SJ, de Waal PP, Teunissen AWRH, de Bont JAM, Nijland JG, Driessen AJM, Hauer B. Improved xylose uptake in *Saccharomyces cerevisiae* due to directed evolution of galactose permease Gal2 for sugar co-consumption. *J Appl Microbiol.* 2015;119:99-111.
133. Shin HY, Nijland JG, de Waal PP, de Jong RM, Klaassen P, Driessen AJM. An engineered cryptic Hxt11 sugar transporter facilitates glucose-xylose co-consumption in *Saccharomyces cerevisiae*. *Biotechnol Biofuels.* 2015;8:176.
134. Young EM, Tong A, Bui H, Spofford C, Alper HS. Rewiring yeast sugar transporter preference through modifying a conserved protein motif. *Proc Natl Acad Sci USA.* 2014;111:131-36.

135. Nijland JG, Vos E, Shin HY, de Waal PP, Klaassen P, Driessen AJM. Improving pentose fermentation by preventing ubiquitination of hexose transporters in *Saccharomyces cerevisiae*. *Biotechnol Biofuels*. 2016;9:158.
136. Krahulec S, Klimacek M, Nidetzky B. Engineering of a matched pair of xylose reductase and xylitol dehydrogenase for xylose fermentation by *Saccharomyces cerevisiae*. *Biotechnol J*. 2009;4:684-94.
137. Petschacher B, Leitgeb S, Kavanagh Kathryn L, Wilson David K, Nidetzky B. The coenzyme specificity of *Candida tenuis* xylose reductase (*AKR2B5*) explored by site-directed mutagenesis and X-ray crystallography. *Biochem J*. 2005;385:75-83.
138. Petschacher B, Nidetzky B. Altering the coenzyme preference of xylose reductase to favor utilization of NADH enhances ethanol yield from xylose in a metabolically engineered strain of *Saccharomyces cerevisiae*. *Microb Cell Fact*. 2008;7:9.
139. Watanabe S, Abu Saleh A, Pack SP, Annaluru N, Kodaki T, Makino K. Ethanol production from xylose by recombinant *Saccharomyces cerevisiae* expressing protein-engineered NADH-preferring xylose reductase from *Pichia stipitis*. *Microbiology*. 2007;153:3044-54.
140. Lee SM, Jellison T, Alper HS. Directed Evolution of xylose isomerase for improved xylose catabolism and fermentation in the yeast *Saccharomyces cerevisiae*. *Appl Environ Microbiol*. 2012;78:5708-16.
141. Moon J, Liu ZL. Engineered NADH-dependent *GRE2* from *Saccharomyces cerevisiae* by directed enzyme evolution enhances HMF reduction using additional cofactor NADPH. *Enzyme Microb Technol*. 2012;50:115-20.
142. Sander JD, Joung JK. CRISPR-Cas systems for editing, regulating and targeting genomes. *Nat Biotech*. 2014;32:347-55.
143. DiCarlo JE, Norville JE, Mali P, Rios X, Aach J, Church GM. Genome engineering in *Saccharomyces cerevisiae* using CRISPR-Cas systems. *Nucleic Acids Res*. 2013:gkt135.
144. Mans R, van Rossum HM, Wijsman M, Backx A, Kuijpers NG, van den Broek M, Daran-Lapujade P, Pronk JT, van Maris AJA, Daran J-MG. CRISPR/Cas9: a molecular Swiss army knife for simultaneous introduction of multiple genetic modifications in *Saccharomyces cerevisiae*. *FEMS Yeast Res*. 2015;15::fov004.
145. Tsai C-S, Kong II, Lesmana A, Million G, Zhang G-C, Kim SR, Jin Y-S. Rapid and marker-free refactoring of xylose-fermenting yeast strains with Cas9/CRISPR. *Biotechnol Bioeng*. 2015;112:2406-11.
146. Shi S, Liang Y, Zhang MM, Ang EL, Zhao H. A highly efficient single-step, markerless strategy for multi-copy chromosomal integration of large biochemical pathways in *Saccharomyces cerevisiae*. *Metab Eng*. 2016;33:19-27.
147. Verhoeven MD, Lee M, Kamoen L, van den Broek M, Janssen DB, Daran J-MG, van Maris AJA, Pronk JT. Mutations in *PMR1* stimulate xylose isomerase activity and anaerobic growth on xylose of engineered *Saccharomyces cerevisiae* by influencing manganese homeostasis. *Sci Rep*. 2017;7:46155.
148. Stovicek V, Borodina I, Forster J. CRISPR-Cas system enables fast and simple genome editing of industrial *Saccharomyces cerevisiae* strains. *Metab Eng Commun*. 2015;2:13-22.
149. Van Rossum HM, Kozak BU, Niemeijer MS, Dykstra JC, Luttik MAH, Daran J-MG, van Maris AJA, Pronk JT. Requirements for carnitine shuttle-mediated translocation of mitochondrial acetyl moieties to the yeast cytosol. *mBio*. 2016;7.
150. Jeffries TW, Jin Y. Metabolic engineering for improved fermentation of pentoses by yeasts. *Appl Microbiol Biotechnol*. 2004;63:495-509.
151. van Maris AJA, Winkler AA, Kuyper M, De Laat WT, van Dijken JP, Pronk JT: Development of efficient xylose fermentation in *Saccharomyces cerevisiae*: xylose isomerase as a key component. In: *Biofuels*. Springer; 2007: 179-204.
152. Jeffries TW. Engineering yeasts for xylose metabolism. *Curr Opin Biotechnol*. 2006;17:320-26.

153. Runquist D, Hahn-Hägerdal B, Bettiga M. Increased ethanol productivity in xylose-utilizing *Saccharomyces cerevisiae* via a randomly mutagenized xylose reductase. *Appl Environ Microbiol.* 2010;76:7796-802.
154. Watanabe S, Saleh AA, Pack SP, Annaluru N, Kodaki T, Makino K. Ethanol production from xylose by recombinant *Saccharomyces cerevisiae* expressing protein-engineered NADH-preferring xylose reductase from *Pichia stipitis*. *Microbiology.* 2007;153:3044-54.
155. Sedlak M, Ho NW: Production of ethanol from cellulosic biomass hydrolysates using genetically engineered *Saccharomyces* yeast capable of cofermenting glucose and xylose. In *Proceedings of the Twenty-Fifth Symposium on Biotechnology for Fuels and Chemicals*; Breckenridge, CO. Springer; 2003: 403-16.
156. Wahlbom CF, Hahn-Hägerdal B. Furfural, 5-hydroxymethyl furfural, and acetoin act as external electron acceptors during anaerobic fermentation of xylose in recombinant *Saccharomyces cerevisiae*. *Biotechnol Bioeng.* 2002;78:172-78.
157. Moniruzzaman M, Dien B, Skory C, Chen Z, Hespell R, Ho N, Dale B, Bothast R. Fermentation of corn fibre sugars by an engineered xylose utilizing *Saccharomyces* yeast strain. *World J Microbiol Biotechnol.* 1997;13:341-46.
158. Katahira S, Mizuike A, Fukuda H, Kondo A. Ethanol fermentation from lignocellulosic hydrolysate by a recombinant xylose-and cellooligosaccharide-assimilating yeast strain. *Appl Microbiol Biotechnol.* 2006;72:1136-43.
159. Karhumaa K, Sanchez RG, Hahn-Hägerdal B, Gorwa-Grauslund MF. Comparison of the xylose reductase-xylitol dehydrogenase and the xylose isomerase pathways for xylose fermentation by recombinant *Saccharomyces cerevisiae*. *Microb Cell Fact.* 2007;6:5.
160. Harhangi HR, Akhmanova AS, Emmens R, van der Drift C, de Laat WT, van Dijken JP, Jetten MS, Pronk JT, den Camp HJO. Xylose metabolism in the anaerobic fungus *Piromyces* sp. strain E2 follows the bacterial pathway. *Arch Microbiol.* 2003;180:134-41.
161. Kuyper M, Hartog MM, Toirkens MJ, Almering MJ, Winkler AA, van Dijken JP, Pronk JT. Metabolic engineering of a xylose-isomerase-expressing *Saccharomyces cerevisiae* strain for rapid anaerobic xylose fermentation. *FEMS Yeast Res.* 2005;5:399-409.
162. Brat D, Boles E, Wiedemann B. Functional expression of a bacterial xylose isomerase in *Saccharomyces cerevisiae*. *Appl Environ Microb.* 2009;75:2304-11.
163. Dun B, Wang, Z., Ye, K., Zhang, B., Li, G., Lu, M. Functional expression of *Arabidopsis thaliana* xylose isomerase in *Saccharomyces cerevisiae*. *Xinjiang Agric Sci.* 2012;49:681-86.
164. Hector RE, Dien BS, Cotta MA, Mertens JA. Growth and fermentation of D-xylose by *Saccharomyces cerevisiae* expressing a novel D-xylose isomerase originating from the bacterium *Prevotella ruminicola* TC2-24. *Biotechnol Biofuels.* 2013;6:84.
165. Hou J, Shen Y, Jiao C, Ge R, Zhang X, Bao X. Characterization and evolution of xylose isomerase screened from the bovine rumen metagenome in *Saccharomyces cerevisiae*. *J Biosci Bioeng.* 2016;121:160-65.
166. Madhavan A, Tamalampudi S, Ushida K, Kanai D, Katahira S, Srivastava A, Fukuda H, Bisaria VS, Kondo A. Xylose isomerase from polycentric fungus *Orpinomyces*: gene sequencing, cloning, and expression in *Saccharomyces cerevisiae* for bioconversion of xylose to ethanol. *Appl Microbiol Biotechnol.* 2009;82:1067-78.
167. Demeke MM, Foulquié-Moreno MR, Dumortier F, Thevelein JM. Rapid evolution of recombinant *Saccharomyces cerevisiae* for xylose fermentation through formation of extra-chromosomal circular DNA. *PLOS Genet.* 2015;11:e1005010.
168. Crook N, Abatamarco J, Sun J, Wagner JM, Schmitz A, Alper HS. *In vivo* continuous evolution of genes and pathways in yeast. *Nat Commun.* 2016;7.
169. Verhoeven MD, Lee M, Kamoen L, van der Broek M, Janssen DB, Daran JM, van Maris AJA, Pronk JT. Mutations in *PMR1* stimulate xylose isomerase activity and anaerobic growth on xylose of engineered *Saccharomyces cerevisiae* by influencing manganese homeostasis. *Sci Rep.* 2017;7:46155.

170. Xia PF, Zhang GC, Liu JJ, Kwak S, Tsai CS, Kong II, Sung BH, Sohn JH, Wang SG, Jin YS. GroE chaperonins assisted functional expression of bacterial enzymes in *Saccharomyces cerevisiae*. *Biotechnol Bioeng*. 2016.
171. Van Vleet JH, Jeffries TW, Olsson L. Deleting the para-nitrophenyl phosphatase (pNPPase), *PHO13*, in recombinant *Saccharomyces cerevisiae* improves growth and ethanol production on D-xylose. *Metab Eng*. 2008;10:360-69.
172. Xu H, Kim S, Sorek H, Lee Y, Jeong D, Kim J, Oh EJ, Yun EJ, Wemmer DE, Kim KH. *PHO13* deletion-induced transcriptional activation prevents sedoheptulose accumulation during xylose metabolism in engineered *Saccharomyces cerevisiae*. *Metab Eng*. 2016;34:88-96.
173. Ni H, Laplaza JM, Jeffries TW. Transposon mutagenesis to improve the growth of recombinant *Saccharomyces cerevisiae* on D-xylose. *Appl Environ Microbiol*. 2007;73:2061-66.
174. Bamba T, Hasunuma T, Kondo A. Disruption of *PHO13* improves ethanol production via the xylose isomerase pathway. *Amb Express*. 2016;6:4.
175. Sato TK, Tremaine M, Parreiras LS, Hebert AS, Myers KS, Higbee AJ, Sardi M, McIlwain SJ, Ong IM, Breuer RJ. Directed evolution reveals unexpected epistatic interactions that alter metabolic regulation and enable anaerobic xylose use by *Saccharomyces cerevisiae*. *PLOS Genet*. 2016;12:e1006372.
176. Dos Santos LV, Carazzolle MF, Nagamatsu ST, Sampaio NMV, Almeida LD, Pirolla RAS, Borelli G, Corrêa TLR, Argueso JL, Pereira GAG. Unraveling the genetic basis of xylose consumption in engineered *Saccharomyces cerevisiae* strains. *Sci Rep*. 2016;6.
177. Lee N, Gielow W, Martin R, Hamilton E, Fowler A. The organization of the *araBAD* operon of *Escherichia coli*. *Gene*. 1986;47:231-44.
178. Bettiga M, Hahn-Hägerdal B, Gorwa-Grauslund MF. Comparing the xylose reductase/xylitol dehydrogenase and xylose isomerase pathways in arabinose and xylose fermenting *Saccharomyces cerevisiae* strains. *Biotechnol Biofuels*. 2008;1:16.
179. Kou S, Christensen MS, Cirillo VP. Galactose transport in *Saccharomyces cerevisiae* II. Characteristics of galactose uptake and exchange in galactokinaseless cells. *J Bacteriol*. 1970;103:671-78.
180. Subtil T, Boles E. Competition between pentoses and glucose during uptake and catabolism in recombinant *Saccharomyces cerevisiae*. *Biotechnol Biofuels*. 2012;5:1.
181. Wisselink HW, Cipollina C, Oud B, Crimi B, Heijnen JJ, Pronk JT, van Maris AJA. Metabolome, transcriptome and metabolic flux analysis of arabinose fermentation by engineered *Saccharomyces cerevisiae*. *Metab Eng*. 2010;12:537-51.
182. Hamacher T, Becker J, Gárdonyi M, Hahn-Hägerdal B, Boles E. Characterization of the xylose-transporting properties of yeast hexose transporters and their influence on xylose utilization. *Microbiology*. 2002;148:2783-88.
183. Lee W, Kim M, Ryu Y, Bisson L, Seo J. Kinetic studies on glucose and xylose transport in *Saccharomyces cerevisiae*. *Appl Microbiol Biotechnol*. 2002;60:186-91.
184. Saloheimo A, Rauta J, Stasyk V, Sibirny AA, Penttilä M, Ruohonen L. Xylose transport studies with xylose-utilizing *Saccharomyces cerevisiae* strains expressing heterologous and homologous permeases. *Appl Microbiol Biotechnol*. 2007;74:1041-52.
185. Reifenberger E, Boles E, Ciriacy M. Kinetic characterization of individual hexose transporters of *Saccharomyces cerevisiae* and their relation to the triggering mechanisms of glucose repression. *Eur J Biochem*. 1997;245:324-33.
186. Diderich JA, Schepper M, van Hoek P, Luttk MA, van Dijken JP, Pronk JT, Klaassen P, Boelens HF, de Mattos MJT, van Dam K. Glucose uptake kinetics and transcription of *HXT* genes in chemostat cultures of *Saccharomyces cerevisiae*. *J Biol Chem*. 1999;274:15350-59.
187. Horak J, Regelman J, Wolf DH. Two distinct proteolytic systems responsible for glucose-induced degradation of fructose-1,6-bisphosphatase and the Gal2p transporter in the yeast *Saccharomyces cerevisiae* share the same protein components of the glucose signaling pathway. *J Biol Chem*. 2002;277:8248-54.

188. Horak J, Wolf DH. Catabolite inactivation of the galactose transporter in the yeast *Saccharomyces cerevisiae*: ubiquitination, endocytosis, and degradation in the vacuole. *J Bacteriol.* 1997;179:1541-49.
189. Sedlak M, Ho NW. Characterization of the effectiveness of hexose transporters for transporting xylose during glucose and xylose co-fermentation by a recombinant *Saccharomyces* yeast. *Yeast.* 2004;21:671-84.
190. Demeke MM, Dumortier F, Li Y, Broeckx T, Foulquié-Moreno MR, Thevelein JM. Combining inhibitor tolerance and D-xylose fermentation in industrial *Saccharomyces cerevisiae* for efficient lignocellulose-based bioethanol production. *Biotechnol Biofuels.* 2013;6:120.
191. Ask M, Bettiga M, Duraiswamy VR, Olsson L. Pulsed addition of HMF and furfural to batch-grown xylose-utilizing *Saccharomyces cerevisiae* results in different physiological responses in glucose and xylose consumption phase. *Biotechnol Biofuels.* 2013;6:181.
192. Bellissimi E, van Dijken JP, Pronk JT, van Maris AJA. Effects of acetic acid on the kinetics of xylose fermentation by an engineered, xylose-isomerase-based *Saccharomyces cerevisiae* strain. *FEMS Yeast Res.* 2009;9:358-64.
193. Kim SR, Ha S-J, Wei N, Oh EJ, Jin Y-S. Simultaneous co-fermentation of mixed sugars: a promising strategy for producing cellulosic ethanol. *Trends Biotechnol.* 2012;30:274-82.
194. Moysés DN, Reis VCB, de Almeida JRMM, Lidia Maria Pepe de, Torres FAG. Xylose fermentation by *Saccharomyces cerevisiae*: challenges and prospects. *Int J Mol Sci.* 2016;17:207.
195. Sanchez RG, Karhumaa K, Fonseca C, Nogué VS, Almeida JR, Larsson CU, Bengtsson O, Bettiga M, Hahn-Hägerdal B, Gorwa-Grauslund MF. Improved xylose and arabinose utilization by an industrial recombinant *Saccharomyces cerevisiae* strain using evolutionary engineering. *Biotechnol Biofuels.* 2010;3:1.
196. Shin H, Nijland J, de Waal P, de Jong R, Klaassen P, Driessen AJ. An engineered cryptic Hxt11 sugar transporter facilitates glucose-xylose co-consumption in *Saccharomyces cerevisiae*. *Biotechnol Biofuels.* 2015;8:176.
197. Wisselink HW, van Maris AJA, Pronk JT, Klaassen P, De Jong RM: Polypeptides with permease activity. US Patent 9034608 B2. 2015.
198. Reznicek O, Facey SJ, Waal P, Teunissen AW, Bont J, Nijland JG, Driessen AJ, Hauer B. Improved xylose uptake in *Saccharomyces cerevisiae* due to directed evolution of galactose permease Gal2 for sugar co-consumption. *J Appl Microbiol.* 2015.
199. Runquist D, Hahn-Hägerdal B, Rådström P. Comparison of heterologous xylose transporters in recombinant *Saccharomyces cerevisiae*. *Biotechnol Biofuels.* 2010;3:1.
200. Weierstall T, Hollenberg CP, Boles E. Cloning and characterization of three genes (*SUT1-3*) encoding glucose transporters of the yeast *Pichia stipitis*. *Mol Microbiol.* 1999;31:871-83.
201. Young EM, Comer AD, Huang H, Alper HS. A molecular transporter engineering approach to improving xylose catabolism in *Saccharomyces cerevisiae*. *Metab Eng.* 2012;14:401-11.
202. Colabardini AC, Ries LNA, Brown NA, Dos Reis TF, Savoldi M, Goldman MHS, Menino JF, Rodrigues F, Goldman GH. Functional characterization of a xylose transporter in *Aspergillus nidulans*. *Biotechnol Biofuels.* 2014;7:1.
203. Du J, Li S, Zhao H. Discovery and characterization of novel D-xylose-specific transporters from *Neurospora crassa* and *Pichia stipitis*. *Mol Biosyst.* 2010;6:2150-56.
204. Ferreira D, Nobre A, Silva ML, Faria-Oliveira F, Tulha J, Ferreira C, Lucas C. *XYLH* encodes a xylose/H⁺ symporter from the highly related yeast species *Debaryomyces fabryi* and *Debaryomyces hansenii*. *FEMS Yeast Res.* 2013;13:585-96.
205. Katahira S, Ito M, Takema H, Fujita Y, Tanino T, Tanaka T, Fukuda H, Kondo A. Improvement of ethanol productivity during xylose and glucose co-fermentation by xylose-assimilating *S. cerevisiae* via expression of glucose transporter Sut1. *Enzyme Microb Technol.* 2008;43:115-19.
206. Knoshaug EP, Vidgren V, Magalhães F, Jarvis EE, Franden MA, Zhang M, Singh A. Novel transporters from *Kluyveromyces marxianus* and *Pichia guilliermondii* expressed in

- Saccharomyces cerevisiae* enable growth on L-arabinose and D-xylose. *Yeast*. 2015;32:615-28.
207. Leandro MJ, Gonçalves P, Spencer-Martins I. Two glucose/xylose transporter genes from the yeast *Candida intermedia*: first molecular characterization of a yeast xylose-H⁺ symporter. *Biochem J*. 2006;395:543-49.
208. Li J, Xu J, Cai P, Wang B, Ma Y, Benz JP, Tian C. Functional analysis of two L-arabinose transporters from filamentous fungi reveals promising characteristics for improved pentose utilization in *Saccharomyces cerevisiae*. *Appl Environ Microbiol*. 2015;81:4062-70.
209. Reis TF, Lima PBA, Parachin NS, Mingossi FB, Oliveira JVC, Ries LNA, Goldman GH. Identification and characterization of putative xylose and cellobiose transporters in *Aspergillus nidulans*. *Biotechnol Biofuels*. 2016;9:204.
210. Wang M, Yu C, Zhao H. Directed evolution of xylose specific transporters to facilitate glucose-xylose co-utilization. *Biotechnol Bioeng*. 2016;113:484-91.
211. Lewis Liu Z, Moon J, Andersh BJ, Slininger PJ, Weber S. Multiple gene-mediated NAD(P)H-dependent aldehyde reduction is a mechanism of *in situ* detoxification of furfural and 5-hydroxymethylfurfural by *Saccharomyces cerevisiae*. *Appl Microbiol Biotechnol*. 2008;81:743-53.
212. Almeida JRM, Bertilsson M, Hahn-Hägerdal B, Lidén G, Gorwa-Grauslund M-F. Carbon fluxes of xylose-consuming *Saccharomyces cerevisiae* strains are affected differently by NADH and NADPH usage in HMF reduction. *Appl Microbiol Biotechnol*. 2009;84:751-61.
213. Jeppsson M, Johansson B, Jensen PR, Hahn-Hägerdal B, Gorwa-Grauslund MF. The level of glucose-6-phosphate dehydrogenase activity strongly influences xylose fermentation and inhibitor sensitivity in recombinant *Saccharomyces cerevisiae* strains. *Yeast*. 2003;20:1263-72.
214. Adeboye PT, Bettiga M, Olsson L. *ALD5*, *PAD1*, *ATF1* and *ATF2* facilitate the catabolism of coniferyl aldehyde, ferulic acid and p-coumaric acid in *Saccharomyces cerevisiae*. *Sci Rep*. 2017;7:42635.
215. Liu ZL. Molecular mechanisms of yeast tolerance and *in situ* detoxification of lignocellulose hydrolysates. *Appl Microbiol Biotechnol*. 2011;90:809-25.
216. Li BZ, Yuan YJ. Transcriptome shifts in response to furfural and acetic acid in *Saccharomyces cerevisiae*. *Appl Microbiol Biotechnol*. 2010;86:1915-24.
217. Mira NP, Palma M, Guerreiro JF, Sá-Correia I. Genome-wide identification of *Saccharomyces cerevisiae* genes required for tolerance to acetic acid. *Microb Cell Fact*. 2010;9:79.
218. Abbott DA, Knijnenburg TA, de Poorter LMI, Reinders MJT, Pronk JT, van Maris AJA. Generic and specific transcriptional responses to different weak organic acids in anaerobic chemostat cultures of *Saccharomyces cerevisiae*. *FEMS Yeast Res*. 2007;7:819-33.
219. Guo Z, Olsson L. Physiological response of *Saccharomyces cerevisiae* to weak acids present in lignocellulosic hydrolysate. *FEMS Yeast Res*. 2014;14:1234-48.
220. Chen Y, Sheng J, Jiang T, Stevens J, Feng X, Wei N. Transcriptional profiling reveals molecular basis and novel genetic targets for improved resistance to multiple fermentation inhibitors in *Saccharomyces cerevisiae*. *Biotechnol Biofuels*. 2016;9.
221. González-Ramos D, Gorter de Vries AR, Grijseels SS, Berkum MC, Swinnen S, Broek M, Nevoigt E, Daran J-MG, Pronk JT, van Maris AJA. A new laboratory evolution approach to select for constitutive acetic acid tolerance in *Saccharomyces cerevisiae* and identification of causal mutations. *Biotechnol Biofuels*. 2016;9:1.
222. Thompson OA, Hawkins GM, Gorsich SW, Doran-Peterson J. Phenotypic characterization and comparative transcriptomics of evolved *Saccharomyces cerevisiae* strains with improved tolerance to lignocellulosic derived inhibitors. *Biotechnol Biofuels*. 2016;9.
223. Wright J, Bellissimi E, de Hulster E, Wagner A, Pronk JT, van Maris AJA. Batch and continuous culture-based selection strategies for acetic acid tolerance in xylose-fermenting *Saccharomyces cerevisiae*. *FEMS Yeast Res*. 2011;11:299-306.

224. Swinnen S, Fernández-Niño M, González-Ramos D, van Maris AJA, Nevoigt E. The fraction of cells that resume growth after acetic acid addition is a strain-dependent parameter of acetic acid tolerance in *Saccharomyces cerevisiae*. *FEMS Yeast Res.* 2014;14:642-53.
225. Field SJ, Ryden P, Wilson D, James SA, Roberts IN, Richardson DJ, Waldron KW, Clarke TA. Identification of furfural resistant strains of *Saccharomyces cerevisiae* and *Saccharomyces paradoxus* from a collection of environmental and industrial isolates. *Biotechnol Biofuels.* 2015;8.
226. Favaro L, Basaglia M, Trento A, Van Rensburg E, García-Aparicio M, Van Zyl WH, Casella S. Exploring grape marc as trove for new thermotolerant and inhibitor-tolerant *Saccharomyces cerevisiae* strains for second-generation bioethanol production. *Biotechnol Biofuels.* 2013;6:168.
227. Wimalasena TT, Greetham D, Marvin ME, Liti G, Chandelia Y, Hart A, Louis EJ, Phister TG, Tucker GA, Smart KA. Phenotypic characterisation of *Saccharomyces spp.* yeast for tolerance to stresses encountered during fermentation of lignocellulosic residues to produce bioethanol. *Microb Cell Fact.* 2014;13:47.
228. Wisselink HW, Toirkens MJ, Wu Q, Pronk JT, van Maris AJA. Novel evolutionary engineering approach for accelerated utilization of glucose, xylose, and arabinose mixtures by engineered *Saccharomyces cerevisiae* strains. *Appl Environ Microbiol.* 2009;75:907-14.
229. Costa CE, Romaní A, Cunha JT, Johansson B, Domingues L. Integrated approach for selecting efficient *Saccharomyces cerevisiae* for industrial lignocellulosic fermentations: Importance of yeast chassis linked to process conditions. *Bioresour Technol.* 2017;227:24-34.
230. Li H, Shen Y, Wu M, Hou J, Jiao C, Li Z, Liu X, Bao X. Engineering a wild-type diploid *Saccharomyces cerevisiae* strain for second-generation bioethanol production. *Bioresour Bioprocess.* 2016;3:51.
231. Basso LC, De Amorim HV, De Oliveira AJ, Lopes ML. Yeast selection for fuel ethanol production in Brazil. *FEMS Yeast Res.* 2008;8:1155-63.
232. Della-Bianca BE, de Hulster E, Pronk JT, van Maris AJA, Gombert AK. Physiology of the fuel ethanol strain *Saccharomyces cerevisiae* PE-2 at low pH indicates a context-dependent performance relevant for industrial applications. *FEMS Yeast Res.* 2014;14:1196-205.
233. Gorter De Vries AR, Pronk JT, Daran J-MG. Industrial relevance of chromosomal copy number variation in *Saccharomyces* yeasts. *Appl Environ Microbiol.* 2017;83:e03206-16.
234. Zhang K, Zhang L-J, Fang Y-H, Jin X-N, Qi L, Wu X-C, Zheng D-Q. Genomic structural variation contributes to phenotypic change of industrial bioethanol yeast *Saccharomyces cerevisiae*. *FEMS Yeast Res.* 2016;16:fov118.
235. Hahn-Hägerdal B, Karhumaa K, Fonseca C, Spencer-Martins I, Gorwa-Grauslund MF. Towards industrial pentose-fermenting yeast strains. *Appl Microbiol Biotechnol.* 2007;74:937-53.
236. Pronk JT. Auxotrophic yeast strains in fundamental and applied research. *Appl Environ Microbiol.* 2002;68:2095-100.
237. Karim AS, Curran KA, Alper HS. Characterization of plasmid burden and copy number in *Saccharomyces cerevisiae* for optimization of metabolic engineering applications. *FEMS Yeast Res.* 2013;13:107-16.
238. Wang BL, Ghaderi A, Zhou H, Agresti J, Weitz DA, Fink GR, Stephanopoulos G. Microfluidic high-throughput culturing of single cells for selection based on extracellular metabolite production or consumption. *Nat Biotechnol.* 2014;32:473-78.
239. Snoek T, Nicolino MP, van den Breemt S, Mertens S, Saels V, Verplaetse A, Steensels J, Verstrepen KJ. Large-scale robot-assisted genome shuffling yields industrial *Saccharomyces cerevisiae* yeasts with increased ethanol tolerance. *Biotechnol Biofuels.* 2015;8:32.
240. Jacques KA, Lyons TP, Kelsall DR: *The alcohol textbook: a reference for the beverage, fuel and industrial alcohol industries.* Nottingham University Press; 2003.

241. Nielsen F, Tomás-Pejó E, Olsson L, Wallberg O. Short-term adaptation during propagation improves the performance of xylose-fermenting *Saccharomyces cerevisiae* in simultaneous saccharification and co-fermentation. *Biotechnol Biofuels*. 2015;8:1.
242. Alkasrawi M, Rudolf A, Lidén G, Zacchi G. Influence of strain and cultivation procedure on the performance of simultaneous saccharification and fermentation of steam pretreated spruce. *Enzyme Microb Technol*. 2006;38:279-86.
243. Sánchez i Nogué V, Narayanan V, Gorwa-Grauslund MF. Short-term adaptation improves the fermentation performance of *Saccharomyces cerevisiae* in the presence of acetic acid at low pH. *Appl Microbiol Biotechnol*. 2013;97:7517-25.
244. Narendranath NV, Lewis SM: Systems and methods for yeast propagation. US Patent 9034631 B2. 2013.
245. Steiner G: Use of ethanol plant by-products for yeast propagation. US Patent 8183022 B2. 2008.
246. Yuan WJ, Chang BL, Ren JG, Liu JP, Bai FW, Li YY. Consolidated bioprocessing strategy for ethanol production from Jerusalem artichoke tubers by *Kluyveromyces marxianus* under high gravity conditions. *J Appl Microbiol*. 2012;112:38-44.
247. Ryabova OB, Chmil OM, Sibirny AA. Xylose and cellobiose fermentation to ethanol by the thermotolerant methylotrophic yeast *Hansenula polymorpha*. *FEMS Yeast Res*. 2003;4:157-64.
248. Goshima T, Tsuji M, Inoue H, Yano S, Hoshino T, Matsushika A. Bioethanol production from lignocellulosic biomass by a novel *Kluyveromyces marxianus* strain. *Biosci Biotechnol Biochem*. 2013;77:1505-10.
249. Radecka D, Mukherjee V, Mateo RQ, Stojiljkovic M, Foulquié-Moreno MR, Thevelein JM. Looking beyond *Saccharomyces*: the potential of non-conventional yeast species for desirable traits in bioethanol fermentation. *FEMS Yeast Res*. 2015;15:fov053.
250. Caspeta L, Chen Y, Ghiaci P, Feizi A, Buskov S, Hallström BM, Petranovic D, Nielsen J. Altered sterol composition renders yeast thermotolerant. *Science*. 2014;346:75-78.
251. Fletcher E, Feizi A, Bisschops MMM, Hallström BM, Khoomrung S, Siewers V, Nielsen J. Evolutionary engineering reveals divergent paths when yeast is adapted to different acidic environments. *Metab Eng*. 2017;39:19-28.
252. Van Maris AJA, Abbott DA, Bellissimi E, van den Brink J, Kuyper M, Luttik MAH, Wisselink HW, Scheffers WA, van Dijken JP, Pronk JT. Alcoholic fermentation of carbon sources in biomass hydrolysates by *Saccharomyces cerevisiae*: current status. *Antonie Van Leeuwenhoek*. 2006;90:391-418.
253. Yang F, Hanna MA, Sun R. Value-added uses for crude glycerol-a byproduct of biodiesel production. *Biotechnol Biofuels*. 2012;5:13.
254. De Bont JAM, Teunissen AWRH, Klaassen P, Hartman WWA, van Beusekom S: Yeast strains engineered to produce ethanol from acetic acid and glycerol. US Patent 20150176032 A1. 2012.
255. Klaassen P, Hartman WWA: Glycerol and acetic acid converting yeast cells with improved acetic acid conversion. US Patent 20160208291 A1. 2014.
256. Kumar D, Singh V. Dry-grind processing using amylase corn and superior yeast to reduce the exogenous enzyme requirements in bioethanol production. *Biotechnol Biofuels*. 2016;9:228.
257. Katahira S, Fujita Y, Mizuike A, Fukuda H, Kondo A. Construction of a xylan-fermenting yeast strain through codisplay of xylanolytic enzymes on the surface of xylose-utilizing *Saccharomyces cerevisiae* cells. *Appl Environ Microbiol*. 2004;70:5407-14.
258. Lee JH, Heo S-Y, Lee J-W, Yoon K-H, Kim Y-H, Nam S-W. Thermostability and xylan-hydrolyzing property of endoxylanase expressed in yeast *Saccharomyces cerevisiae*. *Biotechnol Bioprocess Eng*. 2009;14:639-44.
259. La Grange DC, Pretorius IS, Claeysens M, Van Zyl WH. Degradation of xylan to D-xylose by recombinant *Saccharomyces cerevisiae* coexpressing the *Aspergillus niger* β -xylosidase

(*xlnD*) and the *Trichoderma reesei* xylanase II (*xyn2*) genes. *Appl Environ Microbiol.* 2001;67:5512-19.

Chapter 2

Optimizing anaerobic growth rate and fermentation kinetics in *Saccharomyces cerevisiae* strains expressing Calvin-cycle enzymes for improved ethanol yield

Ioannis Papapetridis, Maaïke Goudriaan, Maria Vazquez-Vitali, Nikita A. de Keijzer, Marcel van den Broek, Antonius J.A. van Maris and Jack T. Pronk

Essentially as published in *Biotechnology for Biofuels* 2018 11:17
(<https://doi.org/10.1186/s13068-017-1001-z>)

Abstract

Reduction or elimination of by-product formation is of immediate economic relevance in fermentation processes for industrial bioethanol production with the yeast *Saccharomyces cerevisiae*. Anaerobic cultures of wild-type *S. cerevisiae* require formation of glycerol to maintain the intracellular NADH/NAD⁺ balance. Previously, functional expression of the Calvin-cycle enzymes ribulose-1,5-bisphosphate carboxylase (RuBisCO) and phosphoribulokinase (PRK) in *S. cerevisiae* was shown to enable reoxidation of NADH with CO₂ as electron acceptor. In slow-growing cultures, this engineering strategy strongly decreased glycerol yield, while increasing the ethanol yield on sugar. The present study explores engineering strategies to improve rates of growth and alcoholic fermentation in yeast strains that functionally express RuBisCO and PRK, while maximizing the positive impact on the ethanol yield. Multi-copy integration of a bacterial-RuBisCO expression cassette was combined with expression of the *E. coli* GroEL/GroES chaperones and expression of PRK from the anaerobically inducible *DAN1* promoter. In anaerobic, glucose-grown bioreactor batch cultures, the resulting *S. cerevisiae* strain showed a 31% lower glycerol yield and a 31% lower specific growth rate than a non-engineered reference strain. Growth of the engineered strain in anaerobic, glucose-limited chemostat cultures revealed a negative correlation between its specific growth rate and the contribution of the Calvin-cycle enzymes to redox homeostasis. Additional deletion of *GPD2*, which encodes an isoenzyme of NAD⁺-dependent glycerol-3-phosphate dehydrogenase, combined with overexpression of the structural genes for enzymes of the non-oxidative pentose-phosphate pathway, yielded a CO₂-reducing strain that grew at the same rate as a non-engineered reference strain in anaerobic bioreactor batch cultures, while exhibiting a 86% lower glycerol yield and a 15% higher ethanol yield. The metabolic engineering strategy presented here enables an almost complete elimination of glycerol production in anaerobic, glucose-grown batch cultures of *S. cerevisiae*, with an associated increase in ethanol yield, while retaining near wild-type growth rates and a capacity for glycerol formation under osmotic stress. Using current genome-editing techniques, the required genetic modifications can be introduced in one or a few

transformations. Evaluation of this concept in industrial strains and conditions is therefore a realistic next step towards its implementation for improving the efficiency of first- and second-generation bioethanol production.

2.1 Introduction

Transport fuels derived from microbial fermentation combine compatibility with current combustion-engine technology with the potential to achieve lower carbon footprints than those of petrochemistry-derived fuels [1]. Bioethanol, the biofuel with the highest current global production volume (ca. 100 billion liters in 2015 [2]), is almost exclusively made via the fermentation of sugars by the yeast *Saccharomyces cerevisiae* [3, 4]. First-generation bioethanol processes, which mainly use hydrolysed corn starch or sucrose from sugar cane as feedstocks, reach high ethanol productivities and yields [5]. For example, sugar-cane based bioethanol production in Brazil often approaches 92% of the theoretical maximum of $0.51 \text{ g g}_{\text{hexose}}^{-1}$ [6]. Since the feedstock is the largest cost contributor in first-generation industrial ethanol production [7], even modest improvements in ethanol yield can significantly improve process economics.

Carbon losses during anaerobic bioethanol production result from the formation of biomass, CO_2 , and by-products, with glycerol formation requiring up to 4% of the sugar substrate in industrial processes [2, 8]. Glycerol plays multiple roles in the physiology of *S. cerevisiae*. While sugar dissimilation via the enzymes of glycolysis and alcoholic fermentation is redox-neutral, yeast cells still need to reoxidize an 'excess' of NADH formed in biosynthetic reactions [9, 10]. In anaerobic cultures, which cannot reoxidize NADH by respiration, this essential role is fulfilled by NADH-dependent reduction of dihydroxyacetone-phosphate to glycerol-3-phosphate (catalysed by the isoenzymes Gpd1 and Gpd2), followed by its dephosphorylation to glycerol (catalysed by the isoenzymes Gpp1 and Gpp2) [9, 10]. Glycerol-3P, an intermediate in this pathway, also provides the glycerol backbone of glycerolipids [11, 12]. This role of glycerol-3P is, however, non-essential, since glycerolipids can also be formed from dihydroxyacetone-phosphate via the reactions catalysed by dihydroxyacetone-phosphate

acyltransferase and 1-acylglycerol-3-phosphate acyltransferase [12]. Furthermore, glycerol has been identified as the major compatible solute in osmotically stressed, glucose-grown *S. cerevisiae* cultures [13, 14]. In contrast, trehalose has recently been reported to be the predominant compatible solute in ethanol-grown cultures [15].

In *S. cerevisiae*, *GPD1* is up-regulated under osmotic stress, while *GPD2* is up-regulated during anaerobiosis [16-19]. Despite their differential regulation, complete elimination of glycerol production requires deletion of both genes. Anaerobic growth of *Gpd⁻* strains requires addition of external electron acceptors such as acetoin, which can be reduced to 2,3-butanediol [19]. Additionally, acetate-dependent anaerobic growth of *gpd1Δ gpd2Δ S. cerevisiae* strains has been demonstrated in strains expressing an engineered pathway for NADH-linked reduction of acetate to ethanol [20]. When the decreased osmotolerance of these strains is addressed by evolutionary or targeted metabolic engineering [21, 22], this acetate reduction strategy is particularly attractive for ethanol production from lignocellulosic hydrolysates, in which acetic acid is a ubiquitous inhibitor of yeast performance [23, 24].

Several strategies have been explored to decrease glycerol production by *S. cerevisiae* in first-generation bioethanol processes, including redox engineering of ammonium assimilation [8], expression of a non-phosphorylating, NADP⁺-dependent glyceraldehyde-3-phosphate dehydrogenase [25] and reduction of biomass yields by forcing increased ATP turnover, e.g. by addition of weak organic acids to bioreactors [26, 27]. While resulting in significantly reduced glycerol yields in laboratory cultures, these strategies also led to reduced growth rates and/or depended on specific growth conditions.

In a previous study, our group functionally expressed the Calvin-cycle enzymes phosphoribulokinase (PRK) and ribulose-1,5-bisphosphate carboxylase/oxygenase (RuBisCO) in *S. cerevisiae*, thereby enabling the use of CO₂ as alternative electron acceptor for reoxidation of cytosolic NADH [28]. Together, these enzymes convert one mol of the pentose-phosphate-pathway intermediate ribulose-5-phosphate and one mol of CO₂ into two moles of 3-phosphoglycerate, thus bypassing NADH formation in glycolysis. Since CO₂ is abundantly present

in fermenting yeast cultures, implementation of this strategy is not limited by the composition of industrial media. Co-expression of a plant PRK gene (*Spinacia oleracea prk*), a bacterial RuBisCO gene (*Thiobacillus denitrificans cbbm*), and the *Escherichia coli* chaperone genes *groEL* and *groES* yielded a *S. cerevisiae* strain that displayed a 90% decrease in glycerol yield in anaerobic glucose/galactose-grown chemostat cultures and a 60% decrease in glycerol yield in anaerobic galactose-grown batch cultures [28]. These results were obtained without deletion of *GPD1* or *GPD2*, indicating that, especially in the chemostat cultures, NADH oxidation enabled by expression of the RuBisCO/PRK pathway could compete efficiently with the native glycerol pathway for NADH oxidation. Retaining a low background capacity for glycerol production is attractive for industrial application in view of its positive impact on osmotolerance [22]. The proof-of-principle strain described in our earlier paper required galactose as a carbon source to induce gene expression, which led to low specific growth rates in batch cultures [28]. Moreover, its different performance in batch and chemostat cultures indicated that further analysis and optimization of this redox-engineering strategy is required before implementation in industry can be considered.

The goal of the present study was to investigate and address requirements for efficient carbon dioxide reduction via heterologously expressed Calvin-cycle enzymes in fast-growing anaerobic batch cultures on glucose. To this end, we used CRISPR-Cas9-mediated genome editing for integration of constitutively expressed gene cassettes for RuBisCO and PRK in the yeast genome. The performance of the constructed strains was quantitatively analysed in anaerobic glucose-limited chemostats and batch cultures. Based on the results of these analyses, additional metabolic engineering steps were implemented, yielding *S. cerevisiae* strains that displayed the full benefit of glycerol yield reduction and ethanol yield improvement in anaerobic, glucose-grown batch cultures growing at near-wild-type specific growth rates.

2.2 Methods

2.2.1 Maintenance of strains

All yeast strains used in this study (Table 1) originate from the CEN.PK lineage of *S. cerevisiae* strains [29, 30]. Cultures were propagated in synthetic medium [31] supplemented with 20 g L⁻¹ glucose. Uracil (0.14 g L⁻¹) was added when auxotrophic strains were propagated. *E. coli XL-1* blue stock cultures were grown in LB medium (5 g L⁻¹ Bacto yeast extract, 10 g L⁻¹ Bacto tryptone, 5 g L⁻¹ NaCl), supplemented with 100 µg mL⁻¹ ampicillin or 50 µg mL⁻¹ kanamycin. Frozen stocks were prepared by addition of glycerol (30% v/v final concentration) to growing cultures and subsequent storage at -80 °C.

2.2.2 Plasmid and cassette construction

All plasmids used in this study are listed in Table 2. CRISPR/Cas9-based genome editing was used to perform genetic modifications in all constructed strains [32]. Unique CRISPR/Cas9 sequences targeting *GPD2*, *SGA1* or X-2 were identified using a publicly available list [32]. A list of all primers and oligonucleotides used in this study is given in Additional File 1. Phusion High Fidelity DNA Polymerase (Thermo-Scientific, Waltham, MA) was used for PCR amplification of plasmids and expression cassettes in all cases, according to the manufacturer's guidelines.

Table 1. *S. cerevisiae* strains used in this study.

Strain name	Relevant Genotype	Parental strain	Origin
CEN.PK113-5D	<i>MATa ura3-52</i>	-	[29]
CEN.PK122	<i>MATa/MATα</i>	-	[29]
IMX585	<i>MATa URA3 can1::cas9-natNT2</i>	CEN.PK113-7D	[34]
IMX581	<i>MATa ura3-52 can1::cas9-natNT2</i>	CEN.PK113-5D	[34]
IMX673	<i>MATa/MATα ura3-52/ura3-52 CAN1/can1Δ::cas9-natNT2</i>	CEN.PK115	[34]
IME324	<i>MATa ura3-52 can1::cas9-natNT2 p426-TEF</i> (empty)	IMX581	[22]
IMX765*	<i>MATa/MATa ura3-52/ura3-52 can1::cas9-natNT2/can1::cas9-natNT2 sga1::cbbM</i> (9 copies), <i>groES, groEL</i>	IMX581	This study
IMX773	<i>MATa/MATa ura3-52/ura3-52 can1::cas9-natNT2/can1::cas9-natNT2 sga1::cbbM</i> (9 copies), <i>groES, groEL X-2::pYEN1-prk/X-2::pYEN1-prk pUDR164</i>	IMX765	This study
IMX774	<i>MATa/MATa ura3-52/ura3-52 can1::cas9-natNT2/can1::cbbM</i> (9 copies), <i>groES, groEL X-2::pDANI-prk/X-2::pDANI-prk pUDR164</i>	IMX765	This study
IMX949	<i>MATa/MATa ura3-52/ura3-52 can1::cas9-natNT2/can1::cbbM</i> (9 copies), <i>groES, groEL X-2::pDANI-prk/X-2::pDANI-prk gpd2Δ/gpd2Δ pROS10-gRNA.GPD2</i>	IMX774	This study
IMX1443	<i>MATa/MATa ura3-52/ura3-52 can1::cas9-natNT2/can1::cbbM</i> (9 copies), <i>groES, groEL X-2::pDANI-prk/X-2::pDANI-prk gpd2::pTDH3-RPE1, pPGK1-TKL1, pTEFI-TALL, pPGI1-NQM1, pTPII-RK11, pPYK1-TKL2/gpd2::pTDH3-RPE1, pPGK1-TKL1, pTEFI-TALL, pPGI1-NQM1, pTPII-RK11, pPYK1-TKL2 pUDR164</i>	IMX774	This study
IME369	<i>MATa/MATα ura3-52/ura3-52 CAN1/can1Δ::cas9-natNT2 p426-TEF</i> (empty)	IMX673	This study
IMX1472	<i>MATa ura3-52 can1::cas9-natNT2 gpd2::pTDH3-RPE1, pPGK1-TKL1, pTEFI-TALL, pPGI1-NQM1, pTPII-RK11, pPYK1-TKL2 pROS11-gRNA.GPD2</i>	IMX581	This study
IMX1489	<i>MATa ura3-52 can1::cas9-natNT2 gpd2::pTDH3-RPE1, pPGK1-TKL1, pTEFI-TALL, pPGI1-NQM1, pTPII-RK11, pPYK1-TKL2 sga1::pDANI-prk cbbM</i> (9 copies), <i>groES, groEL pUDR103</i>	IMX1472	This study

* indicates spontaneous diploidization; see Results section.

Table 2. Plasmids used in this study.

Name	Characteristics	Origin
p426-TEF	2 μ m ori, <i>URA3</i> , p <i>TEF1-tCYC1</i> empty vector	[38]
pMEL10	2 μ m ori, <i>KIURA3</i> , p <i>SNR52-gRNA.CAN1-tSUP4</i>	[34]
pMEL11	2 μ m ori, <i>amdS</i> , p <i>SNR52-gRNA.CAN1-tSUP4</i>	[34]
pROS10	<i>URA3</i> , gRNA. <i>CAN1-2</i> μ m ori-gRNA. <i>ADE2</i>	[34]
pROS11	<i>amdS</i> , gRNA. <i>CAN1-2</i> μ m ori-gRNA. <i>ADE2</i>	[34]
pUD232	Delivery vector, p <i>TEF1-groEL-tACT1</i>	[28]
pUD233	Delivery vector, p <i>TPI1-groES-tPGI1</i>	[28]
pUDE046	2 μ m ori, p <i>GAL1-prk-tCYC1</i>	[28]
pBTWW002	2 μ m ori, <i>URA3</i> , p <i>TDH3-cbbM-tCYC1</i>	[28]
pUD344	p <i>PGI1-NQM1-tNQM1</i> PCR template vector	[48]
pUD345	p <i>TPI1-RKI1-tRKI1</i> PCR template vector	[48]
pUD346	p <i>PYK1-TKL2-tTKL2</i> PCR template vector	[48]
pUD347	p <i>TDH3-RPE1-tRPE1</i> PCR template vector	[48]
pUD348	p <i>PGK1-TKL1-tTKL1</i> PCR template vector	[48]
pUD349	p <i>TEF1-TAL1-tTAL1</i> PCR template vector	[48]
pUDR103	2 μ m ori, <i>KIURA3</i> , p <i>SNR52-gRNA.SGA1-tSUP4</i>	[22]
pUDR119	2 μ m ori, <i>amdS</i> , p <i>SNR52-gRNA.SGA1-tSUP4</i>	This study
pUDR164	2 μ m ori, <i>KIURA3</i> , p <i>SNR52-gRNA.X-2-tSUP4</i>	This study
pJET-cbbM	PCR template vector for <i>cbbM</i> amplification	This study

For markerless genomic integration of gene cassettes, plasmids expressing unique gRNAs targeting the *SGA1* locus or the intergenic region X-2 [33] were constructed. The plasmid backbones of puDR119 and pURD164 were obtained by PCR amplification using the primer combination 5792-5980 and plasmids pMEL11 and pMEL10 [34], respectively, as templates. The plasmid inserts of pUDR119 and pUDR164, containing the expression cassettes coding for the unique 20-bp gRNA sequences targeting *SGA1* and X-2 respectively, were obtained by PCR amplification using the primer combinations 5979-7023 for *SGA1*, 5979-7374 for X-2, and plasmids pMEL11 and pMEL10, respectively, as templates. The assembly of plasmids pUDR119 and pUDR164 was performed *in vitro* using the Gibson Assembly Cloning kit (New England Biolabs, Ipswich, MA) following the supplier's guidelines. The assembly was enabled by homologous sequences present at the 5' and 3' ends of the PCR-amplified plasmid backbones and inserts. In each case, 1 μ l of the Gibson-assembly mix was used for *E. coli* XL-1 blue transformation by electroporation, performed in a Gene PulserXcell Electroporation System (Biorad, Hercules, CA). Correct assembly of plasmids was confirmed by diagnostic PCR

(Dreamtaq, Thermo-Scientific) or restriction digestion. The constructed plasmids pUDR119 and pUDR164 were isolated from transformed *E. coli* cultures using a Sigma GenElute Plasmid kit (Sigma-Aldrich, St. Louis, MO) and used in transformations of *S. cerevisiae*.

For markerless deletion of *GPD2*, the plasmid backbone of pROS10 (*URA3* marker) or pROS11 (*amdS* marker) was PCR amplified using primer combination 5793-5793 (double-binding). The plasmid insert, containing the expression cassette coding for the unique 20-bp gRNA sequence targeting *GPD2*, was obtained using primer combination 6966-6966 (double binding) and plasmid pROS10 as template.

A yeast codon-optimized cassette for *T. denitrificans cbbm* overexpression [28] was obtained by PCR amplification using plasmid pBTWW002 as template and primer combination 7549-7550. The resulting fragment was ligated to a pJET/1.2 blunt vector (Thermo-Scientific) following the supplier's protocol and cloned to *E. coli*. The resulting plasmid was used as PCR template to generate *cbbm* integration cassettes, using primer combinations 11206-6285, 6280-6273, 6281-6270, 6282-6271, 6284-6272, 6283-6275, 6287-6276, 6288-6277, 6289-7075. The overexpression cassettes of *cbbm* (pTDH3-*cbbm*-tCYC1) were genetically identical, except for different overhangs present at the 5' and 3' ends of the fragments to allow for *in vivo* homologous recombination. Codon-optimized yeast expression cassettes of *groEL* (pTEF1-*groEL*-tACT1) and *groES* (pTPI1-*groES*-tPGI1) were obtained using plasmids pUD232 and pUD233 as templates and primer combinations 7076-7077 and 7078-7079 respectively.

The genomic sequence corresponding to the constitutive promoter of *YEN1* [35] was obtained by PCR amplification with primer combination 7933-7295 and genomic DNA of IMX585 as template. The genomic sequence of the anaerobically-inducible promoter of *DAN1* [35] was obtained by PCR amplification with primer combinations 7930-7931 (integration at X-2) and 7978-7931 (integration at *SGA1*), using genomic DNA of IMX585 as template. The terminator sequence of *PGK1* was obtained by PCR amplification using primer combinations 7084-7934 (integration at X-2) and 7084-11205 (integration at *SGA1*), using genomic DNA of IMX585 as template.

The *S. oleracea* *prk*-ORF was obtained by PCR amplification using primer combinations 7297-7081 (p*YEN1-prk* cassette construction), 7932-7081 (p*DAN1-prk* cassette construction), and plasmid pUDE046 as template. The various primer combinations resulted in *prk*-ORF fragments with homologous overhangs to the different promoter sequences and the terminator sequence of *PGK1*. The complete expression cassettes (p*YEN1-prk-tPGK1* and p*DAN1-prk-tPGK1*) were assembled by *in vivo* homologous recombination after transformation to yeast and correct assembly was verified by diagnostic PCR and Sanger sequencing (Baseclear, Leiden, The Netherlands).

An integration cassette for *RPE1* overexpression (p*TDH3-RPE1-tRPE1*) was PCR amplified using primer combination 11593-3290 and pUD347 as a template. Similarly, integration cassettes for overexpression of *TKL1* (p*PGK1-TKL1-tTKL1*), *TAL1* (p*TEF1-TAL1-tTAL1*), *NQM1* (p*PGI1-NQM1-tNQM1*), *RKI1* (p*TPI1-RKI1-tRKI1*) and *TKL2* (p*PYK1-TKL2-tTKL2*) were obtained by PCR amplification using primer combinations 5909-4068, 3274-3275, 3847-3276, 4691-3277, and 3283-11595, respectively, with plasmids pUD348, pUD349, pUD344, pUD345, and pUD346, respectively, as templates. The integration cassettes included overhang sequences to allow for *in vivo* assembly of overexpression cassettes of the complete non-oxidative pentose-phosphate pathway and integration at the *GPD2* locus.

2.2.3 Yeast genome editing and strain construction

The lithium-acetate transformation protocol [36] was used for yeast transformations. Transformation mixtures were plated on synthetic medium agar plates [31] (2% Bacto Agar, BD, Franklin Lakes, NJ), supplemented with 20 g L⁻¹ glucose (final concentration) in the case of transformations with plasmids expressing the *URA3* marker. In transformations with plasmids expressing the *amdS* marker, agar plates were prepared as described previously [37]. Confirmation of the desired genotypes in each case was performed by diagnostic colony PCR using Dreamtaq polymerase (Thermo-Scientific), according to manufacturer's guidelines (Additional File 1). Counter-selection of plasmids expressing *URA3* was performed using 5-

fluoro-orotic acid (Zymo Research, Irvine, CA), following the supplier's guidelines. Counter-selection of plasmids expressing *amdS* was performed as described previously [12].

Co-transformation and chromosomal integration of pUDR119, 9 copies of the *cbm* expression cassette and single copies of the expression cassettes of *groEL* and *groES* to IMX581 (after plasmid recycling from the correct mutant) yielded the RuBisCO-expressing strain IMX765. Overhangs present at the 5' and 3' ends of the molecules allowed for *in vivo* assembly of the entire construct (11 fragments) and for integration at the *SGA1* locus.

Co-transformation of the *pYEN1* and *pDAN1* sequences, respectively, the *prk*-ORF and the *tPGK1* fragments, along with plasmid pUDR164 to strain IMX765 yielded strains IMX773 and IMX774. For construction of strain IMX949, in which *GPD2* was deleted, the two fragments of the gRNA-expressing plasmid (pROS10 backbone) and the repair oligo-nucleotides 6969-6970 were co-transformed to IMX774 (after recycling of pUDR164). For construction of strain IMX1443, in which *GPD2* was deleted and the genes of the non-oxidative branch of the pentose-phosphate pathway were overexpressed, the two fragments of the gRNA-expressing plasmid (pROS11 backbone), along with the integration cassettes *pTDH3-RPE1-tRPE1*, *pPGK1-TKL1-tTKL1*, *pTEF1-TAL1-tTAL1*, *pPGI1-NQM1-tNQM1*, *pTPI1-RK11-tRK11* and *pPYK1-TKL2-tTKL2*, were co-transformed to IMX774. The entire construct (6 fragments) was assembled *in vivo* and integrated at the *GPD2* locus. Before stocking of strain IMX1443, the *GPD2*-targeting CRISPR plasmid was recycled by counter-selection against its *amdS* marker [12].

Co-transformation of the two fragments of the *GPD2*-targeting CRISPR plasmid (pROS11 backbone) and the non-oxidative pentose-phosphate pathway integration cassettes to strain IMX581 yielded strain IMX1472. The RuBisCO/PRK-expressing strain IMX1489 was obtained by co-transformation of pUDR103, the *pDAN1*, *prk*-ORF, *tPGK1* sequences, 9 copies of the expression cassette of *cbm* and the expression cassettes of *groEL* and *groES* (14 fragments) to strain IMX1472 (integration at the *SGA1* locus, *GPD2*-targeting CRISPR plasmid recycled). The reference strains IME324 and IME369 were obtained by transformation of p426-*TEF* (empty) [38] to strains IMX581 and IMX673, respectively.

2.2.4 Bioreactor cultivation

Physiological characterization of *S. cerevisiae* strains was performed in anaerobic batch and chemostat cultures in 2-L bioreactors (Applikon, Delft, The Netherlands), with 1-L working volume. Salt solutions were sterilized by autoclaving at 120 °C for 20 min.

Glucose solutions were autoclaved separately at 110 °C for 20 min and subsequently added to the sterile salt solutions. All cultures were grown on synthetic medium with vitamins [31], supplemented with 20 g L⁻¹ glucose and with sterile solutions of the anaerobic growth factors ergosterol (10 mg L⁻¹) and Tween 80 (420 mg L⁻¹), as well as with 0.2 g L⁻¹ sterile antifoam C (Sigma-Aldrich). Anaerobic conditions were maintained by sparging of a gas mixture of N₂/CO₂ (90%/10%, <10 ppm oxygen) at a rate of 0.5 L min⁻¹ and culture pH was maintained at 5 by automatic addition of 2 M KOH. All cultures were grown at a stirrer speed of 800 rpm and at a temperature of 30 °C. Oxygen diffusion in the bioreactors was minimized by equipping them with Norprene tubing and Viton O-rings, and evaporation was minimized by cooling of outlet gas to 4 °C.

To generate bioreactor inocula, two pre-culture shake flasks were grown in 500-mL flasks containing 100 mL synthetic medium (20 g L⁻¹ glucose). Initial pH was adjusted to 6 by addition of KOH. Cultures were grown, under an air atmosphere, at 30 °C and shaken at 200 rpm. In each case, initial pre-culture flasks were inoculated from frozen *S. cerevisiae* stock cultures. After incubation for 8-12 h, cultures from these flasks were used to inoculate fresh pre-culture flasks for bioreactor inoculum propagation. In all cases, bioreactors were inoculated when pre-cultures reached mid-exponential phase (OD₆₆₀ 4-5), to a starting OD₆₆₀ of 0.15-0.25.

2.2.5 Analytical methods

Off-gas analysis, biomass dry weight measurements, HPLC analysis of culture supernatants and correction for ethanol evaporation in bioreactor experiments were performed as described previously [20]. Optical density was determined at 660 nm, using a Libra S11 spectrophotometer (Biochrom, Cambridge, United Kingdom). In batch cultures, yields of products were calculated from samples taken at mid-exponential phase (minimum of five

samples), as described previously [39]. Biomass and product yields in chemostat cultures were determined from residual glucose, biomass and metabolite concentrations in steady-state cultures, analysed after rapid quenching of culture samples [40].

For calculation of the degree of reduction (electron) balances in cultures, the degrees of reduction of biomass, CO₂, NH₄⁺ and extracellular metabolites (glucose, ethanol, glycerol, succinate, pyruvate, lactate, acetate) were defined as described in [41].

Calculations of statistical significance of differences in yields between strains were determined with two-tailed Student's *t*-tests. All values are represented as averages ± mean deviation of independent biological replicate cultures, performed at least in duplicate.

2.2.6 Enzyme-activity assays

For *in vitro* enzyme activity assays of PRK [28], cells (65 mL culture volume) from exponentially growing (OD₆₆₀ 4), anaerobic shake-flask cultures (100 mL working volume in 500 mL conical shake-flasks) on glucose synthetic medium were harvested and cell extracts were prepared as described previously [42]. The harvesting and sonication buffer contained 100 mM Tris-HCl, 20 mM MgCl₂·6H₂O and 5 mM 1,4-dithiothreitol (pH 8.2). The assay mixture [43] contained 50 mM Tris-HCl (pH 8.2), 40 mM KCl, 10 mM MgCl₂·6H₂O, 0.15 mM NADH, 1 mM ATP, 3 mM phosphoenolpyruvate, 1 mM 1,4-dithiothreitol, 5 U of pyruvate kinase (EC 2.7.1.40, Sigma-Aldrich), 6 U of L-lactate dehydrogenase (EC 1.1.1.27, Honeywell Fluka, Bucharest, Romania) and 20, 30, 40 or 50 µL cell extract in 1 mL total volume. Reactions were started by addition of D-ribulose-5-phosphate (2.5 mM final concentration) and PRK activity was measured at 30 °C using a Hitachi 100-60 spectrophotometer, by monitoring of NADH oxidation at 340 nm over time. Protein concentrations in cell extracts were quantified with the Lowry method [44].

2.2.7 Protein extraction and proteomics analysis

For proteomics analysis, 5 mL were harvested from mid-exponential-phase (OD₆₆₀ 2), anaerobic shake-flask cultures on synthetic medium (20 g L⁻¹ glucose or 20 g L⁻¹ galactose), washed with ice-cold MilliQ H₂O, and subsequently stored at -80 °C. Frozen cells were lysed using mechanical disruption in a Precellys-24 homogeniser (Bertin Technologies, Montigny-le-

Bretonneux, France) in 0.5 mL cold methanol (-20 °C, Sigma-Aldrich). The protein concentration of the disrupted cell suspension was measured using a Qubit 2.0 fluorometer (Thermo-Scientific). A total of 250 µg protein was taken from each methanol suspension and 10 µg bovine-serum albumin was spiked to all samples for quality control. Proteins were extracted from the disrupted cell suspension using chloroform (Sigma-Aldrich) and 20% TCA (Sigma-Aldrich). The obtained protein pellet was dissolved in 100 mM NH₄HCO₃ buffer (pH 7) to a final concentration of 0.5 g L⁻¹. In each sample, 5 µl of 500 mM Tris-(2-carboxyethyl)phosphine hydrochloride solution (TCEP, Sigma-Aldrich) was added, and samples were incubated at 55 °C for 30 min to facilitate disulfide reduction. Alkylation was performed through the addition of 5 µl of 550 mM iodoacetamide and subsequent incubation at 25 °C in the dark for 30 min.

Proteolysis was carried out overnight at 37 °C with Trypsin Gold (Promega, WI, USA), which specifically cleaves C-terminally at lysine and arginine, at an enzyme to substrate ratio of 1:25. Gradient elution of peptides was performed on a C18 (Acquity UPLC CSH C18 Column, 130 Å, 1.7 µm, 2.1 mm X 100 mm, Ultimate 3000) (Thermo-Scientific). 20 µL of injected peptides were separated using a gradient ratio of mobile phase A (99.9% water and 0.1% formic acid; VWR) to 20% B (99.9% acetonitrile and 0.1% formic acid; VWR) for 20 min, and to 50% B for 30 min (60 min total duration).

Data acquisition was carried out using a data-dependent method using a Q Exactive Plus mass spectrometer (Thermo-Scientific). The top 15 precursors were selected for tandem-MS/MS (MS2) analysis after higher-energy collisional dissociation (HCD) fragmentation. Full MS scans covering a mass range of 400 to 1600 were acquired at a resolution of 70000 (at m/z 200), with a maximum fill time of 75 ms, and an automatic gain control (AGC) target value of 3·10⁶. MS2 scans were acquired at a resolution of 17500 (at m/z 200), with a maximum fill time of 75 ms, and an AGC target value of 10⁵. An isolation window of 2 m/z with a fixed first mass of 110 m/z was applied in all experiments. HCD fragmentation was induced with a normalized collision energy of 27 for all peptides. Charge-state exclusion was set to ignore unassigned 1 charge. Isotope exclusion was enabled and peptide match was preferred.

All LC-MS/MS results were searched against the *S. cerevisiae* protein database, to which the amino acid sequences of the heterologous introduced enzymes (PRK, CbbM, GroEL, GroES) were manually added, in Proteome Discoverer 1.4 Sequest HT (Thermo-Scientific). The cleavage preference of trypsin was selected, allowing for up to 2 missed cleavages (C-Term K/R restrict P). Dynamic modifications were set to carbamidomethyl (C), deamidation (N/Q) and oxidation (M). Precursor mass tolerance was set to 10 ppm and fragment mass tolerance 0.6 Da. Following peptide identification, their q-values were calculated based on a target decoy approach with a 1% false discovery rate.

2.2.8 Spot plate assay

Spot plates on synthetic medium (pH 6) were prepared as described previously [45]. Sterile solutions of glucose (180 g L⁻¹) and of the anaerobic growth factors ergosterol (10 mg L⁻¹) and Tween 80 (420 mg L⁻¹) were additionally supplemented. All plates were inoculated with serial dilutions of exponentially growing shake-flask cultures in sterile demineralized water, prepared as described above. Plates were incubated under anaerobic conditions (10% CO₂) at 30 °C for 48 h.

2.2.9 Ploidy determination by flow cytometry

For determination of yeast ploidy, ca. 10⁷ cells were harvested from mid-exponential phase shake-flask cultures on synthetic medium (20 g L⁻¹ glucose), washed twice with demineralized water and stored in 70% ethanol at 4 °C. Sample preparation and staining was performed as described previously [46]. Samples were processed using a BD Accuri C6 flow-cytometer (BD Biosciences, San Jose, CA) and analysed using the FlowJo software package (Flowjo LLC, Ashland, OR).

2.2.10 Genome sequencing

DNA was isolated from yeast cells harvested from shake-flask cultures of strain IMX774 on synthetic medium (20 g L⁻¹ glucose) using a Qiagen Blood & Cell Culture DNA kit (Qiagen, Germantown, MD), following manufacturer's specifications. Paired-end sequencing (22 mln reads) was performed on a 350-bp PCR-free insert library using an Illumina HiSeq PE150

sequencer (Novogene Company Limited, Hong Kong) with a sample size of 3.3 Gb, accounting for a total coverage of 275x. Sequence data was mapped to the CEN.PK113-7D genome [30], to which the sequences of the *pDAN1-prk-tPGK1*, *pTDH3-cbbm-tCYC1*, *pTEF1-groEL-tACT1*, and *pTPI1-groES-tPGI1* cassettes were manually added. Data processing and chromosome copy number analysis were carried out as described previously [47-51].

2.3 Results

2.3.1 Impact of PRK expression levels on *in vivo* CO₂ reduction via the RuBisCO pathway in glucose-grown batch cultures

In the engineered strain used for the first demonstration of the effect of expression of the Calvin-cycle enzymes RuBisCO and PRK on the anaerobic physiology of *S. cerevisiae*, the coding sequence of *S. oleracea prk* was placed under the control of the galactose-inducible *GAL1* promoter [28]. Use of galactose as an inducer of gene expression in *S. cerevisiae* is, however, not a realistic option in large-scale industrial fermentations for ethanol production due to the price of galactose and repression of the *GAL1* promoter by glucose [52]. Furthermore, this strain expressed the *T. denitrificans* RuBisCO gene *cbbm*, as well as the *E. coli* chaperones *groEL/groES*, from a centromeric plasmid. Expression from plasmids with auxotrophic markers limits applicability in industrial processes [53] and the use of a centromeric vector restricted the number of *cbbm*-cassettes per cell to 1-2 [54]. The low RuBisCO activity in cell extracts of strain IMU033 (4.6 ± 0.3 nmol (mg protein)⁻¹ min⁻¹) [28] suggested that introduction of additional copies of the *cbbm* cassette might be relevant for improved strain performance.

In vivo tandem assembly by homologous recombination and CRISPR-mediated targeted integration at a single locus was previously shown to be an effective way to introduce multiple copies of expression cassettes without the use of multi-copy plasmids [48, 55]. To construct a galactose-independent RuBisCO-expressing platform strain with an increased number of *cbbm* cassettes, 9 copies of the *cbbm* overexpression cassette, along with single expression cassettes of *groEL/groES*, were first integrated at the *SGA1* locus of IMX581 using CRISPR/Cas9 single-step transformation and assembly [34], yielding strain IMX765. Since high-level expression of

heterologous PRK in microbes has been previously shown to be toxic [56, 57], two expression cassettes were constructed, in which the *prk* open reading frame was either placed under the control of *pYEN1* (low-level constitutive expression under a wide range of cultivation conditions, [35]) or under the control of *pDAN1* (medium-level expression induced under anaerobic conditions, [35]). These expression cassettes were integrated at the X-2 locus [33] of strain IMX765, yielding strains IMX773 and IMX774 respectively.

Enzyme-activity assays in cell extracts of anaerobic, glucose-grown shake-flask cultures of strains IMX773 and IMX774 showed PRK activities of 0.14 ± 0.01 and 0.68 ± 0.33 $\mu\text{mol (mg protein)}^{-1} \text{ min}^{-1}$ respectively. These activities were 100-fold and 20-fold lower than previously measured in cell extracts of strain IMU033 under galactose-induced conditions (14.4 ± 1.5 $\mu\text{mol (mg protein)}^{-1} \text{ min}^{-1}$) [28]. Analysis of protein abundance of RuBisCO and PRK in strains IMU033 (*pGAL1-prk cbbm*) and IMX774 revealed 10-fold higher CbbM levels and 9-fold lower PRK levels in the latter, newly engineered strain (Figure 1).

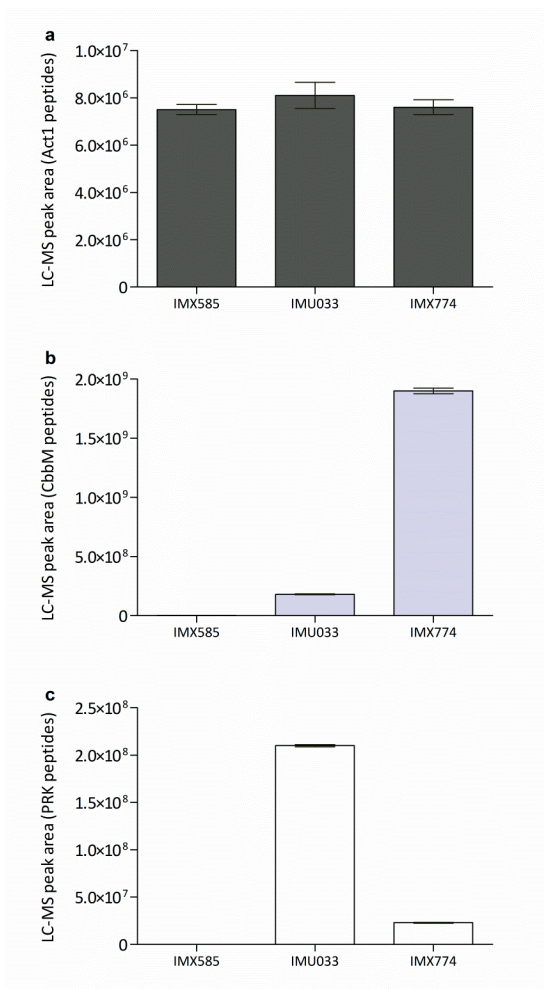


Figure 1. Peptide abundance in cells harvested from mid-exponential anaerobic shake-flask cultures of strains IMX585 (CEN.PK reference), IMU033 (*pGAL1-prk cbbm*), and IMX774 (*pDAN1-prk cbbm*), displayed as the sum of LC-MS peak areas of unique peptides identified per protein. A: Act1 (internal control); B: CbbM; C: PRK. Cultures of IMX585 and IMX774 were grown on 20 g L⁻¹ glucose (initial pH 6); cultures of IMU033 were grown on 20 g L⁻¹ galactose (initial pH 6). Values represent averages ± mean deviations of measurements on independent duplicate cultures.

To investigate the effect of PRK and RuBisCO expression on the physiology of glucose-grown *S. cerevisiae*, growth and metabolite formation of strains IME324 (congenic reference strain not expressing Calvin-cycle enzymes or *E. coli* chaperones), IMX773 (*pYEN1-prk cbbm*) and IMX774 (*pDAN1-prk cbbm*) were analysed in anaerobic bioreactor batch cultures on 20 g L⁻¹ glucose (Table 3; Additional File 2). In these cultures, the maximum specific growth rates of strains IMX773 and IMX774 were 13% and 31% lower, respectively, than that of the reference strain IME324 (Table 3). A lower specific growth rate of the engineered *S. cerevisiae* strains overexpressing PRK, RuBisCO and GroEL/GroES might reflect a metabolic burden resulting from increased protein synthesis (Figure 1) [58]. This interpretation is consistent with the

observation that biomass yields on glucose of strains IMX774 and IME324 were the same, even though stoichiometric analyses predicted that use of the RuBisCO/PRK pathway can lead to an up to 13.5% higher biomass yield [28]. Comparison of PRK activities in cell extracts and specific growth rates (Table 3) of strains IMX773 and IMX774 suggested that, in particular, high-level expression of PRK might have negatively affected the specific growth rate. Toxicity of high-level PRK expression is consistent with observations on galactose-grown cultures of *S. cerevisiae* IMU033 (p*GAL1-prk cbbm*) [28] and on PRK overexpression in *E. coli* [56, 57].

Table 3. Specific growth rate (μ), yields (Y) of biomass, ethanol and glycerol on glucose and stoichiometric relationships between glycerol production and biomass formation in anaerobic bioreactor batch cultures of *S. cerevisiae* strains carrying different genetic modifications. Cultures were grown on synthetic medium containing 20 g L⁻¹ glucose (pH 5). Specific growth rates and stoichiometries were calculated from multiple sample points in the mid-exponential growth phase. Values represent averages \pm mean deviations of measurements on independent cultures. Cultures of IME324, IMX949, and IMX1443 were performed in triplicate. Cultures of IMX774 were performed in quadruplicate and cultures of IMX773 were performed in duplicate. * ($p < 0.05$) and ** ($p < 0.01$) denote statistical significance of value differences between IME324 and each engineered strain in Student's *t*-tests. Degree of reduction balances constructed over the exponential growth phase yielded electron recoveries between 96% and 101%.

Strain	IME324	IMX773	IMX774	IMX949	IMX1443
Relevant Genotype	<i>GPD1 GPD2</i>	<i>GPD1 GPD2 pYEN1-prk cbbm</i>	<i>GPD1 GPD2 pDANI-prk cbbm</i>	<i>GPD1 gpd2Δ pDANI-prk cbbm</i>	<i>GPD1 gpd2Δ pDANI-prk cbbm non-ox PPPT</i>
μ (h⁻¹)	0.32 \pm 0.02	0.28 \pm 0.01 *	0.22 \pm 0.02 **	0.22 \pm 0.01 **	0.30 \pm 0.01
Y biomass/glucose (g g⁻¹)	0.090 \pm 0.002	0.089 \pm 0.001	0.087 \pm 0.004	0.095 \pm 0.004	0.099 \pm 0.005 *
Y ethanol/glucose (g g⁻¹)	0.364 \pm 0.015	0.385 \pm 0.002	0.400 \pm 0.006 **	0.411 \pm 0.002 **	0.419 \pm 0.001 **
Y glycerol/glucose (g g⁻¹)	0.101 \pm 0.003	0.098 \pm 0.000	0.070 \pm 0.005 **	0.038 \pm 0.001 **	0.013 \pm 0.000 **
Glycerol produced/biomass (mmol (g biomass)⁻¹)	12.239 \pm 0.095	11.880 \pm 0.008 *	7.622 \pm 0.409 **	4.314 \pm 0.245 **	1.507 \pm 0.119 **

Strain IMX773, in which *prk* was expressed from the weak constitutive *YEN1* promoter, did not show significant differences in glycerol or ethanol yields relative to the reference strain IME324 (Table 3). This result confirms that functional expression of PRK is essential for the use of CO₂ as an electron acceptor for NADH oxidation by the engineered *S. cerevisiae* strains. In contrast, strain IMX774, which expressed *prk* from the anaerobically induced, medium-strength *pDAN1* promoter, exhibited a 31% lower glycerol yield and a 10% higher ethanol yield than the reference strain (Table 3). Furthermore, the glycerol production per gram biomass of strain IMX774 was 38% lower than that of the reference strain (Table 3). These observations indicated that the engineered PRK/RuBisCO pathway significantly contributed to NADH oxidation in anaerobic cultures of this engineered strain.

2.3.2 The impact of the RuBisCO pathway on NADH oxidation is negatively correlated with the specific growth rate

The reduced glycerol yield of strain IMX774 (*pDAN1-prk cbbm*) in anaerobic, glucose-grown bioreactor batch cultures resembled the change in glycerol yield that was previously observed in similar galactose-grown cultures of strain IMU033 (*pGAL1-prk cbbm*) [28]. However, the observed reduction in glycerol yield relative to the reference strain IME324, which did not express RuBisCO or PRK, was still far from the 90% reduction that was previously observed in sugar-limited anaerobic chemostat cultures of strain IMU033, grown at a dilution rate of 0.05 h⁻¹ on glucose/galactose mixtures [28]. Specific growth rates in the batch cultures were much higher than in those in chemostat cultures (Table 3, [28]). To investigate a possible relation between specific growth rate and relative contribution of NADH oxidation via the engineered PRK/RuBisCO pathway, growth and product formation of strains IMX774 (*pDAN1-prk cbbm*) and IME324 (reference) were analysed in anaerobic, glucose-limited chemostat cultures grown at dilution rates of 0.05 h⁻¹ and 0.15 h⁻¹ (Table 4; Additional File 2).

At a dilution rate of 0.05 h⁻¹, strain IMX774 showed glycerol and ethanol yields on glucose of 0.005 g g⁻¹ and 0.451 g g⁻¹, respectively. These yields were 90% lower and 7% higher, respectively, than in chemostat cultures of the reference strain IME324 grown at the same

dilution rate (Table 4; Figure 2). In these slow-growing chemostat cultures the glycerol production per gram biomass of strain IMX774 was only 0.66 mmol (g biomass)⁻¹, which was 90% lower than observed for strain IME324 (Figure 2). These results indicate that, at this low specific growth rate, the RuBisCO pathway almost completely replaced reoxidation of ‘excess’ NADH via glycerol formation, in agreement with previous results on IMU033 glucose/galactose-grown chemostat cultures on the same dilution rate [28].

Table 4. Yields (Y) of biomass and ethanol on glucose in anaerobic chemostat cultures of *S. cerevisiae* reference strain IME324 and the RuBisCO/PRK-expressing strain IMX774. Cultures were grown on synthetic medium containing 20 g L⁻¹ glucose (pH 5). Values represent averages ± mean deviations of measurements on independent duplicate cultures. * (p<0.05) denotes statistical significance of differences between strains IME324 and IMX774 at the same dilution rate, and # (p<0.01) indicates statistical significance of differences between analyses at different dilution rates in cultures of the same strain in Student’s *t*-tests. Degree of reduction balances of steady-state analyses yielded electron recoveries between 99% and 101%.

Strain	IME324		IMX774	
	<i>GPD1</i>	<i>GPD2</i>	<i>GPD1</i>	<i>GPD2</i> p <i>DAN1-prk cbbm</i>
Dilution rate (h ⁻¹)	0.05	0.15	0.05	0.15
Y biomass/glucose (g g ⁻¹)	0.083 ± 0.001	0.087 ± 0.007	0.082 ± 0.002	0.086 ± 0.002
Y ethanol/glucose (g g ⁻¹)	0.421 ± 0.001	0.411 ± 0.006	0.451 ± 0.001 *, #	0.432 ± 0.001 *, #

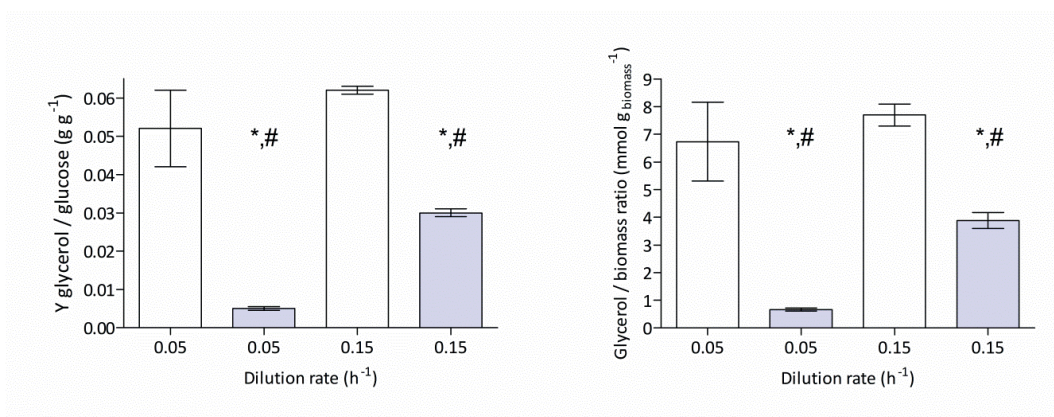


Figure 2. Yields (Y) of glycerol on glucose and stoichiometric relationships between glycerol production and biomass formation in anaerobic chemostat cultures of *S. cerevisiae* reference strain IME324 (white bars) and the RuBisCO/PRK-expressing strain IMX774 (p*DAN1-prk cbbm*, blue bars). Cultures were grown on synthetic medium containing 20 g L⁻¹ glucose (pH 5). Values represent averages \pm mean deviations of measurements on independent duplicate cultures. * ($p < 0.05$) denotes statistical significance of value differences between IME324 and IMX774 at the same dilution rate, and # ($p < 0.01$) indicates statistical significance of differences between the two dilution rates in cultures of the same strain in Student's t -tests.

The reference strain IME324 showed no significant differences in glycerol yield on glucose or in glycerol production per gram biomass when grown at a dilution rate of either 0.05 h⁻¹ or 0.15 h⁻¹ in anaerobic, glucose-limited chemostat cultures (Figure 2). In contrast, strain IMX774 showed a 5-fold higher glycerol yield on glucose and glycerol production per gram biomass when grown at a dilution rate of 0.15 h⁻¹ than in cultures grown at 0.05 h⁻¹ (Figure 2). The glycerol production per gram biomass of strain IMX774 at 0.15 h⁻¹ (3.88 mmol (g biomass)⁻¹) was only 50% lower than that of strain IME324 grown at the same dilution rate (Figure 2). These results demonstrated that, in strain IMX774, higher specific growth rates, which coincided with a higher glycolytic flux, resulted in a smaller contribution of the engineered PRK/RuBisCO pathway to NADH reoxidation, thereby reducing its beneficial impact on (by)product formation.

2.3.3 Deletion of *GPD2* improves CO₂ reduction to ethanol in anaerobic batch cultures of RuBisCO/PRK-expressing *S. cerevisiae*

The lower impact on product formation of RuBisCO/PRK expression at high specific growth rates identified the glycerol-3-phosphate dehydrogenases Gpd1 and Gpd2 as potential engineering targets for increasing the contribution of the engineered PRK/RuBisCO pathway to NADH reoxidation. Deletion of *GPD2* was previously reported to decrease glycerol formation in other engineered *S. cerevisiae* strains, without affecting osmotolerance [16-19, 22]. *GPD2* was therefore deleted in strain IMX774 (*GPD1 GPD2 pDAN1-prk cbbm*), yielding strain IMX949 (*GPD1 gpd2Δ pDAN1-prk cbbm*). This deletion did not affect the specific growth rate in anaerobic bioreactor batch cultures grown on 20 g L⁻¹ glucose (Table 3). Since deletion of *GPD2* has a strong negative effect on anaerobic growth of wild-type *S. cerevisiae* in the absence of an external electron acceptors [59, 60], this result further supported our conclusion that the RuBisCO pathway can effectively contribute to redox cofactor balancing in fast-growing anaerobic *S. cerevisiae* cultures. In these anaerobic bioreactor batch cultures, the glycerol and ethanol yields on glucose of strain IMX949 were 62% lower and 13% higher, respectively, than those of the reference strain IME324 (*GPD1 GPD2*) (Table 3). Furthermore, glycerol production per gram biomass of strain IMX949 was 65% and 43% lower than that of strains IME324 and IMX774, respectively (Table 3). These results clearly indicated that deletion of *GPD2* enables a higher contribution of the engineered PRK/RuBisCO pathway to anaerobic NADH reoxidation in engineered *S. cerevisiae* strains.

2.3.4 Optimization of precursor supply to the RuBisCO pathway further decreases glycerol yield and enables wild-type specific growth rates in anaerobic cultures

In *S. cerevisiae*, the substrate of PRK, ribulose-5-phosphate, can be formed either by NADPH-generating oxidative decarboxylation of 6-phosphogluconate, or from glyceraldehyde-3-phosphate and fructose-6-phosphate via the re-arrangement reactions of the non-oxidative pentose-phosphate pathway (PPP, [28]). If ribulose-5-phosphate used in the RuBisCO pathway were exclusively derived from 6-phosphogluconate, this would cause an NADPH/NADP⁺

imbalance when the RuBisCO pathway completely replaces glycerol formation [10]. While formation of ribulose-5-phosphate via the non-oxidative PPP does not present such a redox constraint, extensive research on metabolic engineering of *S. cerevisiae* for pentose fermentation indicates that this pathway has a limited capacity in wild-type strains [61-64].

To test if fermentation performance of strain IMX949 (*GPD1 gpd2Δ pDAN1-prk cbbm*) could be further improved by optimization of the ribulose-5-phosphate supply, overexpression cassettes for the non-oxidative PPP genes *RPE1*, *TKL1*, *TAL1*, *NQM1*, *RK11* and *TKL2* were simultaneously integrated at the *GPD2* locus of IMX774, yielding strain IMX1443 (*GPD1 gpd2Δ non-ox PPP↑ pDAN1-prk cbbm*). In anaerobic, glucose-grown bioreactor batch cultures, grown under identical conditions to the previously discussed RuBisCO/PRK-expressing strains, the specific growth rate of strain IMX1443 was virtually identical to that of the reference strain IME324 (*GPD1 GPD2*) and 36% higher than that of its parental strain IMX774 (*GPD1 GPD2 pDAN1-prk cbbm*) and of strain IMX949 (Table 3; Additional File 2). Furthermore, strain IMX1443 showed a 9% higher biomass yield on glucose than the reference strain IME324 (Table 3), which closely corresponds to the maximum theoretical increase for a RuBisCO/PRK-expressing strain of 13.5% [28]. These observations showed that the reduced growth rates of strains IMX774 and IMX949 were not primarily caused by accumulation of ribulose-1,5-biphosphate or ATP depletion, resulting from an imbalance of the *in vivo* activities of PRK and RuBisCO. Instead, they indicate that the reduced growth rates of these strains resulted from a reduced intracellular pool of ribulose-5-phosphate, which is a key precursor for the formation of the PPP-derived biosynthetic building blocks ribose-5-phosphate and erythrose-4-phosphate.

The glycerol yield on glucose of strain IMX1443 (*GPD1 gpd2Δ non-ox PPP↑ pDAN1-prk cbbm*) was 81% and 87% lower than that of its parental strain IMX774 (*GPD1 GPD2 pDAN1-prk cbbm*) and of the reference strain IME324 (*GPD1 GPD2*), respectively (Table 3). Consistent with an almost complete replacement of redox cofactor balancing via glycerol production by the RuBisCO pathway, its glycerol production per gram biomass was 88% lower than that of strain IME324 and closely matched the phenotype observed in slow-growing glucose-limited

chemostat cultures of strain IMX774 (Table 4). Furthermore, the ethanol yield on glucose of strain IMX1443 was 15% and 5% higher than that of the reference strain IME324 and of its parental strain IMX774, respectively. The phenotype of strain IMX1443 thereby approaches the theoretical maximum benefits in glycerol reduction and increased ethanol yield, without a reduction of its specific growth rate in anaerobic, glucose-grown batch cultures. Further, the osmotolerance of strain IMX1443 was not impacted by these modifications, as shown by plate growth tests on high osmolarity (1M glucose) medium (Additional File 3).

2.3.5 The physiological benefit of RuBisCO/PRK-expression in *S. cerevisiae* is independent of strain ploidy

In the context of another study, the ploidy of strains IMX765, IMX773, and IMX774 was analysed by flow cytometry. Surprisingly, strain IMX765, the parental strain of all RuBisCO/PRK-expressing strains constructed in this study, was found to have undergone a whole-genome duplication (Additional File 4). To determine whether this diploidization was accompanied by any other chromosomal copy number variations or rearrangements, the genome of strain IMX774 (*GPD1 GPD2 pDAN1-prk cbbm*) was sequenced [Genbank PRJNA415562] and compared to that of the haploid congenic reference strain CENPK.113-7D [30]. This analysis showed that a 'clean' genome duplication had occurred, without chromosomal or segmental aneuploidies (Additional File 5).

The differences in glycerol and ethanol yields between strains IME324 (haploid, *GPD1 GPD2* reference) and IMX774 (diploid, *GPD1 GPD2 pDAN1-prk cbbm*) were not expected to be influenced by ploidy variation, as biomass formation and requirements for NADH oxidation are stoichiometrically linked and the biomass yields on glucose of these strains were not significantly different (Table 3). However, as ploidy variation might affect specific growth rate [65], two additional strains were constructed to investigate whether ploidy differences affected the interpretation of our results.

Strain IME369 was constructed by transformation of p426-*TEF* (empty) to IMX673, thereby generating a new diploid reference strain (*GPD1/GPD1 GPD2/GPD2*). Additionally, the

genetic modifications introduced in the best performing RuBisCO/PRK-expressing strain (IMX1443) were reconstructed in a haploid background, resulting in strain IMX1489 (Additional File 4). Anaerobic growth of both strains was analysed in bioreactor batch cultures, under the same conditions used for the other strains analysed in this study (Table 5; Additional File 2). The new diploid reference strain IME369 showed no significant differences in specific growth rate, biomass or ethanol yields on glucose or glycerol production per gram biomass when compared to the haploid reference strain IME324 (*GPD1 GPD2*) (Tables 3 and 5). Furthermore, the specific growth rates of the engineered strains IMX1489 (haploid) and IMX1443 (diploid) were the same, while their biomass and product yields also very closely corresponded (Tables 3 and 5, Figure 3). Similarly to strain IMX1443, the osmotolerance of IMX1489 did not differ from that of a *GPD1 GPD2* reference strain (Additional File 3). These results indicate that the impact of the engineering strategy presented in this study does not differ for haploid and diploid *S. cerevisiae* strains.

Table 5. Specific growth rates (μ), yields (Y) of biomass, ethanol and glycerol on glucose and stoichiometric relationships between glycerol production and biomass formation in anaerobic bioreactor batch cultures of *S. cerevisiae* strains IME369 and IMX1489. Cultures were grown on synthetic medium containing 20 g L⁻¹ glucose (pH 5). Specific growth rates and stoichiometries were calculated from sample points during the mid-exponential growth phase. Values represent averages \pm mean deviations of measurements on independent duplicate cultures. * ($p < 0.02$) and ** ($p < 0.01$) denote statistical significance of differences between IME324 (Table 3) and strains IME369 and IMX1489 in Student's *t*-tests. Degree of reduction balances constructed over the exponential growth phase yielded electron recoveries between 96% and 100%.

Strain	IME369	IMX1489
Relevant Genotype	<i>GPD1 GPD2</i>	<i>GPD1 gpd2Δ pDAN1-prk cbbm non-ox PPP↑</i>
μ (h⁻¹)	0.31 \pm 0.00	0.30 \pm 0.01
Y biomass/glucose (g g⁻¹)	0.091 \pm 0.009	0.096 \pm 0.001 *
Y ethanol/glucose (g g⁻¹)	0.376 \pm 0.005	0.421 \pm 0.002 *
Y glycerol/glucose (g g⁻¹)	0.107 \pm 0.004	0.014 \pm 0.000 **
Glycerol produced/biomass (mmol (g biomass)⁻¹)	12.189 \pm 1.080	1.669 \pm 0.082 **

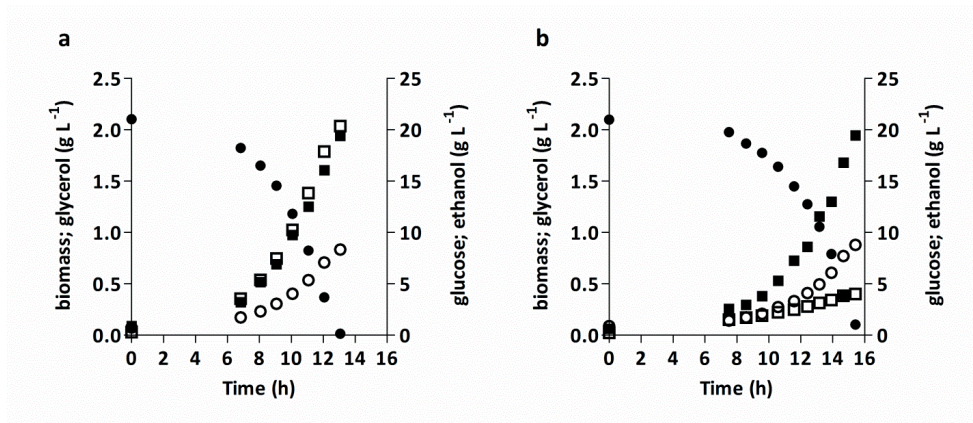


Figure 3. Growth, glucose consumption and product formation in anaerobic bioreactor batch cultures of *S. cerevisiae* strains IME324 (*GPD1 GPD2*) (A) and IMX1489 (*GPD1 gpd2Δ pTDH3-RPE1, pPGK1-TKL1, pTEF1-TAL1, pPGI1-NQM1, pTPI1-RK11, pPYK1-TKL2 pDAN1-prk cbbm*) (B). Cultures were grown on synthetic medium containing 20 g L⁻¹ glucose (pH 5). Symbols: ●, glucose; ■, biomass; □, glycerol; ○, ethanol. Representative cultures of independent duplicate experiments are shown.

2.4 Discussion

Fixation of CO₂ via the Calvin-cycle enzymes RuBisCO and phosphoribulokinase (PRK) plays a key role in the biological carbon cycle [66]. The Calvin cycle's role in carbon fixation by photo- and chemoautotrophs is well established and its improvement remains a major target of research [67, 68]. Additionally, in nature as well as in engineered industrial microorganisms, Calvin-cycle enzymes can increase the flexibility of intracellular redox cofactor balancing in chemoorganoheterotrophs [69, 70].

Here, we present a metabolic engineering strategy, based on expression of Calvin-cycle enzymes for redox cofactor balancing in *S. cerevisiae* [28], that enabled a near-complete elimination of glycerol production in anaerobic, glucose-grown batch cultures, with an associated increase in ethanol yield. In addition to multi-copy chromosomal integration of expression cassettes for *T. denitrificans cbbm*, this strategy encompassed expression of the *E. coli* chaperone genes *groEL* and *groES* [28], expression of the spinach *prk* gene from the

anaerobically inducible *DAN1* promoter, deletion of *GPD2* and overexpression of the *S. cerevisiae* structural genes for the enzymes of non-oxidative pentose-phosphate pathway.

A high specific growth rate of industrial *S. cerevisiae* strains is important in view of its impact on volumetric productivity and competition with microbial contaminants [2, 71]. Many previously reported redox engineering strategies for decreasing glycerol formation in *S. cerevisiae* resulted in reduced specific growth rates or requirements for specific media [8, 20, 59, 72]. Reduced growth rates of metabolically engineered microorganisms are often attributed to the metabolic burden caused by high-level expression of heterologous and/or homologous proteins [58, 73]. Despite the high-level expression of RuBisCO and yeast PPP-enzymes, the specific growth rates of haploid and diploid engineered *S. cerevisiae* strains in anaerobic batch cultures were the same as those of non-engineered reference strains.

Previous research had already shown that co-expression of the *E. coli* chaperones GroEL and GroES is required for functional heterologous expression of CbbM in *S. cerevisiae* [28]. Functional expression of a plant RuBisCO in *E. coli* was also recently shown to require co-expression of no fewer than five plant chaperones [74], highlighting the importance of expression of folding-assisting proteins in the formation of functional RubisCO complexes. In the case of GroEL and GroES specifically, it was recently shown that their expression facilitates functional expression of several heterologous proteins in yeasts [28, 75, 76]. Further, their expression can potentially be beneficial in improving strain robustness against industrial fermentation conditions [77]. In the present study, their expression may have contributed to the apparent absence of a metabolic burden in the engineered strains, by preventing cellular stress and increased protein-turnover caused by incorrect protein folding. Since multi-copy integration of expression cassettes for the form-II RuBisCO CbbM supported wild-type growth rates in anaerobic glucose-grown cultures, its replacement by an alternative RuBisCO with superior catalytic properties [68, 78] is not necessary in this experimental context. The high K_m of RuBisCO for CO_2 [67] implies that microorganisms that heterologously express Calvin-cycle enzymes require high CO_2 concentrations in the cultures for *in vivo* pathway activity [28, 70].

Since industrial ethanol production processes very rapidly become CO₂ saturated, implementation of this redox engineering strategy in industry does not impose specific requirements on process design or medium composition [8].

As recently demonstrated in engineered *E. coli* strains expressing RuBisCO and PRK [56, 57], expression levels of PRK in engineered *S. cerevisiae* strains needed to be ‘tuned’ to strike a balance between generating sufficient ribulose-1,5-bisphosphate for *in vivo* RuBisCO activity and avoiding negative effects of high-level PRK overexpression. Use of the medium-strength, anaerobically inducible *DAN1* promoter was shown to meet these requirements. An additional advantage of using an anaerobically inducible promoter for *prk* expression is that it minimizes any negative effects of PRK expression during the aerobic biomass propagation phase that precedes anaerobic industrial processes for bioethanol production [79].

In the original strain design, which carried a functional *GPD2* gene and in which the PPP enzymes were not overexpressed, the contribution of the engineered PRK/RuBisCO pathway to *in vivo* NADH oxidation was negatively correlated with specific growth rate. The effect of additional overexpression of the non-oxidative pentose-phosphate pathway genes *RPE1*, *TKL1*, *TAL1*, *NQM1*, *RK11*, and *TKL2* identified supply of ribulose-5-phosphate and/or other intermediates of the PPP as a key factor in the PRK/RuBisCO-mediated CO₂ reduction in *S. cerevisiae*. Overexpression of non-oxidative PPP genes is a well-documented element in the construction of xylose- and arabinose-fermenting *S. cerevisiae* strains for fermentation of lignocellulosic hydrolysates [61, 80, 81], which should facilitate implementation of PRK/RuBisCO-enabled CO₂ reduction in such strains. The positive effect of the deletion of *GPD2* on CO₂ reduction is consistent with its reported beneficial effect on strains utilizing acetic acid as an external electron acceptor for redox cofactor balancing [22].

A mechanistic, quantitative understanding of the mechanisms by which glycerol formation and RuBisCO/PRK-mediated CO₂ reduction interact in a growth-rate dependent manner would require advanced analyses of intracellular metabolite concentrations in the yeast cytosol, which are beyond the scope of the present study. Clearly, the cytosolic NADH/NAD⁺

ratio, which affects regulation of *GPD2* [17] and is involved in the reductive reactions in both pathways, would be of special interest in such studies. In addition, the triose-phosphate node in glycolysis is of special interest, since Gpd1 and Gpd2 use dihydroxyacetone phosphate (DHAP) as a substrate, while the glycolytic intermediate glyceraldehyde-3-phosphate (GAP) is a substrate of transketolase, a key enzyme for provision of the RuBisCO substrate ribulose-5-phosphate via the non-oxidative PPP. Intracellular concentrations of DHAP in glucose-grown cultures of *S. cerevisiae* increase with increasing specific growth rate [82], presumably reflecting the higher glycolytic flux in fast-growing cultures. The equilibrium of the triose phosphate isomerase lies far toward DHAP [83], whose intracellular concentrations in *S. cerevisiae* have been reported to be in the low mM range [84]. Intracellular concentrations of GAP are therefore likely to be below the reported high K_m value of yeast transketolase for this substrate (ca. 5 mM, [85]), which may well contribute to the impact of overexpression of the PPP pathway on flux distribution at this branchpoint.

Whole genome duplications have been previously shown in *S. cerevisiae* strains obtained by evolutionary engineering [86, 87]. However, its occurrence in our initially constructed strains, which were only subjected to targeted, CRISPR-mediated genetic modification, was unexpected. Since 5-fluoro-orotic acid has been reported to affect chromosome segregation in yeasts [88], we cannot exclude the possibility that genome duplication was related to counter-selection with 5-fluoro-orotic acid to recycle the gRNA-expressing plasmid during the construction of strain IMX765, the parental strain of IMX773 and IMX774. When using traditional genetic modification techniques, such as one-step gene replacement, aneuploidies or genome duplications are easily identified by simple diagnostic PCR experiments. However, the high efficiency of CRISPR/Cas9-based genome editing generally results in simultaneous modification of both copies of a target locus in diploid or aneuploid strains [89]. In this light, it is advisable to perform flow-cytometry-based ploidy analysis and whole genome sequencing to detect genome duplications and aneuploidy, respectively [65], when CRISPR technology is used for strain construction.

The characteristics of the engineered strains make this engineering strategy very interesting for further testing in industrial settings. In contrast to a previously published strategy for minimizing glycerol production by the reduction of acetic acid, by expression of a heterologous acetylating-acetaldehyde dehydrogenase in combination with the native alcohol dehydrogenases [20, 22], the current strategy does not require an organic electron acceptor. It is therefore compatible with fermentation of 'first generation' feedstocks that contain little or no acetic acid.

Research on production of alternative compatible solutes is ongoing, with trehalose production being a promising candidate, but so far glycerol remains the key metabolite involved in tolerance of sugar-grown *S. cerevisiae* cultures to osmotic stress [90-92]. The presence, in the CO₂-reducing strains described in this study, of a functional *GPD1* gene was sufficient to maintain osmotolerance. At high osmolarity, upregulation of *GPD1* [16, 93] might reduce the stoichiometric benefits of CO₂-fixation in RuBisCO/PRK-expressing yeast strains. It may be possible to prevent such an effect by promoter replacement of *GPD1* by lower-strength ones [59]. Alternatively, the entire *GPD1* gene may be replaced by a heterologous gene encoding an NADP⁺-linked glycerol-3-phosphate dehydrogenase, thereby uncoupling the roles of glycerol in redox homeostasis and osmotolerance [22].

2.5 Conclusions

Overexpression of the Calvin-cycle enzymes RuBisCO and PRK, in combination with deletion of *GPD2* and overexpression of the genes of the non-oxidative branch of the pentose-phosphate pathway, yielded a *S. cerevisiae* strain that displayed a ca. 90% decreased glycerol production and a 15% increase in the ethanol yield on sugar, without affecting the maximum specific growth rate of the strain. Based on our experiments in synthetic media, the presented metabolic engineering strategy has the potential to enable significant improvements in the ethanol yields in industrial processes. The industrial application of this strategy should not require special

process conditions or media compositions and is ready for implementation in industrial strain backgrounds and subsequent evaluation in first- and second-generation industrial substrates.

2.6 Acknowledgements

We thank Jean-Marc Daran and Pilar de la Torre for advice on molecular biology, Erik de Hulster for advice on fermentations, and Marijke Luttkik, Astrid van der Meer and Victor Guadalupe-Medina for advice on enzymatic activity determinations. We thank Mark Bisschops for advice on statistical analysis, and Maarten Verhoeven and Jasmine Bracher for advice on strain construction.

2.7 Additional Files

Additional File 1. Primers used in this study.

Primer	Sequence 5'-3'	Purpose
5792	GTTTTAGAGCTAGAAATAGCAAGTTAAAAATAAG	pUDR119 and pUDR164 construction
5980	CGACCGAGTTGCTCTTG	pUDR119 and pUDR164 construction
5979	TAATTGACGGCGGCAAGAGC	pUDR119 and pUDR164 construction
7023	GTTGATAACGGGACTAGCCTTAATTTAACTTGCTATTTCTAGCTCTAAAAACGAAGAATTCCAGTGGTCAATGATCAATTTATCTTTTAC TCCGGAGAAAGTTTCGAACGCCGGAACATGGCCA	pUDR119 construction
7374	GTTGATAACGGGACTAGCCTTAATTTAACTTGCTATTTCTAGCTCTAAAAACCTACTCTCTCCTAGTCCGGGATCATTATCTTTTAC TCCGGAGAAAGTTTCGAACGCCGGAACATGGCCA	pUDR164 construction
7375	CTACTCTCTCCTAGTCGCC	pUDR164 diagnostic PCR
5793	GATCATTTATCTTTTCACTGGGGAG	<i>GPD2</i> -targeting CRISPR plasmid construction
6966	GTGGCCATGTTTTCGGCGTTTCGAAACTTCTCCGCAGTGAAAGATAAATGATCCCAAGAAATTCGCCATTTATTCGGGTTTATAGAGCTAGAAA TAGCAAGTTAAAAATAAG	<i>GPD2</i> -targeting CRISPR plasmid construction
7549	GGGATACCCCTGGGATCTTCACAGCTATGACCATGATTACG	Addition of 20 bp primer-binding sequence to <i>cbbM</i>
7550	CGCGGAGATTAGCGAAGCCTCACTATAGGGGGAATTGG	Addition of 20 bp primer-binding sequence to <i>cbbM</i>
11206	CATAGCTTGAAACTACGGCAAAAGGATTGTCAGATCGCTTCATACAGGGGAAAGCTTCGGCACGGGCAGATTAGCGAAGC	<i>cbbM</i> cassette construction - F tag addition

	GC	<i>cbbM</i> cassette construction - <i>SGAI</i> tag addition	<i>cbbM</i> cassette construction - <i>G</i> tag addition	<i>cbbM</i> cassette construction - <i>A</i> tag addition	<i>cbbM</i> cassette construction - <i>G</i> tag addition	<i>cbbM</i> cassette construction - <i>B</i> tag addition	<i>cbbM</i> cassette construction - <i>A</i> tag addition	<i>cbbM</i> cassette construction - <i>C</i> tag addition	<i>cbbM</i> cassette construction - <i>B</i> tag addition	<i>cbbM</i> cassette construction - <i>D</i> tag addition	<i>cbbM</i> cassette construction - <i>M</i> tag addition	<i>cbbM</i> cassette construction - <i>M</i> tag addition	<i>cbbM</i> cassette construction - <i>N</i> tag addition	<i>cbbM</i> cassette construction - <i>N</i> tag addition	<i>cbbM</i> cassette construction - <i>O</i> tag addition	<i>cbbM</i> cassette construction - <i>O</i> tag addition	<i>cbbM</i> cassette construction - <i>J</i> tag addition	Diagnostic primer <i>cbbM</i> integration	Diagnostic primer <i>cbbM</i> integration
7548		GCATAGAACATTTATCCGGCGAAAGGGGTATTAGGGGTGAGGTGAATAAGAAAGTCAAGAAATCGGGCCGGCAGATTAGCGAA																	
6285		AAGGGCCATGACACCTGATGCACCAATTAGGTAGGTCTGGCTATGTCTATACCTCTGGGGGATACCCCTGGGATCTTC																	
6280		CTGCCATTGATGATCTGGCGGAATCTCTGCCGTGCCATAGCCATGCCTTCACATATAGTGGCATACCCCTGGCATCTTC																	
6273		GCCAGAGGTATAGACATAGCAGACCTACCTAATTGGTGCATCAGTGTCTATGGCCCTTCGGCGAGATTAGGGAAGC																	
6281		GTTGAACATTTCTTAGCTGTGCAATCATTTAGACACGGGGATCGTCTCGAAAGGTGGGATACCCCTGGATCTTTC																	
6270		ACTATATGTGAAGGCATGGCTATGGCACGGCAGACATTCGGCCAGATCAATAAGCACCGGGCAGATTAGGGAAGC																	
6282		CTAGCGTCTCGCATAGTTCTTAGATTGTGCTAGCGCATATACGATCCGTGAGACGTGGGATACCCCTGGGATCTTTC																	
6271		CACCTTTCGAGAGGATGCCCGTGTAAATGATTTGGACCCAGCTAAGAAATGTTCAACCGGGCAGATTAGGGAAGC																	
6284		AATCACTCTCCATACAGGGTTTCATACATTTCTCCAGGGACCCACAGTGGTAGATGGCTGGGATACCCCTGGGATCTTC																	
6272		ACGCTCACGGATCGTATATGCCGTAGGGACAATCTAAGAACTATGCGAGACAGCTAGGGGGCAGATTAGGGAAGC																	
6283		ACGCCATCTAGGACTGTGGTCCCGTGGAGAAATGTATGAAAGCCCTGTATGGAGATGATTGGGATACCCCTGGGATCTTC																	
6275		ACGAGATGAAGGCTCACCGATGGACTTACTATGATGCCATGTGGAAGCTCCGCTATCGGGCAGATTAGCGAAGC																	
6287		ATGACCGGAGCTTCCAGCATGGCATCATACTAAGTCCATCGGTGAGCCTTTCATCTCTCGTGGGATACCCCTGGGATCTTC																	
6276		TTCTAGGCTTTGATGCAAGGTCCACATATCTTTCGTTAGGACTCAA TCGTGGTGTGATCCGGCGAGATTAGCGGAAGC																	
6288		GATCAGCACCCAGATTGAGTCTTAAGGAAGATATGTGACCTTGCATCAAAGCCCTAGAAGCCATACCCCTGGGATCTTTC																	
6277		ATACTCCCTGCCACAGATGAGTCAAGCTATTTGACACCGEAGACGGGCTCAAGGATCATTTCCGGGGCAGATTAGGGAAGC																	
6289		GAAATGATCGTTCCAGCGGTTCTCGGTCTTCAATAGCTTACTCATCTCTGACGGGAGTATGGGATACCCCTGGGATCTTTC																	
7075		CGACGAGATGCTCAGACTATGTGTTCTACCTGCTTGGACATCTTCGGGTATATGACGGGCGGGCGCAAAATTAAGGCCTT																	
7298		TTGTTCAATGGATGCGGTTTC																Diagnostic primer <i>cbbM</i> integration	
4692		AAGGGCCATGACCACCTG																Diagnostic primer <i>cbbM</i> integration	

4870	GCCAGAGGTATAGACATAGCC	Diagnostic primer <i>cbbM</i> integration
3275	GTGCCATTGATGATCTGGGGGAATG	Diagnostic primer <i>cbbM</i> integration
3847	ACTATACTGAAGGCATGGCTATCG	Diagnostic primer <i>cbbM</i> integration
3276	GTTGAACATTCTTAGGCTGGTCGAATC	Diagnostic primer <i>cbbM</i> integration
4691	CACCTTTCGAGAGGACGATG	Diagnostic primer <i>cbbM</i> integration
3277	CTAGGGTGTCTCGCATAGTCTTAGATTG	Diagnostic primer <i>cbbM</i> integration
3283	ACGTCTACGGATCGTATATGC	Diagnostic primer <i>cbbM</i> integration
7226	ATACATTTCTCCACGGGACC	Diagnostic primer <i>cbbM</i> integration
7225	GTCCCGTGGAGAAATGTATG	Diagnostic primer <i>cbbM</i> integration
6629	ACGAGAGATCAAGGCTCACC	Diagnostic primer <i>cbbM</i> integration
4184	ATGACGGGAGCTTCCAGCATG	Diagnostic primer <i>cbbM</i> integration
3842	TTCTAGGCTTTTGATGCAAGGTC	Diagnostic primer <i>cbbM</i> integration
3843	GATCAGCACCCACGATTG	Diagnostic primer <i>cbbM</i> integration
3840	ATACTCCCTGCACAGATGA	Diagnostic primer <i>cbbM</i> integration
3837	GAATGATCGTTCAGCGCG	Diagnostic primer <i>cbbM</i> integration
7228	TCTACCTGCTGGACATCTTC	Diagnostic primer <i>cbbM</i> integration
7227	ATACGGAAAGATGTCCAAGC	Diagnostic primer <i>cbbM</i> integration
3290	GTCACGGGTTCTCAGCAATTCC	Diagnostic primer <i>cbbM</i> integration
3291	CTCTAACGGCTCAGGCATCATCG	Diagnostic primer <i>cbbM</i> integration
4229	TGGTCGACAGATACAATCTCTGG	Diagnostic primer <i>cbbM</i> integration
1370	GTTTCATGCTCCAGCTACAG	Diagnostic primer <i>cbbM</i> integration

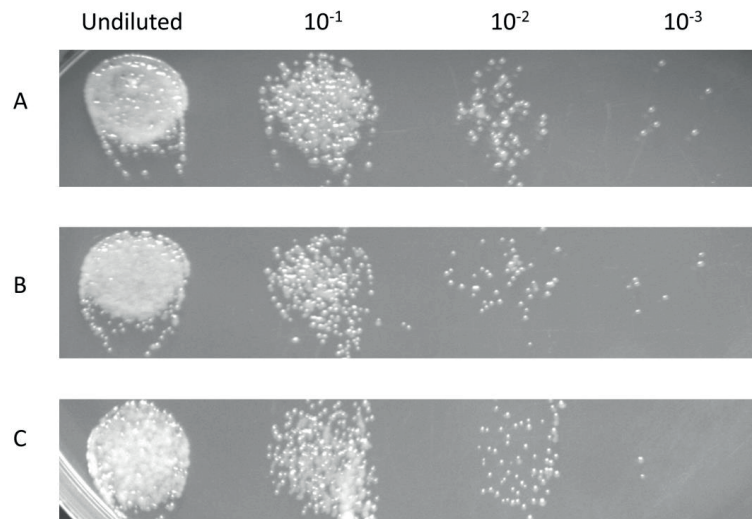
1371	AAATAGCACGAGCAGGAG	Diagnostic primer <i>cbhM</i> integration
7076	GGCCGTCATATACGGGAAGATGCCAAGCAGGTAGAACACATAGTCTGAGCATCTCGTCGGGACCATAGCTTCAAAATGTTTC	<i>groEL</i> cassette construction - J tag addition
7077	GTCACGGGTTCTCAGCAATTCGAGCTATTACCGATGATGGCTGAGGGCTTAGAGTAACTGCTGGACATTTTATGATGGAATG	<i>groEL</i> cassette construction - H tag addition
7078	AGATTTACTTAAGCCCTCAGCCATCATCGGTAATAGCTCGAAATGCTGAAACCGGTGACGGGATCTACGTATGGTCAATTTTC	<i>groES</i> cassette construction - H tag addition
7079	TATAATTTGATGTAATATCTAGGAAATACACTTGTGTATFACTTCTCGCTTTCTTTTATTGGGCCCTTTTAAACAGTTGATG	<i>groES</i> cassette construction - <i>SGAI</i> tag addition
7933	TCACAGAGGGATCCCGTTACCCATCTATGCTGAAGATTTATCATACTATTCTCCGGCTCGGGAATTCAGGCAATAGCGTTTC	<i>pYEN1-prk</i> cassette construction
7295	TTTCTTGTGCAGTATCCAGAATAAT	<i>pYEN1-prk</i> cassette construction
7930	TCACAGAGGGATCCCGTTACCCATCTATGCTGAAGATTTATCATACTATTCTCCGGCTCGGAGAAATGCAAGGGCAACAGG	<i>pDANI1-prk</i> cassette construction
7931	TACTTGGGGTATATATTTAGTATCC	<i>pDANI1-prk</i> cassette construction
7978	GCATAGAACAATTATCCGGGAAACGGGTATTAGGGGTGAGGGTGAATAAGGAAAGTCAGGAAATCGGGCAGAATGCAAGGGCAAA	<i>prk</i> cassette construction (<i>pDANI1-SGAI</i> tag addition)
7084	ATTGAAATGAAATGAAATCGATAG	<i>prk</i> cassette construction (<i>tPGK1</i>)
7934	GTCATAACTCAATTTGCCCTATTTCTTACGGCTTCTCATAAAACGTCCACACTATTCAGGGCTTCAAGCTTACACAACAGG	<i>prk</i> cassette construction (<i>tPGK1</i>) - X-2 tag addition
7081	ATTGATCTATCGAATTTCAATTTCAATTTCAATCTAGGCTTTAGCAGCTGTTG	<i>prk</i> amplification
11205	TCCCGCACTTCCCTGTATCAAGGGATCTGACCAATCCCTTTGCCGTAGTTTCAAGGTATGGCTTCAAGCTTACACAACAC	<i>prk</i> cassette construction (<i>tPGK1</i>) - F tag addition
7297	ACTTGTATATTTCTGGATCTGCAAGAAAATGTCAACAACAACAACAATTTGTG	<i>prk</i> amplification (<i>pYEN1</i> cassette)

7932	TTGCAGATAAAAGTGTAGCAGATAAAAAGTGTAGCATACTAAATATA TACCCCAAGTAATGTCACACAACAACAATTGTG	<i>prk</i> amplification (pDAM1 cassette)
11593	GTATTTTGGTAGATTCAATTTCTTCCCTTTCCTTCCCTCCCTCCCTTATCAGTCAAAAAATTAGCCCTTTTAAATCTTCC	<i>GPD2_RPE1_H</i> cassette construction
3290	GTCACGGGTTCTCAGCAATTTCG	<i>GPD2_RPE1_H</i> cassette construction
5909	AGATTTACTCTAAGCCCTCAGCC	<i>H_TKL1_I</i> cassette construction
4068	GCCTACGGTTCGGGAAGTATGC	<i>H_TKL1_I</i> cassette construction
3274	TATTCACGTAGACGGATAGGTATAGC	<i>I_TAL1_A</i> cassette construction
3275	GTCCTATTGATGATCTGGCGGAATG	<i>I_TAL1_A</i> cassette construction
3847	ACTATATGTGAAGGCATGGCTATGG	<i>A_NQM1_B</i> cassette construction
3276	GTTGAACATTCTTAGGCTGGTCGAATC	<i>A_NQM1_B</i> cassette construction
4691	CACCTTTCGAGAGGAGGATG	<i>B_RK11_C</i> cassette construction
3277	CTAGGGTGTCTCGCATAGTCTTAGATTG	<i>B_RK11_C</i> cassette construction
3283	AGGTCTCAGGGATCGTATATGC	<i>C_TKL2_GPD2</i> cassette construction
11595	ATAACTGTAGTAAATGTTACTAGTAGTAGTTCGTAGAACTTGTGTATAAATGATAAAATGGTTTACTATTGGCTGCTTGTAC	<i>C_TKL2_GPD2</i> cassette construction
7376	GGTCTAGGCCCTGCATAATCG	Diagnostic primer <i>prk</i> integration in <i>X-2</i>
7377	TGGGCATCATGTCTACTTG	Diagnostic primer <i>prk</i> integration in <i>X-2</i>
2375	TCAGCCACTTAAATTTTCGTGAATG	Diagnostic primer <i>prk</i> integration in <i>X-2</i>
2376	GCCTTTGAGTGACGTGATACC	Diagnostic primer <i>prk</i> integration in <i>X-2</i>
2018	GTTACAGCAGCTCTTCTCTAC	Diagnostic primer non-ox PPP integration
4496	CCGGGTTTGA TGACCTTATG	Diagnostic primer non-ox PPP integration
7868	CAACTTGGCTTGGGAATGC	Diagnostic primer non-ox PPP integration
7876	ACTGCTAGCACCATCGATAG	Diagnostic primer non-ox PPP integration

7875	TTGATAAGCTAGCGGCTCTCC	Diagnostic primer non-ox PPP integration
7872	TCGGCTTCACCCTTGTAATC	Diagnostic primer non-ox PPP integration
7871	GGTGATTTGGGGCTCTATTGC	Diagnostic primer non-ox PPP integration
7874	AAATCTGGGTGCCGAATTCC	Diagnostic primer non-ox PPP integration
7873	ACCCATGTGGTTGCTGATTC	Diagnostic primer non-ox PPP integration
7870	CTTCATCAGCACCGTCAAAC	Diagnostic primer non-ox PPP integration
7869	CTTTGGGCAATCCTTTGGAG	Diagnostic primer non-ox PPP integration
7877	CAACCATATGCCCTCGTATCG	Diagnostic primer non-ox PPP integration
7923	ACTAGGATTGGCACCAGTTG	Diagnostic primer non-ox PPP integration
2015	CCAAATGGCACATGAGTCAC	Diagnostic primer non-ox PPP integration
2018	GTTCAGCAGCTCTTCTCTAC	Diagnostic primer non-ox PPP integration
2015	CCAAATGGCACATGAGTCAC	Diagnostic primer non-ox PPP integration

Additional File 2. Organic acid production in anaerobic bioreactor batch and chemostat cultures of *S. cerevisiae* strains constructed in this study. Cultures were grown on synthetic medium containing 20 g L⁻¹ glucose (pH 5). Values represent averages ± mean deviations of measurements taken at the end of the fermentations in the case of batch cultures, and during steady-state in chemostat cultures. Batch cultures of IME324 and IMX1443 were performed in triplicate. Batch cultures of IMX774 were performed in quadruplicate and cultures of all other strains were performed in duplicate.

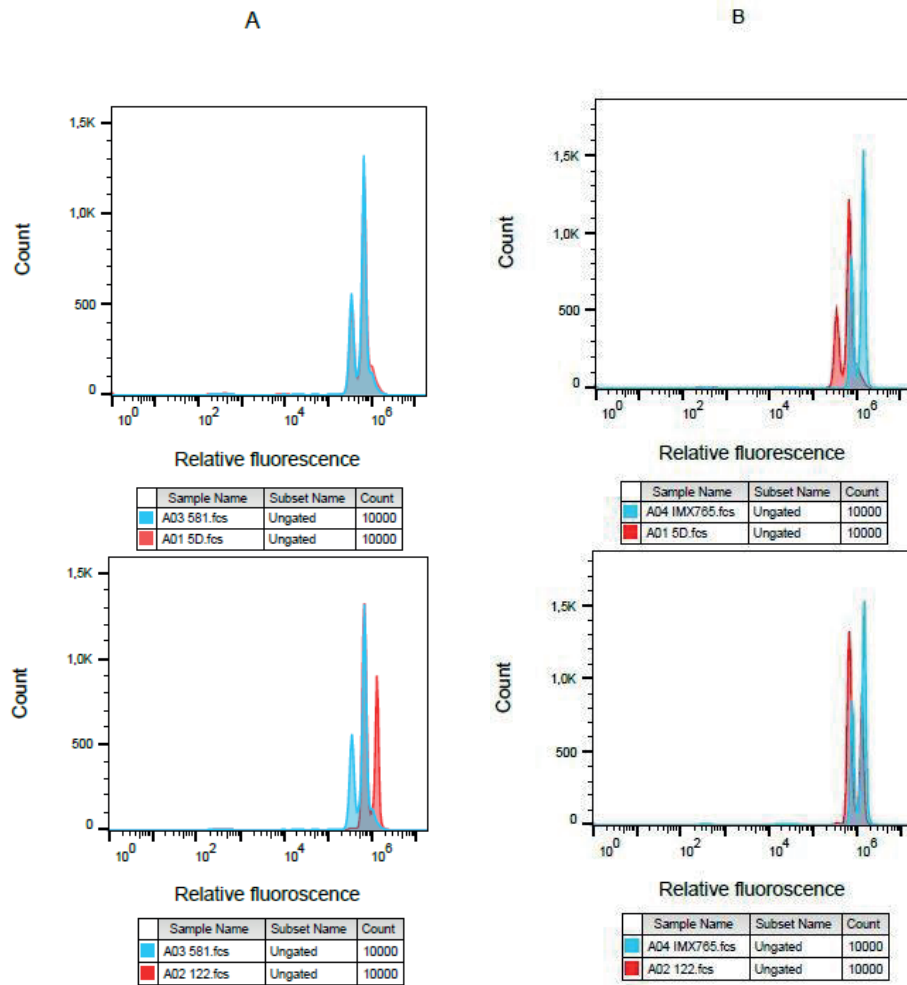
Culture mode	Strain name	Acetate (mM)	Pyruvate (mM)	Succinate (mM)	Lactate (mM)
Batch	IME324	2.79 ± 0.11	0.71 ± 0.02	0.80 ± 0.05	2.01 ± 0.07
	IME369	2.71 ± 0.58	0.61 ± 0.06	0.59 ± 0.01	1.71 ± 0.18
	IMX773	2.63 ± 0.14	0.57 ± 0.01	1.12 ± 0.03	1.79 ± 0.02
	IMX774	4.17 ± 0.48	0.86 ± 0.10	0.76 ± 0.07	1.65 ± 0.14
	IMX949	1.99 ± 0.06	0.91 ± 0.01	0.65 ± 0.01	1.97 ± 0.01
	IMX1443	4.13 ± 0.18	0.81 ± 0.02	0.88 ± 0.06	1.99 ± 0.13
	IMX1489	4.60 ± 0.30	0.90 ± 0.00	0.83 ± 0.06	1.98 ± 0.06
Chemostat D = 0.05 h⁻¹	IME324	0.55 ± 0.11	0.12 ± 0.15	0.92 ± 0.03	1.06 ± 0.25
Chemostat D = 0.05 h⁻¹	IMX774	2.46 ± 0.31	0.27 ± 0.08	0.82 ± 0.00	1.28 ± 0.01
Chemostat D = 0.15 h⁻¹	IME324	0.71 ± 0.18	0.40 ± 0.07	0.79 ± 0.01	1.80 ± 0.08
Chemostat D = 0.15 h⁻¹	IMX774	1.75 ± 0.16	0.60 ± 0.04	1.07 ± 0.04	1.76 ± 0.02



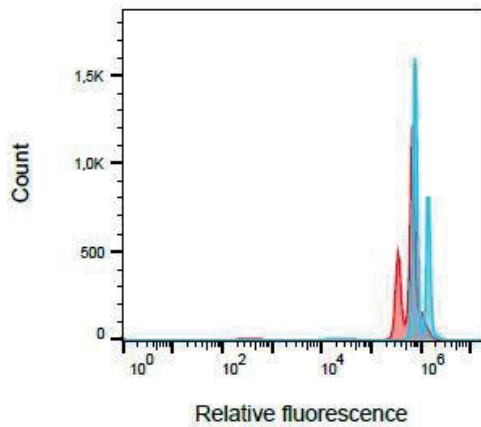
2

Additional File 3. Osmotolerance assay of engineered strains. Cells were grown on synthetic medium (180 g L⁻¹ (1M) glucose, initial pH 6) and incubated at 30 °C for 48h under anaerobic conditions (10% CO₂). A: IME324 (*GPD1 GPD2*); B: IMX1443 (*GPD1 gpd2Δ pDAN1-prk cbbm non-ox PPP↑*, diploid); C: IMX1489 (*GPD1 gpd2Δ pDAN1-prk cbbm non-ox PPP↑*, haploid).

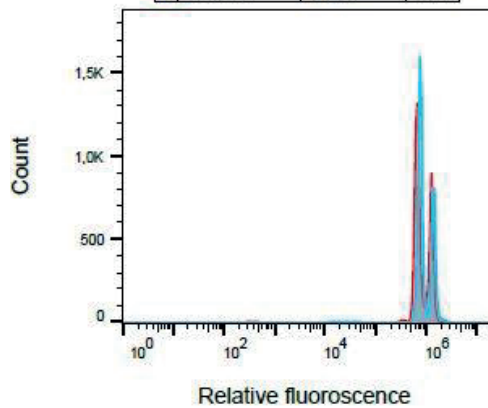
Additional File 4. Ploidy assessment of engineered RuBisCO/PRK-expressing strains. DNA content of each strain (blue) was measured by flow cytometric analysis and compared to the haploid strain CEN.PK113-5D (red; upper panel) and the diploid strain CEN.PK122 (red; bottom panel). A: IMX581 (*GPD1 GPD2*, parental of lineage); B: IMX765 (*GPD1 GPD2 cbbm*); C: IMX773 (*GPD1 GPD2 pYEN1-prk cbbm*); D: IMX774 (*GPD1 GPD2 pDAN1-prk cbbm*); E: IMX1489 (*GPD1 gpd2Δ pDAN1-prk cbbm*).



C

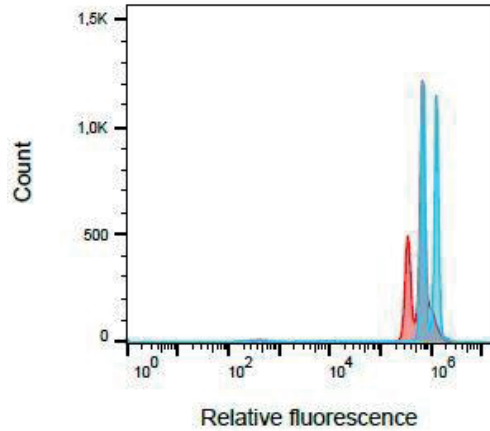


Sample Name	Subset Name	Count
A05 IMX773.fcs	Ungated	10000
A01 5D.fcs	Ungated	10000

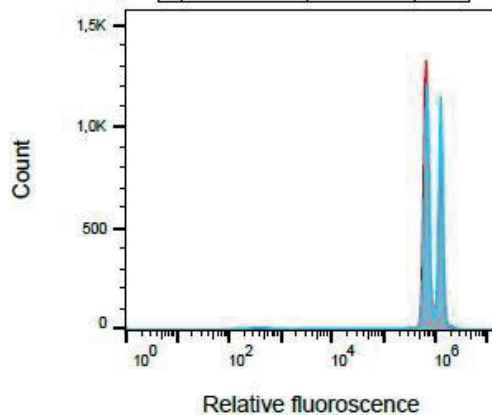


Sample Name	Subset Name	Count
A05 IMX773.fcs	Ungated	10000
A02 122.fcs	Ungated	10000

D

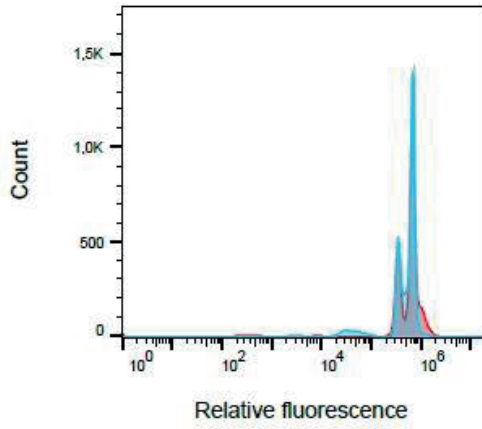


Sample Name	Subset Name	Count
A04 774.fcs	Ungated	10000
A01 5D.fcs	Ungated	10000

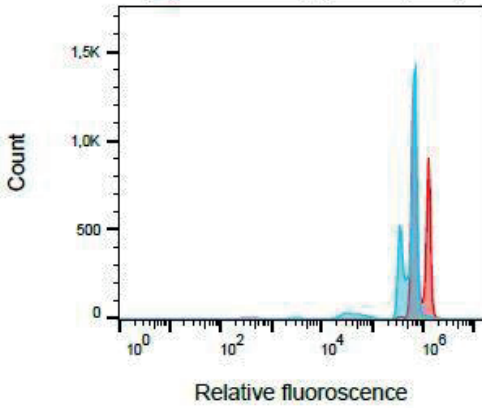


Sample Name	Subset Name	Count
A04 774.fcs	Ungated	10000
A02 122.fcs	Ungated	10000

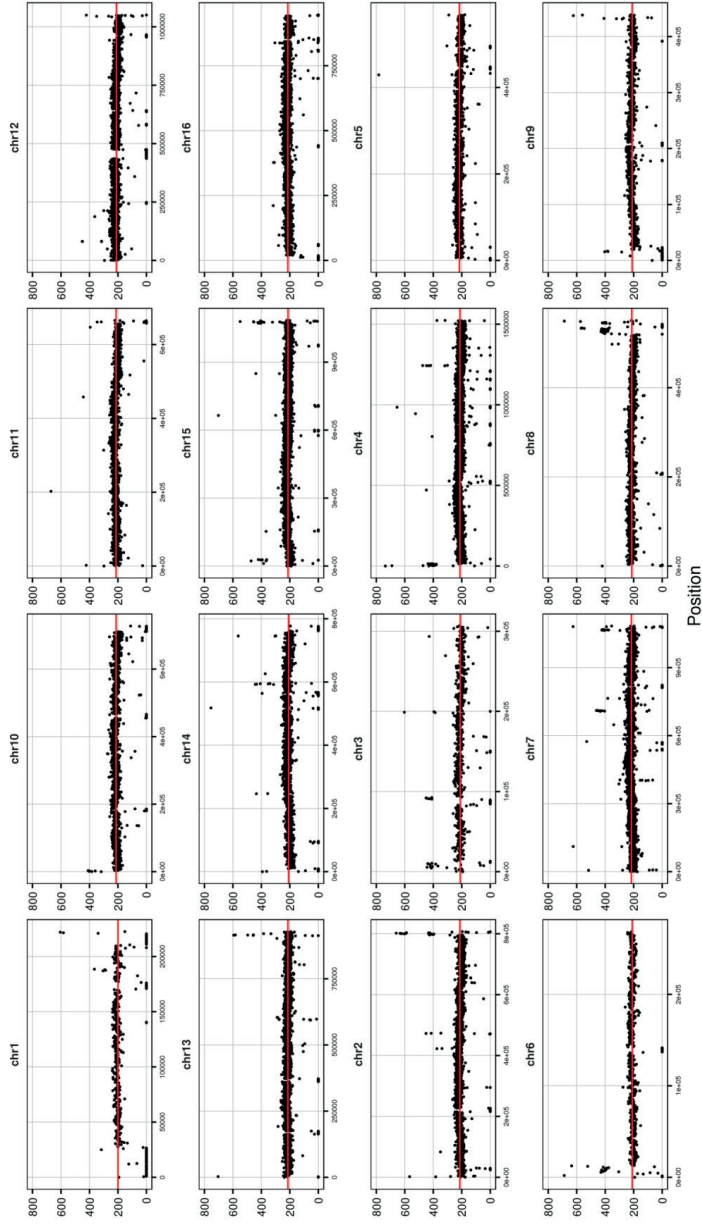
E



Sample Name	Subset Name	Count
A03 IMX1489.fcs	Ungated	10000
A01 5D.fcs	Ungated	10000



Sample Name	Subset Name	Count
A03 IMX1489.fcs	Ungated	10000
A02 122.fcs	Ungated	10000



Additional File 5. Sequence coverage plots comparing the genome of RuBisCO/PRK-expressing strain IMX774 to a published genome of CEN.PK113-7D [30], generated using BWA to map the sequence reads from IMX774 to the CEN.PK113-7D reference. Further processed by SAMtools to extract the per base sequence depth and an in-house script to calculate the average coverage for 500 bp non-overlapping windows. R script was used to plot the 500 bp windows (black dots) and median coverage (red line).

2.8 Reference list

1. Hermann BG, Blok K, Patel MK. Producing bio-based bulk chemicals using industrial biotechnology saves energy and combats climate change. *Environ Sci Technol.* 2007;41:7915-21.
2. Jansen MLA, Bracher JM, Papapetridis I, Verhoeven MD, de Bruijn H, de Waal PP, van Maris AJA, Klaassen P, Pronk JT. *Saccharomyces cerevisiae* strains for second-generation ethanol production: from academic exploration to industrial implementation. *FEMS Yeast Res.* 2017;fox044.
3. Della-Bianca BE, Basso TO, Stambuk BU, Basso LC, Gombert AK. What do we know about the yeast strains from the Brazilian fuel ethanol industry? *Appl Microbiol Biotechnol.* 2013;97:979-91.
4. Nielsen J, Larsson C, van Maris AJA, Pronk JT. Metabolic engineering of yeast for production of fuels and chemicals. *Curr Opin Biotechnol.* 2013;24:398-404.
5. Gombert AK, van Maris AJA. Improving conversion yield of fermentable sugars into fuel ethanol in 1st generation yeast-based production processes. *Curr Opin Biotechnol.* 2015;33:81-86.
6. Lopes ML, de Lima Paulillo SC, Godoy A, Cherubin RA, Lorenzi MS, Giometti FHC, Bernardino CD, Berbert de Amorim Neto H, Vianna de Amorim H. Ethanol production in Brazil: a bridge between science and industry. *Braz J Microbiol.* 2016;47:64-76.
7. Maiorella BL, Blanch HW, Wilke CR, Charles EWIB. Economic evaluation of alternative ethanol fermentation processes. *Biotechnol Bioeng.* 2009;104:419-43.
8. Nissen TL, Kielland-Brandt MC, Nielsen J, Villadsen J. Optimization of ethanol production in *Saccharomyces cerevisiae* by metabolic engineering of the ammonium assimilation. *Metab Eng.* 2000;2:69-77.
9. Van Dijken JP, Scheffers WA. Redox balances in the metabolism of sugars by yeasts. *FEMS Microbiol Lett.* 1986;32:199-224.
10. Verduyn C, Postma E, Scheffers WA, van Dijken JP. Physiology of *Saccharomyces cerevisiae* in anaerobic glucose-limited chemostat cultures. *J Gen Microbiol.* 1990;136:395-403.
11. Bishop WR, Bell RM. Assembly of phospholipids into cellular membranes: biosynthesis, transmembrane movement and intracellular translocation. *Ann Rev Cell Biol.* 1988;4:579-610.
12. Athenstaedt K, Daum G. 1-Acyldihydroxyacetone-phosphate reductase (Ayr1p) of the yeast *Saccharomyces cerevisiae* encoded by the open reading frame *YIL124w* is a major component of lipid particles. *J Biol Chem.* 2000;275:235-40.
13. Hohmann S. Osmotic stress signaling and osmoadaptation in yeasts. *Microbiol Mol Biol Rev.* 2002;66:300-72.
14. Nevoigt E, Stahl U. Osmoregulation and glycerol metabolism in the yeast *Saccharomyces cerevisiae*. *FEMS Microbiol Rev.* 1997;21:231-41.
15. Babazadeh R, Lahtvee P-J, Adiels CB, Goksör M, Nielsen JB, Hohmann S. The yeast osmostress response is carbon source dependent. *Sci Rep.* 2017;7:990.
16. Albertyn J, Hohmann S, Thevelein JM, Prior BA. *GPD1*, which encodes glycerol-3-phosphate dehydrogenase, is essential for growth under osmotic stress in *Saccharomyces cerevisiae*, and its expression is regulated by the high-osmolarity glycerol response pathway. *Mol Cell Biol.* 1994;14:4135-44.
17. Ansell R, Granath K, Hohmann S, Thevelein JM, Adler L. The two isoenzymes for yeast NAD⁺-dependent glycerol 3-phosphate dehydrogenase encoded by *GPD1* and *GPD2* have distinct roles in osmoadaptation and redox regulation. *EMBO J.* 1997;16:2179-87.
18. Larsson K, Ansell R, Eriksson P, Adler L. A gene encoding sn-glycerol 3-phosphate dehydrogenase (NAD⁺) complements an osmosensitive mutant of *Saccharomyces cerevisiae*. *Mol Microbiol.* 1993;10:1101-11.

19. Björkqvist S, Ansell R, Adler L, Lidén G. Physiological response to anaerobicity of glycerol-3-phosphate dehydrogenase mutants of *Saccharomyces cerevisiae*. *Appl Environ Microbiol*. 1997;63:128-32.
20. Guadalupe-Medina V, Almering MJH, van Maris AJA, Pronk JT. Elimination of glycerol production in anaerobic cultures of a *Saccharomyces cerevisiae* strain engineered to use acetic acid as an electron acceptor. *Appl Environ Microbiol*. 2010;76:190-95.
21. Guadalupe-Medina V, Metz B, Oud B, van Der Graaf CM, Mans R, Pronk JT, van Maris AJA. Evolutionary engineering of a glycerol-3-phosphate dehydrogenase-negative, acetate-reducing *Saccharomyces cerevisiae* strain enables anaerobic growth at high glucose concentrations. *Microb Biotechnol*. 2014;7:44-53.
22. Papapetridis I, van Dijk M, van Maris AJA, Pronk JT. Metabolic engineering strategies for optimizing acetate reduction, ethanol yield and osmotolerance in *Saccharomyces cerevisiae*. *Biotechnol Biofuels*. 2017;10:107.
23. Klinke HB, Thomsen AB, Ahring BK. Inhibition of ethanol-producing yeast and bacteria by degradation products produced during pre-treatment of biomass. *Appl Microbiol Biotechnol*. 2004;66:10-26.
24. Palmqvist E, Hahn-Hägerdal B. Fermentation of lignocellulosic hydrolysates. II: inhibitors and mechanisms of inhibition. *Bioresour Technol*. 2000;74:25-33.
25. Bro C, Regenber B, Förster J, Nielsen J. In silico aided metabolic engineering of *Saccharomyces cerevisiae* for improved bioethanol production. *Metab Eng*. 2006;8:102-11.
26. Palmqvist E, Grage H, Meinander NQ, Hahn-Hägerdal B. Main and interaction effects of acetic acid, furfural, and p-hydroxybenzoic acid on growth and ethanol productivity of yeasts. *Biotechnol Bioeng*. 1999;63:46-55.
27. Taherzadeh MJ, Niklasson C, Lidén G. Acetic acid—friend or foe in anaerobic batch conversion of glucose to ethanol by *Saccharomyces cerevisiae*? *Chem Eng Sci*. 1997;52:2653-59.
28. Guadalupe-Medina V, Wisselink HW, Luttik MA, de Hulster E, Daran J-MG, Pronk JT, van Maris AJA. Carbon dioxide fixation by Calvin-Cycle enzymes improves ethanol yield in yeast. *Biotechnol Biofuels*. 2013;6:125-25.
29. Entian K-D, Kötter P. 25 yeast genetic strain and plasmid collections. *Methods Microbiol*. 2007;36:629-66.
30. Nijkamp JF, van den Broek M, Datema E, de Kok S, Bosman L, Luttik MA, Daran-Lapujade P, Vongsangnak W, Nielsen J, Heijne WH, et al. De novo sequencing, assembly and analysis of the genome of the laboratory strain *Saccharomyces cerevisiae* CEN.PK113-7D, a model for modern industrial biotechnology. *Microb Cell Fact*. 2012;11:36.
31. Verduyn C, Postma E, Scheffers WA, van Dijken JP. Effect of benzoic acid on metabolic fluxes in yeasts: A continuous-culture study on the regulation of respiration and alcoholic fermentation. *Yeast*. 1992;8:501-17.
32. DiCarlo JE, Norville JE, Mali P, Rios X, Aach J, Church GM. Genome engineering in *Saccharomyces cerevisiae* using CRISPR-Cas systems. *Nucleic Acids Res*. 2013;41:4336-43.
33. Mikkelsen MD, Buron LD, Salomonsen B, Olsen CE, Hansen BG, Mortensen UH, Halkier BA. Microbial production of indolyglucosinolate through engineering of a multi-gene pathway in a versatile yeast expression platform. *Metab Eng*. 2012;14:104-11.
34. Mans R, van Rossum HM, Wijsman M, Backx A, Kuijpers NGA, van den Broek M, Daran-Lapujade P, Pronk JT, van Maris AJA, Daran J-MG. CRISPR/Cas9: a molecular Swiss army knife for simultaneous introduction of multiple genetic modifications in *Saccharomyces cerevisiae*. *FEMS Yeast Res*. 2015;15:fov004.
35. Knijnenburg TA, Daran J-MG, van den Broek MA, Daran-Lapujade P, de Winde JH, Pronk JT, Reinders MJT, Wessels LFA. Combinatorial effects of environmental parameters on transcriptional regulation in *Saccharomyces cerevisiae*: A quantitative analysis of a compendium of chemostat-based transcriptome data. *BMC Genom*. 2009;10:53-53.

36. Daniel Gietz R, Woods RA. Transformation of yeast by lithium acetate/single-stranded carrier DNA/polyethylene glycol method. *Methods Enzymol.* 2002;350:87-96.
37. Solis-Escalante D, Kuijpers NGA, Bongaerts N, Bolat I, Bosman L, Pronk JT, Daran J-MG, Daran-Lapujade P. *amdSYM*, a new dominant recyclable marker cassette for *Saccharomyces cerevisiae*. *Fems Yeast Res.* 2013;13:126-39.
38. Mumberg D, Müller R, Funk M. Yeast vectors for the controlled expression of heterologous proteins in different genetic backgrounds. *Gene.* 1995;156:119-22.
39. Papapetridis I, van Dijk M, Dobbe AP, Metz B, Pronk JT, van Maris AJA. Improving ethanol yield in acetate-reducing *Saccharomyces cerevisiae* by cofactor engineering of 6-phosphogluconate dehydrogenase and deletion of *ALD6*. *Microb Cell Fact.* 2016;15:67.
40. Mashego MR, van Gulik WM, Vinke JL, Heijnen JJ. Critical evaluation of sampling techniques for residual glucose determination in carbon-limited chemostat culture of *Saccharomyces cerevisiae*. *Biotechnol Bioeng.* 2003;83:395-99.
41. Heijnen JJ, Van Dijken JP. In search of a thermodynamic description of biomass yields for the chemotrophic growth of microorganisms. *Biotechnol Bioeng.* 1992;39:833-58.
42. Postma E, Verduyn C, Scheffers WA, van Dijken JP. Enzymic analysis of the crabtree effect in glucose-limited chemostat cultures of *Saccharomyces cerevisiae*. *Appl Environ Microbiol.* 1989;55:468-77.
43. MacElroy RD, Mack HM, Johnson EJ. Properties of phosphoribulokinase from *Thiobacillus neapolitanus*. *J Bacteriol.* 1972;112:532-38.
44. Lowry OH, Rosebrough NJ, Farr AL, Randall RJ. Protein measurement with the folin phenol reagent. *J Biol Chem.* 1951;193:265-75.
45. Van Rossum HM, Kozak BU, Niemeijer MS, Dykstra JC, Luttik MAH, Daran J-MG, van Maris AJA, Pronk JT. Requirements for carnitine shuttle-mediated translocation of mitochondrial acetyl moieties to the yeast cytosol. *mBio.* 2016;7.
46. Haase S, Reed S. Improved flow cytometric analysis of the budding yeast cell cycle. *Cell Cycle.* 2002;1:132-6.
47. Bracher JM, de Hulster E, Koster CC, van den Broek M, Daran J-MG, van Maris AJA, Pronk JT. Laboratory evolution of a biotin-requiring *Saccharomyces cerevisiae* strain for full biotin prototrophy and identification of causal mutations. *Appl Environ Microbiol.* 2017.
48. Verhoeven MD, Lee M, Kamoen L, van den Broek M, Janssen DB, Daran J-MG, van Maris AJA, Pronk JT. Mutations in *PMR1* stimulate xylose isomerase activity and anaerobic growth on xylose of engineered *Saccharomyces cerevisiae* by influencing manganese homeostasis. *Sci Rep.* 2017;7:46155.
49. Walker BJ, Abeel T, Shea T, Priest M, Abouelliel A, Sakthikumar S, Cuomo CA, Zeng Q, Wortman J, Young SK, Earl AM. Pilon: An integrated tool for comprehensive microbial variant detection and genome assembly improvement. *PLOS ONE.* 2014;9:e112963.
50. Li H, Durbin R. Fast and accurate long-read alignment with Burrows-Wheeler transform. *Bioinformatics.* 2010;26:589-95.
51. Li H, Handsaker B, Wysoker A, Fennell T, Ruan J, Homer N, Marth G, Abecasis G, Durbin R, Genome Project Data Processing S. The sequence alignment/map format and SAMtools. *Bioinformatics.* 2009;25:2078-79.
52. Van den Brink J, Akeroyd M, van der Hoeven R, Pronk JT, de Winde JH, Daran-Lapujade P. Energetic limits to metabolic flexibility: responses of *Saccharomyces cerevisiae* to glucose-galactose transitions. *Microbiology.* 2009;155:1340-50.
53. Pronk JT. Auxotrophic yeast strains in fundamental and applied research. *App Environ Microbiol.* 2002;68:2095-100.
54. Da Silva NA, Srikrishnan S. Introduction and expression of genes for metabolic engineering applications in *Saccharomyces cerevisiae*. *FEMS Yeast Res.* 2012;12:197-214.
55. Shi S, Liang Y, Zhang MM, Ang EL, Zhao H. A highly efficient single-step, markerless strategy for multi-copy chromosomal integration of large biochemical pathways in *Saccharomyces cerevisiae*. *Metab Eng.* 2016;33:19-27.

56. Parikh MR, Greene DN, Woods KK, Matsumura I. Directed evolution of RuBisCO hypermorphs through genetic selection in engineered *E.coli*. *Protein Eng Des Sel*. 2006;19:113-19.
57. Hudson G, Morell M, Arvidsson Y, Andrews T. Synthesis of spinach phosphoribulokinase and ribulose 1,5-bisphosphate in *Escherichia coli*. *Funct Plant Biol*. 1992;19:213-21.
58. Snoep JL, Yomano LP, Westerhoff HV, Ingram LO. Protein burden in *Zymomonas mobilis*: negative flux and growth control due to overproduction of glycolytic enzymes. *Microbiology*. 1995;141:2329-37.
59. Hubmann G, Guillouet S, Nevoigt E. Gpd1 and Gpd2 fine-tuning for sustainable reduction of glycerol formation in *Saccharomyces cerevisiae*. *Appl Environ Microbiol*. 2011;77:5857-67.
60. Nissen TL, Hamann CW, Kielland-Brandt MC, Nielsen J, Villadsen J. Anaerobic and aerobic batch cultivations of *Saccharomyces cerevisiae* mutants impaired in glycerol synthesis. *Yeast*. 2000;16:463-74.
61. Kuyper M, Hartog MMP, Toirkens MJ, Almering MJH, Winkler AA, van Dijken JP, Pronk JT. Metabolic engineering of a xylose-isomerase-expressing *Saccharomyces cerevisiae* strain for rapid anaerobic xylose fermentation. *FEMS Yeast Res*. 2005;5:399-409.
62. Wisselink HW, Cipollina C, Oud B, Crimi B, Heijnen JJ, Pronk JT, van Maris AJA. Metabolome, transcriptome and metabolic flux analysis of arabinose fermentation by engineered *Saccharomyces cerevisiae*. *Metab Eng*. 2010;12:537-51.
63. Walfridsson M, Hallborn J, Penttilä M, Keränen S, Hahn-Hägerdal B. Xylose-metabolizing *Saccharomyces cerevisiae* strains overexpressing the *TKL1* and *TAL1* genes encoding the pentose phosphate pathway enzymes transketolase and transaldolase. *Appl Environ Microbiol*. 1995;61:4184-90.
64. Karhumaa K, Hahn-Hägerdal B, Gorwa-Grauslund M-F. Investigation of limiting metabolic steps in the utilization of xylose by recombinant *Saccharomyces cerevisiae* using metabolic engineering. *Yeast*. 2005;22:359-68.
65. Gorter de Vries AR, Pronk JT, Daran J-MG. Industrial relevance of chromosomal copy number variation in *Saccharomyces* yeasts. *Appl Environ Microbiol*. 2017;83:e03206-16.
66. Calvin M, Benson AA. The path of carbon in photosynthesis. *Science*. 1948;107:476-80.
67. Ducat DC, Silver PA. Improving carbon fixation pathways. *Curr Opin Chemical Biol*. 2012;16:337-44.
68. Lin MT, Occhialini A, Andralojc PJ, Parry MAJ, Hanson MR. A faster RubisCO with potential to increase photosynthesis in crops. *Nature*. 2014;513:547-50.
69. McKinlay JB, Harwood CS. Carbon dioxide fixation as a central redox cofactor recycling mechanism in bacteria. *PNAS*. 2010;107:11669-75.
70. Gong F, Liu G, Zhai X, Zhou J, Cai Z, Li Y. Quantitative analysis of an engineered CO₂-fixing *Escherichia coli* reveals great potential of heterotrophic CO₂ fixation. *Biotechnol Biofuels*. 2015;8:86.
71. Bischoff KM, Liu S, Leathers TD, Worthington RE, Rich JO. Modeling bacterial contamination of fuel ethanol fermentation. *Biotechnol Bioeng*. 2009;103:117-22.
72. Jain VK, Divol B, Prior BA, Bauer FF. Elimination of glycerol and replacement with alternative products in ethanol fermentation by *Saccharomyces cerevisiae*. *J Ind Microbiol Biotechnol*. 2011;38:1427-35.
73. Wu G, Yan Q, Jones JA, Tang YJ, Fong SS, Koffas MAG. Metabolic burden: Cornerstones in synthetic biology and metabolic engineering applications. *Trends Biotechnol*. 2016;34:652-64.
74. Aigner H, Wilson RH, Bracher A, Calisse L, Bhat JY, Hartl FU, Hayer-Hartl M. Plant RuBisCo assembly in *E. coli* with five chloroplast chaperones including BSD2. *Science*. 2017;358:1272-78.
75. Temer B, dos Santos LV, Negri VA, Galhardo JP, Magalhães PHM, José J, Marschalk C, Corrêa TLR, Carazzolle MF, Pereira GAG. Conversion of an inactive xylose isomerase into a functional enzyme by co-expression of GroEL-GroES chaperonins in *Saccharomyces cerevisiae*. *BMC Biotechnol*. 2017;17:71.

76. Jariyachawalid K, Laowanapiban P, Meevootisom V, Wiyakrutta S. Effective enhancement of *Pseudomonas stutzeri* D-phenylglycine aminotransferase functional expression in *Pichia pastoris* by co-expressing *Escherichia coli* GroEL-GroES. *Microb Cell Fact*. 2012;11:47.
77. Xia PF, Turner TL, Jayakody LN. The role of GroE chaperonins in developing biocatalysts for biofuel and chemical production. *Enz Eng*. 2016;5.
78. Li Y-J, Wang M-M, Chen Y-W, Wang M, Fan L-H, Tan T-W. Engineered yeast with a CO₂-fixation pathway to improve the bio-ethanol production from xylose-mixed sugars. *Sci Rep*. 2017;7:43875.
79. Bellissimi E, Ingledew WM. Metabolic acclimatization: preparing active dry yeast for fuel ethanol production. *Process Biochem*. 2005;40:2205-13.
80. Wisselink HW, Toirkens MJ, del Rosario Franco Berriel M, Winkler AA, van Dijken JP, Pronk JT, van Maris AJA. Engineering of *Saccharomyces cerevisiae* for efficient anaerobic alcoholic fermentation of l-arabinose. *App Environ Microbiol*. 2007;73:4881-91.
81. Becker J, Boles E. A modified *Saccharomyces cerevisiae* strain that consumes l-arabinose and produces ethanol. *App Environ Microbiol*. 2003;69:4144-50.
82. Boer VM, Crutchfield CA, Bradley PH, Botstein D, Rabinowitz JD. Growth-limiting intracellular metabolites in yeast growing under diverse nutrient limitations. *Mol Biol Cell*. 2010;21:198-211.
83. Nickbarg EB, Knowles JR. Triosephosphate isomerase: energetics of the reaction catalyzed by the yeast enzyme expressed in *Escherichia coli*. *Biochemistry*. 1988;27:5939-47.
84. Christen S, Sauer U. Intracellular characterization of aerobic glucose metabolism in seven yeast species by ¹³C flux analysis and metabolomics. *FEMS Yeast Res*. 2011;11:263-72.
85. Schenk G, Duggleby RG, Nixon PF. Properties and functions of the thiamin diphosphate dependent enzyme transketolase. *Int J Biochem Cell Biol*. 1998;30:1297-318.
86. Oud B, Guadalupe-Medina V, Nijkamp JF, De Ridder D, Pronk JT, van Maris AJA, Daran J-MG. Genome duplication and mutations in *ACE2* cause multicellular, fast-sedimenting phenotypes in evolved *Saccharomyces cerevisiae*. *PNAS*. 2013;110.
87. Voordeckers K, Kominek J, Das A, Espinosa-Cantú A, De Maeyer D, Arslan A, Van Pee M, van der Zande E, Meert W, Yang Y, et al. Adaptation to high ethanol reveals complex evolutionary pathways. *PLoS Genet*. 2015;11:e1005635.
88. Wellington M, Rustchenko E. 5-fluoro-oroic acid induces chromosome alterations in *Candida albicans*. *Yeast*. 2005;15:57-70.
89. Stovicek V, Borodina I, Forster J. CRISPR-Cas system enables fast and simple genome editing of industrial *Saccharomyces cerevisiae* strains. *Metab Eng Commun*. 2015;2:13-22.
90. Shen B, Hohmann S, Jensen RG, Bohnert, Hans J. Roles of sugar alcohols in osmotic stress adaptation. Replacement of glycerol by mannitol and sorbitol in yeast. *Plant Physiol*. 1999;121:45-52.
91. Hounsa C-G, Brandt EV, Thevelein J, Hohmann S, Prior BA. Role of trehalose in survival of *Saccharomyces cerevisiae* under osmotic stress. *Microbiology*. 1998;144:671-80.
92. Guo Z-P, Zhang L, Ding Z-Y, Shi G-Y. Minimization of glycerol synthesis in industrial ethanol yeast without influencing its fermentation performance. *Metab Eng*. 2011;13:49-59.
93. Hirayama T, Maeda T, Saito H, Shinozaki K. Cloning and characterization of seven cDNAs for hyperosmolarity-responsive (HOR) genes of *Saccharomyces cerevisiae*. *Mol Gen Genet*. 1995;249:127-38.

Chapter 3

Improving ethanol yield in acetate-reducing *Saccharomyces cerevisiae* by cofactor engineering of 6-phosphogluconate dehydrogenase and deletion of *ALD6*

Ioannis Papapetridis, Marlous van Dijk, Arthur PA Dobbe, Benjamin Metz, Jack T Pronk and Antonius JA van Maris

Essentially as published in *Microbial Cell Factories* 2016 15:67 (doi: 10.1186/s12934-016-0465-z)

Abstract

Acetic acid, an inhibitor of sugar fermentation by yeast, is invariably present in lignocellulosic hydrolysates which are used or considered as feedstocks for yeast-based bioethanol production. *Saccharomyces cerevisiae* strains have been constructed, in which anaerobic reduction of acetic acid to ethanol replaces glycerol formation as a mechanism for reoxidizing NADH formed in biosynthesis. An increase in the amount of acetate that can be reduced to ethanol should further decrease acetic acid concentrations and enable higher ethanol yields in industrial processes based on lignocellulosic feedstocks. The stoichiometric requirement of acetate reduction for NADH implies that increased generation of NADH in cytosolic biosynthetic reactions should enhance acetate consumption. Replacement of the native NADP⁺-dependent 6-phosphogluconate dehydrogenase in *S. cerevisiae* by a prokaryotic NAD⁺-dependent enzyme resulted in increased cytosolic NADH formation, as demonstrated by a ca. 15% increase in the glycerol yield on glucose in anaerobic cultures. Additional deletion of *ALD6*, which encodes an NADP⁺-dependent acetaldehyde dehydrogenase, led to a 39% increase in the glycerol yield compared to a non-engineered strain. Subsequent replacement of glycerol formation by an acetate reduction pathway resulted in a 44% increase of acetate consumption per amount of biomass formed, as compared to an engineered, acetate-reducing strain that expressed the native 6-phosphogluconate dehydrogenase and *ALD6*. Compared to a non-acetate reducing reference strain under the same conditions, this resulted in a ca. 13% increase in the ethanol yield on glucose. The combination of NAD⁺-dependent 6-phosphogluconate dehydrogenase expression and deletion of *ALD6* resulted in a marked increase in the amount of acetate that was consumed in these proof-of-principle experiments, and this concept is ready for further testing in industrial strains as well as in hydrolysates. Altering the cofactor specificity of the oxidative branch of the pentose-phosphate pathway in *S. cerevisiae* can also be used to increase glycerol production in wine fermentation and to improve NADH generation and/or generation of precursors derived from the pentose-phosphate pathway in other industrial applications of this yeast.

3.1 Introduction

The intensive use of fossil resources by mankind presents one of the great challenges of our time and many research efforts focus on seeking sustainable alternatives for petrochemistry-based production of transport fuels and chemicals. One of these alternatives is the microbial conversion of hydrolysates of lignocellulosic plant biomass into fuel ethanol. *Saccharomyces cerevisiae* is a major candidate for this application, because of its naturally high ethanol yield on sugar and tolerance to inhibitors and low pH values [22,38,64]. In addition to these natural attributes, robust performance of *S. cerevisiae* in lignocellulosic hydrolysates requires tolerance to the organic acids, furans and phenols that are released during biomass pre-treatment.

One of the most important inhibitors released during hemicellulose hydrolysis is acetic acid, whose concentration in lignocellulosic hydrolysates can exceed 10 g L^{-1} [28]. As for all weak organic acids in solution, the relative concentrations of the un- and dissociated (acetate) forms of acetic acid are determined by its acid-dissociation constant (pKa) and by the extant pH. Industrial fermentation processes with *S. cerevisiae* are typically performed at pH values close to the pKa of acetic acid (4.75). This implies that a substantial fraction of the acid will be present in its non-dissociated form, which can diffuse across the yeast plasma membrane. Upon entry into the near-neutral yeast cytosol (pH 6.5-7 during exponential growth [42]), acetic acid will dissociate and release a proton. To avoid acidification of the cytosol, protons have to be expelled by the yeast plasma membrane ATPase. This proton export requires 1 ATP per proton, while additional metabolic energy may be required to expel the acetate anion [44,46]. At low to moderate concentrations of acetic acid ($1\text{-}3 \text{ g L}^{-1}$) and at pH values of 4 to 5, this increased demand for ATP results in lower biomass and glycerol yields and a higher ethanol yield on glucose in anaerobic cultures of *S. cerevisiae* [2,27,46]. However, at higher acetic acid concentrations (or at a lower pH), cells can no longer meet the energy requirements for pH homeostasis and can no longer prevent acidification of the cytosol, leading to inhibition of fermentation and growth [32,60]. Inhibition by acetic acid is even more pronounced when engineered yeast strains utilise xylose, a major component of lignocellulosic hydrolysates, as a

carbon source [2]. The variability in acetic acid sensitivity of glucose- and xylose-grown cultures has been attributed to the sugar fermentation rates with these sugars, with a slower fermentation of xylose constraining the maximum rate of proton export via the plasma-membrane ATPase. In addition to the impact of acetic acid on intracellular pH homeostasis, intracellular accumulation of the acetate anion has been linked to increased oxidative stress and inhibition of key enzymes, such as aldolase [45], transaldolase and transketolase [23].

Although removal of acetic acid and other inhibitors from lignocellulosic hydrolysates can be achieved through chemical or biological detoxification, such additional steps are costly and can cause loss of fermentable substrate [28,43,47,59]. Therefore, development of stress-resistant yeast strains has received considerable attention. Acetic acid tolerance, which differs among *S. cerevisiae* strains, is a multi-gene trait [23,35,58] which has been the objective of metabolic and evolutionary engineering studies [51,55,70]. Guadalupe-Medina et al. [20] first explored the *in situ* reduction of acetic acid to ethanol as an alternative strategy to combat acetic acid toxicity. Under anaerobic conditions, wild-type strains of *S. cerevisiae* cannot metabolise acetic acid [44]. Expression of the *E. coli mhpF* gene, which encodes an NAD⁺-dependent acetylating acetaldehyde dehydrogenase, introduced a pathway for NADH-dependent reduction of acetic acid to ethanol into *S. cerevisiae*. When combined with inactivation of the *GPD1* and *GPD2* genes, which encode glycerol-3-phosphate dehydrogenase and are essential for glycerol production, reoxidation of NADH formed in biosynthesis was coupled to the reduction of acetic acid to ethanol [20]. This approach completely abolished the formation of glycerol which, after biomass and CO₂, is the most important by-product of industrial ethanol production. The ensuing 13% increase in the apparent ethanol yield on sugar was caused by the elimination of carbon loss to glycerol and the conversion of acetic acid to additional ethanol. In addition to improving the ethanol yield on sugar, this metabolic engineering strategy enabled a partial *in situ* detoxification of acetic acid by the yeast. However, the amount of acetic acid that can be converted by the engineered yeast strain is limited by the amount of NADH resulting from

biosynthesis which, in anaerobic cultures of wild-type yeast, is reoxidized via the formation of glycerol [63,68].

The goal of the present study is to explore a metabolic engineering strategy for increasing the amount of acetic acid that can be reduced to ethanol in anaerobic *S. cerevisiae* cultures. The proposed strategy aims to increase the formation of surplus cytosolic NADH in biosynthesis by replacing the native NADP⁺-dependent yeast 6-phosphogluconate dehydrogenase (encoded by *GND1* and *GND2* [54]) with a prokaryotic NAD⁺-dependent enzyme. 6-phosphogluconate dehydrogenase (6-PGDH) catalyses the oxidative decarboxylation of 6-phospho-D-gluconate to D-ribulose-5-phosphate. In *S. cerevisiae*, this reaction is strictly NADP⁺-dependent and part of the oxidative pentose-phosphate pathway, the major NADPH-providing pathway in this yeast [4,54]. First, the predicted impact of this strategy on increasing NADH availability was evaluated by a theoretical stoichiometric analysis. Subsequently, three candidate genes encoding heterologous NAD⁺-dependent 6-phosphogluconate dehydrogenases were tested for functional expression in *S. cerevisiae*. One of these genes was then expressed in a reference strain of *S. cerevisiae* and in strain backgrounds that contained additional modifications. The final set of strains also included strains in which the glycerol production pathway had been replaced by an acetate reduction pathway. The physiological impact of these redox-cofactor engineering interventions on product yields and acetate conversion was quantitatively analysed in anaerobic bioreactor cultures.

3.2 Methods

3.2.1 Strains and maintenance

All *S. cerevisiae* strains used in this study (Table 1) were based on the CEN.PK lineage [13,39]. Stock cultures of *S. cerevisiae* were propagated in synthetic medium [67] or YP medium (10 g L⁻¹ Bacto yeast extract, 20 g L⁻¹ Bacto peptone). 20 g L⁻¹ glucose was added as carbon source. Stock cultures of *E. coli* *XL-1* blue were propagated in LB medium (10 g L⁻¹ Bacto tryptone, 5 g L⁻¹ Bacto yeast extract, 5 g L⁻¹ NaCl), supplemented with 100 µg mL⁻¹ ampicillin or 50 µg mL⁻¹ kanamycin.

After addition of glycerol to a concentration of 30% v/v to stationary-phase cultures, samples were frozen and stored at -80 °C.

Table 1. *S. cerevisiae* strains used in this study.

Strain name	Relevant Genotype	Origin
CEN.PK113-7D	<i>MATa MAL2-8c SUC2</i>	[13]
IMX585	<i>MATa MAL2-8c SUC2 can1::cas9-natNT2</i>	[33]
IMX643	<i>MATa MAL2-8c SUC2 can1::cas9-natNT2 gnd2Δ</i>	This work
IMX899	<i>MATa MAL2-8c SUC2 can1::cas9-natNT2 ald6Δ</i>	This work
IMX705	<i>MATa MAL2-8c SUC2 can1::cas9-natNT2 gnd2Δ gnd1::gndA</i>	This work
IMX706	<i>MATa MAL2-8c SUC2 can1::cas9-natNT2 gnd2Δ gnd1::6pgdh</i>	This work
IMX707	<i>MATa MAL2-8c SUC2 can1::cas9-natNT2 gnd2Δ gnd1::gox1705</i>	This work
IMX756	<i>MATa MAL2-8c SUC2 can1::cas9-natNT2 gnd2Δ gnd1::gndA ald6Δ</i>	This work
IMX817	<i>MATa MAL2-8c SUC2 can1::cas9-natNT2 gnd2Δ gnd1::gndA ald6Δ gpd2::eutE</i>	This work
IMX860	<i>MATa MAL2-8c SUC2 can1::cas9-natNT2 gnd2Δ gnd1::gndA ald6Δ gpd2::eutE gpd1Δ</i>	This work
IMX883	<i>MATa MAL2-8c SUC2 can1::cas9-natNT2 gpd2::eutE</i>	This work
IMX888	<i>MATa MAL2-8c SUC2 can1::cas9-natNT2 gpd2::eutE gpd1Δ</i>	This work

Table 2. Plasmids used in this study.

Name	Characteristics	Origin
pBOL199	Delivery vector, p426- <i>TDH3p-eutE</i>	[36]
pMEL11	2 μm ori, <i>amdS</i> , <i>SNR52p-gRNA.CAN1.Y-SUP4t</i>	[33]
pROS11	<i>AmdSYM-gRNA.CAN1-2mu-gRNA.ADE2</i>	[33]
pUDE197	2 μm ori, p426- <i>TDH3p-eutE-CYC1t</i>	This work
pUDI076	pRS406- <i>TDH3p-eutE-CYC1t</i>	This work
pUDR122	2 μm ori, <i>amdS</i> , <i>SNR52p-gRNA.GND2.Y-SUP4t</i>	This work
pUDR123	2 μm ori, <i>amdS</i> , <i>SNR52p-gRNA.GND1.Y-SUP4t</i>	This work
pMK-RQ- <i>gndA</i>	Delivery vector, <i>TP1p-gndA-CYC1t</i>	GeneArt, Germany
pMK-RQ- <i>6pgdH</i>	Delivery vector, <i>TP1p-6pgdh-CYC1t</i>	GeneArt, Germany
pMK-RQ- <i>gox1705</i>	Delivery vector, <i>TP1p-gox1705-CYC1t</i>	GeneArt, Germany

3.2.2 Plasmid and cassette construction

Yeast genetic modifications were performed using a chimeric CRISPR/Cas9 genome-editing system [11]. Plasmid pMEL11 [33] was used to individually delete *GND1*, *GND2* and *ALD6*. Plasmid pROS11 [33] was used to delete *GPD1* and *GPD2*. Unique CRISPR/Cas9 target sequences in each of these genes were identified based on a provided list [11]. Plasmid backbones of pMEL11 and pROS11 were PCR amplified using primers 5792-5980 and the double-binding primer 5793 (Supplementary Table S1), respectively. Oligonucleotides were custom synthesized

by Sigma-Aldrich, St. Louis, MO, USA. Plasmid insert sequences, expressing the 20 bp gRNA-targeting sequence, were obtained by PCR with primer combinations 5979-7365 for *GND1*, 5979-7231 for *GND2* and 5979-7610 for *ALD6*, using pMEL11 as a template. Insert sequences expressing the gRNA sequences targeting *GPD1* and *GPD2* were obtained by PCR using the double-binding primers 6965 and 6966, respectively, with pROS11 as template. PCR amplifications for construction of plasmids and expression cassettes were performed using Phusion® High Fidelity DNA Polymerase (Thermo Scientific, Waltham, MA, USA), according to the manufacturer's guidelines. Plasmid pre-assembly was performed using the Gibson Assembly® Cloning kit (New England Biolabs, Ipswich, MA, USA) according to the supplier's protocol, downscaled to 10 µl total volume. Assembly was enabled by homologous sequences at the 5' and 3' ends of the generated PCR fragments.

Assembly of the pMEL11 backbone and the insert sequences coding for the gRNAs targeting *GND1* and *GND2* yielded plasmids pUDR122 and pUDR123, respectively. In each case, 1 µL of the Gibson-assembly mix was used for electroporation of *E. coli XL-1* blue cells in a Gene PulserXcell Electroporation System (Biorad, Hercules, CA, USA). Plasmids were re-isolated from *E. coli* cultures using a Sigma GenElute Plasmid kit (Sigma-Aldrich). Correct assembly of plasmids was confirmed by diagnostic PCR (Dreamtaq®, Thermo Scientific) or restriction analysis. A list of the plasmids used in this study is presented in Table 2. The *ALD6*-, *GPD1*- and *GPD2*-gRNA-expressing plasmids were not pre-assembled. Instead, the backbone and insert fragments were transformed directly into yeast and plasmids were assembled *in vivo*.

Sequences of *Methylobacillus flagellatus* KT *gndA* [Genbank: AAF34407.1], *Gluconobacter oxydans* 621H *gox1705* [Genbank: AAW61445.1] and *Bradyrhizobium japonicum* USDA 110 *6pgdh* were codon optimized based on the codon composition of highly expressed glycolytic genes [69]. In the case of *B. japonicum*, the sequence of *6pgdh* was obtained by aligning its translated genomic sequence [Genbank: NC_004463.1] with the other two proteins (45% and 57% similarity respectively). In yeast integration cassettes, the codon-optimized coding sequences of these bacterial genes were flanked by the native yeast promoter of *TPI1* and the

terminator of *CYC1*. Complete expression cassettes [Genbank: KU601575, KU601576, KU601577] were synthesized by GeneArt GmbH (Regensburg, Germany) and delivered in pMK-RQ vectors (GeneArt). After cloning in *E. coli*, plasmids were re-isolated and used as templates for PCR amplification of the integration cassettes. The integration cassettes *TPI1p-gndA-CYC1t*, *TPI1p-6pgdH-CYC1t* and *TPI1p-gox1705-CYC1t* were obtained by PCR using, respectively, primer combination 7380-7381 and plasmids pMK-RQ-*gndA*, pMK-RQ-*6pgdH* and pMK-RQ-*gox1705* as templates.

A gene encoding *E. coli eutE* [Genbank: WP_001075673.1], codon-pair optimized for expression in *S. cerevisiae* [49] was obtained from pBOL199 by digestion with *XhoI/SpeI* and ligated into pAG426GPD-*ccdB* (Addgene, Cambridge, MA, USA), yielding the multi-copy plasmid pUDE197. For integration cassette preparation, *SacI/EagI*-digested pRS406 (Addgene) was used as a plasmid backbone and ligated with the *TDH3p-eutE-CYC1t* cassette [Genbank: KU601578], which was obtained from pUDE197 by digestion with the same restriction enzymes, yielding plasmid pUDI076.

The integration cassette *TDH3p-eutE-CYC1t* was amplified using primers 7991 and 7992 with plasmid pUDI076 as template. These primers were designed to add 60 bp of DNA sequence at the 5' and 3' ends of the PCR products, corresponding to the sequences directly upstream and downstream of the open-reading frames of the targeted chromosomal genes. The *TPI1p-gndA-CYC1t*, *TPI1p-6pgdH-CYC1t* and *TPI1p-gox1705-CYC1t* expression cassettes were targeted to *GND1* and the *TDH3p-eutE-CYC1t* cassette was targeted to *GPD2*.

3.2.3 Strain construction

Yeast transformations were performed using the lithium acetate method [16]. Selection of mutants was performed on synthetic medium agar plates (2% Bacto Agar, BD, Franklin Lakes, NJ) [67] with 20 g L⁻¹ glucose as carbon source and with acetamide as sole nitrogen source [56]. In each case, correct integration was verified by diagnostic PCR, using primer combinations binding outside the targeted loci as well as inside the coding sequences of the integrated

cassettes (Supplementary Table S1). Plasmid recycling after each transformation was performed as described previously [56].

Strain IMK643 was obtained by markerless CRISPR/Cas9-based deletion of *GND2* by co-transformation of the gRNA-expressing plasmid pUDR123 and the repair oligo nucleotides 7299-7300. The *TPI1p-gndA-CYC1t*, *TPI1p-6pgdH-CYC1t* and *TPI1p-gox1705-CYC1t* integration cassettes were transformed to IMK643, along with the gRNA expressing plasmid pUDR122, yielding strains IMX705, IMX706 and IMX707 respectively. Co-transformation of the pMEL11 backbone, the *ALD6*-targeting gRNA-expressing plasmid insert and the repair oligonucleotides 7608-7609 to strains IMX705 and IMX585 yielded strains IMX756 and IMX899 respectively, in which *ALD6* was deleted without integration of a marker. Co-transformation of the pROS11 backbone, the *GPD2*-targeting gRNA-expressing plasmid insert and the *TDH3p-eutE-CYC1t* integration cassette to strains IMX756 and IMX585 yielded strains IMX817 and IMX883 respectively. Markerless deletion of *GPD1* in strains IMX817 and IMX883 was performed by co-transformation of the pROS11 backbone, the *GPD1*-targeting gRNA-expressing plasmid insert and the repair oligo nucleotides 6967-6968, yielding strains IMX860 and IMX888 respectively.

3.2.4 Cultivation and media

Shake-flask cultures were grown in 500-mL flasks containing 100 mL of synthetic medium [67] supplemented with glucose to a final concentration of 20 g L⁻¹ under an air atmosphere. The pH was adjusted to 6 by addition of 2 M KOH before autoclaving at 120 °C for 20 min. Glucose solutions were autoclaved separately at 110 °C for 20 min and added to the sterile flasks. Vitamin solutions [67] were filter sterilized and added to the sterile flasks separately. Cultures were grown at 30 °C and shaken at 200 rpm. Initial pre-culture shake flasks were inoculated from frozen stocks in each case. After 8 to 12h, fresh pre-culture flasks were inoculated from the initial flasks. Cultures prepared in this way were used for shake-flask experiments or as inoculum for anaerobic bioreactor experiments. Bioreactors were inoculated from exponentially growing pre-culture flasks to an initial OD₆₆₀ of 0.2-0.3. Anaerobic batch cultivations were performed in 2-L Applikon bioreactors (Applikon, Schiedam, The Netherlands) with a 1-L

working volume. All anaerobic batch fermentations were performed in synthetic medium (20 g L⁻¹ glucose), prepared as described above. Anaerobic growth media additionally contained 0.2 g L⁻¹ sterile antifoam C (Sigma-Aldrich), ergosterol (10 mg L⁻¹) and Tween 80 (420 mg L⁻¹), added separately. Bioreactor cultivations were performed at 30 °C and at a stirrer speed of 800 rpm. Nitrogen gas (<10 ppm oxygen) was sparged through the cultures at 0.5 L min⁻¹ and culture pH was maintained at 5 by automated addition of 2 M KOH. Bioreactors were equipped with Norprene tubing and Viton O-rings to minimize oxygen diffusion. All strains and conditions were tested in independent duplicate cultures.

3.2.5 Analytical methods

Determination of optical density at 660 nm was done using a Libra S11 spectrophotometer (Biochrom, Cambridge, UK). Off-gas analysis, biomass dry weight measurements, HPLC analysis of culture supernatants and correction for ethanol evaporation in bioreactor experiments were performed as described previously [20]. For anaerobic batch cultures, biomass concentrations were estimated from OD₆₆₀ measurements, using calibration curves based of a minimum of six samples taken in mid-exponential phase for which both biomass dry weight and OD₆₆₀ were measured. Yields of each fermentation were calculated from a minimum of six samples taken during the mid-exponential growth phase by plotting either biomass against substrate, ethanol against substrate, glycerol against substrate, acetate against substrate, glycerol against biomass or acetate against biomass and calculating the absolute value of the slopes of the resulting linear fits.

3.2.6 Enzyme-activity assays

Cell extracts for *in vitro* enzyme-activity assays were prepared as described previously [30] from exponentially growing shake-flask cultures harvested at an OD₆₆₀ between 4 and 5. Spectrophotometric assays were performed at 30 °C and conversion of NAD⁺/NADP⁺ to NADH/NADPH was monitored by measuring absorbance at 340 nm. For NAD⁺- or NADP⁺-linked 6-phosphogluconate dehydrogenase, the 1-mL assay mixture contained 50 mM Tris-HCl (pH 8.0), 5 mM MgCl₂, 0.4 mM NAD⁺ or NADP⁺ and 50 or 100 μL of cell extract. Reactions were

started by addition of 6-phosphogluconate to a concentration of 5 mM. Glucose-6-phosphate dehydrogenase activity was routinely measured as a quality check of the cell extracts, using an assay mix containing 50 mM Tris-HCl (pH 8.0), 5 mM MgCl₂, 0.4 mM NADP⁺ and 50 or 100 μl of cell extract in a volume of 1 mL. The reaction was started by addition of glucose-6-phosphate to a concentration of 5 mM. NADP⁺-linked glucose-6-phosphate dehydrogenase activities in different cell extracts varied between 0.43 and 0.55 μmol (mg protein)⁻¹ min⁻¹. All assays were performed in duplicate and reaction rates were proportional to the amount of cell extract added.

3.3 Results

3.3.1 Theoretical analysis of the stoichiometric impact of altering the cofactor specificity of 6-PGDH

Based on the assumption that the oxidative pentose-phosphate pathway is the predominant source of NADPH in glucose-grown cultures of *S. cerevisiae* [4,68], replacing the native NADP⁺-dependent 6-phosphogluconate dehydrogenase with an NAD⁺-dependent enzyme should result in an increased growth-coupled formation of cytosolic NADH. To predict the impact of this cofactor switch on the glycerol yield in anaerobic, glucose-grown cultures, a stoichiometric analysis with lumped reactions for biosynthesis, NADPH formation, NADH reoxidation and ATP-generating alcoholic fermentation was performed (Supplementary Table S2). Calculations were based on a previous analysis of anaerobic, glucose-limited chemostat cultures of wild-type *S. cerevisiae* growing at a fixed specific growth rate of 0.10 h⁻¹ [68]. The flux distribution in central metabolism was determined for the formation of 1 g of biomass (indicated as g_x; Fig. 1; top numbers) based on an experimentally determined biomass yield on glucose of 0.103 g_x g⁻¹ [68], which corresponds to a glucose requirement of 53.94 mmol g_x⁻¹. In the analysis, lumped stoichiometries for biosynthesis, NADPH formation via the pentose-phosphate pathway, NADH reoxidation through glycerol formation and redox-neutral, ATP-generating alcoholic fermentation were described by Equations 1, 2, 3 and 4, respectively [68].

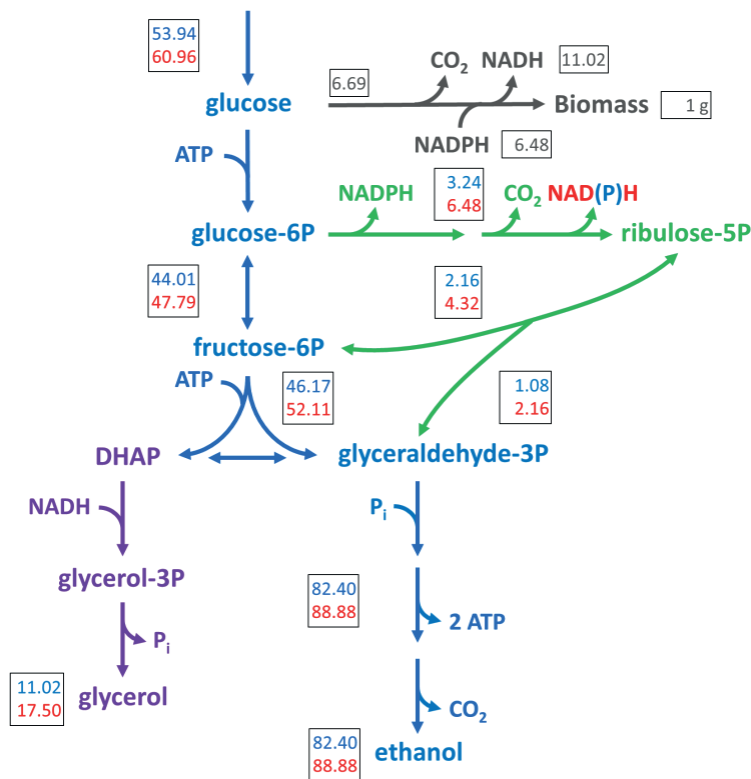
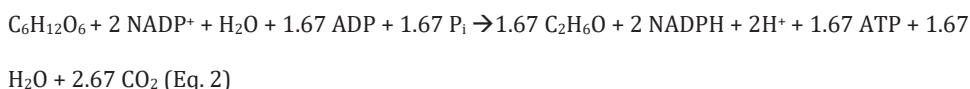
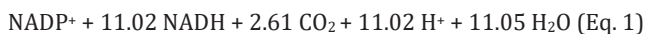
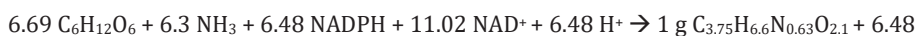
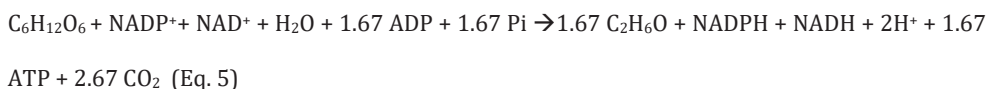


Figure 1. Theoretical stoichiometric comparison of the anaerobic metabolism of *S. cerevisiae* expressing a strictly NAD⁺-dependent 6-PGDH to wild-type *S. cerevisiae*. Numbers in boxes represent the carbon distribution and grey numbers in boxes represent the requirement for glucose and cofactors in mmol g⁻¹, normalized for the formation of 1 g of biomass in the two scenarios: native, NAD⁺-dependent 6-PGDH (top, blue colour) and heterologous, NAD⁺-dependent 6-PGDH (bottom, red colour). Blue: Glycolysis and alcoholic fermentation; Green: Pentose-phosphate pathway; Purple: Glycerol formation pathway; Grey: Biosynthesis according to [68], which, together with the ATP requirement for biosynthesis, was assumed to be identical for both scenarios. The oxidative branch of the pentose phosphate pathway was assumed to be the only NADPH formation pathway. Figure adapted from [21].



From Equations 1-4, anaerobic formation of 1 g of wild-type *S. cerevisiae* biomass from glucose can be calculated to require 71.38 mmol ATP for biosynthesis and 11.02 mmol ATP for NAD⁺ regeneration and to result in the formation of 11.02 mmol glycerol g^{x-1} and 82.4 mmol ethanol g^{x-1}. This corresponds to a predicted glycerol yield on glucose of 0.104 g g⁻¹ and an ethanol yield on glucose of 0.391 g g⁻¹.

When the cofactor specificity of 6-phosphogluconate dehydrogenase is changed from NADP⁺ to NAD⁺, formation of NADPH in the oxidative branch of the pentose-phosphate pathway only occurs in the glucose-6-phosphate dehydrogenase reaction. As a result, only 1 mol of NADPH is formed for each mol of glucose converted via this pathway and, moreover, its formation is coupled to the formation of 1 mol of NADH (Fig. 1; bottom numbers). In this scenario, Eq. 2 should therefore be replaced by NADPH formation according to Eq. 5.



Assuming an identical ATP, NAD⁺ and NADPH requirement for biosynthesis of 1 g of biomass (Eq. 1) and exclusive formation of NADPH via this modified version of the oxidative pentose-phosphate pathway (Eq. 5), the flux through the pentose-phosphate pathway should, at the same specific growth rate, be twice as high in the engineered strain as in the wild type (Fig. 1). As a result, an additional 6.48 mmol g^{x-1} NADH are generated which, under anaerobic conditions, need to be reoxidized to NAD⁺ via glycerol formation (Eq. 3). The increased ATP requirement for glycerol formation also requires an increased conversion of glucose into ethanol, according to the stoichiometry shown in Equation 4. The total amount of glucose that is

required for production of 1 g of biomass in this scenario increases to 60.96 mmol g_x⁻¹ (Fig. 1). As a result, the glycerol yield on glucose is predicted to increase to 0.147 g g⁻¹ (41% increase relative to wild type), while the ethanol yield on glucose is predicted to decrease to 0.373 g g⁻¹ (5% decrease relative to wild type). Furthermore, the biomass yield on glucose is predicted to decrease to 0.091 g_x g⁻¹ (12% decrease relative to wild type) in the engineered strain. This corresponds to an increase of 59% on the glycerol formed per g of biomass relative to wild type.

3.3.2 Characterization of *S. cerevisiae* strains expressing NAD⁺-dependent 6-PGDH

To assess the feasibility of changing the cofactor specificity of 6-PGDH from NADP⁺ to NAD⁺, two bacterial genes expressing NAD⁺-dependent enzymes (from *M. flagellatus* and *B. japonicum*) [8,57] and one expressing an NAD⁺-preferring enzyme (from *G. oxydans*) [48] were expressed in *S. cerevisiae*. To this end, *GND1* and *GND2*, which encode the major and minor isoform respectively, of NADP⁺-dependent 6-PGDH in *S. cerevisiae*, were first deleted using CRISPR/Cas9 genome-editing. The three bacterial genes were codon-optimized for expression in *S. cerevisiae*, placed under the control of the strong constitutive *TPI1* promoter and individually integrated at the *GND1* locus. In shake-flask cultures on glucose-containing synthetic medium, the *gnd1Δ gnd2Δ* strains expressing either *M. flagellatus gndA* or *G. oxydans gox1705* grew at nearly the specific growth rate of the parental *GND1 GND2* strain (Table 3). Strain IMX706, which expressed *B. japonicum 6pgdh*, showed a 22% lower growth rate than the reference strain.

Expression of the heterologous 6-PGDH enzymes in *S. cerevisiae* was further investigated by measuring NAD⁺- and NADP⁺-linked enzyme activities in cell extracts of glucose-grown shake-flask cultures (Fig. 2). All three *gnd1Δ gnd2Δ* strains expressing bacterial 6-PGDH genes showed high specific activities with NAD⁺ as the electron acceptor and low activities with NADP⁺ (Fig. 2). Therefore, replacing the native *S. cerevisiae* 6-PGDH isoenzymes with the bacterial enzymes resulted in an up to 4000-fold increase of the ratio of the *in vitro* activities, with NAD⁺ and NADP⁺ as the cofactors (Table 3). Strain IMX705, expressing *gndA* from *M. flagellatus*, showed the highest *in vitro* NAD⁺-dependent 6-PGDH activity (0.49 ± 0.1 μmol mg protein⁻¹ min⁻¹) (Fig. 2) as well as the highest ratio of NAD⁺- versus NADP⁺-linked activities (46 ± 10) (Table 3).

Based on these results, strain IMX705 (*gnd2Δ gnd1::gndA*) was used to further investigate the physiological impact of changing the cofactor specificity of 6-PGDH from NADP⁺ to NAD⁺.

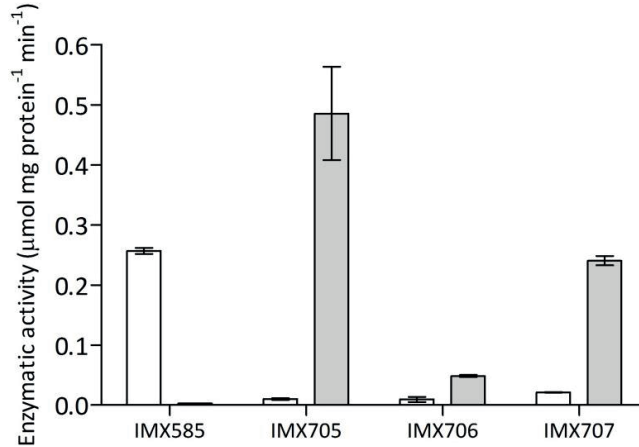


Figure 2. Activities of NADP⁺-dependent 6-PGDH (left, white bars) and NAD⁺-dependent 6-PGDH (right, grey bars) in cell extracts of exponentially growing shake-flask cultures on synthetic medium containing 20 g L⁻¹ glucose. From left to right: *S. cerevisiae* strains IMX585 (*GND1 GND2*), IMX705 (*gnd2Δ gnd1::gndA*), IMX706 (*gnd2Δ gnd1::6pgdh*) and IMX707 (*gnd2Δ gnd1::gox1705*). Data represent the average and mean deviation of independent duplicate experiments.

Table 3. Maximum specific growth rates in shake-flask cultures and ratio of NAD⁺- and NADP⁺-linked 6-phosphogluconate dehydrogenase activity in cell extracts of a reference *S. cerevisiae* strain with native NADP⁺-dependent 6-phosphogluconate dehydrogenase (IMX585) and three strains expressing different heterologous NAD⁺-dependent 6-phosphogluconate dehydrogenases (IMX705-707). Shake-flask cultures (initial pH 6) were grown on synthetic medium containing 20 g L⁻¹ glucose under an air atmosphere and cell extracts were prepared from exponentially growing cultures. Data represent the average and mean deviation of data from independent duplicate cultures.

Strain	Relevant genotype	μ (h ⁻¹)	NAD ⁺ /NADP ⁺ linked activity ratio
IMX585	<i>GND1 GND2</i>	0.38 ± 0.01	<0.01
IMX705	<i>gnd2Δ gnd1::gndA</i>	0.36 ± 0.00	46 ± 10
IMX706	<i>gnd2Δ gnd1::6pgdh</i>	0.28 ± 0.01	5 ± 0.2
IMX707	<i>gnd2Δ gnd1::gox1705</i>	0.36 ± 0.00	11 ± 0.5

For a quantitative analysis of the impact of the 6-PGDH cofactor change, growth and product formation were studied in anaerobic, glucose-grown bioreactor batch cultures of *S. cerevisiae* strains IMX585 (*GND1 GND2*) and IMX705 (*gnd2Δ gnd1::gndA*). Glycerol formation of strain IMX585 was 12.19 mmol g_x⁻¹ (Table 4), which closely corresponded to the theoretically predicted 11.02 mmol g_x⁻¹. As observed in the shake-flask experiments, the specific growth rate of the two strains in anaerobic bioreactors was similar (Table 4), resulting in complete consumption of glucose within ca. 12 h after inoculation (Fig. 3a-b). This result is consistent with earlier reports [6,7] which show that NADPH metabolism in *S. cerevisiae* is sufficiently flexible and likely still able to provide a sufficient flux of NADPH formation following a switch in cofactor specificity of 6-PGDH. Glycerol formation of strain IMX705 (*gnd2Δ gnd1::gndA*) was 15.14 mmol g_x⁻¹, which corresponds to an increase of 24% compared to the reference strain IMX585. The corresponding glycerol yield on glucose of strain IMX705 in these anaerobic batch cultures was 0.121 g g⁻¹, which was 15% higher than that of the reference strain IMX585 (*GND1 GND2*) (Table 4). Although the change in cofactor specificity of 6-PGDH resulted in increased glycerol formation, the magnitude of the increase was below the predicted 59% increase in glycerol per biomass and 41% increase of the glycerol yield on glucose.

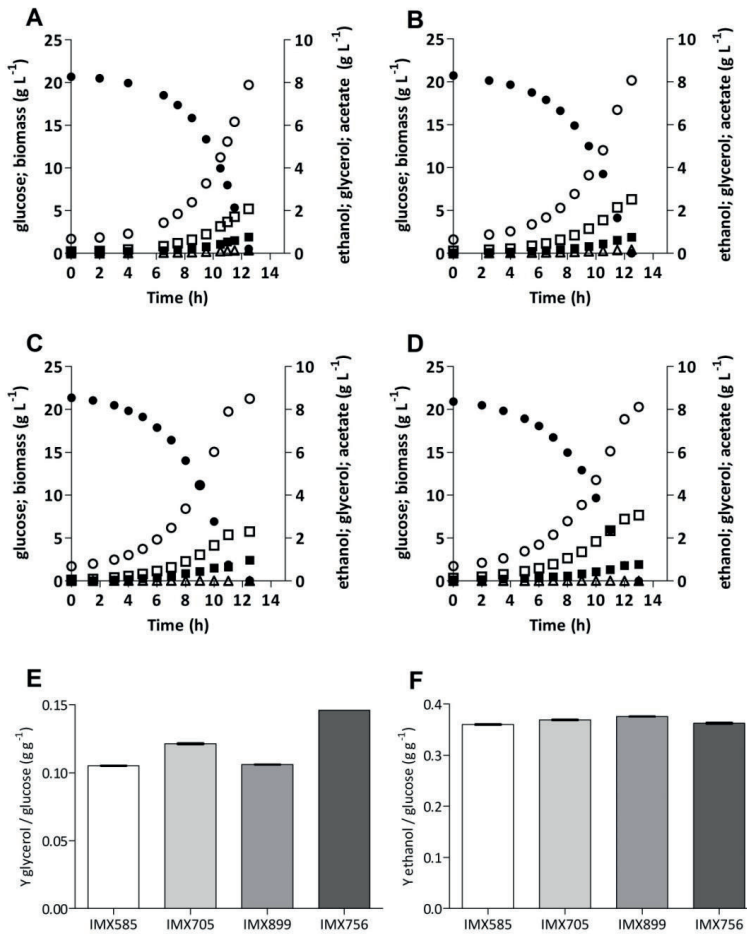


Figure 3. Fermentation product profiles in anaerobic bioreactor batch cultures of *S. cerevisiae* strains IMX585 (panel A; *GND1 GND2*), IMX705 (panel B; *gnd2Δ gnd1::gndA*), IMX899 (panel C; *GND1 GND2 ald6Δ*) and IMX756 (panel D; *gnd2Δ gnd1::gndA ald6Δ*). Glucose = filled circles; Biomass = filled squares; Glycerol = open squares; Ethanol = open circles; Acetate = open triangles. All cultures were grown on synthetic medium containing 20 g L^{-1} glucose (pH 5; Panel E: Glycerol yields on glucose of the above cultures; Panel F: Ethanol yields on glucose of the above cultures, corrected for ethanol evaporation. Panels A-D display single representative cultures from a set of two independent duplicate cultures for each strain. Data on yields represent the average and mean deviation of independent duplicate cultures.

Table 4. Maximum specific growth rate (μ), yields (Y) of glycerol, biomass and ethanol on glucose and the ratios of glycerol and acetate formation to biomass formation in anaerobic bioreactor batch cultures of *S. cerevisiae* strains IMX585, IMX705, IMX899 and IMX756. Cultures were grown on synthetic medium containing 20 g L⁻¹ glucose (pH 5). Yields and ratios were calculated from the exponential growth phase. The ethanol yield on glucose was corrected for evaporation. Values represent average and mean deviation of data from independent duplicate cultures. Carbon recovery in all fermentations was between 95-100%.

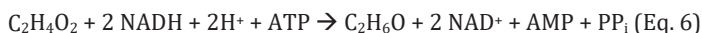
Strain	IMX585	IMX705	IMX899	IMX756
Relevant genotype	<i>GND1 GND2</i>	<i>gnd2Δ gnd1::gndA</i>	<i>GND1 GND2 ald6Δ</i>	<i>gnd2Δ gnd1::gndA ald6Δ</i>
μ (h ⁻¹)	0.32 ± 0.00	0.30 ± 0.01	0.29 ± 0.01	0.26 ± 0.01
Y glycerol/glucose (g g ⁻¹)	0.105 ± 0.000	0.121 ± 0.001	0.106 ± 0.000	0.146 ± 0.000
Y biomass/glucose (g _x g ⁻¹)	0.094 ± 0.004	0.087 ± 0.002	0.088 ± 0.001	0.083 ± 0.002
Y EtOH/glucose (g g ⁻¹)	0.372 ± 0.001	0.379 ± 0.001	0.386 ± 0.000	0.374 ± 0.002
Ratio glycerol formed/biomass (mmol g _x ⁻¹)	12.19 ± 0.44	15.14 ± 0.22	12.83 ± 0.39	18.90 ± 0.56
Ratio acetate formed/biomass (mmol g _x ⁻¹)	1.50 ± 0.03	1.63 ± 0.02	< 0.05	< 0.05

Anaerobic cultures of strain IMX705 (*gnd2Δ gnd1::gndA*) showed a ca. 9% higher production of extracellular acetate than those of the reference strain IMX585 (Table 4). Acetate can be formed via cytosolic NADP⁺-dependent acetaldehyde dehydrogenase, which is encoded by *ALD6* and provides an alternative route of cytosolic NADPH formation [18]. NADPH formation through Ald6 is not desirable in an ethanol producing strain, since it decreases the impact of the cofactor switch of 6-PGDH and results in the production of acetate instead of ethanol. To eliminate this alternative NADPH-forming route, *ALD6* was deleted in strain IMX705, yielding strain IMX756 (*gnd2Δ gnd1::gndA ald6Δ*). To distinguish the impact of *ALD6* deletion alone and in combination with NAD⁺-dependent 6-PGDH, *ALD6* was also deleted in strain IMX585, yielding strain IMX899 (*GND1 GND2 ald6Δ*). Strains IMX899 (*GND1 GND2 ald6Δ*) and IMX756 (*gnd2Δ gnd1::gndA ald6Δ*) were then characterized in anaerobic bioreactor experiments under the same conditions as the previous experiments with their parental strains IMX585 and IMX705 (Table 4, Fig. 3 c-d). Deletion of *ALD6* in strains of IMX899 (*GND1 GND2 ald6Δ*) and IMX756 (*gnd2Δ gnd1::gndA ald6Δ*) resulted in slightly lower specific growth rates (90% and 81%, respectively) than those observed in the case of the reference strain IMX585 (*GND1 GND2*). The additional growth rate decrease of strain IMX756 could be an indication of a limited capacity of NADPH formation in the absence of both Ald6 and NADP⁺-dependent 6-PGDH.

Inactivation of *ALD6* resulted in a strong decrease in the production of acetate during the early stages of the anaerobic cultures, and acetate concentrations even dropped to below detection level during the later stages of cultivation in both IMX899 (*GND1 GND2 ald6Δ*) and IMX756 (*gnd2Δ gnd1::gndA ald6Δ*) (Fig. 3). In strain IMX899, the deletion of *ALD6* resulted in a glycerol production of 12.83 mmol g_x⁻¹ compared to 12.19 mmol g_x⁻¹ for IMX585 (Table 4). This small difference suggested that, in the presence of native 6-PGDH, the contribution of Ald6 to NADPH formation is limited in this strain background. However, in combination with *gndA* overexpression and deletion of *GND1* and *GND2*, deletion of *ALD6* resulted in a 55% increase of the glycerol formation, from 12.19 mmol g_x⁻¹ in IMX585 to 18.90 mmol g_x⁻¹ in strain IMX756 (Table 4), which closely corresponds to the theoretically predicted 59% increase. The biomass yield of strain IMX756 (*gnd2Δ gnd1::gndA ald6Δ*) was 13% lower than the reference strain IMX585 (*GND1 GND2*), as compared to a theoretically predicted 12% decrease. The corresponding glycerol yield on glucose of strain IMX756 was 39% higher (0.146 g g⁻¹ compared to 0.105 g g⁻¹) than the glycerol yield of the *GND1 GND2* reference strain IMX585 (Table 4).

3.3.3 Theoretical analysis of the impact of changing the cofactor specificity of 6-PGDH in an acetate-reducing strain

Guadalupe Medina *et al.* [20] showed that expression of an *E. coli* acetylating acetaldehyde dehydrogenase (MhpF, EC 1.2.1.10) could complement the anaerobic growth defect on glucose of a *gpd1Δ gpd2Δ S. cerevisiae* strain when acetate was added to growth media. Expression of the *E. coli mhpF* gene completed a functional pathway for NADH-dependent reduction of acetate to ethanol in *S. cerevisiae* that further involved the native acetyl-CoA synthetases Acs1 and/or Acs2 [62] and the native alcohol dehydrogenases Adh1-Adh5 [9]. As a result, NADH reoxidation through glycerol formation (Eq. 3) was functionally replaced by reduction of acetate to ethanol, according to the following lumped stoichiometry:



First, the stoichiometry of central metabolism for the formation of 1 g of biomass was analysed for such an acetate-reducing strain under the assumption of identical to wild-type ATP,

NAD⁺ and NADPH requirements for biosynthesis (Eq. 1) and cofactor regeneration according to Eq. 2 and Eq. 6 (Supplementary Table S2). Under these conditions, a glucose requirement of 48.43 mmol g⁻¹ (Fig. 4; top numbers) is predicted for an acetate-reducing strain. NADH reoxidation in this scenario requires 5.51 mmol g⁻¹ acetate which, together with ATP-generating alcoholic fermentation (Eq. 4), results in the formation of 87.91 mmol ethanol per gram of biomass (Fig. 4; top numbers). In this situation, the glycerol yield on glucose is assumed to be zero and the predicted ethanol yield on glucose increases to 0.464 g g⁻¹, compared to 0.391 g g⁻¹ in anaerobic cultures of wild-type *S. cerevisiae*.

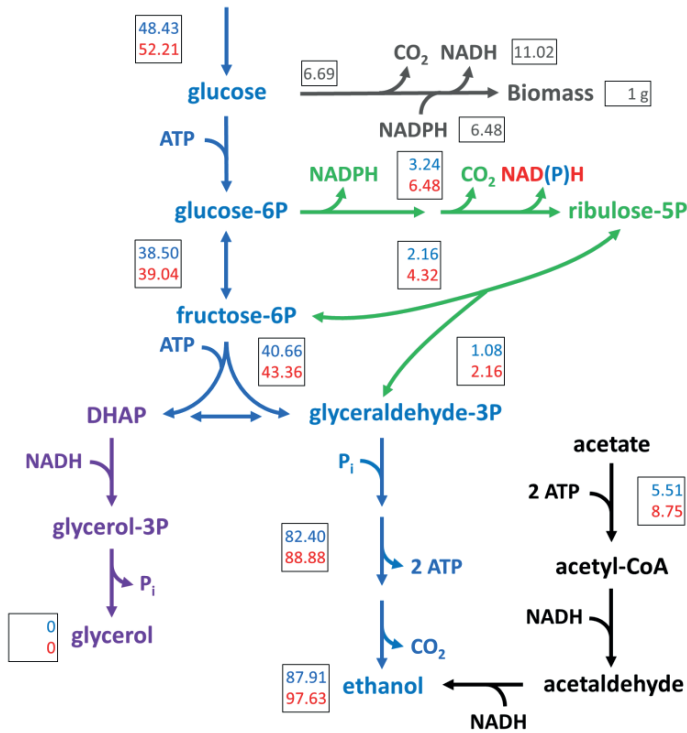


Figure 4. Theoretical stoichiometric comparison of the anaerobic metabolism of acetate reducing *S. cerevisiae* expressing a strictly NAD⁺-dependent 6-PGDH to acetate reducing *S. cerevisiae* expressing the native 6-PGDH. Numbers in boxes represent the carbon distribution and grey numbers in boxes represent the requirement for glucose and cofactors in mmol g⁻¹, normalized for the formation of 1 g of biomass in the two scenarios: native, NADP⁺-dependent 6-PGDH (top, blue colour) and heterologous, NAD⁺-dependent 6-PGDH (bottom, red colour). Blue: Glycolysis and alcoholic fermentation; Green: Pentose-phosphate pathway; Purple: Glycerol formation pathway; Black: Acetate to ethanol reduction pathway.

Grey: Biosynthesis according to [68], which, together with the ATP requirement for biosynthesis, was assumed to be identical for both scenarios. Glycerol formation in this case was assumed to be zero. The Acs-catalysed reaction requires the hydrolysis of ATP to AMP and pyrophosphate, which is stoichiometrically equivalent to hydrolysis of 2 ATP to 2 ADP. The oxidative branch of the pentose phosphate pathway was assumed to be the only NADPH formation pathway. Figure adapted from [21].

Changing the cofactor specificity of 6-PGDH from NADP⁺ to NAD⁺ (Eq. 5) in an acetate-reducing strain should result in an increase in the acetate requirement to 8.75 mmol g_x⁻¹ (Figure 4; bottom numbers). This corresponds to an increase of 59% relative to the strain expressing the native enzyme. As reduction of acetate to ethanol requires ATP (Eq. 6), the requirement for glucose in this scenario increases to 52.21 mmol g_x⁻¹, resulting in the formation of 97.63 mmol g_x⁻¹ ethanol. This scenario, therefore, results in an increase in acetate consumption per g of consumed glucose to 0.056 g, which corresponds to an increase of 47% relative to an acetate-reducing strain expressing native, NADP⁺-dependent 6-PGDH. Additionally, the apparent ethanol yield on glucose is predicted to further increase, by an additional 3%, to 0.478 g g⁻¹.

3.3.4 Physiological impact of *gndA* expression and *ALD6* deletion in an acetylating acetaldehyde dehydrogenase expressing strain

To experimentally investigate the combined effect of changing the cofactor specificity of 6-PGDH, deleting cytosolic NADP⁺-dependent acetaldehyde dehydrogenase, implementing a NADH-dependent pathway for reduction of acetate to ethanol and eliminating the glycerol production pathway, an overexpression cassette for *E. coli eutE* (encoding acetylating acetaldehyde dehydrogenase) was integrated at the *GPD2* locus of strain IMX756, yielding *S. cerevisiae* IMX817 (*gnd2Δ gnd1::gndA ald6Δ GPD1 gpd2::eutE*). Subsequent deletion of *GPD1* yielded strain IMX860 (*gnd2Δ gnd1::gndA ald6Δ gpd1Δ gpd2::eutE*). The acetate-reducing IMX888 (*GND1 GND2 gpd1Δ gpd2::eutE*) was used as a reference strain. Growth, substrate consumption and product formation of strains IMX860 (*gnd2Δ gnd1::gndA ald6Δ gpd1Δ gpd2::eutE*) and IMX888 (*GND1 GND2 gpd1Δ gpd2::eutE*) were investigated in anaerobic bioreactor batch cultures (Fig. 5). Except for the supplementation of 3 g L⁻¹ acetic acid, growth conditions were identical to those

described above. The impact of acetic-acid addition was also investigated in the parental, non-acetate reducing strain IMX585 (*GND1 GND2 GPD1 GPD2*).

In the cultures of the non-acetate reducing reference strain IMX585, addition of acetic acid caused a slight decrease in its specific growth rate, from 0.32 h⁻¹ to 0.28 h⁻¹ (Table 4 and 5). Furthermore, in the presence of 3 g L⁻¹ acetic acid, the biomass yield on glucose decreased by 19% from 0.094 g g⁻¹ to 0.076 g g⁻¹ and the glycerol yield on glucose decreased by 43% from 0.105 g g⁻¹ to 0.060 g g⁻¹. Simultaneously, the ethanol yield on glucose (corrected for ethanol evaporation) increased by 17% to 0.433 g g⁻¹ (Table 4 and 5). This physiological response of the reference strain IMX585 to acetic acid addition reflects the increased requirement for ATP and, hence, for alcoholic fermentation to meet the increased energy requirements associated with acetic-acid diffusion into the cells, and is consistent with previously reported results [2,46]. Contrary to the assumption in the stoichiometric analysis, strain IMX585 (*GND1 GND2 GPD1 GPD2*) showed an acetate consumption of 2.44 mmol g_x⁻¹ (Table 5), which probably reflects a combination of acetate accumulation inside the cells as well as acetate consumed for synthesis of acetyl-CoA; an acetate consumption of ca. 1.04 mmol g_x⁻¹ for synthesis of cytosolic acetyl-CoA is expected if no acetate is formed from glucose [15]. To compare the impact of the 6-PGDH cofactor switch in strains IMX860 and IMX888, this basal-level acetate consumption will have to be taken into account. In the presence of acetate, the formation of glycerol by IMX585 decreased from 12.19 mmol g_x⁻¹ to 8.50 mmol g_x⁻¹, which is in line with the observation that the glycerol yield on glucose decreased more than the biomass yield and that some acetate was used for acetyl-CoA synthesis, thereby decreasing NADH formation.

The maximum specific growth rate of the acetate reducing strain with native 6-PGDH (IMX888) in the presence of acetate was 93% of that of the reference strain IMX585 (Table 5). This represents a significant improvement in the specific growth rate relative to what was previously reported for a *gpd1Δ gpd2Δ* strain expressing *mhpF* from *E. coli* which, in the same genetic background, displayed only half the growth rate of a *GPD1 GPD2* reference strain [20]. This difference indicates that, in the previous study, the *in vivo* activity of the heterologous

acetylating acetaldehyde dehydrogenase limited the rate of acetate reduction and, thereby, the specific growth rate. The apparent ethanol yield on glucose (corrected for ethanol evaporation but not for use of acetate as a substrate for ethanol formation) of strain IMX888 (*GND1 GND2 gpd1Δ gpd2::eutE*) was 0.474 g g⁻¹, compared to 0.433 g g⁻¹ of the reference strain IMX585 (*GND1 GND2 GPD1 GPD2*) (Table 5). This corresponds to an increase of 9% and is consistent with a previous report on a *gpd1Δ gpd2Δ* strain that overexpressed *mhpF* [20]. Strain IMX888 (*GND1 GND2 gpd1Δ gpd2::eutE*) showed an acetate consumption of 6.92 mmol g_x⁻¹ (Table 5). Corrected for the acetate-consumption of strain IMX585 as described above, it follows that 4.48 mmol g_x⁻¹ acetate were reduced to ethanol via the EutE-dependent pathway. The corresponding regeneration of 8.96 mmol NAD⁺ g_x⁻¹ is very close to the regeneration of 8.50 mmol NAD⁺ g_x⁻¹ via glycerol production of strain IMX585 (Table 5).

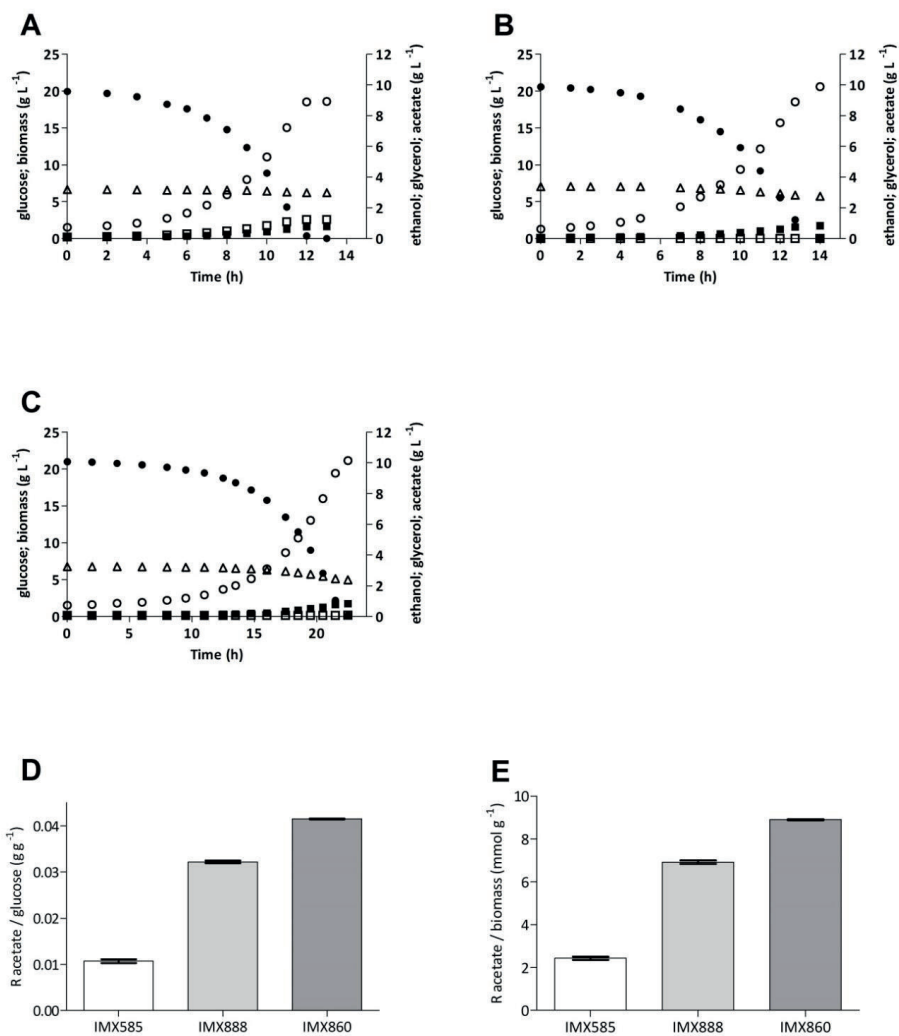


Figure 5. Fermentation product profiles in anaerobic bioreactor batch cultures of *S. cerevisiae* strains IMX585 (panel A; *GND1 GND2 GPD1 GPD2*), IMX888 (panel B; *GND1 GND2 gpd2::eutE gpd1Δ*), IMX860 (panel C; *gnd2Δ gnd1::gndA gpd2::eutE gpd1Δ*). Glucose = filled circles; Biomass = filled squares; Glycerol = open squares; Ethanol = open circles; Acetate = open triangles. All cultures were grown on synthetic medium containing 20 g L⁻¹ glucose and 3 g L⁻¹ acetic acid (pH 5); Panel E: Ratio of acetate to glucose consumption of the above cultures; Panel F: Ratio of acetate consumption per biomass formed of the above cultures. Panels A-C display single representative cultures from a set of two independent duplicate cultures for each strain. Data on ratios represent the average and mean deviation of independent duplicate cultures.

Table 5. Maximum specific growth rate (μ), yields (Y) of glycerol, biomass and ethanol on glucose and the ratios of glycerol production to biomass formation and acetate consumption to glucose consumption and biomass formation in anaerobic bioreactor batch cultures of *S. cerevisiae* strains IMX585, IMX888 and IMX860. Cultures were grown on synthetic medium containing 20 g L⁻¹ glucose and 3 g L⁻¹ acetic acid (pH 5). Yields and ratios were calculated from the exponential growth phase. The ethanol yield on glucose was corrected for evaporation. Values represent average and mean deviation of data from independent duplicate cultures. Carbon recovery in all fermentations was between 95-100%.

Strain	IMX585		IMX888		IMX860	
	<i>GND1 GND2 GPD1 GPD2</i>	<i>GND1 GND2 GPD2::eutE gpd1Δ</i>	<i>GND1 GND2 GPD2::eutE gpd1Δ</i>	<i>gnd2Δ gnd1::gndA alde6Δ gpd2::eutE gpd1Δ</i>		
μ (h ⁻¹)	0.28 ± 0.01	0.26 ± 0.01	0.26 ± 0.01	0.20 ± 0.01		
Y glycerol/glucose (g g ⁻¹)	0.060 ± 0.000	< 0.001	< 0.001	< 0.001		
Y biomass/glucose (g·g ⁻¹)	0.076 ± 0.003	0.075 ± 0.000	0.075 ± 0.000	0.077 ± 0.000		
Y EtOH/glucose (g g ⁻¹)	0.433 ± 0.001	0.474 ± 0.001	0.474 ± 0.001	0.489 ± 0.000		
Ratio glycerol produced/biomass (mmol g ⁻¹)	8.50 ± 0.04	< 0.01	< 0.01	< 0.01		
Ratio acetate consumed/biomass (mmol g ⁻¹)	2.44 ± 0.10	6.92 ± 0.12	6.92 ± 0.12	8.90 ± 0.04		
Ratio acetate consumed/glucose (g g ⁻¹)	0.011 ± 0.00	0.032 ± 0.00	0.032 ± 0.00	0.042 ± 0.00		

The NAD⁺-dependent 6-PGDH-expressing strain IMX860 (*gnd2Δ gnd1::gndA ald6Δ gpd1Δ gpd2::eutE*) showed a growth rate that was 29% lower than that of the reference strain IMX585 (*GND1 GND2 GPD1 GPD2*) (Table 5). This difference in growth rate increased the overall fermentation time by ca. 5 h (Fig. 5). The acetate consumption of strain IMX860 (*gnd2Δ gnd1::gndA ald6Δ gpd1Δ gpd2::eutE*) was 8.9 mmol g_x⁻¹ (Table 5). Corrected for the acetate consumption of IMX585, this corresponds to the regeneration of 12.92 mmol NADH g_x⁻¹ via reduction of 6.46 mmol g_x⁻¹ acetate to ethanol via the EutE-dependent pathway. These calculations indicate that increased NADH generation via NAD⁺-dependent 6-PGDH resulted in a 44% increase in the EutE-dependent acetate consumption per g biomass of strain IMX860, compared to the native 6-PGDH expressing strain IMX888. In regard to the overall fermentation performance, strain IMX860 consumed 0.042 g acetate per g of consumed glucose, which is 31% higher than the observed consumption of strain IMX888 (*GND1 GND2 gpd1Δ gpd2::eutE*) (Fig. 5; Table 5). Furthermore, strain IMX860 (*gnd2Δ gnd1::gndA ald6Δ gpd1Δ gpd2::eutE*) showed an apparent ethanol yield on glucose of 0.489 g g⁻¹, which corresponded to an increase of 3% compared to strain IMX888 (*GND1 GND2 gpd1Δ gpd2::eutE*) and an increase of 13% compared to strain IMX585 under the same conditions (Table 5). In comparison to IMX585 in the absence of (added) acetate, the combined effects of weak-acid uncoupling, acetate-consumption and the redox-cofactor of 6-PGDH in IMX860 increased the (apparent) ethanol yield on glucose by 32% from 0.372 to 0.489 g g⁻¹.

3.4 Discussion

This study demonstrates that altering the cofactor specificity of 6-PGDH can be used to increase generation of NADH in the yeast cytosol, as demonstrated by the increased glycerol yield of a *gnd1Δ gnd2Δ S. cerevisiae* strain expressing *Methylobacillus flagellatus gndA*. However, the observed increase was lower than anticipated based on theoretical calculations. Additional deletion of *ALD6*, which encodes an NADP⁺-dependent cytosolic acetaldehyde dehydrogenase, was required to further increase the glycerol yield to a value close to the theoretical prediction. Previous reports already indicated that NADP⁺-dependent oxidation of acetaldehyde via *ALD6*

accounts for ca. 20% of the NADPH demand in wild type *S. cerevisiae* [6,7]. Formation of acetyl-CoA and/or acetate via Ald6, instead of via the NAD⁺-dependent Ald2, Ald3 or Ald4 acetaldehyde dehydrogenases [50], also decreases the formation of NADH. A limited capacity for NADPH formation via the pentose-phosphate pathway in the engineered *gndA* expressing strain may well lead to an increased contribution of *ALD6* to NADPH regeneration, as also indicated by its increased production of acetate. A similar response has been observed in strains in which *ZWF1*, encoding NADP⁺-dependent glucose-6-phosphate dehydrogenase, was deleted and which showed increased expression of *ALD6* [18]. In strains engineered for acetate reduction via an acetylating acetaldehyde dehydrogenase, deletion of *ALD6* may additionally affect product formation in another way. In combination with the heterologous acetylating acetaldehyde dehydrogenase and acetyl-coenzyme A synthetase, Ald6 could form an ATP-driven transhydrogenase cycle, converting cytosolic NADH into NADPH (Fig. 6), thereby decreasing the formation of NADH from biosynthesis. In view of our results, deletion of *ALD6* should be an integral part of engineering strategies that rely on NADH-dependent acetate reduction via acetylating acetaldehyde dehydrogenase, especially when NADH for acetate reduction is derived from pathways that are also involved in NADPH formation.

The cofactor switch from NADP⁺-dependent 6-PGDH to an NAD⁺-dependent enzyme, in combination with deletion of *ALD6*, elimination of glycerol formation and heterologous expression of acetylating acetaldehyde dehydrogenase, resulted in a strain with significantly increased acetic acid consumption per g of biomass formed in synthetic media. However, even when corrected for acetate consumption independent of acetylating acetaldehyde dehydrogenase, the experimentally observed acetate consumption increase of 44% was lower than the theoretically predicted 59%. This deviation can, for instance, be caused by differences in biomass composition due to differences between strain backgrounds and/or their specific growth rates (specific growth rate is known to affect RNA and protein content [66]), or by suboptimal enzyme kinetics due to lower than predicted *in vivo* activity/affinity of GndA with NAD⁺ instead of NADP⁺, which could result in some NADPH formation. One clear possibility for

further improvement is the maximum specific growth rate of the acetate-reducing strains. In strain IMX860 (*gnd2Δ gnd1::gndA ald6Δ gpd1Δ gpd2::eutE*) the specific growth rate was 29% lower than that of the reference strain IMX585 under the same conditions. The superior growth rates of strains expressing the EutE acetylating acetaldehyde dehydrogenase, instead of the previously used MhpF [20], identifies the *in vivo* capacity of this enzyme as a relevant target for further engineering studies, especially in strains with an increased requirement for NADH-regeneration. In addition to a systematic evaluation of alternative acetylating acetaldehyde-dehydrogenase genes, the copy number of the corresponding expression cassettes can also vary. Alternatively, a limited *in vivo* capacity of NAD⁺-dependent 6-PGDH, for which only 3 candidate genes were screened, and/or of the non-oxidative pentose-phosphate pathway may be responsible for the suboptimal growth rates of the engineered strains. As an alternative approach, cofactor engineering of the native NADP⁺-dependent glucose-6-phosphate dehydrogenase [41] might be considered. The stoichiometric impact of such an intervention is expected to be identical to that of the strategy presented in this study.

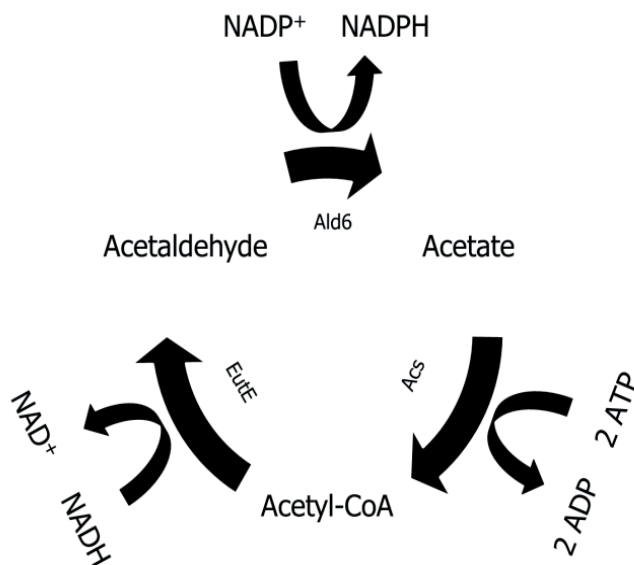


Figure 6. Putative ATP-driven transhydrogenase cycle for converting cytosolic NADH to NADPH involving Ald6. Acetate can be converted to acetyl-CoA via *Acs1p/Acs2* at the net cost of 2 ATP (ATP to AMP and pyrophosphate, followed by pyrophosphate hydrolysis). Acetyl-CoA can be converted to acetaldehyde via *EutE*, using cytosolic NADH as electron donor. Lastly, acetaldehyde is converted back to acetate via *Ald6*, thereby forming NADPH.

Recently, an alternative metabolic engineering strategy to increase the reduction of acetate to ethanol was described [24]. This alternative strategy is based on introduction of a heterologous NADPH-dependent alcohol dehydrogenase in combination with overexpression of *ZWF1* and/or *ACS2*. In contrast to the strategy described in the present study, this alternative strategy is not dependent on NADH generation in biosynthesis. The absence of a stoichiometric coupling to growth potentially provides more flexibility in acetate reduction but might also lead to cells that are less stable during long-term cultivation, since mutational loss of either *ZWF1* overexpression or NADPH-dependent alcohol dehydrogenase provides a benefit for the cells. Further research is required to study how these two strategies, which can in principle be combined, can be used to maximize acetic-acid detoxification and optimization of ethanol yields in lignocellulosic hydrolysates. Such research should also address the question of how changes in NADPH formation affect cellular robustness in lignocellulosic hydrolysates, since NADPH can play a key role in the reductive detoxification of, for example, 2-furaldehyde (furfural) and 5-hydroxymethyl furfuraldehyde (HMF) to the corresponding less toxic alcohols [10,17,26]. Although the strains in this study have a *gpd1Δ gpd2Δ* (*Gpd*⁻) genotype, which can affect strain performance in industrial fermentations that are operated at high osmotic pressures [1,3], this phenotype can be overcome by additional metabolic engineering steps, such as expression of alternative compatible solutes [53], tuning of expression of *Gpd1/2* [25,37], or by evolutionary engineering of growth in high osmolarity media [19].

The possible applications of the cofactor engineering strategy presented in this study extend beyond increasing acetate consumption in second-generation ethanol production. Altering the balance between glycerol and ethanol production is, for example, of interest to wine fermentation, in which a shift of carbon away from ethanol production is desirable during

fermentation of grapes with high sugar content [31,52]. Several previous studies have investigated increased glycerol production as a means to decrease the ethanol content of the wine [34,61,65] without negatively affecting its organoleptic properties [40]. A benefit of the strategy presented in this work is that formation of the NADH required for additional glycerol formation is coupled to carbon dioxide production rather than to increased formation of organic products such as acetate, pyruvate or acetaldehyde, which negatively affect wine quality [5,12,52]. However, it must be noted that, in spite of an increased glycerol formation, the ethanol yield on glucose in our study did not decrease in a strain containing NAD⁺-dependent 6-phosphogluconate dehydrogenase, caused by a larger than predicted decrease in the biomass yield. Analysis of the applicability in wine fermentation, therefore, requires a careful analysis of product formation under actual wine fermentation conditions. In general, this novel approach can be used to improve production of compounds that are more reduced than glucose in glucose-based industrial processes using *S. cerevisiae*. Expression of a NAD⁺-dependent 6-PGDH can also be applied in metabolic engineering strategies for production of compounds that require pentose-phosphate pathway derived precursors, such as for example erythrose-4-phosphate for 2-phenylethanol [14] or flavonoid production [29], but that do not require (all) the accompanying NADPH formation.

3.5 Conclusions

This work demonstrates an efficient and versatile strategy to increase cytosolic NADH generation in *S. cerevisiae* by engineering the cofactor specificity of the oxidative part of the pentose-phosphate pathway. The strategy was successfully applied to the generation of a strain that was able to reduce more acetate and produce more ethanol than a non-engineered, acetate-reducing reference strain.

3.6 Acknowledgments

We thank Jean-Marc Daran, Pilar de la Torre and Paul Klaassen for advice on molecular biology, Matthijs Niemeijer and Erik de Hulster for advice on fermentations, Marcel van der Broek for assistance with 6-PGDH sequence data screening, Marijke Luttik for advice on enzymatic activity determinations and Susan Weening for pre-screening of acetylating acetaldehyde dehydrogenases.

Supplementary Table S2. Lumped stoichiometric analysis of strategy impact on non- and acetate-reducing strains. Compounds in mmol (except for biomass). Stoichiometry for formation of 1 g biomass taken from [68]. Ethanol production in reference scenario (red font) taken from [68]. ATP requirement for formation of 1 g biomass was calculated from experimental data taken from [68].

Reference (non acetate-reducing)	Stoichiometry of the lumped pathway							Multiplier for balancing		Multiplier x Stoichiometry of the lumped pathways							
	glucose	NADPH	NADH	CO ₂	g biomass	ATP	ethanol	glycerol	#	glucose	NADPH	NADH	CO ₂	g biomass	ATP	ethanol	glycerol
Biomass formation	-6.69	-6.48	11.02	2.61	1.00	-71.38	0.00	0.00	1	-6.69	-6.48	11.02	2.61	1.00	-71.38	0.00	0.00
NADPH formation (PPP to ethanol)	-1	2	0	2.67	0	1.67	1.67	0	3.24	-3.24	6.48	0.00	8.64	0.00	5.40	5.40	0.00
Glycerol formation	-1	0	-2	0	0	-2	0	2	5.51	-5.51	0.00	-11.02	0.00	0.00	-11.02	0.00	11.02
Alcoholic fermentation (glycolysis + ethanol)	-1	0	0	2	0	2	2	0	38.5	-38.50	0.00	0.00	77.00	0.00	77.00	77.00	0.00
total										53.94	0.00	0.00	88.25	1.00	0.00	82.40	11.02
NAD+-linked 6-PGDH (non acetate-reducing)																	
Biomass formation	-6.69	-6.48	11.02	2.61	1.00	-71.38	0.00	0.00	1	-6.69	-6.48	11.02	2.61	1.00	-71.38	0.00	0.00
NADPH formation (PPP to ethanol)	-1	1	1	2.67	0	1.67	1.67	0	6.48	-6.48	6.48	17.28	0.00	10.80	10.80	0.00	0.00
Glycerol formation	-1	0	-2	0	0	-2	0	2	8.75	-8.75	0.00	-17.50	0.00	0.00	-17.50	0.00	17.50
Alcoholic fermentation (glycolysis + ethanol)	-1	0	0	2	0	2	2	0	39.04	-39.04	0.00	0.00	78.08	0.00	78.08	78.08	0.00
total										-60.96	0.00	0.00	97.97	1.00	0.00	88.88	17.50
Reference (acetate-reducing)																	
Biomass formation	-6.69	-6.48	11.02	2.61	1.00	-71.38	0.00	0.00	1	-6.69	-6.48	11.02	2.61	1.00	-71.38	0.00	0.00
NADPH generation (PPP to ethanol)	-1	2	0	2.67	0	1.67	1.67	0	3.24	-3.24	6.48	0.00	8.64	0.00	5.40	5.40	0.00
Glycerol formation	-1	0	-2	0	0	-2	0	2	0	0.00	0.00	0.00	0.00	0.00	0.00	0.00	0.00
Alcoholic fermentation (glycolysis + ethanol)	-1	0	0	2	0	2	2	0	38.5	-38.50	0.00	0.00	77.00	0.00	77.00	77.00	0.00
Acetate reduction to ethanol	0	0	-2	0	0	-2	1	0	5.51	0.00	0.00	-11.02	0.00	0.00	-11.02	5.51	0.00
total										-48.43	0.00	0.00	88.25	1.00	0.00	87.91	0.00
NAD+-linked 6-PGDH (acetate-reducing)																	
Biomass formation	-6.69	-6.48	11.02	2.61	1.00	-71.38	0.00	0.00	1	-6.69	-6.48	11.02	2.61	1.00	-71.38	0.00	0.00
NADPH generation (PPP to ethanol)	-1	1	1	2.67	0	1.67	1.67	0	6.48	-6.48	6.48	17.28	0.00	10.80	10.80	0.00	0.00
Glycerol formation	0	0	0	0	0	0	0	0	0	0.00	0.00	0.00	0.00	0.00	0.00	0.00	0.00
Alcoholic fermentation (glycolysis + ethanol)	-1	0	0	2	0	2	2	0	39.04	-39.04	0.00	0.00	78.08	0.00	78.08	78.08	0.00
Acetate reduction to ethanol	0	0	-2	0	0	-2	1	0	8.75	0.00	0.00	-17.50	0.00	0.00	-17.50	8.75	0.00
total										-52.21	0.00	0.00	97.97	1.00	0.00	97.63	0.00

3.8 References

1. Albertyn J, Hohmann S, Thevelein JM, Prior BA. *GPD1*, which encodes glycerol-3-phosphate dehydrogenase, is essential for growth under osmotic stress in *Saccharomyces cerevisiae*, and its expression is regulated by the high-osmolarity glycerol response pathway. *Mol Cell Biol*. 1994;14:4135-44.
2. Bellissimi E, van Dijken JP, Pronk JT, van Maris AJA. Effects of acetic acid on the kinetics of xylose fermentation by an engineered, xylose-isomerase-based *Saccharomyces cerevisiae* strain. *FEMS Yeast Res*. 2009;9:358-64.
3. Blomberg A, Adler L. Roles of glycerol and glycerol-3-phosphate dehydrogenase (NAD⁺) in acquired osmotolerance of *Saccharomyces cerevisiae*. *J Bacteriol*. 1989;171:1087-92.
4. Bruinenberg PM, van Dijken JP, Scheffers WA. A theoretical analysis of NADPH production and consumption in yeasts. *J Gen Microbiol*. 1983;129:953-64.
5. Cambon B, Monteil V, Remize F, Camarasa C, Dequin S. Effects of *GPD1* overexpression in *Saccharomyces cerevisiae* commercial wine yeast strains lacking *ALD6* genes. *Appl Environ Microb*. 2006;72:4688-94.
6. Celton M, Goelzer A, Camarasa C, Fromion V, Dequin S. A constraint-based model analysis of the metabolic consequences of increased NADPH oxidation in *Saccharomyces cerevisiae*. *Metab Eng*. 2012;14:366-79.
7. Celton M, Sanchez I, Goelzer A, Fromion V, Camarasa C, Dequin S. A comparative transcriptomic, fluxomic and metabolomic analysis of the response of *Saccharomyces cerevisiae* to increases in NADPH oxidation. *BMC Genomics*. 2012;13:317.
8. Chistoserdova L, Gomelsky L, Vorholt JA, Gomelsky M, Tsygankov YD, Lidstrom ME. Analysis of two formaldehyde oxidation pathways in *Methylobacillus flagellatus* KT, a ribulose monophosphate cycle methylotroph. *Microbiology*. 2000;146:233-8.
9. Ciriacy M. Genetics of alcohol dehydrogenase in *Saccharomyces cerevisiae*. *Mutat Res-Fund Mol M*. 1975;29:315-25.
10. Cunha JT, Aguiar TQ, Romani A, Oliveira C, Domingues L. Contribution of *PRS3*, *RPB4* and *ZWF1* to the resistance of industrial *Saccharomyces cerevisiae* CUG53310 and PE-2 strains to lignocellulosic hydrolysate-derived inhibitors. *Bioresour Technol*. 2015;191:7-16.
11. DiCarlo JE, Norville JE, Mali P, Rios X, Aach J, Church GM. Genome engineering in *Saccharomyces cerevisiae* using CRISPR-Cas systems. *Nucleic Acids Res*. 2013;41:4336-43.
12. Eglinton JM, Heinrich AJ, Pollnitz AP, Langridge P, Henschke PA, de Barros Lopes M. Decreasing acetic acid accumulation by a glycerol overproducing strain of *Saccharomyces cerevisiae* by deleting the *ALD6* aldehyde dehydrogenase gene. *Yeast*. 2002;19:295-301.
13. Entian KD, Kötter P. Yeast genetic strain and plasmid collections. *Method Microbiol*. 2007;36:629-66.
14. Etschmann M, Bluemke W, Sell D, Schrader J. Biotechnological production of 2-phenylethanol. *Appl Microbiol Biotechnol*. 2002;59:1-8.
15. Flikweert MT, de Swaaf M, van Dijken JP, Pronk JT. Growth requirements of pyruvate-decarboxylase-negative *Saccharomyces cerevisiae*. *FEMS Microbiol Lett*. 1999;174:73-9.
16. Gietz RD, Woods RA. Transformation of yeast by lithium acetate/single-stranded carrier DNA/polyethylene glycol method. *Methods Enzymol*. 2002;350:87-96.
17. Gorsich SW, Dien BS, Nichols NN, Slininger PJ, Liu ZL, Skory CD. Tolerance to furfural-induced stress is associated with pentose phosphate pathway genes *ZWF1*, *GND1*, *RPE1*, and *TKL1* in *Saccharomyces cerevisiae*. *Appl Microbiol Biotechnol*. 2006;71:339-49.
18. Grabowska D, Chelstowska A. The *ALD6* gene product is indispensable for providing NADPH in yeast cells lacking glucose-6-phosphate dehydrogenase activity. *J Biol Chem*. 2003;278:13984-8.
19. Guadalupe-Medina V, Metz B, Oud B, van der Graaf CM, Mans R, Pronk JT, van Maris AJA. Evolutionary engineering of a glycerol-3-phosphate dehydrogenase-negative, acetate-

- reducing *Saccharomyces cerevisiae* strain enables anaerobic growth at high glucose concentrations. *Microb Biotechnol.* 2014;7:44-53.
20. Guadalupe-Medina V, Almering MJH, van Maris AJA, Pronk JT. Elimination of glycerol production in anaerobic cultures of a *Saccharomyces cerevisiae* strain engineered to use acetic acid as an electron acceptor. *Appl Environ Microb.* 2010;76:190-5.
 21. Guadalupe-Medina V, Wisselink H, Luttik M, de Hulster E, Daran J-MG, Pronk JT, van Maris AJA. Carbon dioxide fixation by Calvin-Cycle enzymes improves ethanol yield in yeast. *Biotechnol Biofuels.* 2013;6:125.
 22. Hahn-Hägerdal B, Karhumaa K, Fonseca C, Spencer-Martins I, Gorwa-Grauslund MF. Towards industrial pentose-fermenting yeast strains. *Appl Microbiol Biotechnol.* 2007;74:937-53.
 23. Hasunuma T, Sanda T, Yamada R, Yoshimura K, Ishii J, Kondo A. Metabolic pathway engineering based on metabolomics confers acetic and formic acid tolerance to a recombinant xylose-fermenting strain of *Saccharomyces cerevisiae*. *Microb Cell Fact.* 2011;10:2.
 24. Henningsen BM, Hon S, Covalla SF, Sonu C, Argyros DA, Barrett TF, Wiswall E, Froehlich AC, Zelle RM. Increasing anaerobic acetate consumption and ethanol yield in *Saccharomyces cerevisiae* with NADPH-specific alcohol dehydrogenase. *Appl Environ Microbiol.* 2015;81:8108-17.
 25. Hubmann G, Guillouet S, Nevoigt E. Gpd1 and Gpd2 fine-tuning for sustainable reduction of glycerol formation in *Saccharomyces cerevisiae*. *Appl Environ Microbiol.* 2011;77:5857-67.
 26. Jeppsson M, Johansson B, Jensen PR, Hahn-Hägerdal B, Gorwa-Grauslund MF. The level of glucose-6-phosphate dehydrogenase activity strongly influences xylose fermentation and inhibitor sensitivity in recombinant *Saccharomyces cerevisiae* strains. *Yeast.* 2003;20:1263-72.
 27. Keating JD, Panganiban C, Mansfield SD. Tolerance and adaptation of ethanologenic yeasts to lignocellulosic inhibitory compounds. *Biotechnol Bioeng.* 2006;93:1196-206.
 28. Klinke HB, Thomsen AB, Ahring BK. Inhibition of ethanol-producing yeast and bacteria by degradation products produced during pre-treatment of biomass. *Appl Microbiol Biotechnol.* 2004;66:10-26.
 29. Koopman F, Beekwilder J, Crimi B, van Houwelingen A, Hall RD, Bosch D, van Maris AJA, Pronk JT, Daran J-MG. De novo production of the flavonoid naringenin in engineered *Saccharomyces cerevisiae*. *Microb Cell Fact.* 2012;11:155.
 30. Kozak BU, van Rossum HM, Benjamin KR, Wu L, Daran J-MG, Pronk JT, van Maris AJA. Replacement of the *Saccharomyces cerevisiae* acetyl-CoA synthetases by alternative pathways for cytosolic acetyl-CoA synthesis. *Metab Eng.* 2014;21:46-59.
 31. Kutyna DR, Varela C, Henschke PA, Chambers PJ, Stanley GA. Microbiological approaches to lowering ethanol concentration in wine. *Trends Food Sci Tech.* 2010;21:293-302.
 32. Larsson S, Palmqvist E, Hahn-Hägerdal B, Tengborg C, Stenberg K, Zacchi G, Nilvebrant NO. The generation of fermentation inhibitors during dilute acid hydrolysis of softwood. *Enzyme Microb Tech.* 1999;24:151-9.
 33. Mans R, van Rossum HM, Wijsman M, Backx A, Kuijpers NG, van den Broek M, Daran-Lapujade P, Pronk JT, van Maris AJA, Daran J-MG. CRISPR/Cas9: a molecular Swiss army knife for simultaneous introduction of multiple genetic modifications in *Saccharomyces cerevisiae*. *FEMS Yeast Res.* 2015;15:fov004.
 34. Michnick S, Roustan JL, Remize F, Barre P, Dequin S. Modulation of glycerol and ethanol yields during alcoholic fermentation in *Saccharomyces cerevisiae* strains overexpressed or disrupted for *GPD1* encoding glycerol 3-phosphate dehydrogenase. *Yeast.* 1997;13:783-93.
 35. Mira N, Palma M, Guerreiro J, Sa-Correia I. Genome-wide identification of *Saccharomyces cerevisiae* genes required for tolerance to acetic acid. *Microb Cell Fact.* 2010;9:79.
 36. Müller UM, Wu L, Raamsdonk LM, Winkler AA. Acetyl-coa producing enzymes in yeast. *PCT/EP2008/059119 (WO2009013159 A2).* 30-9-2010.

37. Nevoigt E, Kohnke J, Fischer CR, Alper H, Stahl U, Stephanopoulos G. Engineering of promoter replacement cassettes for fine-tuning of gene expression in *Saccharomyces cerevisiae*. *Appl Environ Microbiol.* 2006;72:5266-73.
38. Nielsen J, Larsson C, van Maris AJA, Pronk JT. Metabolic engineering of yeast for production of fuels and chemicals. *Curr Opin Biotechnol.* 2013;24:398-404.
39. Nijkamp JF, van den Broek M, Datema E, de Kok S, Bosman L, Luttkik MA, Daran-Lapujade P, Vongsangnak W, Nielsen J, Heijne WHM, Klaassen P, Paddon CJ, Platt D, Kötter P, van Ham RC, Reinders MJT, Pronk JT, de Ridder D, Daran J-MG. De novo sequencing, assembly and analysis of the genome of the laboratory strain *Saccharomyces cerevisiae* CEN.PK113-7D, a model for modern industrial biotechnology. *Microb Cell Fact.* 2012;11:36.
40. Noble AC, Bursick GF. The contribution of glycerol to perceived viscosity and sweetness in white wine. *Am J Enol Viticult.* 1984;35:110-2.
41. Nogue I, Johnston M. Isolation and characterization of the *ZWF1* gene of *Saccharomyces cerevisiae*, encoding glucose-6-phosphate dehydrogenase. *Gene.* 1990;96:161-9.
42. Orij R, Urbanus M, Vizeacoumar F, Giaever G, Boone C, Nislow C, Brul S, Smits G. Genome-wide analysis of intracellular pH reveals quantitative control of cell division rate by pHc in *Saccharomyces cerevisiae*. *Genome Biol.* 2012;13:R80.
43. Palmqvist E, Hahn-Hägerdal B. Fermentation of lignocellulosic hydrolysates. I: inhibition and detoxification. *Bioresour Technol.* 2000;74:17-24.
44. Palmqvist E, Hahn-Hägerdal B. Fermentation of lignocellulosic hydrolysates. II: inhibitors and mechanisms of inhibition. *Bioresour Technol.* 2000;74:25-33.
45. Pampulha ME, Loureiro-Dias MC. Activity of glycolytic enzymes of *Saccharomyces cerevisiae* in the presence of acetic acid. *Appl Microbiol Biotechnol.* 1990;34:375-80.
46. Pampulha ME, Loureiro-Dias MC. Energetics of the effect of acetic acid on growth of *Saccharomyces cerevisiae*. *FEMS Microbiol Lett.* 2000;184:69-72.
47. Parawira W, Tekere M. Biotechnological strategies to overcome inhibitors in lignocellulose hydrolysates for ethanol production: review. *Crit Rev Biotechnol.* 2010;31:20-31.
48. Rauch B, Pahlke J, Schweiger P, Deppenmeier U. Characterization of enzymes involved in the central metabolism of *Gluconobacter oxydans*. *Appl Microbiol Biotechnol.* 2010;88:711-8.
49. Roubos JA, van Noel N, Peij VNNM. A method for achieving improved polypeptide expression. PCT/EP2007/055943(WO2008000632 A1). 3-1-2008.
50. Saint-Prix F, Bönquist L, Dequin S. Functional analysis of the *ALD* gene family of *Saccharomyces cerevisiae* during anaerobic growth on glucose: the NADP⁺-dependent Ald6p and Ald5p isoforms play a major role in acetate formation. *Microbiology.* 2004;150:2209-20.
51. Sanda T, Hasunuma T, Matsuda F, Kondo A. Repeated-batch fermentation of lignocellulosic hydrolysate to ethanol using a hybrid *Saccharomyces cerevisiae* strain metabolically engineered for tolerance to acetic and formic acids. *Bioresour Technol.* 2011;102:7917-24.
52. Schmidtke LM, Blackman JW, Agboola SO. Production technologies for reduced alcoholic wines. *J Food Sci.* 2012;77:R25-R41.
53. Shen B, Hohmann S, Jensen RG, Bohnert H. Roles of sugar alcohols in osmotic stress adaptation. Replacement of glycerol by mannitol and sorbitol in yeast. *Plant Physiol.* 1999;121:45-52.
54. Sinha A, Maitra PK. Induction of specific enzymes of the oxidative pentose phosphate pathway by glucono- δ -lactone in *Saccharomyces cerevisiae*. *J Gen Microbiol.* 1992;138:1865-73.
55. Smith J, van Rensburg E, Gorgens J. Simultaneously improving xylose fermentation and tolerance to lignocellulosic inhibitors through evolutionary engineering of recombinant *Saccharomyces cerevisiae* harbouring xylose isomerase. *BMC Biotechnol.* 2014;14:41.

56. Solis-Escalante D, Kuijpers NGA, Bongaerts N, Bolat I, Bosman L, Pronk JT, Daran J-M, Daran-Lapujade P. amdSYM, a new dominant recyclable marker cassette for *Saccharomyces cerevisiae*. FEMS Yeast Res. 2013;13:126-39.
57. Sosa-Saavedra F, León-Barrios M, Pérez-Galdona R. Pentose phosphate pathway as the main route for hexose catabolism in *Bradyrhizobium sp.* lacking Entner-Doudoroff pathway. A role for NAD⁺-dependent 6-phosphogluconate dehydrogenase (decarboxylating). Soil Biol Biochem. 2001;33:339-43.
58. Swinnen S, Fernández-Niño M, González-Ramos D, van Maris AJA, Nevoigt E. The fraction of cells that resume growth after acetic acid addition is a strain-dependent parameter of acetic acid tolerance in *Saccharomyces cerevisiae*. FEMS Yeast Res. 2014;14:642-53.
59. Taherzadeh MJ, Karimi K: Chapter 12 - Fermentation inhibitors in ethanol processes and different strategies to reduce their effects. In *Biofuels*. Edited by Gnansounou APL. Amsterdam: Academic Press; 2011:287-311.
60. Thomas KC, Hynes SH, Ingledew WM. Influence of medium buffering capacity on inhibition of *Saccharomyces cerevisiae* growth by acetic and lactic acids. Appl Environ Microbiol. 2002;68:1616-23.
61. Tilloy V, Ortiz-Julien A, Dequin S. Reduction of ethanol yield and improvement of glycerol formation by adaptive evolution of the wine yeast *Saccharomyces cerevisiae* under hyperosmotic conditions. Appl Environ Microbiol. 2014;80:2623-32.
62. Van den Berg MA, de Jong-Gubbels P, Kortland CJ, van Dijken JP, Pronk JT, Steensma HY. The two acetyl-coenzyme A synthetases of *Saccharomyces cerevisiae* differ with respect to kinetic properties and transcriptional regulation. J Biol Chem. 1996;271:28953-9.
63. Van Dijken JP, Scheffers WA. Redox balances in the metabolism of sugars by yeasts. FEMS Microbiol Lett. 1986;32:199-224.
64. Van Maris AJA, Abbott DA, Bellissimi E, van den Brink J, Kuyper M, Luttik MA, Wisselink HW, Scheffers WA, van Dijken JP, Pronk JT. Alcoholic fermentation of carbon sources in biomass hydrolysates by *Saccharomyces cerevisiae*: current status. Antonie van Leeuwenhoek. 2006;90:391-418.
65. Varela C, Kutyna DR, Solomon MR, Black CA, Borneman A, Henschke PA, Pretorius IS, Chambers PJ. Evaluation of gene modification strategies for the development of low-alcohol-wine yeasts. Appl Environ Microbiol. 2012;78:6068-77.
66. Verduyn C, Postma E, Scheffers WA, van Dijken JP. Energetics of *Saccharomyces cerevisiae* in anaerobic glucose-limited chemostat cultures. J Gen Microbiol. 1990;136:405-12.
67. Verduyn C, Postma E, Scheffers WA, van Dijken JP. Effect of benzoic acid on metabolic fluxes in yeasts: A continuous-culture study on the regulation of respiration and alcoholic fermentation. Yeast. 1992;8:501-17.
68. Verduyn C, Postma E, Scheffers WA, van Dijken JP. Physiology of *Saccharomyces cerevisiae* in anaerobic glucose-limited chemostat cultures. J Gen Microbiol. 1990;136:395-403.
69. Wiedemann B, Boles E. Codon-optimized bacterial genes improve l-arabinose fermentation in recombinant *Saccharomyces cerevisiae*. Appl Environ Microbiol. 2008;74:2043-50.
70. Wright J, Bellissimi E, de Hulster E, Wagner A, Pronk JT, van Maris AJA. Batch and continuous culture-based selection strategies for acetic acid tolerance in xylose-fermenting *Saccharomyces cerevisiae*. FEMS Yeast Res. 2011;11:299-306.

Chapter 4

**Metabolic engineering strategies for optimizing acetate reduction,
ethanol yield and osmotolerance in *Saccharomyces cerevisiae***

Ioannis Papapetridis, Marlous van Dijk, Antonius J.A. van Maris and Jack T. Pronk

Essentially as published in *Biotechnology for Biofuels* 2017 10:7

(<https://doi.org/10.1186/s13068-017-0791-3>)

Abstract

Glycerol, whose formation contributes to cellular redox balancing and osmoregulation in *Saccharomyces cerevisiae*, is an important by-product of yeast-based bioethanol production. Replacing the glycerol pathway by an engineered pathway for NAD⁺-dependent acetate reduction has been shown to improve ethanol yields and contribute to detoxification of acetate-containing media. However, the osmosensitivity of glycerol non-producing strains limits their applicability to high-osmolarity industrial processes. This study explores engineering strategies for minimizing glycerol production by acetate-reducing strains, while retaining osmotolerance. *GPD2* encodes one of two *S. cerevisiae* isoenzymes of NAD⁺-dependent glycerol-3-phosphate dehydrogenase (G3PDH). Its deletion in an acetate-reducing strain yielded a 4-fold lower glycerol production in anaerobic, low-osmolarity cultures but hardly affected glycerol production at high osmolarity. Replacement of both native G3PDHs by an archaeal NADP⁺-preferring enzyme, combined with deletion of *ALD6*, yielded an acetate-reducing strain whose phenotype in low-osmolarity cultures resembled that of a glycerol-negative *gpd1Δ gpd2Δ* strain. This strain grew anaerobically at high osmolarity (1 mol L⁻¹ glucose), while consuming acetate and producing virtually no extracellular glycerol. Its ethanol yield in high-osmolarity cultures was 13% higher than that of an acetate-reducing strain expressing the native glycerol pathway. Deletion of *GPD2* provides an attractive strategy for improving product yields of acetate-reducing *S. cerevisiae* strains in low, but not in high-osmolarity media. Replacement of the native yeast G3PDHs by a heterologous NADP⁺-preferring enzyme, combined with deletion of *ALD6*, virtually eliminated glycerol production in high-osmolarity cultures while enabling efficient reduction of acetate to ethanol. After further optimization of growth kinetics, this strategy for uncoupling the roles of glycerol formation in redox homeostasis and osmotolerance can be applicable for improving performance of industrial strains in high-gravity acetate-containing processes.

4.1 Introduction

By functionally replacing fossil-fuel derived compounds, microbial production of chemicals and transport fuels can contribute to a transition to a sustainable, low-carbon global economy [1]. The total industrial production of fuel ethanol, which reached ca. 100 billion liters in 2015, is predicted to increase further [2]. The yeast *Saccharomyces cerevisiae* is the established microbial cell factory for conversion of starch- and sucrose-derived hexose sugars to ethanol, as it combines a high ethanol yield and productivity with robustness under process conditions [3-5]. Efforts in yeast strain improvement and process optimization of corn-starch and cane-sugar-based bioethanol production have further improved product yields and productivity [5]. Furthermore, intensive metabolic and evolutionary engineering studies have yielded yeast strains capable of efficiently fermenting the pentose sugars xylose and arabinose, thus paving the way for yeast-based 'second-generation' bioethanol production from lignocellulosic hydrolysates [6-8].

In industrial bioethanol production, the carbohydrate feedstock represents the single largest cost factor [9]. Maximizing ethanol yield on sugar is therefore a key requirement, especially in second-generation processes, whose ethanol yields and productivity are generally still lower than those of first-generation processes [6-8]. Adequate yeast performance in lignocellulosic hydrolysates also requires tolerance to inhibitors that are released during biomass pre-treatment and hydrolysis [10-12]. Suboptimal ethanol yields in industrial processes are caused by formation of biomass and low-molecular-weight metabolites, of which glycerol accounts for a loss of up to 4% of the carbohydrate substrate [13]. Under anaerobic conditions, wild-type *S. cerevisiae* strains require glycerol formation to re-oxidize NADH formed during biosynthesis or during production of metabolites whose formation results in net NADH formation [14,15]. As the major compatible solute in *S. cerevisiae*, glycerol also plays a key role in osmotolerance [16,17].

In *S. cerevisiae*, glycerol formation is initiated by reduction of the glycolytic intermediate dihydroxyacetone phosphate to glycerol-3-phosphate, a reaction catalysed by two isoenzymes of

NAD⁺-dependent glycerol-3P dehydrogenase (G3PDH), Gpd1 and Gpd2 [18]. Glycerol-3P is subsequently hydrolysed to glycerol and inorganic phosphate by glycerol-3P phosphatase, isoenzymes of which are encoded by *GPP1* and *GPP2*. Reoxidation of one mol of NADH through glycerol production requires 0.5 mol glucose and 1 mol ATP [18]. Several metabolic engineering strategies have demonstrated that altering redox-cofactor specificity of reactions in biosynthesis [13] or in sugar dissimilation [19] can be used to decrease glycerol formation from sugars.

GPD1 and *GPD2* are differentially regulated, as transcriptional upregulation of *GPD1* mainly occurs in response to osmotic stress, while regulation of *GPD2* is linked to redox homeostasis [20-22]. Complete elimination of glycerol production by inactivation of both *GPD1* and *GPD2* has been reported to abolish anaerobic growth and to greatly increase osmosensitivity [20,21,23]. Anaerobic growth of *gpd1Δ gpd2Δ* cultures can be restored by addition of an external electron acceptor, such as acetoin, to growth media [23]. Recently, *S. cerevisiae* strains have been engineered to use acetic acid or CO₂ as external electron acceptors [24-28]. Functional expression of a heterologous acetylating-acetaldehyde dehydrogenase (A-ALD), together with the activities of the native acetyl-CoA synthetases and alcohol dehydrogenases, enabled the NADH-dependent reduction of acetic acid to ethanol [25]. CO₂ is abundantly present in all industrial ethanol fermentation processes, while acetic acid is an important, ubiquitous inhibitor of yeast performance in lignocellulosic hydrolysates [10,11]. Use of acetic acid as external 'redox sink' is highly attractive for second-generation bioethanol processes, since its reduction to ethanol not only increases product yields, but simultaneously contributes to detoxification of the fermentation medium [25,29,30].

Although metabolic engineering has enabled replacement of glycerol production by the reduction of acetic acid to ethanol, the increased osmosensitivity of *gpd1Δ gpd2Δ* strains has not been fully resolved. Process intensification of bioethanol production via the introduction of high-gravity fermentation processes will make osmotolerance ever more important [31-36]. Previous research on improving osmotolerance of *gpd1Δ gpd2Δ* strains explored production of alternative compatible solutes, including the polyols mannitol and sorbitol [37], trehalose [38-40] and

proline [41,42]. These alternative compounds, however, did not confer the same osmotolerance as glycerol. Evolutionary engineering of an acetate-reducing *gpd1Δ gpd2Δ* strain yielded a strain that could grow anaerobically at 1 mol L⁻¹ glucose without loss of acetate reduction potential or ethanol yield [43]. However, the underlying genetic changes were not fully resolved [43]. Tuning the expression of the native G3PDH genes can lead to decreased glycerol production, but the resulting strains still require the production of considerable amounts of this by-product to maintain the redox cofactor balance [34,35,44]. To uncouple the roles of glycerol formation in NADH reoxidation and osmotolerance in *S. cerevisiae*, it would be of interest to alter the redox cofactor specificity of G3PDH. Specifically, making this reaction NADPH-dependent might uncouple glycerol production from NAD⁺ regeneration. In such a scenario, NAD⁺ could then be exclusively regenerated via acetate or CO₂ reduction. Simultaneously, NADPH-dependent formation of intracellular glycerol would enable the synthesis of a compatible solute with minimal losses in ethanol yield. Recently, an NADP⁺-preferring G3PDH, encoded by the *gpsA* gene from the thermophilic archaeon *Archaeoglobus fulgidus* was described [45]. Based on its unusual cofactor preference and, due to its thermophilic origin, anticipated low *in vivo* activity in yeast, it was hypothesized that *A. fulgidus* GpsA might be an interesting candidate to replace the NAD⁺-dependent Gpd1 and Gpd2 enzymes in *S. cerevisiae*.

The goal of this study is to explore new metabolic engineering strategies for construction of acetate-reducing, osmotolerant *S. cerevisiae* strains with a minimal, non-zero production of glycerol. To this end, acetate-reducing strains with different configurations of the native glycerol production pathway, as well as strains in which *GPD1* and *GPD2* were replaced by *A. fulgidus* *gpsA*, were constructed. To construct acetate-reducing strains the ethanolamine utilization protein of *E. coli*, encoded by *eutE* [Genbank: WP_001075673.1], was overexpressed, as it was previously shown to support near-wild-type anaerobic growth rates in a *gpd1Δ gpd2Δ* strain background [29]. The impact of these engineering strategies on acetate reduction and glycerol production was quantitatively analysed in anaerobic bioreactor batch cultures grown on low and high osmolarity media.

4.2 Methods

4.2.1 Strain propagation and maintenance

All *S. cerevisiae* strains used in this study belong to the CEN.PK lineage [46] (Table 1). *S. cerevisiae* cultures were propagated in synthetic medium [47] containing 20 g L⁻¹ glucose. *E. coli* XL-1 blue cultures for plasmid cloning were propagated in LB medium (10 g L⁻¹ Bacto tryptone, 5 g L⁻¹ Bacto yeast extract, 5 g L⁻¹ NaCl) containing 100 mg L⁻¹ ampicillin. All strains were stored at -80°C, after addition of sterile glycerol (30% v/v) to growing cultures.

4.2.2 Construction of expression cassettes and plasmids

Plasmids used in this study are listed in Table 2. Plasmids expressing chimeric gRNAs were used for CRISPR/Cas9-mediated genome editing [48]. Unique Cas9-recognition sequences in *GPD1*, *GPD2*, *SGA1* and *ALD6* were selected as described previously [29]. PCR for construction of expression cassettes and diagnostic PCR were performed with Phusion High Fidelity DNA Polymerase and Dreamtaq polymerase (Thermo Scientific, Waltham, MA), respectively, according to the manufacturer's guidelines. For construction of pUDR240, the backbone of the plasmid was PCR amplified using the double-binding primer 5793 (Additional File S1) and pROS10 as template. The insert fragment, expressing the *GPD1*-targeting and *GPD2*-targeting gRNA cassettes, was amplified using primers 6965-6966 and pROS10 as template. For construction of pUDR103, the plasmid backbone of pMEL10 was PCR amplified using primers 5792-5980. The *SGA1*-targeting gRNA expression cassette was PCR amplified using primers 5979-7023 and pMEL10 as template. For construction of pUDR264, the plasmid backbone of pMEL11 was PCR amplified using primers 5792-5980. The *ALD6*-targeting gRNA expression cassette was PCR amplified using primers 5979-7610 and pMEL11 as a template. Plasmids were assembled with the Gibson Assembly Cloning kit (New England Biolabs, Ipswich, MA), after downscaling the supplier's protocol to 10 µl reaction volumes. Plasmids pUDR240 and pUDR264 were cloned in *E. coli* XL-1 blue cells after transformation by electroporation and plasmid re-isolation with a miniprep kit (Sigma-Aldrich, St. Louis, MO). Correct clones were

verified by restriction digestion or by diagnostic PCR (DreamTaq polymerase, Additional File S1). For single deletion of *GPD2*, a plasmid backbone was PCR amplified with the double-binding primer 5793 and pROS10 as template. The insert fragment, expressing two identical *GPD2*-targeting gRNA cassettes, was amplified with primer 6966 and pROS10 as template. For single deletion of *GPD2*, the two plasmid fragments were transformed directly into yeast cells and assembled *in vivo*.

An *S. cerevisiae* codon-optimized version of *Archaeoglobus fulgidus gpsA* [Genbank: AAB90367.1], based on the codon preference of highly expressed yeast glycolytic genes [49], was synthesized by GeneArt GmbH (Regensburg, Germany) [Genbank: KY554758]. An integration cassette for replacing the coding region of *GPD1* by the codon-optimized *gpsA* sequence was PCR amplified with primers 7862-7863 and pMK-RQ-*gpsA* as template. Codon-optimized expression cassettes for the *E. coli* EutE acetylating-acetaldehyde dehydrogenase gene (*TDH3p-eutE-CYC1t*), aimed at integration in the *GPD2* or *SGA1* locus, were amplified with primers 7991-7992 or 7211-7025, respectively, using pUDI076 [29] as a template. A cassette expressing *ALD6* from its native promoter and terminator sequences, aimed at integration in the *SGA1* locus, was amplified with primers 9809-9810, using genomic DNA of *S. cerevisiae* IMX581 as a template. Integration cassettes were flanked by 60-bp sequences that enabled integration by homologous recombination after CRISPR/Cas9-mediated introduction of double-strand breaks in selected *S. cerevisiae* genomic loci.

Table 1. *S. cerevisiae* strains used in this study.

Strain name	Relevant Genotype	Origin
IMX585	<i>MAL2-8c SUC2 can1::cas9-natNT2</i>	[48]
IMX581	<i>ura3-52 MAL2-8c SUC2 can1::cas9-natNT2</i>	[48]
IMZ160	<i>ura3 leu2::LEU2 [pRS405] gpd1::loxP gpd2::hphMX4 pUDE43</i>	[43]
IME324	<i>ura3-52 MAL2-8c SUC2 can1::cas9-natNT2 p426-TEF (empty)</i>	This work
IMX884	<i>ura3-52 MAL2-8c SUC2 can1::cas9-natNT2 gpd2::eutE pROS10 (GPD2-targeting)</i>	This work
IMX992	<i>ura3-52 MAL2-8c SUC2 can1::cas9-natNT2 sga1::eutE pUDR119</i>	This work
IMX776	<i>ura3-52 MAL2-8c SUC2 can1::cas9-natNT2 gpd1::gpsA gpd2::eutE pUDR240</i>	This work
IMX901	<i>ura3-52 MAL2-8c SUC2 can1::cas9-natNT2 gpd1::gpsA gpd2::eutE ald6Δ pUDR240</i>	This work
IMX888	<i>MAL2-8c SUC2 can1::cas9-natNT2 gpd1Δ gpd2::eutE</i>	[29]
IMX900	<i>MAL2-8c SUC2 can1::cas9-natNT2 gpd1Δ gpd2::eutE ald6Δ</i>	This work
IMX1039	<i>ura3-52 MAL2-8c SUC2 can1::cas9-natNT2 gpd1::gpsA gpd2::eutE ald6Δ</i>	This work
IMX1120	<i>MAL2-8c SUC2 can1::cas9-natNT2 gpd1Δ gpd2::eutE ald6Δ sga1::ALD6</i>	This work
IMX1142	<i>ura3-52 MAL2-8c SUC2 can1::cas9-natNT2 gpd1::gpsA gpd2::eutE ald6Δ sga1::ALD6 pUDR103</i>	This work

Table 2. Plasmids used in this study.

Plasmid	Characteristics	Origin
p426-TEF (empty)	2 μ, <i>URA3, TEF1p-CYC1t</i>	[75]
pMEL10	2 μ, <i>KIURA3, SNR52p-gRNA.CAN1.Y-SUP4t</i>	[48]
pMEL11	2 μ, <i>amdS, SNR52p-gRNA.CAN1.Y-SUP4t</i>	[48]
pROS10	<i>KIURA3-gRNA.CAN1-2mu-gRNA.ADE2</i>	[48]
pUDI076	pRS406- <i>TDH3p-eutE-CYC1t</i>	[29]
pUDR103	2 μ, <i>KIURA3, SNR52p-gRNA.SGA1.Y-SUP4t</i>	This work
pUDR119	2 μ, <i>amdS, SNR52p-gRNA.SGA1.Y-SUP4t</i>	[76]
pUDR240	<i>KIURA3-gRNA.GPD1-2mu-gRNA.GPD2</i>	This work
pUDR264	2 μ, <i>amdS, SNR52p-gRNA.ALD6.Y-SUP4t</i>	This work
pMK-RQ-gpsA	Delivery vector, codon-optimized <i>gpsA</i> ORF	GeneArt, Germany

4.2.3 Strain construction

The lithium acetate/polyethylene glycol method [50] was used for yeast transformation. After transformation with plasmids pUDR103, pUDR240 and after single deletion of *GPD2*, transformants were selected on synthetic medium agar plates [47] containing 20 g L⁻¹ glucose. After transformation with plasmids pUDR119 and pUDR264, selection and counter selection were performed as described [51]. Counter selection of plasmids carrying *URA3* was performed on YP agar plates (10 g L⁻¹ Bacto yeast extract, 20 g L⁻¹ Bacto peptone) supplemented with glucose (20 g L⁻¹ final concentration) and 5-fluoroorotic acid (1 g L⁻¹ final concentration). Diagnostic colony PCR was used for genotypic analysis of selected colonies. Co-transformation of pUDR119 and the *SGA1*-flanked *TDH3p-eutE-CYC1t* cassette into strain IMX581 yielded strain IMX992, in which *eutE* was overexpressed in the presence of functional *GPD1* and *GPD2* genes. Co-transformation of the two fragments of the *GPD2*-targeting gRNA plasmid and the *GPD2*-flanked *TDH3p-eutE-CYC1t* cassette to strain IMX581 yielded strain IMX884, in which *GPD2* was deleted and *eutE* was overexpressed. Co-transformation of pUDR240, the *GPD1*-flanked *gpsA* coding sequence and the *GPD2*-flanked *TDH3p-eutE-CYC1t* cassette to strain IMX581 yielded strain IMX776, in which *gpsA* was expressed from the native *GPD1* promoter and terminator, *GPD2* was deleted and *eutE* was overexpressed. Co-transformation of pUDR264 and the repair oligonucleotides 7608-7609, followed by pUDR264 counter-selection, into strains IMX776 and IMX888 yielded strains IMX901 and IMX900 respectively, in which *ALD6* was deleted. Counter-selection of pUDR240 from IMX901 yielded strain IMX1039. Strain IMX1142, in which the native *ALD6* gene was re-introduced in the *SGA1* locus, was obtained by co-transformation of pUDR103 and the *SGA1*-flanked *ALD6* cassette into strain IMX1039. Co-transformation of pUDR119 and the *SGA1*-flanked *ALD6* cassette into strain IMX900, following pUDR119 counter-selection, yielded strain IMX1120. The empty-vector reference strain IME324 was obtained by transformation of IMX581 with p426-*TEF*.

4.2.4 Bioreactor batch cultivation

Anaerobic batch cultures were grown in 2-L bioreactors (Applikon, Schiedam, The Netherlands) on synthetic medium [47] supplemented with acetic acid (3 g L⁻¹ final concentration). In high-osmolarity cultures of the acetate-consuming strains IMX776, IMX901 and IMX1142, the concentration of acetic acid was re-set to 3 g L⁻¹ when it reached a value below 1.5 g L⁻¹, by addition of glacial acetic acid, to prevent acetic-acid limitation [43]. After autoclaving the mineral salt components of the synthetic medium and acetic acid at 120 °C for 20 min, anaerobic growth media were supplemented with sterile antifoam C (0.2 g L⁻¹) (Sigma-Aldrich), ergosterol (10 mg L⁻¹), Tween 80 (420 mg L⁻¹) and filter-sterilized vitamin solution [47]. Glucose solutions were autoclaved separately at 110 °C for 20 min and added to low- and high-osmolarity media at final concentrations of 20 g L⁻¹ and 180 g L⁻¹ (1 M), respectively. Shake-flask cultures (100 mL) were inoculated with frozen glycerol stock cultures (1 mL) and grown on synthetic medium supplemented with glucose (20 g L⁻¹ final concentration). Samples from these cultures were used as inocula for 100 mL shake-flask pre-cultures on the same medium, yielding an initial OD₆₆₀ of 0.1 to 0.3. Upon reaching mid-exponential phase (OD₆₆₀ 4-6), samples from these pre-cultures were used to inoculate anaerobic bioreactor cultures, yielding an initial OD₆₆₀ of 0.15-0.2. Anaerobic conditions were maintained by continuously sparging nitrogen gas (<10 ppm oxygen) at a rate of 0.5 L min⁻¹. Norprene tubing and Viton O-rings were used to minimize oxygen diffusion into the reactors. In low-osmolarity cultures, the culture pH was automatically controlled at 5 by addition of 2 M KOH. In high-osmolarity cultures (pH 5), a 12.5% v v⁻¹ NH₄OH solution was used as titrant to prevent nitrogen limitation. The stirrer speed was set at 800 rpm and temperature was controlled at 30 °C. Evaporation was minimized by cooling the outlet gas to 4 °C in a condenser.

4.2.5 Enzyme-activity assays

Cell extracts were prepared by sonication [52] of biomass from exponential-phase shake-flask cultures (OD₆₆₀ 5-6) grown on synthetic medium (20 g L⁻¹ glucose) in an aerobic incubator.

Enzyme-activity assays were performed at 30 °C by continuous spectrophotometric monitoring of the conversion of NAD(P)H to NAD(P)⁺ at 340 nm. For determination of acetylating-acetaldehyde dehydrogenase activity [25], cells were sonicated in 100 mM potassium phosphate buffer (KPB, pH 7.5) with 2 mM MgCl₂ and 1 mM dithiothreitol. The 1-mL reaction mixture contained 50 mM KPB (pH 7.5), 0.15 mM NADH and 50 or 70 μL cell extract. Reactions were started by addition of acetyl-CoA to a final concentration of 0.5 mM. To assess if expression of *A. fulgidus gpsA* resulted in a change in the cofactor preference of glycerol-3-phosphate dehydrogenase (G3PDH) in *S. cerevisiae*, G3PDH activities were measured with a modified version of a published assay optimized for GpsA [45]. In the modified assay, 20 mM Tris-HCl (pH 8.2) buffer supplemented with 10 mM EDTA was used for harvesting and storage of cells and sonication was performed in 20 mM Tris-HCl (pH 8.2) buffer with 2 mM EDTA. The 1-mL reaction mixture contained 50 mM Tris-HCl (pH 6.6), 2 mM EDTA, 0.15 mM NADH or NADPH and 50 or 70 μL cell extract. The reaction was started by addition of dihydroxy-acetone phosphate to a final concentration of 4 mM. All assays were performed on samples from two independent cultures and enzyme activities were proportional to the volume of cell extract added to the assay.

4.2.6 Intracellular glycerol determination

Shake-flask pre-cultures on synthetic medium (20 g L⁻¹ glucose) were inoculated from frozen stocks. After reaching mid-exponential phase, cells were washed with sterile demineralized water and used as inoculum for anaerobic shake-flask cultures on the same medium as the high-osmolarity bioreactor batch cultivations. Anaerobic shake-flask cultures were grown in a Bactron anaerobic chamber (Sheldon Manufacturing, Cornelius, OR) at 30 °C. Mid-exponential phase cultures were harvested and centrifuged at 4000 x g for 5 min. The supernatant was discarded, cells were resuspended in 0.005 mol L⁻¹ H₂SO₄ and incubated at 100 °C for 5 min. The cell suspension was centrifuged at 4000 x g for 5 min and the supernatant was used for HPLC analysis. For calculation of the pellet volume, an average density of the pellet of 1.1 g mL⁻¹ was

used [53]. For conversion of intracellular glycerol concentration from g (g dry weight)⁻¹ to g L⁻¹, an intracellular volume of 2.6 mL (g dry weight)⁻¹ was used [54].

4.2.7 Analytical methods

Biomass dry weight determination, HPLC analysis of extracellular metabolites and correction for ethanol evaporation were performed as previously described [25]. Culture offgas composition was analysed as previously described [25], except for batch cultures grown under high-osmolarity conditions with strains IMX992, IMX884, IMX776 and IMX901, in which production of CO₂ was calculated from ethanol production, assuming formation of 1 mol CO₂ per mol ethanol produced. Prior to glucose and ethanol concentration measurements in high-osmolarity fermentations, culture supernatant was diluted 1:1 with demineralized water. Product yields and ratios in batch cultures were calculated from a minimum of five samples taken during the mid-exponential growth phase [29]. Biomass concentrations corresponding to samples taken before the mid-exponential growth phase (OD₆₆₀ < 1) were calculated based on OD₆₆₀ measurements, using calibration curves based on a minimum of five samples taken in mid-exponential phase for which biomass dry weight and OD₆₆₀ were measured [29].

4.3 Results

4.3.1 Limited impact of the expression of an acetate-reduction pathway in *GPD1 GPD2 S. cerevisiae*

Previous studies on acetate reduction by anaerobic, glucose-grown *S. cerevisiae* cultures were based on *gpd1Δ gpd2Δ* strains [25,29]. In these strains, the role of the native glycerol pathway in NADH reoxidation was entirely replaced by reduction of externally supplied acetate to ethanol. To investigate the impact of co-expressing an acetate-reduction pathway with a fully functional glycerol pathway, growth and product formation of strain IMX992 (*GPD1 GPD2 sga1::eutE*) were analysed in anaerobic, glucose-grown bioreactor batch cultures on 20 g L⁻¹ glucose, supplemented with 3 g L⁻¹ acetic acid (Fig. 1, Table 3) and compared with the acetate non-

reducing reference strain IME324. Under these conditions and consistent with previous reports [29,43], IME324 (*GPD1 GPD2*) showed an acetate consumption of 2.43 mmol (g biomass)⁻¹ (Table 3). In acetate non-reducing strains, consumption of small amounts of acetate can reflect intracellular accumulation and/or use of extracellular-acetate-derived acetyl-CoA as a biosynthetic precursor [55]. Strain IMX992 (*GPD1 GPD2 sga1::eutE*) showed an acetate consumption of 3.35 mmol (g biomass)⁻¹, which was only 0.92 mmol (g biomass)⁻¹ higher than the acetate consumption by the *GPD1 GPD2* reference strain. Conversely, under identical conditions, strain IMX888 (*gpd1Δ gpd2::eutE*) showed an acetate consumption of 6.92 mmol (g biomass)⁻¹ in a previous study [29]. Consistent with its marginally higher acetate consumption, glycerol production by strain IMX992 decreased only slightly, from 9.19 to 8.28 mmol glycerol (g biomass)⁻¹, relative to strain IME324 (Table 3). Clearly, in glucose-fermenting engineered *S. cerevisiae* strains, EutE-based acetate reduction could not efficiently compete for NADH with a fully functional native glycerol pathway.

4.3.2 Deletion of *GPD2* improves acetate reduction by an *eutE*-expressing strain

GPD2 encodes the redox-regulated isoenzyme of G3PDH and its deletion has been reported to cause impaired anaerobic growth of *S. cerevisiae* [23,35]. In acetate-supplemented anaerobic cultures of strain IMX884 (*GPD1 gpd2::eutE*), *eutE* expression fully compensated for the absence of a functional Gpd2 enzyme, both in terms of specific growth rate and in terms of biomass yield on glucose (Table 3, Fig. 1, Additional File S3). Compared to strain IMX992 (*GPD1 GPD2 sga1::eutE*), strain IMX884 showed a 4-fold lower production of glycerol (1.92 and 8.28 mmol glycerol (g biomass)⁻¹, respectively) and a correspondingly higher EutE-based acetate consumption (3.34 and 0.92 mmol acetate (g biomass)⁻¹, respectively, corrected for acetate consumption by the acetate non-reducing reference strain IME324, resulting in an ethanol yield on glucose of 0.46 g g⁻¹ (Additional File S3). These results indicate that, at least in low-osmolarity media, inactivation of *GPD2* enables the EutE-based acetate reduction pathway to efficiently compete for redox equivalents with the glycerol pathway. This engineering strategy not only

resulted in a markedly higher acetate consumption, but also in a higher ethanol yield on glucose than observed in the acetate non-reducing reference strain IME324 (Table 3, Additional File S3).

Table 3. Specific growth rate (μ) and stoichiometric relationships between glycerol production and biomass formation, acetate consumption and glucose consumption, and acetate consumption and biomass formation in anaerobic bioreactor batch cultures of *S. cerevisiae* strains with different genetic modifications in glycerol and acetate metabolism. Cultures were grown on synthetic medium containing 20 g L⁻¹ glucose and 3 g L⁻¹ acetic acid (pH 5). Specific growth rates and stoichiometries were calculated from the mid-exponential growth phase and represent averages \pm mean deviations of data obtained from independent duplicate cultures. In all cultures, carbon recoveries were between 95 and 100%. Enzyme activities of acetylating-acetaldehyde dehydrogenase in cell extracts of *eutE*-expressing strains were similar (Additional File S2).

Strain	IME324	IMX992	IMX884	IMX776	IMX901	IMX888*
Relevant Genotype	<i>GPD1 GPD2</i>	<i>GPD1 GPD2 sga1::eutE</i>	<i>GPD1 gpd2::eutE</i>	<i>gpd1::gpsA gpd2::eutE</i>	<i>gpd1::gpsA gpd2::eutE ald6Δ</i>	<i>gpd1Δ gpd2::eutE</i>
μ (h⁻¹)	0.31 \pm 0.01	0.30 \pm 0.00	0.31 \pm 0.01	0.24 \pm 0.01	0.24 \pm 0.01	0.26 \pm 0.01
Ratio glycerol produced/biomass (mmol (g biomass)⁻¹)	9.19 \pm 0.08	8.28 \pm 0.14	1.92 \pm 0.06	< 0.1	< 0.1	< 0.1
Ratio acetate consumed/biomass (mmol (g biomass)⁻¹)	2.43 \pm 0.16	3.35 \pm 0.08	5.77 \pm 0.25	6.66 \pm 0.01	6.41 \pm 0.28	6.92 \pm 0.12
Ratio acetate consumed/glucose (g g⁻¹)	0.010 \pm 0.000	0.015 \pm 0.000	0.026 \pm 0.001	0.031 \pm 0.001	0.031 \pm 0.000	0.032 \pm 0.000

*Data on strain IMX888 were taken from [29].

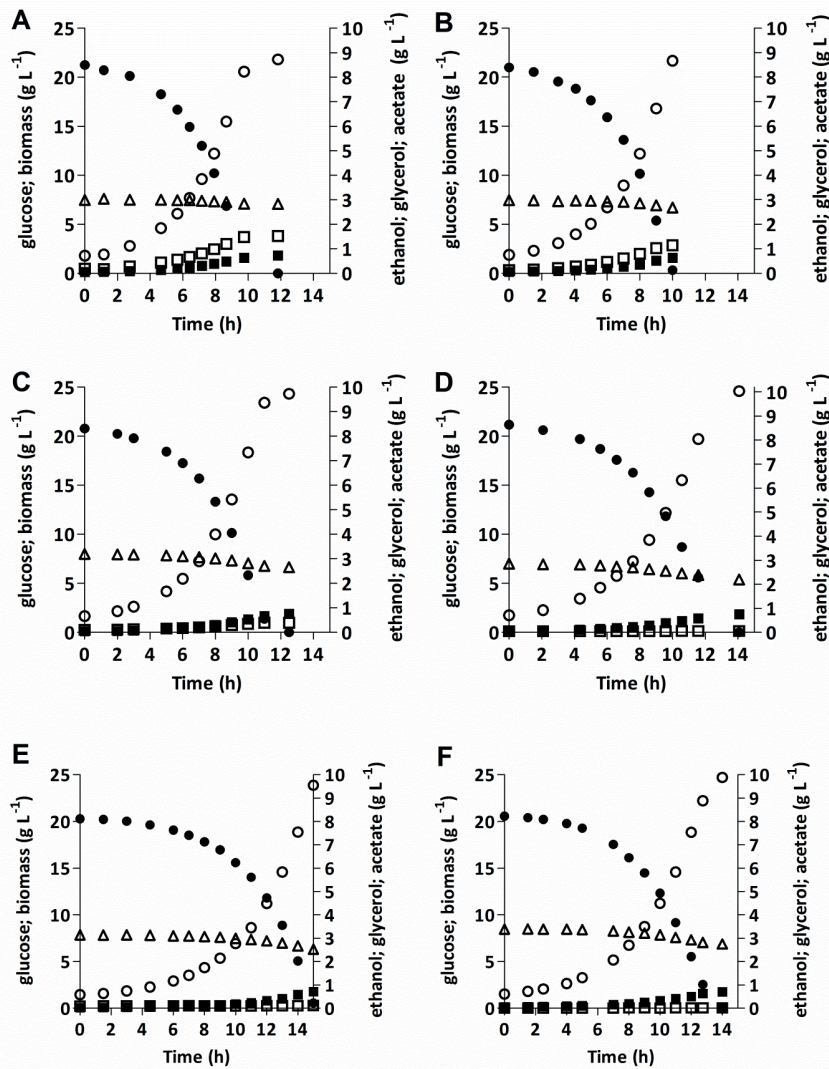


Figure 1. Growth, glucose consumption and product formation in anaerobic bioreactor batch cultures of *S. cerevisiae* strains with different genetic modifications in glycerol and acetate metabolism. Cultures were grown on synthetic medium containing 20 g L^{-1} glucose and 3 g L^{-1} acetic acid (pH 5). A, strain IME324 (*GPD1 GPD2*); B, strain IMX992 (*GPD1 GPD2 sga1::eutE*); C, strain IMX884 (*GPD1 gpd2::eutE*); D, strain IMX776 (*gpd1::gpsA gpd2::eutE*); E, strain IMX901 (*gpd1::gpsA gpd2::eutE ald6Δ*); F, strain IMX888 (*gpd1Δ gpd2::eutE*). Symbols: ●, glucose; ■, biomass; □, glycerol; ○, ethanol; △, acetate. Panels A-F display single representative cultures from a set of two independent duplicate cultures for each strain. Data on strain IMX888 were taken from [29].

4.3.3 Functional expression of an NADPH-preferring G3PDH in *S. cerevisiae*

As outlined above, expression of the NADP⁺-preferring G3PDH encoded by *A. fulgidus* *gpsA* might enable strategies to uncouple the roles of glycerol metabolism in yeast osmotolerance and redox balancing. To investigate whether *gpsA* can be functionally expressed in *S. cerevisiae*, its coding sequence was codon-optimized for expression in yeast and integrated at the *GPD1* locus of strain IMX581 (along with integration of *eutE* at the *GPD2* locus), yielding strain IMX776 (*gpd1::gpsA gpd2::eutE*). This insertion was designed to place *gpsA* under the control of the *GPD1* promoter and terminator, in order to enable upregulation of its expression at high-osmolarity [20,21].

Enzyme activity assays in cell extracts showed that, in strain IMX776, replacement of the native *GPD1* and *GPD2* genes by *gpsA* resulted in a switch in cofactor preference of glycerol-3-phosphate dehydrogenase (G3PDH, Fig. 2). The *gpsA*-expressing strain showed *in vitro* activities of $0.103 \pm 0.004 \mu\text{mol mg protein}^{-1} \text{ min}^{-1}$ and $0.006 \mu\text{mol mg protein}^{-1} \text{ min}^{-1}$ with NADPH and NADH, respectively. As a result, the ratio of NADPH- and NADH-linked rates of dihydroxyacetone phosphate reduction was ca. 500-fold higher in strain IMX776 than in the reference strain IMX992, which expresses the native *GPD1* and *GPD2* genes. These observations are consistent with a previous report on the cofactor preference of GpsA, expressed in *E. coli* [45], and show that the enzyme was functionally expressed in yeast.

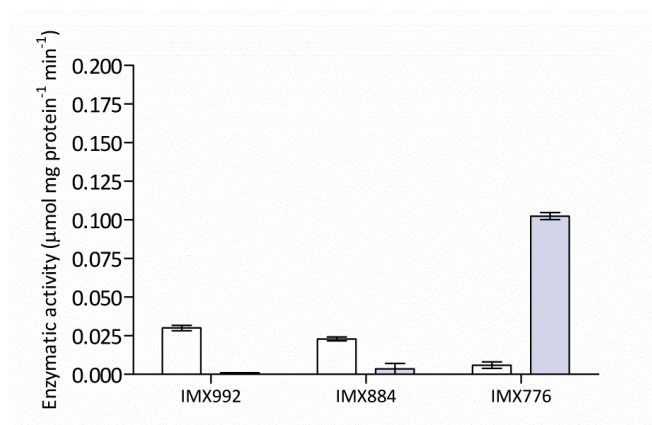


Figure 2. Specific rates of NADH-dependent (white bars) and NADPH-dependent (blue bars) reduction of dihydroxy-acetone phosphate by cell extracts of shake-flask cultures on synthetic medium (20 g L⁻¹ glucose) of *S. cerevisiae* strains IMX992 (*GPD1 GPD2*), IMX884 (*GPD1 gpd2::eutE*) and IMX776 (*gpd1::gpsA gpd2::eutE*). Data represent averages \pm mean deviations of assays on independent duplicate cultures.

4.3.4 Increased acetate reduction and decreased glycerol production in a *gpsA*-expressing yeast strain

The combined activity of acetyl-CoA synthetase and EutE, both of which are essential for acetate reduction and Ald6, the major NADP⁺-dependent, cytosolic isoform of acetaldehyde dehydrogenase [56], could potentially form an ATP-driven dehydrogenase cycle (NADH + NADP⁺ \rightarrow NADPH + NAD⁺ [29]). In *gpsA*-expressing strains, NADPH formed via this cycle might increase glycerol production and, consequently, decrease ethanol yields (Additional File S8). Therefore, *ALD6* was deleted in the *gpsA*-expressing, acetate-reducing strain IMX776 (*gpd1::gpsA gpd2::eutE*), yielding strain IMX901.

In anaerobic, acetate-supplemented bioreactor batch cultures the specific growth rate of strain IMX776 (*gpd1::gpsA gpd2::eutE*) was 0.24 h⁻¹, which was ca. 20% lower than that of the reference strain IME324 (*GPD1 GPD2*). The physiology of strain IMX776 in these anaerobic low-osmolarity cultures, including the stoichiometry of biomass formation and acetate consumption, closely resembled that of strain IMX888 (*gpd1Δ gpd2::eutE*) (Table 3, Fig. 1, Additional File S3). Virtually no extracellular glycerol was formed by strain IMX776, indicating that, under these conditions, the *in vivo* activity of NADPH-dependent glycerol production in this strain was

minimal. Consistent with this notion, growth and product formation in anaerobic cultures of strain IMX901 (*gpd1::gpsA gpd2::eutE ald6Δ*) was similar to the observed performance of strains IMX776 or IMX888 under these conditions.

4.3.5 Growth at high-osmolarity negatively affects acetate reduction by a *gpd2A* strain

To assess the impact of high-osmolarity on the acetate reduction observed in the *GPD1 gpd2::eutE* strain IMX884, its performance was compared with that of strain IMX992 (*GPD1 GPD2 sga1::eutE*) in anaerobic bioreactor batch cultures grown on 1 mol L⁻¹ (180 g L⁻¹) glucose. In contrast to the low-osmolarity cultures, in which strains continued to grow exponentially until glucose was depleted (Fig. 1), high-osmolarity conditions showed a biphasic growth profile, in which the exponential phase was followed by second, slower growth phase (Fig. 3). This biphasic growth profile probably reflects a nutritional limitation other than carbon source depletion. For example, concentrations of the anaerobic growth factors Tween-80 and ergosterol were not increased in high-osmolarity media to avoid potential toxic effects [15]. A similar growth pattern in high-glucose cultures has been reported previously [43].

Consistent with previously reported data on a congeneric, non-acetate reducing *GPD1 GPD2* strain grown under high-osmolarity conditions [43], the initial specific growth rate of strain IMX992 (*GPD1 GPD2 sga1::eutE*) was not affected by increasing the glucose concentration in the medium to 1 mol L⁻¹ (Tables 3 and 4). Acetate consumption in the high-osmolarity cultures by this strain was even slightly lower than observed during growth on 20 g L⁻¹ glucose (2.67 and 3.35 mmol (g biomass⁻¹), respectively). This observation indicates that, also under high-osmolarity conditions, EutE-mediated acetate reduction could not efficiently compete for NADH with a fully functional glycerol pathway.

Strain IMX884 (*GPD1 gpd2::eutE*) showed a 10% lower specific growth rate in high-osmolarity medium than in cultures grown on a low glucose concentration (Tables 3 and 4). This, only minor, difference is consistent with the reported predominant role of the Gpd1 isoenzyme in osmoregulation [20,21,57]. Relative to its performance in low-osmolarity cultures,

growth on 1 mol L⁻¹ glucose led to a three-fold increase in extracellular glycerol production (6.34 mmol (g biomass)⁻¹ versus 1.92 mmol (g biomass)⁻¹) and a corresponding decrease in acetate consumption (2.98 mmol (g biomass)⁻¹ versus 5.77 mmol (g biomass)⁻¹) (Tables 3 and 4). These changes largely eliminated the four-fold difference in glycerol production between strains IMX992 and IMX884 that was observed in low-osmolarity cultures (Tables 3 and 4). After complete glucose consumption, concentrations of acetic acid, glycerol and ethanol reached similar concentrations in high-osmolarity cultures of the two strains (Fig. 3). These results indicate that, even when *GPD2* is deleted, high-osmolarity conditions impeded the competition of the EutE-based acetate reduction pathway for NADH with the glycerol pathway, possibly due to osmotic-stress induced upregulation of *GPD1*.

Table 4. Specific growth rate (μ), yields (Y) of biomass, ethanol and glycerol on glucose and stoichiometric relationships between glycerol production and biomass formation, acetate consumption and glucose consumption, and acetate consumption and biomass formation in anaerobic bioreactor batch cultures of *S. cerevisiae* strains with different genetic modifications in glycerol and acetate metabolism. Cultures were grown on synthetic medium containing 180 g L⁻¹ glucose and 3 g L⁻¹ acetic acid (pH 5). Specific growth rates and stoichiometries were calculated from the mid-exponential growth phase and represent averages \pm mean deviations of data obtained from independent duplicate cultures.

Strain	IMX992	IMX884	IMX776	IMX901
Relevant Genotype	<i>GPD1 GPD2 sga1::eutE</i>	<i>GPD1 gpd2::eutE</i>	<i>gpd1::gpsA gpd2::eutE</i>	<i>gpd1::gpsA gpd2::eutE ald6Δ</i>
μ (h⁻¹)	0.28 \pm 0.02	0.27 \pm 0.00	0.14 \pm 0.00	0.12 \pm 0.02
Y biomass/glucose (g g⁻¹)	0.087 \pm 0.001	0.085 \pm 0.000	0.089 \pm 0.000	0.077 \pm 0.013
Y ethanol/glucose (g g⁻¹)	0.43 \pm 0.01	0.42 \pm 0.02	0.47 \pm 0.01	0.49 \pm 0.00
Y glycerol/glucose (g g⁻¹)	0.07 \pm 0.00	0.05 \pm 0.00	0.02 \pm 0.00	< 0.001
Glycerol produced/biomass (mmol (g biomass)⁻¹)	8.76 \pm 0.25	6.34 \pm 0.26	3.29 \pm 0.41	< 0.1
Acetate consumed/biomass (mmol (g biomass)⁻¹)	2.67 \pm 0.96	2.98 \pm 0.08	2.88 \pm 0.17	5.71 \pm 0.15
Acetate consumed/glucose (g g⁻¹)	0.011 \pm 0.001	0.015 \pm 0.000	0.016 \pm 0.000	0.027 \pm 0.003

4.3.6 Replacement of *GPD1* and *GPD2* by *gpsA* uncouples the roles of glycerol formation in redox metabolism and osmoregulation

To test whether replacement of the yeast NAD⁺-dependent Gpd isoenzymes by an NADP⁺-preferring G3PDH can uncouple the roles of glycerol formation in osmoregulation and redox metabolism, growth and product formation of strain IMX776 (*gpd1::gpsA gpd2::eutE*) was investigated in high-osmolarity cultures. In contrast to strains IMX992 and IMX884, strain IMX776 showed a lag phase of ca. 50 h under these conditions (Fig. 3, Additional File S4) and its specific growth rate was 60% lower than in low-osmolarity cultures (Tables 3 and 4). While, under low-osmolarity conditions, this strain did not produce extracellular glycerol, high-osmolarity batch cultures showed a glycerol production of 3.29 mmol (g biomass)⁻¹ (Table 4). After glucose depletion, the glycerol concentration in high-osmolarity cultures of strain IMX776 was 44% lower than observed for strain IMX992 (*GPD1 GPD2 sga1::eutE*) (Fig. 3).

Strain IMX776 showed a much lower acetate consumption in the high-glucose cultures than in low-osmolarity cultures (Tables 3 and 4). This difference could be caused by an increased flux through the cytosolic, NADP⁺-dependent acetaldehyde dehydrogenase Ald6, coupled to the increased demand for NADPH in the cytosolic GpsA reaction. Generating NADPH via the oxidation of acetaldehyde to acetate, which can subsequently be reduced to ethanol via acetyl-CoA synthetase, EutE and NAD⁺-dependent alcohol dehydrogenase, would result in less extracellular acetate being consumed for NADH reoxidation (Additional File S8). An increased production of acetate has been previously observed upon an increase of cytosolic NADPH demand in anaerobic *S. cerevisiae* cultures [29].

Consistent with the hypothesis outlined above, deletion of *ALD6* had a strong impact on the physiology of anaerobic cultures of acetate-reducing *gpsA*-expressing *S. cerevisiae*. Although the specific growth rates of strain IMX776 (*gpd1::gpsA gpd2::eutE*) and strain IMX901 (*gpd1::gpsA gpd2::eutE ald6Δ*) in high-osmolarity cultures were similar (Table 4), complete absence of a lag phase decreased the overall fermentation time of the latter strain by ca. 35 h (Fig. 3, Additional File S4). In addition, strain IMX901 fully relied on exogenous acetic acid

supply for its redox balancing. When, after exponential growth was finished, no additional acetate was provided, growth and glucose consumption slowed down considerably (Additional File S5). A similar addition of acetate to a high-osmolarity batch culture of strain IMX776 did not affect its growth (Additional File S5).

In contrast to strains IMX884 and IMX776, strain IMX901 retained a glycerol non-producing phenotype throughout growth in bioreactor cultures on high-osmolarity medium, resulting in a 13% higher ethanol yield on glucose compared to strain IMX992 (*GPD1 GPD2 sga1::eutE*; Table 4). This, in combination with a measured intracellular glycerol concentration of $5.3 \pm 0.04 \text{ g L}^{-1}$ in anaerobic shake-flask cultures of strain IMX901 on high-osmolarity medium, indicated a complete intracellular retention of glycerol formed via GpsA in this strain. When additional acetate was added to high-osmolarity bioreactor cultures of strain IMX901 immediately after the exponential phase, no extracellular glycerol was detectable (Fig. 3). However, when acetate was added 20 h into the stationary phase (Additional File S5), low concentrations of glycerol were detectable ($< 1 \text{ g L}^{-1}$ final concentration).

4.3.7 Growth of an acetate-reducing *gpd1Δ gpd2Δ* strain in high-osmolarity medium

In the experiments discussed above, the glycerol non-producing, acetate-reducing strain IMX888 (*gpd1Δ gpd2::eutE*) was included as a reference strain. Surprisingly, despite the absence of a functional glycerol pathway, this strain consistently grew in anaerobic high-osmolarity cultures, after a lag phase of ca. 75 h (Additional File S6). Furthermore, the strain retained its acetate-reducing phenotype, with minimal concentrations of acetate and glycerol having been produced upon glucose depletion (Additional File S7). This result contradicts earlier reports of a complete inability of *gpd1Δ gpd2Δ* strains to grow at high-osmolarity [20,21,43]. We therefore re-tested growth of strain IMZ160 (*gpd1Δ gpdΔ mhpF*) [43], which has been previously reported not to grow under the high-osmolarity conditions used in the present study. Consistent with previous observations, this strain failed to grow in high-osmolarity cultures, even after 300 h of incubation (Additional File S6). The different phenotypes of two acetylating-acetaldehyde

expressing, glycerol-negative *S. cerevisiae* strains may reflect the lower *in vivo* activities of heterologously expressed MhpF relative to EutE [25,29]. To investigate a possible involvement of *ALD6* (see above and Additional File S8), this gene was deleted in strain IMX888, yielding strain IMX900 (*gpd1Δ gpd2::eutE ald6Δ*). The latter strain showed a strongly reduced lag phase in high-osmolarity medium relative to its parental strain IMX888, thereby reducing the total fermentation time by ca. 45 h (Additional File S6). However, the overall fermentation time of strain IMX900 was still considerably longer than the *gpsA*-expressing *ald6Δ* strain IMX901 (Additional File S6, Fig. 3). Similar to its parental strain, IMX900 retained its acetate-reducing phenotype and produced only trace amounts of extracellular glycerol (Additional File S7). When the native *S. cerevisiae* *ALD6* gene, including its promoter and terminator sequences, was integrated at the *SGA1* locus of strains IMX900 and IMX901, the resulting strains (IMX1120 and IMX1142), again showed a prolonged lag phase, confirming the detrimental effect of Ald6 in this experimental context (Additional File S6, Fig. 3).

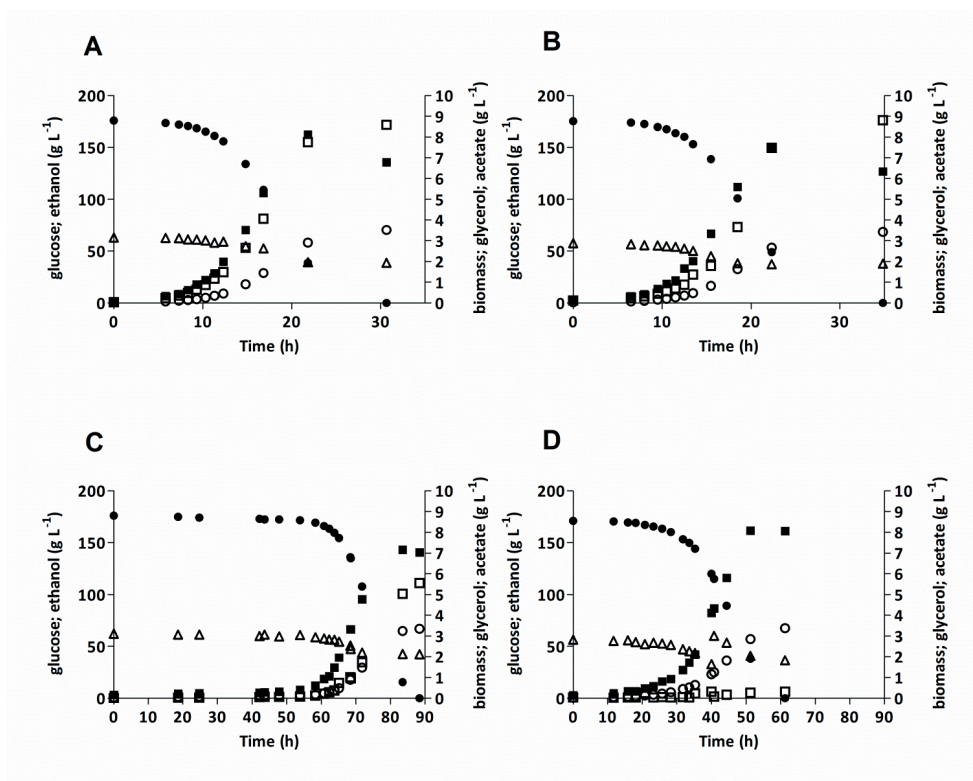


Figure 3. Growth, glucose consumption and product formation in anaerobic bioreactor batch cultures of *S. cerevisiae* strains with different genetic modifications in glycerol and acetate metabolism. Cultures were grown on synthetic medium containing 180 g L⁻¹ glucose and 3 g L⁻¹ acetic acid (pH 5). A, strain IMX992 (*GPD1 GPD2 sga1::eutE*); B, strain IMX884 (*GPD1 gpd2::eutE*); C, strain IMX776 (*gpd1::gpsA gpd2::eutE*); D, strain IMX901 (*gpd1::gpsA gpd2::eutE ald6Δ*). Symbols: ●, glucose; ■, biomass; □, glycerol; ○, ethanol; Δ, acetate. Panels A-C display single representative cultures from a set of two independent duplicate cultures for each strain. In the culture of IMX901, acetic acid was added externally immediately after the exponential growth phase was finished.

4.4 Discussion

Expression of a heterologous acetylating-acetaldehyde dehydrogenase (A-ALD) can fully restore anaerobic growth in acetate-supplemented cultures of *S. cerevisiae* strains that lack a functional glycerol pathway [25,29]. However, the minor decrease in glycerol formation observed upon A-ALD expression in a *GPD1 GPD2* strain (Table 3) indicated that A-ALD-based acetate reduction cannot efficiently compete for NADH with a fully functional, native glycerol pathway. Recently, a 40% decrease in glycerol yield was reported upon A-ALD expression in an industrial *S. cerevisiae* strain [58]. The higher relative impact of A-ALD expression in the industrial strain coincided with a 2-fold lower glycerol yield relative to that of the laboratory reference strain used in this work. These observations identify reduction of the capacity of the native glycerol pathway as an interesting strategy for facilitating NADH reoxidation via acetate reduction. Indeed, deletion of *GPD2*, which encodes the major isoenzyme of G3PDH in anaerobic, low-osmolarity cultures of *S. cerevisiae* [21,23] strongly stimulated acetate reduction (Table 3). By enabling an over four-fold lower glycerol yield and corresponding increase in ethanol production by acetate reduction, without any reduction in specific growth rate, combined deletion of *GPD2* and expression of an A-ALD offers a promising strategy for improving ethanol production in low-osmolarity, acetic-acid containing media. In such processes, osmolarity may be limited by fed-batch cultivation regimes and/or by simultaneous saccharification and fermentation of polymeric feedstocks [59,60]. Reducing the capacity of the glycerol pathway may be similarly effective in other metabolic engineering strategies for redirecting NADH reoxidation in anaerobic yeast cultures, such as the use of CO₂ by Calvin-cycle-enzyme expressing yeast cultures [24], and for expression of A-ALD in engineered xylose-consuming *S. cerevisiae* strains based on expression of heterologous xylose reductase and xylitol dehydrogenase enzymes [26].

Compared to its strong impact under low-osmolarity conditions, deletion of *GPD2* had a much smaller effect on glycerol production and acetate reduction in cultures of A-ALD-expressing *S. cerevisiae* grown on 1 mol L⁻¹ glucose (Table 4). This difference probably reflects the extensively documented, strong upregulation of *GPD1* under hyperosmotic stress [20,61,62],

which is at least partly controlled by the Hog1 MAP-kinase cascade [20,63]. Together with increased intracellular glycerol retention [17,64], upregulation of G3PDH activity plays a key role in the yeast osmotic stress response. The dual role of G3PDH enzymes in redox homeostasis and osmotolerance represents a challenge in redirecting NADH reoxidation in high-osmolarity, anaerobic yeast cultures towards acetate reduction. The results presented here provide a proof of principle for separating the roles of glycerol production in NADH reoxidation and osmotolerance by exchanging the native NAD⁺-dependent G3PDH enzymes for a heterologous, NADP⁺-preferring enzyme (*A. fulgidus* GpsA). In contrast to a *gpd1Δ gpd2Δ* A-ALD expressing strain, the resulting strain was, after a lag phase, able to grow anaerobically on 1 mol L⁻¹ glucose and showed an almost 2-fold lower glycerol yield than a *GPD1 GPD2* reference strain (Table 4). Additional deletion of *ALD6* eliminated the lag phase as well as extracellular glycerol production, yielding a strain with stoichiometric acetate consumption and a ca. 13% higher ethanol yield on glucose in high-osmolarity cultures than observed for a *GPD1 GPD2* reference strain (Table 4). This ethanol yield improvement was consistent with results obtained in studies on glucose-grown, acetate-reducing strains that were not further engineered for osmotolerance [25,29,30] and in an osmotolerant acetate-reducing strain obtained after prolonged laboratory evolution [43].

Several factors may explain the strong impact of deleting *ALD6* on high-osmolarity cultures. In glucose-grown cultures of wild-type *S. cerevisiae* strains, NADP⁺-dependent oxidation of acetaldehyde to acetate by Ald6 can account for ca. 20% of the total cytosolic NADPH requirement [65,66]. Even possibly higher contributions of Ald6 have been reported in genetic backgrounds that affect NADPH supply via other pathways [29,67]. In *gpsA*-expressing strains, NADPH generated by acetate formation via Ald6 can directly contribute to glycerol production. Since, during growth on glucose, NADPH formation by Ald6 is coupled to equimolar generation of NADH in glycolysis, increased acetate formation via Ald6 can help meet an increased NADH demand for glycerol production via Gpd1 and/or Gpd2 during hyper-osmotic stress [20,63]. Furthermore Ald6, together with yeast acetyl-CoA synthetases (*Acs1*, *Acs2*) and

heterologously expressed A-ALD, have been proposed to form an ATP-driven transhydrogenase cycle [29]. Activity of such a cycle in high-osmolarity cultures, possibly stimulated by up-regulation of *ALD6*, could impose an ATP drain that impedes growth under the combined stresses of high osmolarity and acetate uncoupling. Elimination of such an ATP drain could explain why deletion of *ALD6* eliminated lag phases in high-osmolarity, acetate-supplemented cultures. Increased adaptation phases, reflecting a non-genetic population heterogeneity, are well documented in acetate-stressed *S. cerevisiae* cultures [68,69]. Recent studies on engineered A-ALD expressing *S. cerevisiae* strains in low- and medium-osmolarity cultures [26,29] lend further support to the conclusion that deletion of *ALD6* is a key step in engineering efficient pathways for acetate reduction in *S. cerevisiae*.

While a *gpd1Δ gpd2Δ ald6Δ* strain expressing *gpsA* and *eutE* showed an excellent stoichiometry in terms of ethanol yield and acetate reduction, its growth rate in high-osmolarity cultures was substantially lower than that of strains expression *GPD1* and/or *GPD2*. To minimize costs of yeast propagation and to maximize ethanol productivity, a high maximum specific growth rate is important for application in lignocellulosic ethanol production. As previously demonstrated for a *gpd1Δ gpd2Δ* strain expressing *mhpF* [43], evolutionary engineering can enable selection for faster growing mutants. Alternatively, growth kinetics may be improved by optimizing the expression levels of NADPH-dependent G3PDH and/or by improving the availability of cytosolic NADPH [65,66].

In view of the extensively documented, central role of G3PDH in the hyperosmotic stress response of *S. cerevisiae* [17,70], the slow but reproducible anaerobic growth of a *gpd1Δ gpd2Δ ald6Δ, eutE*-expressing *S. cerevisiae* strain in a medium containing 1 mol L⁻¹ glucose was an unexpected result. In addition to possible contributions of the *ald6Δ* mutation and/or *eutE* expression on osmotolerance, the lag phase of *gpd1Δ gpd2Δ* strains in high-osmolarity cultures may have obscured this interesting phenotype in previous short-term growth studies [20,21]. Osmotolerance in *S. cerevisiae* is a complex, multi-gene phenotype [71] and, especially upon sudden exposure to osmotic stress, G3PDH-independent mechanisms have been proposed to

contribute to osmotolerance [64,72], such as trehalose accumulation in osmotically-challenged cultures growing on galactose [73]. Alternatively, intracellular glycerol could be derived via a G3PDH-independent pathway by de-acylation of acyl-glycerol-3-phosphate, which can be formed from dihydroxyacetone phosphate (DHAP) by the combined activities of DHAP acyltransferase and NADPH-linked 1-acylglycerol-3-phosphate acyltransferase [74]. Activity of the latter pathway may explain low levels of glycerol production in an A-ALD-expressing *gpd1Δ gpd2Δ* strain evolved for increased osmotolerance [43]. The acetate-reducing, *gpd1Δ gpd2Δ* strains constructed in this work provide an interesting experimental platform for further fundamental research on G3PDH-independent mechanisms for osmotolerance in *S. cerevisiae*.

4.5 Conclusions

Deletion of *GPD2* provides a straightforward engineering strategy for maximizing the positive impact of A-ALD-based, engineered pathways in low-osmolarity cultures of *S. cerevisiae*, by improving acetate conversion and ethanol yields. Replacement of the NAD⁺-dependent *S. cerevisiae* glycerol-3P dehydrogenases by a heterologous NADP⁺-dependent enzyme enables uncoupling of the function of glycerol as an osmoprotectant from its role in cellular redox cofactor balancing. When combined with a deletion of *ALD6*, thereby eliminating the influence of cytosolic NADP⁺-dependent acetaldehyde oxidation on redox metabolism, this engineering strategy enables anaerobic growth and efficient acetate reduction, with its associated improvement of ethanol yields, in high-osmolarity cultures. If the growth kinetics of the resulting strains can be further improved, this approach is highly promising for application in high-gravity processes for conversion of acetate-containing, lignocellulosic hydrolysates.

4.6 Acknowledgements

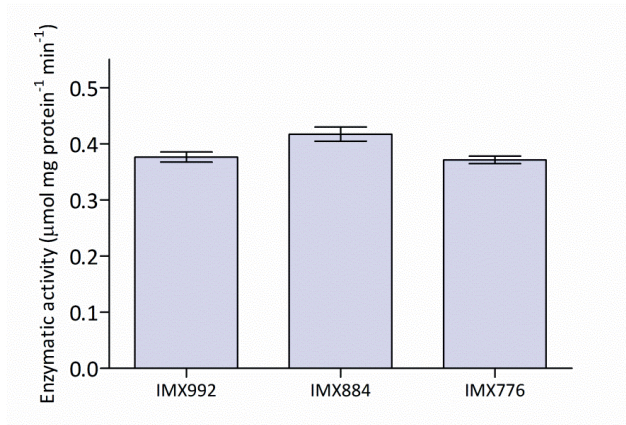
We thank Jean-Marc Daran and Pilar de la Torre for advice on molecular biology, Matthijs Niemeijer and Erik de Hulster for advice on fermentations and Marijke Luttik for advice on enzyme activity assays. We thank Donna Duiker for construction of strain IMX776 and our DSM colleagues for stimulating discussions.

4.7 Additional Files

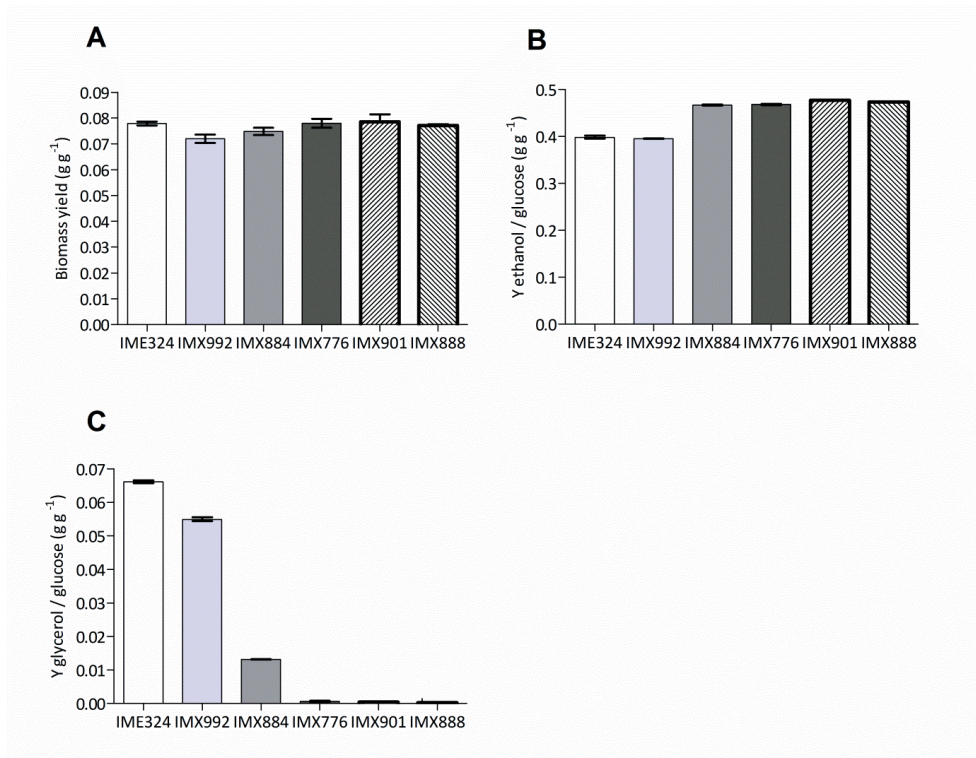
Additional File S1. Primers used in this study

Primer code	Sequence 5'-3'	Purpose
2015	CCAAATGGACATGAGTCAC	Confirmation of <i>GPD2</i> deletion
2112	ACGGACCTATTGCCATTG	Confirmation of <i>GPD2</i> deletion
7298	TTGTTCAAATGGATGGGGTTC	Confirmation of <i>SGA1</i> deletion
4229	TGCTCGACAGATACAATCCTGG	Confirmation of <i>SGA1</i> deletion
2164	ATCCGGGTGGAACATAAAC	Confirmation of <i>ALD6</i> deletion
2171	AGGCACAAGCCTGTTCCTC	Confirmation of <i>ALD6</i> deletion
4397	TCCTCGGTAGATCAGGTCAG	Confirmation of <i>GPD1</i> deletion
4401	ACGGTGAGCTCCGTATTATC	Confirmation of <i>GPD1</i> deletion
5792	GTTTTAGAGCTAGAAATAGCAAGTTAAAATAAG	Amplification of pMEI10 / pMEI11 backbone
5793	GATCATTTATCTTTTCACTGCGGAG	Amplification of pROS10 backbone
5979	TATTGACGCGGGCAAGAGC	Amplification of pMEI10 / pMEI11 insert sequences
5980	CGACCGAGTTGCTCTTG	pMEI11 backbone
6965	GTGGCGATGTTTTGGGGTTTCGAAACTTCCGGCAGTGAAGATAAATGATCGGGCAAGGACTCGACCATAGTTTTAGAGCTAGAAATAGCAAGTTAAAA TAAG	Amplification of pROS10 insert sequence (<i>GPD1</i> targeting)
6966	GTGGCGATGTTTTGGGGTTTCGAAACTTCCGGCAGTGAAGATAAATGATCGGGCAAGGACTCGACCATAGTTTTAGAGCTAGAAATAGCAAGTTAAAA TAAG	Amplification of pROS10 insert sequence (<i>GPD2</i> targeting)
7023	GTTGATAAGGACTAGCCCTTATTTTAACTTGCTATTTCTAGCTCTAAAACGAAATCCAGTGTGTCAAATGATCAATTTATCTTTCACTGCGGAGAAAGTTTC GAAGCCGAAACATCGCCA	Amplification of pMEI10 sequence (<i>SGA1</i> targeting)
7610	GTTGATAAGGACTAGCCCTTATTTTAACTTGCTATTTCTAGCTCTAAAACAAATTCAGAGCTGTTAGCCATGATCAATTTATCTTTCACTGCGGAGAAAGTTTC GAAGCCGAAACATCGCCA	Amplification of pMEI11 insert (<i>ALD6</i> targeting)
7608	TAGAAGAAAAAACATCAAGAAACATCTTTAAACATPACAAAAACACATCTATCAGAAATACATGTACCACCTGGATTTCTTTCCGCTCATATACACAAAAATA CTTTCATATAAACTTACTTG	Repair oligonucleotide (<i>ALD6</i> knockout)

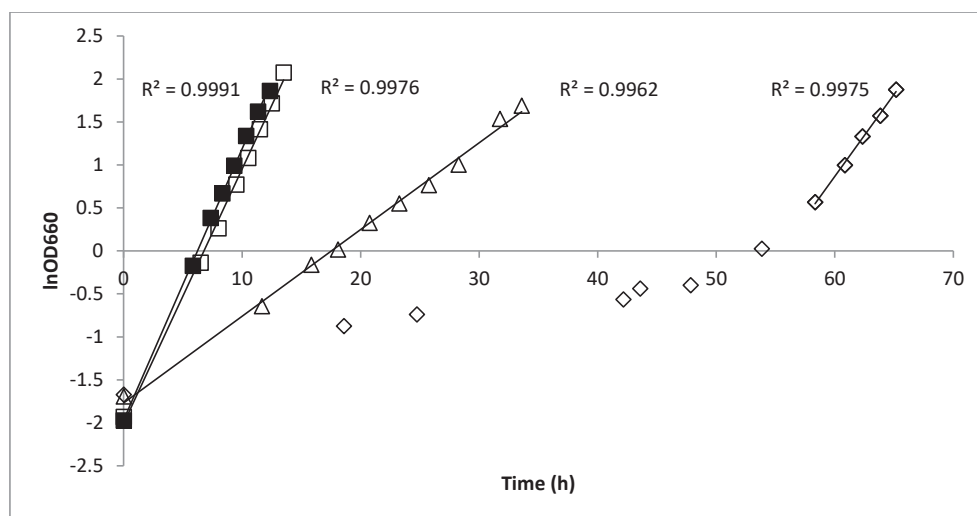
7609	CAAGTAAGTTTATATGAAAGTATTTTGTGTATATGACGGAAAGAAATGCAGGTTGGTGACATATCTCTGATAGTATGTGTTTTGTGTATGCTTAAAGATGTTTCTTGATGTTTTTCTTCTA	Repair oligonucleotide (<i>ALD6</i> knockout)
7025	TATATTTGATGTAATAATCTAGGAAATACACTTGTGTATACTTCTCGGTTTTCTTTTATTGCAAAATTAAGGCCTTCGAGC	Amplification of <i>eutE</i> for integration at <i>SGA1</i> locus
7211	GCATAGAACATTATCCGGGAAACGGGTATTAGGGGTGAGGGTGAATAAGGAAAGTCAGGGAAATCGGGCAAGCTGGAGCTCAGTTTTATCA	Amplification of <i>eutE</i> for integration at <i>SGA1</i> locus
7862	TGTTAITTTGGCAGTTTTCGTAC	Amplification of <i>gpsA</i> for integration at <i>GPD1</i> locus
7863	GTTATGAGAAATGACATAATGC	Amplification of <i>gpsA</i> for integration at <i>GPD1</i> locus
7991	GTATTTTTGTAGATTCAAATTCITTTCCCTTTCCCTTTCCCTTCGGTCCCTTCTTATCACACAGGAAACAGCTATGACC	Amplification of <i>eutE</i> for integration at <i>GPD2</i> locus
7992	ATAACTGTAGTAATGTTACTAGTAGTAGTGTAGAACTTGTGTATAATGATAAAITGGTTGCGCCAAATTAAGGCCTTCG	Amplification of <i>eutE</i> for integration at <i>GPD2</i> locus
8337	CGAACAAAGTTGTCAAGGCTG	Confirmation of <i>eutE</i> integration
8338	GCATCGACCAAAACACAAACG	Confirmation of <i>eutE</i> integration
9809	GCATAGAACATTATCCGGGAAACGGGTATTAGGGGTGAGGGTGAATAAGGAAAGTCAGGGAAATCGGGGTACAATGCCCTGGCATGTTTC	Amplification of <i>ALD6</i> for integration at <i>SGA1</i> locus
9810	TATATTTGATGTAATAATCTAGGAAATACACTTGTGTATACTTCTCGGTTTTCTTTTATTCTCGTCCAGTTGAGTCTAGC	Amplification of <i>ALD6</i> for integration at <i>SGA1</i> locus
7678	ACAATTCAGAGCTGTTAGCC	Confirmation of pUDR264
7611	ACACTGCTGAACCAAGTCAAG	Confirmation of <i>ALD6</i> integration
7612	CACCACCGAATGGAACTCTG	Confirmation of <i>ALD6</i> integration
8034	GGTCTGGTGTATGGGTTTC	Confirmation of <i>gpsA</i> integration
8035	GGTTTCGGTGACTTGAITTC	Confirmation of <i>gpsA</i> integration
8036	GAGTCCAACTTGGTGTCT	Confirmation of <i>gpsA</i> integration
8037	ACCGGTAATAGCAACGGTTC	Confirmation of <i>gpsA</i> integration



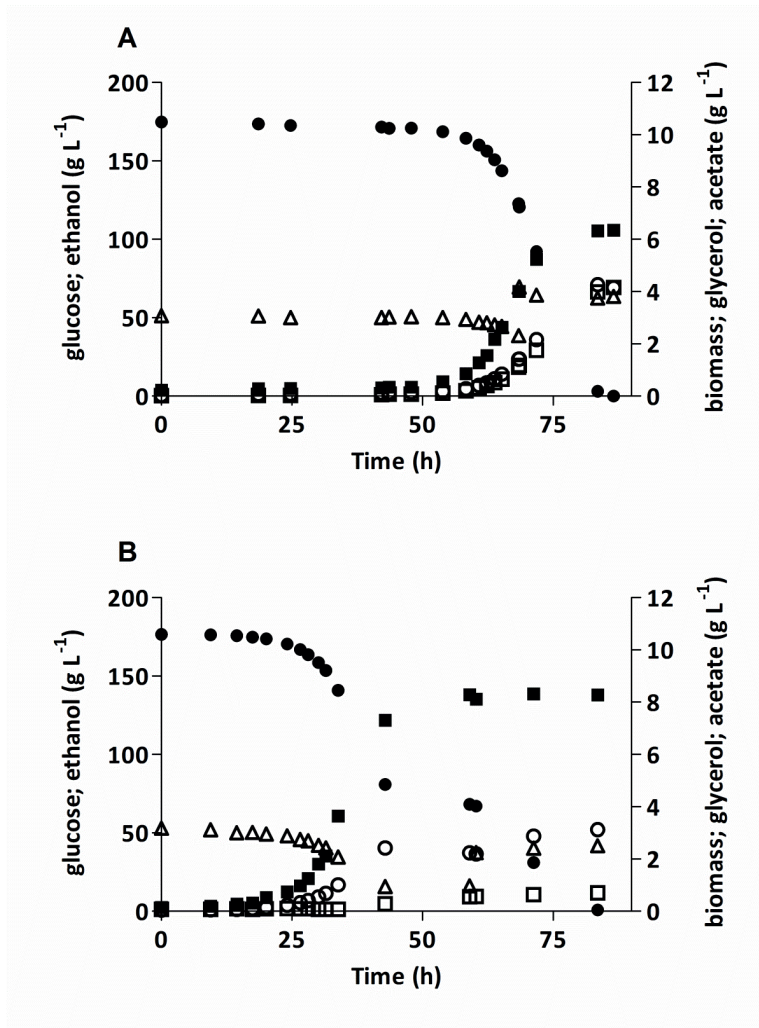
Additional File S2. Specific rates of EutE-dependent reduction of acetyl-CoA by cell extracts of shake-flask cultures on synthetic medium (20 g L^{-1}) glucose. From left to right: *S. cerevisiae* strains IMX992 (*GPD1 GPD2 sga1::eutE*), IMX884 (*GPD1 gpd2::eutE*) and IMX776 (*gpd1::gpsA gpd2::eutE*). Data represent averages \pm mean deviations of assays on independent duplicate cultures.



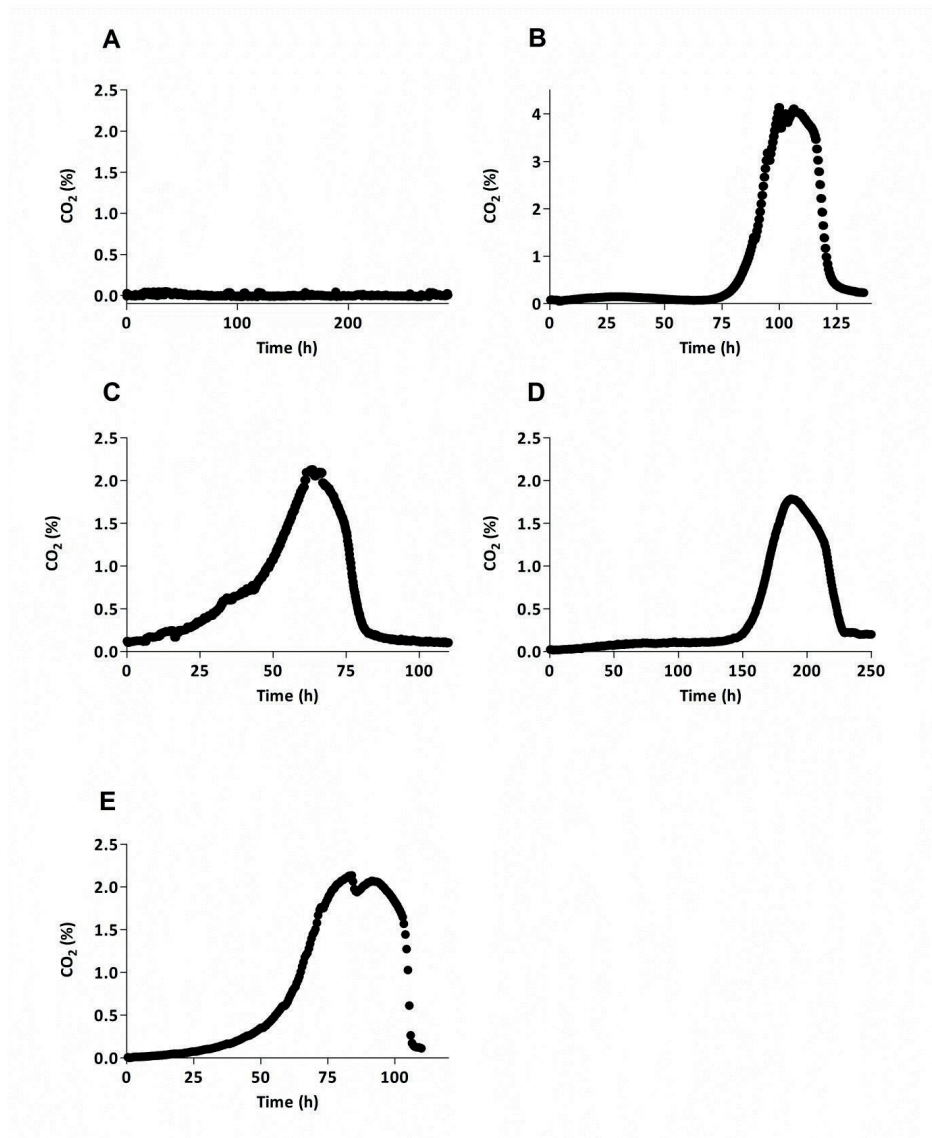
Additional File S3. Biomass and product yields in anaerobic bioreactor batch cultures of *S. cerevisiae* strains with different genetic modifications in glycerol and acetate metabolism. Cultures were grown on synthetic medium containing 20 g L⁻¹ glucose and 3 g L⁻¹ acetic acid (pH 5). Bars refer to the following engineered *S. cerevisiae* strains: IME324 (*GPD1 GPD2*); IMX992 (*GPD1 GPD2 sga1::eutE*); IMX884 (*GPD1 gpd2::eutE*); IMX776 (*gpd1::gpsA gpd2::eutE*); IMX901 (*gpd1::gpsA gpd2::eutE ald6Δ*); IMX888 (*gpd1Δ gpd2::eutE*). A, biomass yield on glucose; B, ethanol yield on glucose (corrected for ethanol evaporation); C, glycerol yield on glucose. Data represent the averages ± mean deviations of measurements on independent duplicate cultures for each strain. Data on strain IMX888 were taken from [29].



Additional File S4. Plots of $\ln(\text{OD}_{660})$ values versus time in anaerobic bioreactor batch cultures of *S. cerevisiae* strains with different genetic modifications in glycerol and acetate metabolism (from inoculation to mid-exponential phase). Cultures were grown on synthetic medium containing 180 g L⁻¹ glucose and 3 g L⁻¹ acetic acid (pH 5). ■, strain IMX992 (*GPD1 GPD2 sga1::eutE*); □, strain IMX884 (*GPD1 gpd2::eutE*); ◇, strain IMX776 (*gpd1::gpsA gpd2::eutE*); Δ, strain IMX901 (*gpd1::gpsA gpd2::eutE ald6Δ*). The figure shows representative cultures of independent duplicate experiments.



Additional File S5. Growth, glucose consumption and product formation in anaerobic bioreactor batch cultures of *S. cerevisiae* strains with different genetic modifications in glycerol and acetate metabolism. Cultures were grown on synthetic medium containing 180 g L^{-1} glucose and 3 g L^{-1} acetic acid (pH 5). A, strain IMX776 (*gpd1::gpsA gpd2::eutE*); B, strain IMX901 (*gpd1::gpsA gpd2::eutE ald6Δ*). Symbols: ●, glucose; ■, biomass; □, glycerol; ○, ethanol; Δ, acetate. In the case of IMX776, acetic acid was added externally immediately after the exponential growth phase was finished. In the case of IMX901, acetic acid was added externally after 20 h in stationary phase.

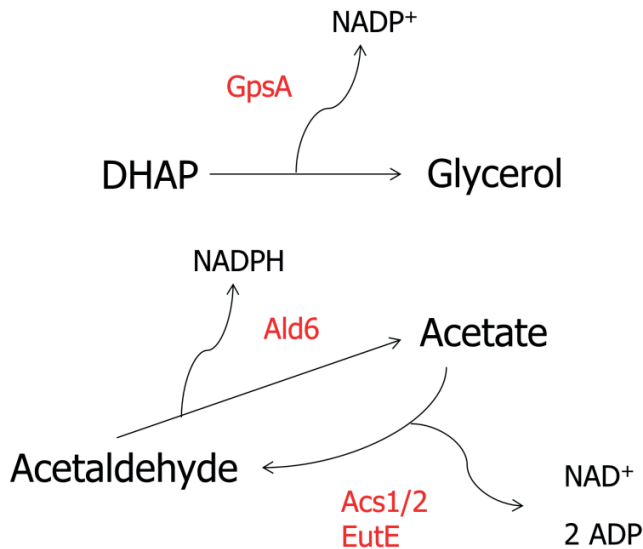


Additional File S6. CO₂ production profiles in anaerobic bioreactor batch cultures of *S. cerevisiae* strains with different genetic modifications in glycerol and acetate metabolism. Cultures were grown on synthetic medium containing 180 g L⁻¹ glucose and 3 g L⁻¹ acetic acid (pH 5). A, IMZ160 (*gpd1::loxP gpd2::hphMX4 mhpF*-overexpressing); B, IMX888 (*gpd1Δ gpd2::eutE*); C, IMX900 (*gpd1Δ gpd2::eutE ald6Δ*); D, IMX1120 (*gpd1Δ gpd2::eutE ald6Δ sga1::ALD6*); E, IMX1142 (*gpd1::gpsA gpd2::eutE ald6Δ sga1::ALD6*). Data collected from online bioreactor offgas measurements. Representative cultures of independent duplicate experiments are shown.

Additional File S7.docx: Starting and end concentrations of acetate and glycerol in anaerobic bioreactor batch cultures of *S. cerevisiae* strains IMX888 (*gpd1Δ gpd2::eutE*) and IMX900 (*gpd1Δ gpd2::eutE ald6Δ*). Cultures were grown on synthetic medium containing 180 g L⁻¹ glucose and 3 g L⁻¹ acetate (pH 5). Values represent averages ± mean deviations of measurements on independent duplicate cultures.

Strain	Acetate g L ⁻¹		Glycerol g L ⁻¹	
	Start	End	Start	End
IMX888	3.26 ± 0.02	0	0.12 ± 0.00	0.30 ± 0.00
IMX900	2.79 ± 0.08	0	0.11 ± 0.00	0.42 ± 0.00

4



Additional File S8. Potential cytosolic transhydrogenase cycle, exchanging NADH with NADPH, catalysed by EutE, Acs1/2 and Ald6. Formed NADPH can be used for DHAP reduction to glycerol by GpsA.

4.8 References

1. Hermann BG, Blok K, Patel MK. Producing bio-based bulk chemicals using industrial biotechnology saves energy and combats climate change. *Environ Sci Technol*. 2007;41:7915-21.
2. Renewable Fuels Association. www.ethanolrfa.org. Accessed November 2016.
3. Gombert AK, van Maris AJA. Improving conversion yield of fermentable sugars into fuel ethanol in 1st generation yeast-based production processes. *Curr Opin Biotech*. 2015;33:81-6.
4. Nielsen J, Larsson C, van Maris AJA, Pronk JT. Metabolic engineering of yeast for production of fuels and chemicals. *Curr Opin Biotechnol*. 2013;24:398-404.
5. Della-Bianca BE, Basso TO, Stambuk BU, Basso LC, Gombert AK. What do we know about the yeast strains from the Brazilian fuel ethanol industry? *Appl Microbiol Biotechnol*. 2013;97:979-91.
6. Hahn-Hägerdal B, Karhumaa K, Fonseca C, Spencer-Martins I, Gorwa-Grauslund MF. Towards industrial pentose-fermenting yeast strains. *Appl Microbiol Biotechnol*. 2007;74:937-53.
7. Moysés ND, Reis CV, Almeida RJ, Moraes ML, Torres AF. Xylose fermentation by *Saccharomyces cerevisiae*: Challenges and prospects. *Int J Mol Sci*. 2016;17:207.
8. Van Maris AJA, Abbott DA, Bellissimi E, van den Brink J, Kuyper M, Luttik MAH, Wisselink HW, Scheffers WA, van Dijken JP, Pronk JT. Alcoholic fermentation of carbon sources in biomass hydrolysates by *Saccharomyces cerevisiae*: current status. *Antonie van Leeuwenhoek*. 2006;90:391-418.
9. Maiorella BL, Blanch HW, Wilke CR. Economic evaluation of alternative ethanol fermentation processes. *Biotechnol Bioeng*. 1984;26:1003-25.
10. Klink HB, Thomsen AB, Ahring BK. Inhibition of ethanol-producing yeast and bacteria by degradation products produced during pre-treatment of biomass. *Appl Microbiol Biotechnol*. 2004;66:10-26.
11. Palmqvist E, Hahn-Hägerdal B. Fermentation of lignocellulosic hydrolysates. II: inhibitors and mechanisms of inhibition. *Bioresour Technol*. 2000;74:25-33.
12. Parawira W, Tekere M. Biotechnological strategies to overcome inhibitors in lignocellulose hydrolysates for ethanol production: review. *Crit Rev Biotechnol*. 2011;31:20-31.
13. Nissen TL, Kielland-Brandt MC, Nielsen J, Villadsen J. Optimization of ethanol production in *Saccharomyces cerevisiae* by metabolic engineering of the ammonium assimilation. *Metab Eng*. 2000;2:69-77.
14. Van Dijken JP, Scheffers WA. Redox balances in the metabolism of sugars by yeasts. *FEMS Microbiol Lett*. 1986;32:199-224.
15. Verduyn C, Postma E, Scheffers WA, van Dijken JP. Physiology of *Saccharomyces cerevisiae* in anaerobic glucose-limited chemostat cultures. *J Gen Microbiol*. 1990;136:395-403.
16. Hohmann S. Osmotic stress signaling and osmoadaptation in yeasts. *Microbiol Mol Biol Rev*. 2002;66:300-72.
17. Nevoigt E, Stahl U. Osmoregulation and glycerol metabolism in the yeast *Saccharomyces cerevisiae*. *FEMS Microbiol Rev*. 1997;21:231-41.
18. Bakker BM, Overkamp KM, van Maris AJA, Kötter P, Luttik MAH, van Dijken JP, Pronk JT. Stoichiometry and compartmentation of NADH metabolism in *Saccharomyces cerevisiae*. *FEMS Microbiol Rev*. 2001;25:15-37.
19. Navarrete C, Nielsen J, Siewers V. Enhanced ethanol production and reduced glycerol formation in *fps1D* mutants of *Saccharomyces cerevisiae* engineered for improved redox balancing. *AMB Express*. 2014;4:86.

20. Albertyn J, Hohmann S, Thevelein JM, Prior BA. *GPD1*, which encodes glycerol-3-phosphate dehydrogenase, is essential for growth under osmotic stress in *Saccharomyces cerevisiae*, and its expression is regulated by the high-osmolarity glycerol response pathway. *Mol Cell Biol*. 1994;14:4135-44.
21. Ansell R, Granath K, Hohmann S, Thevelein JM, Adler L. The two isoenzymes for yeast NAD⁺-dependent glycerol 3-phosphate dehydrogenase encoded by *GPD1* and *GPD2* have distinct roles in osmoadaptation and redox regulation. *EMBO J*. 1997;16:2179-87.
22. Larsson K, Ansell R, Eriksson P, Adler L. A gene encoding sn-glycerol 3-phosphate dehydrogenase (NAD⁺) complements an osmosensitive mutant of *Saccharomyces cerevisiae*. *Mol Microbiol*. 1993;10:1101-11.
23. Björkqvist S, Ansell R, Adler L, Lidén G. Physiological response to anaerobicity of glycerol-3-phosphate dehydrogenase mutants of *Saccharomyces cerevisiae*. *Appl Environ Microbiol*. 1997;63:128-32.
24. Guadalupe-Medina V, Wisselink HW, Luttik MA, de Hulster E, Daran J-MG, Pronk JT, van Maris AJA. Carbon dioxide fixation by Calvin-Cycle enzymes improves ethanol yield in yeast. *Biotechnol Biofuels*. 2013;6:125.
25. Guadalupe-Medina V, Almering MJH, van Maris AJA, Pronk JT. Elimination of glycerol production in anaerobic cultures of a *Saccharomyces cerevisiae* strain engineered to use acetic acid as an electron acceptor. *Appl Environ Microbiol*. 2010;76:190-5.
26. Wei N, Quarterman J, Kim SR, Cate JHD, Jin YS. Enhanced biofuel production through coupled acetic acid and xylose consumption by engineered yeast. *Nat Commun*. 2013;4:2580.
27. Xia PF, Zhang GC, Walker B, Seo SO, Kwak S, Liu JJ, Kim H, Ort DR, Wang SG, Jin YS. Recycling carbon dioxide during xylose fermentation by engineered *Saccharomyces cerevisiae*. *ACS Synth Biol*. 2016;6:276-83.
28. Zhang GC, Kong II, Wei N, Peng D, Turner TL, Sung BH, Sohn JH, Jin YS. Optimization of an acetate reduction pathway for producing cellulosic ethanol by engineered yeast. *Biotechnol Bioeng*. 2016;113:2587-96.
29. Papapetridis I, van Dijk M, Dobbe AP, Metz B, Pronk JT, van Maris AJA. Improving ethanol yield in acetate-reducing *Saccharomyces cerevisiae* by cofactor engineering of 6-phosphogluconate dehydrogenase and deletion of *ALD6*. *Microb Cell Fact*. 2016;15:67.
30. Henningsen BM, Hon S, Covalla SF, Sonu C, Argyros DA, Barrett TF, Wiswall E, Froehlich AC, Zelle RM. Increasing anaerobic acetate consumption and ethanol yields in *Saccharomyces cerevisiae* with NADPH-specific alcohol dehydrogenase. *Appl Environ Microbiol*. 2015;81:8108-17.
31. Koppram R, Tomás-Pejó E, Xiros C, Olsson L. Lignocellulosic ethanol production at high-gravity: challenges and perspectives. *Trends Biotechnol*. 2014;32:46-53.
32. Puligundla P, Smogrovicova D, Obulam VSR, Ko S. Very high gravity (VHG) ethanolic brewing and fermentation: a research update. *J Ind Microbiol Biotechnol*. 2011;38:1133-44.
33. Bayrock DP, Michael Ingledew W. Application of multistage continuous fermentation for production of fuel alcohol by very-high-gravity fermentation technology. *J Chem Technol Biotechnol*. 2001;27:87-93.
34. Ding WT, Zhang GC, Liu JJ. 3' truncation of the *GPD1* promoter in *Saccharomyces cerevisiae* for improved ethanol yield and productivity. *Appl Environ Microbiol*. 2013;79:3273-81.
35. Hubmann G, Guillouet S, Nevoigt E. Gpd1 and Gpd2 fine-tuning for sustainable reduction of glycerol formation in *Saccharomyces cerevisiae*. *Appl Environ Microbiol*. 2011;77:5857-67.
36. Thomas KC, Dhas A, Rossnagel BG, Ingledew WM. Production of fuel alcohol from hull-less barley by very high gravity technology. *Cereal Chem*. 1995;72:360-4.
37. Shen B, Hohmann S, Jensen RG, Bohnert AH. Roles of sugar alcohols in osmotic stress adaptation. Replacement of glycerol by mannitol and sorbitol in yeast. *Plant Physiol*. 1999;121:45-52.

38. D'Amore T, Crumplen R, Stewart GG. The involvement of trehalose in yeast stress tolerance. *J Ind Microbiol.* 1991;7:191-5.
39. Mahmud SA, Nagahisa K, Hirasawa T, Yoshikawa K, Ashitani K, Shimizu H. Effect of trehalose accumulation on response to saline stress in *Saccharomyces cerevisiae*. *Yeast.* 2009;26:17-30.
40. Sharma SC. A possible role of trehalose in osmotolerance and ethanol tolerance in *Saccharomyces cerevisiae*. *FEMS Microbiol Lett.* 1997;152:11.
41. Sasano Y, Haitani Y, Ohtsu I, Shima J, Takagi H. Proline accumulation in baker's yeast enhances high-sucrose stress tolerance and fermentation ability in sweet dough. *Int J Food Microbiol.* 2012;152:40-3.
42. Takagi H. Proline as a stress protectant in yeast: physiological functions, metabolic regulations, and biotechnological applications. *Appl Microbiol Biotechnol.* 2008;81:211.
43. Guadalupe-Medina V, Metz B, Oud B, van Der Graaf CM, Mans R, Pronk JT, van Maris AJA. Evolutionary engineering of a glycerol-3-phosphate dehydrogenase-negative, acetate-reducing *Saccharomyces cerevisiae* strain enables anaerobic growth at high glucose concentrations. *Microb Biotechnol.* 2014;7:44-53.
44. Pagliardini J, Hubmann G, Alfenore S, Nevoigt E, Bideaux C, Guillouet SE. The metabolic costs of improving ethanol yield by reducing glycerol formation capacity under anaerobic conditions in *Saccharomyces cerevisiae*. *Microb Cell Fact.* 2013;12:29.
45. Sakasegawa SI, Hagemeyer CH, Thauer RK, Essen LO, Shima S. Structural and functional analysis of the *gpsA* gene product of *Archaeoglobus fulgidus*: A glycerol-3-phosphate dehydrogenase with an unusual NADP(+) preference. *Protein Sci.* 2004;13:3161-71.
46. Entian KD, Kötter P: 25 Yeast Genetic Strain and Plasmid Collections. *Methods Microbiol.* 2007;629-666.
47. Verduyn C, Postma E, Scheffers WA, van Dijken JP. Effect of benzoic acid on metabolic fluxes in yeasts: A continuous-culture study on the regulation of respiration and alcoholic fermentation. *Yeast.* 1992;8:501-17.
48. Mans R, van Rossum HM, Wijsman M, Backx A, Kuijpers NG, van den Broek M, Daran-Lapujade P, Pronk JT, van Maris AJA, Daran J-MG. CRISPR/Cas9: a molecular Swiss army knife for simultaneous introduction of multiple genetic modifications in *Saccharomyces cerevisiae*. *FEMS Yeast Res.* 2015;15:fov004.
49. Wiedemann B, Boles E. Codon-optimized bacterial genes improve L-arabinose fermentation in recombinant *Saccharomyces cerevisiae*. *Appl Environ Microbiol.* 2008;74:2043-50.
50. Daniel Gietz R, Woods RA. Transformation of yeast by lithium acetate/single-stranded carrier DNA/polyethylene glycol method. *Methods Enzymol.* 2002;87-96.
51. Solis-Escalante D, Kuijpers NGA, Nadine B, Bolat I, Bosman L, Pronk JT, Daran J-MG, Daran-Lapujade P. amdSYM, a new dominant recyclable marker cassette for *Saccharomyces cerevisiae*. *FEMS Yeast Res.* 2013;13:126.
52. Postma E, Verduyn C, Scheffers WA, van Dijken JP. Enzymic analysis of the crabtree effect in glucose-limited chemostat cultures of *Saccharomyces cerevisiae*. *Appl Environ Microbiol.* 1989;55:468-77.
53. Bryan AK, Goranov A, Amon A, Manalis SR. Measurement of mass, density, and volume during the cell cycle of yeast. *PNAS.* 2010;107:999-1004.
54. Albertyn J, Hohmann S, Prior BA. Characterization of the osmotic-stress response in *Saccharomyces cerevisiae*: osmotic stress and glucose repression regulate glycerol-3-phosphate dehydrogenase independently. *Curr Gen.* 1994;25:12-8.
55. Flikweert MT, de Swaaf M, van Dijken JP, Pronk JT. Growth requirements of pyruvate-decarboxylase-negative *Saccharomyces cerevisiae*. *FEMS Microbiol Lett.* 1999;174:73-9.
56. Saint-Prix F, Bönquist L, Dequin S. Functional analysis of the *ALD* gene family of *Saccharomyces cerevisiae* during anaerobic growth on glucose: the NADP⁺-dependent Ald6p and Ald5p isoforms play a major role in acetate formation. *Microbiology.* 2004;150:2209-20.

57. Blomberg A, Adler L. Roles of glycerol and glycerol-3-phosphate dehydrogenase (NAD⁺) in acquired osmotolerance of *Saccharomyces cerevisiae*. *J Bacteriol.* 1989;171:1087-92.
58. Zhang L, Tang Y, Guo Zp, Ding Zy, Shi Gy. Improving the ethanol yield by reducing glycerol formation using cofactor regulation in *Saccharomyces cerevisiae*. *Biotechnol Lett.* 2011;33:1375-80.
59. Hasunuma T, Kondo A. Consolidated bioprocessing and simultaneous saccharification and fermentation of lignocellulose to ethanol with thermotolerant yeast strains. *Process Biochem.* 2012;47:1287-94.
60. Schuster BG, Chinn MS. Consolidated bioprocessing of lignocellulosic feedstocks for ethanol fuel production. *Bioenergy Res.* 2013;6:416-35.
61. Hirayarna T, Maeda T, Saito H, Shinozaki K. Cloning and characterization of seven cDNAs for hyperosmolarity-responsive (HOR) genes of *Saccharomyces cerevisiae*. *Mol Gen Genet.* 1995;249:127-38.
62. Varela JCS, van Beekvelt C, Planta RJ, Mager WH. Osmostress-induced changes in yeast gene expression. *Mol Microbiol.* 1992;6:2183-90.
63. Remize F, Cambon B, Barnavon L, Dequin S. Glycerol formation during wine fermentation is mainly linked to Gpd1p and is only partially controlled by the HOG pathway. *Yeast.* 2003;20:1243-53.
64. Edgley M, Brown AD. Yeast water relations: Physiological changes induced by solute stress in *Saccharomyces cerevisiae* and *Saccharomyces rouxii*. *Microbiology.* 1983;129:3453-63.
65. Celton M, Goelzer A, Camarasa C, Fromion V, Dequin S. A constraint-based model analysis of the metabolic consequences of increased NADPH oxidation in *Saccharomyces cerevisiae*. *Metab Eng.* 2012;14:366-79.
66. Celton M, Sanchez I, Goelzer A, Fromion V, Camarasa C, Dequin S. A comparative transcriptomic, fluxomic and metabolomic analysis of the response of *Saccharomyces cerevisiae* to increases in NADPH oxidation. *BMC Genom.* 2012;13:317.
67. Grabowska D, Chelstowska A. The *ALD6* gene product is indispensable for providing NADPH in yeast cells lacking glucose-6-phosphate dehydrogenase activity. *J Biol Chem.* 2003;278:13984-8.
68. González-Ramos D, Gorter de Vries AR, Grijseels SS, van Berkum MC, Swinnen S, van den Broek M, Nevoigt E, Daran J-MG, Pronk JT, van Maris AJA. A new laboratory evolution approach to select for constitutive acetic acid tolerance in *Saccharomyces cerevisiae* and identification of causal mutations. *Biotechnol Biofuels.* 2016;9:173.
69. Swinnen S, Fernández-Niño M, González-Ramos D, van Maris AJA, Nevoigt E. The fraction of cells that resume growth after acetic acid addition is a strain-dependent parameter of acetic acid tolerance in *Saccharomyces cerevisiae*. *FEMS Yeast Res.* 2014;14:642.
70. Saito H, Posas F. Response to hyperosmotic stress. *Genetics.* 2012;192:289-318.
71. Blomberg A. The osmotic hypersensitivity of the yeast *Saccharomyces cerevisiae* is strain and growth media dependent: Quantitative aspects of the phenomenon. *Yeast.* 1997;13:529-39.
72. Singh KK, Norton RS. Metabolic changes induced during adaptation of *Saccharomyces cerevisiae* to a water stress. *Arch Microbiol.* 1991;156:38-42.
73. García MJ, Ríos G, Ali R, Bellés J.M., Serrano R. Comparative physiology of salt tolerance in *Candida tropicalis* and *Saccharomyces cerevisiae*. *Microbiology.* 1997;143:1125-31.
74. Athenstaedt K, Daum G. 1-Acyldihydroxyacetone-phosphate reductase (Ayr1p) of the yeast *Saccharomyces cerevisiae* encoded by the open reading frame YIL124w is a major component of lipid particles. *J Biol Chem.* 2000;275:235-40.
75. Mumberg D, Müller R, Funk M. Yeast vectors for the controlled expression of heterologous proteins in different genetic backgrounds. *Gene.* 1995;156:119-22.
76. Van Rossum HM, Kozak BU, Niemeijer MS, Duine HJ, Luttik MAH, Boer VM, Kötter P, Daran J-MG, van Maris AJA, Pronk JT. Alternative reactions at the interface of glycolysis and citric acid cycle in *Saccharomyces cerevisiae*. *FEMS Yeast Res.* 2016;16.

Chapter 5

Laboratory evolution for forced glucose-xylose co-consumption enables identification of mutations that improve mixed-sugar fermentation by xylose-fermenting *Saccharomyces cerevisiae*

Ioannis Papapetridis*, Maarten D. Verhoeven*, Sanne J. Wiersma, Maaïke Goudriaan, Antonius J.A. van Maris and Jack T. Pronk

* joint first co-authorship

Submitted for publication

Abstract

Simultaneous fermentation of glucose and xylose can contribute to improved productivity and robustness of yeast-based processes for bioethanol production from lignocellulosic hydrolysates. This study explores a novel laboratory evolution strategy for identifying mutations that contribute to simultaneous utilization of these sugars in batch cultures of *Saccharomyces cerevisiae*. To force simultaneous utilization of xylose and glucose, the genes encoding glucose-6-phosphate isomerase (*PGI1*) and ribulose-5-phosphate epimerase (*RPE1*) were deleted in a xylose-isomerase-based xylose-fermenting strain with a modified oxidative pentose-phosphate pathway. Laboratory evolution of this strain in serial batch cultures on glucose-xylose mixtures yielded mutants that rapidly co-consumed the two sugars. Whole-genome sequencing of evolved strains identified mutations in *HXK2*, *RSP5* and *GAL83*, whose introduction into a non-evolved xylose-fermenting *S. cerevisiae* strain improved co-consumption of xylose and glucose under aerobic and anaerobic conditions. Combined deletion of *HXK2* and introduction of a *GAL83*^{G673T} allele yielded a strain with a 2.5-fold higher xylose and glucose co-consumption ratio than its xylose-fermenting parental strain. These two modifications decreased the time required for full sugar conversion in anaerobic bioreactor batch cultures, grown on 20 g L⁻¹ glucose and 10 g L⁻¹ xylose, by over 24 h. This study demonstrates that laboratory evolution and genome resequencing of microbial strains engineered for forced co-consumption is a powerful approach for studying and improving simultaneous conversion of mixed substrates.

5.1 Introduction

Industrial biotechnology can contribute to reconciling global demands for liquid transport fuels with the almost universally accepted need to limit anthropogenic CO₂ emissions [1]. Bioethanol, the biofuel with the largest annual global production volume, is still predominantly produced by fermentation of sucrose or glucose, derived from sugar cane or corn starch, respectively [2]. These ‘first-generation’ bioethanol processes exploit the natural high fermentation rates and ethanol yield of the yeast *Saccharomyces cerevisiae*. Optimization of yeast strains and production processes enables many industrial processes to operate at >90% of the theoretical ethanol yield on sugar [2-4]. However, the massive scaling up of production volumes that would be required to replace a substantial fraction of petroleum-based transport fuels cannot be sustainably achieved with corn starch and cane sugar as only feedstocks. Instead, a large fraction of the feedstock will have to be derived from lignocellulosic plant biomass, such as agricultural residues and energy crops [5].

In comparison with first-generation feedstocks, lignocellulosic hydrolysates pose additional challenges for yeasts and yeast researchers. In addition to containing mixtures of hexose and pentose (mainly D-xylose and L-arabinose) sugars, the deconstruction of lignocellulosic biomass that precedes yeast-based fermentation releases fermentation inhibitors [6-8]. Intensive metabolic engineering studies, encompassing functional expression of heterologous pathways for xylose and arabinose catabolism, improvements in inhibitor tolerance and minimization of by-product formation have yielded *Saccharomyces cerevisiae* strains that are now applied in the first full-scale ‘second-generation’ industrial bioethanol plants [7, 9]. However, further improvements in ethanol titers, yields and productivities are important to increase the economic viability of this nascent technology.

Current strain engineering strategies for enabling pentose fermentation by *S. cerevisiae* typically yield strains that, in anaerobic batch cultures grown on sugar mixtures, preferentially ferment glucose, while xylose and/or arabinose are predominantly converted in a second, slower fermentation phase [7]. This strong preference for glucose over pentoses persists even

after extensive laboratory evolution on sugar mixtures [10-14]. Achieving efficient co-fermentation of glucose and pentoses, while maintaining a high overall rate of sugar conversion, could increase volumetric productivity of industrial processes. Moreover, since several inhibitors of yeast performance are more harmful during the slower pentose fermentation phase [7, 15-17], simultaneous fermentation of glucose and pentose sugars can also contribute to robustness under industrial process conditions.

Random mutagenesis, laboratory evolution and protein engineering of xylose transporters has yielded transporter variants with improved xylose affinity and reduced glucose inhibition, which enabled the construction of yeast strains with improved xylose consumption in the presence of glucose [18-21]. In an alternative approach, expression of a heterologous cellodextrin transporter and an intracellular β -glucosidase, along with a heterologous xylose reductase/xylitol dehydrogenase pathway, enabled simultaneous consumption of cellobiose and xylose in *S. cerevisiae* by reducing the impact of glucose repression [22]. However, despite progress in this area, engineering of yeast strains showing simultaneous, fast fermentation of glucose and xylose remains a key challenge.

Deletion of *RPE1*, which encodes the pentose-phosphate-pathway (PPP) enzyme ribulose-5-phosphate epimerase, was recently shown to result in coupling of glucose and xylose catabolism, at a ratio of 10:1, in an engineered xylose-utilizing *S. cerevisiae* strain [23]. Despite a low xylose-to-glucose consumption ratio, this strategy indicated the potential of forced stoichiometric coupling of glucose and pentose metabolism in *S. cerevisiae*. In *S. cerevisiae*, phosphoglucose isomerase (Pgi1) catalyses interconversion of glucose-6-phosphate to fructose-6-phosphate in upper glycolysis [24]. Since deletion of *PGI1* blocks glycolysis, *pgi1* Δ strains cannot grow on glucose as the sole carbon source unless all glucose-6-phosphate is rerouted through the pentose-phosphate pathway. Deletion of *eda*, *rpe* and *pgi* in *E. coli* was previously shown to enable co-consumption of xylose and glucose [25]. As conversion of 1 mol glucose-6-phosphate to 1 mol ribulose-5-phosphate via the oxidative branch of the PPP results in a net

generation of 2 mol NADPH, the absence of a redox imbalance relied on conversion of excess NADPH to NADH by the native *E. coli* transhydrogenases.

Wild-type *S. cerevisiae* strains cannot reoxidize all NADPH generated by such a redirection of metabolism and, consequently, *pgi1*-null mutants cannot grow on glucose as sole carbon source [26, 27]. Overexpression of *GDH2*, which encodes NAD⁺-dependent glutamate dehydrogenase, can restore growth of *pgi1Δ* strains by enabling a transhydrogenase-like cycle that couples the interconversion of 2-oxoglutarate and glutamate to the conversion of NADPH and NAD⁺ to NADP⁺ and NADH [26]. Based on the impact of a *pgi1Δ* mutation on glucose metabolism, we reasoned that inactivation of *PGI1* might be used to construct strains with a stringent requirement for co-utilization of xylose and glucose, at much higher ratios than hitherto demonstrated.

The goal of this study was to explore a new strategy for identifying mutations that stimulate glucose-xylose co-consumption by *S. cerevisiae*. The strategy was based on enforcing a strict stoichiometric coupling of glucose and xylose fermentation by the combined deletion of *RPE1* and *PGI1* in an engineered, xylose-isomerase-based *S. cerevisiae* strain [28, 29]. Furthermore, to reduce the impact of these modifications on NADP⁺/NADPH redox cofactor balancing, the native NADP⁺-dependent 6-phosphogluconate dehydrogenases (*Gnd1* and *Gnd2*) were replaced by a heterologous NAD⁺-dependent enzyme [30]. After laboratory evolution for improved growth on glucose-xylose mixtures, the physiology of evolved strains was analysed in aerobic shake-flask and bioreactor batch cultures. Potential causal mutations identified by whole-genome sequencing were introduced into a non-evolved (*PGI1 RPE1 GND1 GND2*) xylose-fermenting strain background. The resulting reverse engineered strains were then analysed in shake-flask and anaerobic bioreactor batch cultures, grown on mixtures of glucose and xylose.

5.2 Materials and Methods

5.2.1 Maintenance of strains

The CEN.PK lineage of *S. cerevisiae* laboratory strains [31] was used to construct and evolve all strains used in this study (Table 1). Depending on strain auxotrophies, cultures were grown in YP (10 g L⁻¹ yeast extract, 20 g L⁻¹ peptone) (BD, Franklin Lakes, NJ) or synthetic medium (SM) [32], supplemented with glucose (20 g L⁻¹), xylose (20 g L⁻¹), a glucose/xylose mixture (10 g L⁻¹ of each sugar) or a xylose/fructose/glucose mixture (20, 10 and 1 g L⁻¹ respectively). Propagation of *E. coli* XL-1 Blue cultures was performed in LB medium (5 g L⁻¹ Bacto yeast extract, 10 g L⁻¹ Bacto tryptone, 5 g L⁻¹ NaCl, 100 µg mL⁻¹ ampicillin). Frozen stock cultures were stored at -80 °C, after addition of glycerol (30% v/v final concentration).

5.2.2 Construction of plasmids and cassettes

PCR amplification for construction of plasmid fragments and yeast integration cassettes was performed with Phusion High Fidelity DNA Polymerase (Thermo-Scientific, Waltham, MA), according to the manufacturer's guidelines. Plasmid assembly was performed *in vitro* with a Gibson Assembly Cloning kit (New England Biolabs, Ipswich, MA), following the supplier's guidelines, or *in vivo* by transformation of plasmid fragments into yeast cells [33]. For all constructs, correct assembly was confirmed by diagnostic PCR with DreamTaq polymerase (Thermo-Scientific), following the manufacturer's protocol. Plasmids used and constructed in this work are described in Table 2. All yeast genetic modifications were performed using CRISPR/Cas9-based genome editing [34]. Unique guide-RNA (gRNA) sequences targeting *GRE3*, *GAL83* and *RSP5* were selected from a publicly available list [35] and synthesized (Baseclear, Leiden, The Netherlands). Primers and oligonucleotides used in this work are listed in Additional File 1.

Table 1. Strains used in this study.

Strain name	Relevant Genotype	Origin
CEN.PK113-7D	<i>MATa MAL2-8c SUC2 can1</i>	[31]
IMX581	<i>MATa urr3-52 MAL2-8c SUC2 can1::cas9-natN2</i>	[34]
IMX705	<i>MATa MAL2-8c SUC2 can1::cas9-natNT2 gnd2Δ gnd1::gndA</i>	[30]
IMX963	<i>MATa MAL2-8c SUC2 can1::cas9-natNT2 gnd2Δ gnd1::gndA gre3::ZWF1, SOL3, TKL1, TAL1, NQM1, RKI1, TKL2</i>	This work
IMX990	<i>MATa MAL2-8c SUC2 can1::cas9-natNT2 gnd2Δ gnd1::gndA gre3::ZWF1, SOL3, TKL1, TAL1, NQM1, RKI1, TKL2 sga1::9*xyIA, XKS1</i>	This work
IMX1046	<i>MATa MAL2-8c SUC2 can1::cas9-natNT2 gnd2Δ gnd1::gndA gre3::ZWF1, SOL3, TKL1, TAL1, NQM1, RKI1, TKL2 sga1::9*xyIA, XKS1 rpe1Δ pgi1Δ</i>	This work
IMS0628	<i>MATa MAL2-8c SUC2 can1::cas9-natNT2 gnd2Δ gnd1::gndA gre3::ZWF1, SOL3, TKL1, TAL1, NQM1, RKI1, TKL2 sga1::9*xyIA, XKS1 rpe1Δ pgi1Δ</i> Evolved isolate 1	This work
IMS0629	<i>MATa MAL2-8c SUC2 can1::cas9-natNT2 gnd2Δ gnd1::gndA gre3::ZWF1, SOL3, TKL1, TAL1, NQM1, RKI1, TKL2 sga1::9*xyIA, XKS1 rpe1Δ pgi1Δ</i> Evolved isolate 2	This work
IMS0630	<i>MATa MAL2-8c SUC2 can1::cas9-natNT2 gnd2Δ gnd1::gndA gre3::ZWF1, SOL3, TKL1, TAL1, NQM1, RKI1, TKL2 sga1::9*xyIA, XKS1 rpe1Δ pgi1Δ</i> Evolved isolate 3	This work
IMS0634	<i>MATa MAL2-8c SUC2 can1::cas9-natNT2 gnd2Δ gnd1::gndA gre3::ZWF1, SOL3, TKL1, TAL1, NQM1, RKI1, TKL2 sga1::9*xyIA, XKS1 rpe1Δ pgi1Δ</i> Evolved isolate 4	This work
IMS0635	<i>MATa MAL2-8c SUC2 can1::cas9-natNT2 gnd2Δ gnd1::gndA gre3::ZWF1, SOL3, TKL1, TAL1, NQM1, RKI1, TKL2 sga1::9*xyIA, XKS1 rpe1Δ pgi1Δ</i> Evolved isolate 5	This work
IMS0636	<i>MATa MAL2-8c SUC2 can1::cas9-natNT2 gnd2Δ gnd1::gndA gre3::ZWF1, SOL3, TKL1, TAL1, NQM1, RKI1, TKL2</i>	This work

<i>sga1::9*xyIA, XKS1 rpe1Δ pgiiΔ</i> Evolved isolate 6	
IMX994	MATa <i>ura3-52 MAL2-8c SUC2 can1::cas9-natN2, gre3::RPE1, TKL1, TAL1, RKI1, XKS1</i> This work
IMU079	MATa <i>ura3-52 MAL2-8c SUC2 can1::cas9-natN2, gre3::RPE1, TKL1, TAL1, RKI1, XKS1 pAKX002</i> This work
IMX1384	MATa <i>ura3-52 MAL2-8c SUC2 can1::cas9-natN2, gre3::RPE1, TKL1, TAL1, RKI1, XKS1 hxxk2Δ pUDE327</i> This work
IMX1385	MATa <i>ura3-52 MAL2-8c SUC2 can1::cas9-natN2, gre3::RPE1, TKL1, TAL1, RKI1, XKS1 gal83Δ pMEL10.GAL83</i> This work
IMX1442	MATa <i>ura3-52 MAL2-8c SUC2 can1::cas9-natN2, gre3::RPE1, TKL1, TAL1, RKI1, XKS1 rsp5Δ pMEL10.RSP5</i> This work
IMX1408	MATa <i>ura3-52 MAL2-8c SUC2 can1::cas9-natN2, gre3::RPE1, TKL1, TAL1, RKI1, XKS1 hxxk2Δ</i> This work
IMX1409	MATa <i>ura3-52 MAL2-8c SUC2 can1::cas9-natN2, gre3::RPE1, TKL1, TAL1, RKI1, XKS1 gal83Δ</i> This work
IMX1451	MATa <i>ura3-52 MAL2-8c SUC2 can1::cas9-natN2, gre3::RPE1, TKL1, TAL1, RKI1, XKS1 rsp5Δ</i> This work
IMX1453	MATa <i>ura3-52 MAL2-8c SUC2 gre3::RPE1, TKL1, TAL1, RKI1, XKS1 gal83::GAL83^{6673T}</i> This work
IMX1484	MATa <i>ura3-52 MAL2-8c SUC2 gre3::RPE1, TKL1, TAL1, RKI1, XKS1 rsp5Δ hxxk2Δ pUDE327</i> This work
IMX1485	MATa <i>ura3-52 MAL2-8c SUC2 gre3::RPE1, TKL1, TAL1, RRRK11, XKS1 hxxk2Δ pAKX002</i> This work
IMX1486	MATa <i>ura3-52 MAL2-8c SUC2 gre3::RPE1, TKL1, TAL1, RKI1, XKS1 gal83Δ pAKX002</i> This work
IMX1487	MATa <i>ura3-52 MAL2-8c SUC2 gre3::RPE1, TKL1, TAL1, RKI1, XKS1 rsp5Δ pAKX002</i> This work
IMX1488	MATa <i>ura3-52 MAL2-8c SUC2 gre3::RPE1, TKL1, TAL1, RKI1, XKS1 gal83::GAL83^{6673T}, pAKX002</i> This work
IMX1510	MATa <i>ura3-52 MAL2-8c SUC2 gre3::RPE1, TKL1, TAL1, RKI1, XKS1 rsp5Δ hxxk2Δ</i> This work
IMX1515	MATa <i>ura3-52 MAL2-8c SUC2 gre3::RPE1, TKL1, TAL1, RKI1, XKS1 rsp5Δ hxxk2Δ pAKX002</i> This work
IMX1563	MATa <i>ura3-52 MAL2-8c SUC2 gre3::RPE1, TKL1, TAL1, RKI1, XKS1 gal83::GAL83^{6673T}, hxxk2Δ pUDE327</i> This work
IMX1571	MATa <i>ura3-52 MAL2-8c SUC2 gre3::RPE1, TKL1, TAL1, RKI1, XKS1 gal83::GAL83^{6673T}, hxxk2Δ</i> This work
IMX1583	MATa <i>ura3-52 MAL2-8c SUC2 gre3::RPE1, TKL1, TAL1, RKI1, XKS1 gal83::GAL83^{6673T}, hxxk2Δ pAKX002</i> This work

Table 2. Plasmids used in this study.

Plasmid	Characteristics	Origin
pMEL10	2 μ m, <i>KIURA3</i> , p <i>SNR52</i> -gRNA. <i>CAN1-tSUP4</i>	[34]
pMEL11	2 μ m, <i>amdS</i> , p <i>SNR52</i> -gRNA. <i>CAN1-tSUP4</i>	[34]
pROS11	<i>amdS</i> , gRNA. <i>CAN1</i> -2 μ m ori-gRNA. <i>ADE2</i>	[34]
pUDE335	2 μ m, <i>KIURA3</i> , p <i>SNR52</i> -gRNA. <i>GRE3-tSUP4</i>	[29]
pUD344	p <i>PGI1-NQM1-tNQM1</i> PCR template vector	[29]
pUD345	p <i>TPI1-RKI1-tRKI1</i> PCR template vector	[29]
pUD346	p <i>PYK1-TKL2-tTKL2</i> PCR template vector	[29]
pUD347	p <i>TDH3-RPE1-tRPE1</i> PCR template vector	[29]
pUD348	p <i>PGK1-TKL1-tTKL1</i> PCR template vector	[29]
pUD349	p <i>TEF1-TAL1-tTAL1</i> PCR template vector	[29]
pUD350	p <i>TPI1-xylA-tCYC1</i> PCR template vector	[29]
pUD353	p <i>TEF1-XKS1-tXKS1</i> PCR template vector	[29]
pUD426	p <i>ADH1-ZWF1-tZWF1</i> PCR template vector	This work
pUD427	p <i>ENO1-SOL3-tSOL3</i> PCR template vector	This work
pUDR119	2 μ m ori, <i>amdS</i> , p <i>SNR52</i> -gRNA. <i>SGA1-tSUP4</i>	[36]
pUDR202	<i>amdS</i> , gRNA. <i>RPE1</i> -2 μ m ori-gRNA. <i>PGI1</i>	This work
pUDR204	2 μ m ori, <i>amdS</i> , p <i>SNR52</i> -gRNA. <i>GRE3-tSUP4</i>	This work
pUDR105	<i>hphNT</i> , gRNA. <i>SynthSite</i> -2 μ m ori-gRNA. <i>SynthSite</i>	[37]
pUDE327	URA3, p <i>SNR52</i> -gRNA. <i>HXK2-tSUP4</i>	[38]
pAKX002	2 μ m ori, URA3, p <i>TPI1-xylA-tCYC1</i>	[39]

To construct the *GRE3*-targeting CRISPR-plasmid pUDR204, the plasmid backbone of pMEL11 was PCR amplified using primer combination 5980/5792. The insert fragment, expressing the *GRE3*-targeting gRNA, was amplified using primer combination 5979/5978 and pMEL11 as template. To construct the *RPE1/PGI1* double-targeting CRISPR-plasmid pUDR202, the plasmid backbone and the insert fragment were PCR amplified using primer combinations 5941/6005 and 9269/9401, respectively, using pROS11 as template. Both plasmids were assembled *in vitro* in yeast and cloned in *E. coli*. To construct CRISPR-plasmids for single deletion of *GAL83* and *RSP5*, the plasmid backbone, the *GAL83*-gRNA insert and the *RSP5*-gRNA insert were amplified using primer combination 5792/5980, 5979/11270 and 5979/11373, respectively, using pMEL10 as template and assembled *in vivo*.

To generate *ZWF1* and *SOL3* overexpression cassettes, promoter regions of *ADH1* and *ENO1* and the coding regions of *ZWF1* and *SOL3* (including their terminator regions) were PCR amplified using primer combinations 8956/8960, 8958/8961, 8953/8964 and 8984/8986, respectively, using CEN.PK113-7D genomic DNA as a template. The resulting products were used as templates for fusion-PCR assembly of the p*ADH1-ZWF1-tZWF1* and p*ENO1-SOL3-tSOL3* overexpression cassettes with primer combinations 8956/8964 and 8958/8986 respectively, which yielded plasmids pUD426 and pUD427 after ligation to pJET-blunt vectors (Thermo-Scientific) and cloning in *E. coli*.

To generate yeast-integration cassettes for overexpression of the major genes of the complete PPP, p*ADH1-ZWF1-tZWF1*, p*ENO1-SOL3-tSOL3*, p*PGK1-TKL1-tTKL1*, p*TEF1-TAL1-tTAL1*, p*PGI1-NQM1-tNQM1*, p*TPI1-RKI1-tRKI1* and p*PYK1-TKL2-tTKL2* cassettes were PCR amplified using primer combinations 4870/7369, 8958/3290, 3291/4068, 3274/3275, 3847/3276, 4691/3277, 3283/3288, respectively, using plasmids pUD426, pUD427, pUD348, pUD349, pUD344, pUD345 and pUD346, respectively, as templates. To generate yeast-integration cassettes of the genes of the non-oxidative PPP, the p*TDH3-RPE1-tRPE1*, p*PGK1-TKL1-tTKL1*, p*TEF1-TAL1-tTAL1*, p*TPI1-RKI1-tRKI1* overexpression cassettes were PCR-

amplified using primer pairs 7133/3290, 3291/4068, 3724/3725, 10460/10461, respectively and plasmids pUD347, pUD348, pUD34 and pUD345 as templates.

Yeast-integration cassettes for overexpression of *Piromyces sp.* xylose isomerase (*pTPI1-xyIA-tCYC1*) were PCR-amplified using primer combinations 6285/7548, 6280/6273, 6281/6270, 6282/6271, 6284/6272, 6283/6275, 6287/6276, 6288/6277 or 6289/6274, using pUD350 as template. Yeast xylulokinase overexpression cassettes (*pTEF1-XKS1-tXKS1*) were PCR-amplified from plasmid pUD353, using primer combination 5920/9029 or 7135/7222. A yeast-integration cassette of *pGAL83-gal83::GAL83^{G673T}-tGAL83* was PCR-amplified from genomic DNA of IMS0629, using primer combination 11273/11274.

5.2.3 Strain construction

Yeast transformation was performed as previously described [40]. Transformation mixtures were plated on SM or YP agar plates (2% Bacto Agar, BD), supplemented with the appropriate carbon sources. For transformations with the *amdS* marker cassette, agar plates were prepared and counter selection was performed as previously described [41]. For transformations with the *URA3* selection marker counter-selection was performed using 5-fluoro-orotic acid (Zymo Research, Irvine, CA), following the supplier's protocol. For transformations with the *hphNT* marker, agar plates were additionally supplemented with 200 mg L⁻¹ hygromycin B (Invivogen, San Diego, CA) and plasmid loss was induced by cultivation in non-selective medium. After each transformation, correct genotypes were confirmed by diagnostic PCR using DreamTaq polymerase (Thermo-Scientific, see Additional File 1 for primer sequences).

Co-transformation of pUDR204 along with the *pADH1-ZWF1-tZWF1*, *pENO1-SOL3-tSOL3*, *pPGK1-TKL1-tTKL1*, *pTEF1-TAL1-tTAL1*, *pPGI1-NQM1-tNQM1*, *pTPI1-RKI1-tRKI1* and *pPYK1-TKL2-tTKL2* integration cassettes to IMX705 [30] and subsequent plasmid counter-selection, yielded strain IMX963, which overexpresses the major enzymes of the PPP. Co-transformation of pUDR119, 9 copies of the *pTPI1-xyIA-tCYC1* integration cassette, along with a single copy of the *pTEF1-XKS1-tXKS1* cassette, to IMX963, followed by plasmid counterselection yielded the xylose-

fermenting strain IMX990. In IMX990, the *pTPI1-xyIA-tCYC1* cassettes recombined *in vivo* to form a multi-copy construct of xylose isomerase overexpression [29]. To construct IMX1046, in which *RPE1* and *PGI1* were deleted, plasmid pUDR202 and the repair oligonucleotides 9279/9280/9281/9282 were co-transformed to IMX990. Transformation mixes of IMX1046 were plated on SM agar supplemented with a xylose/fructose/glucose mixture (20, 10 and 1 g L⁻¹ final concentrations respectively), to avoid potential glucose toxicity [26].

To construct strain IMX994, plasmid pUDE335 was co-transformed to IMX581, along with the *pTDH3-RPE1-tRPE1*, *pPGK1-TKL1-tTKL1*, *pTEF1-TAL1-tTAL1*, *pTPI1-RKI1-tRKI1* and *pTEF1-XKS1-tXKS1* integration cassettes, after which the CRISPR plasmid was recycled. Transformation of pAKX002 to IMX994 yielded the xylose-fermenting strain IMU079. Co-transformation of pUDE327 along with the repair oligonucleotides 5888/5889 to IMX994 yielded strain IMX1384, in which *HXX2* was deleted. Co-transformation of the pMEL10 backbone fragment, along with the *GAL83*-gRNA insert or the *RSP5*-gRNA insert and repair oligonucleotides 11271/11272 or 11374/11375, respectively, yielded strains IMX1385 (*GAL83* deletion) and IMX1442 (*RSP5* deletion). Counterselection of the CRISPR plasmids from IMX1384, IMX1385 and IMX1442 yielded, respectively, strains IMX1408, IMX1409 and IMX1451. Transformation of pAKX002 to IMX1408, IMX1409 and IMX1451 yielded, respectively, the xylose-fermenting strains IMX1485, IMX1486 and IMX1487. To construct strain IMX1453, in which the mutated *GAL83^{G673T}* gene replaced the wild-type *GAL83* allele, plasmid pUDR105 was co-transformed to IMX1409 with the *pGAL83-gal83::GAL83^{G673T}-tGAL83* cassette. Transformation of pAKX002 to IMX1453 yielded the xylose-fermenting strain IMX1488. To construct the *hxx2Δ rsp5Δ* strain IMX1484, plasmid pUDE327 was co-transformed to IMX1451, along with the repair oligonucleotides 5888/5889. Counterselection of pUDE327 from IMX1484 yielded strain IMX1510. Transformation of pAKX002 to IMX1510 yielded the xylose-fermenting strain IMX1515. To construct the *hxx2Δ gal83::GAL83^{G673T}* strain IMX1563, plasmid pUDE327 along with the repair-oligonucleotides 5888/5889 was co-transformed to IMX1453. Counterselection

of pUDE327 from IMX1563 yielded IMX1571. The xylose-fermenting strain IMX1583 was obtained by transformation of pAKX002 to IMX1571.

5.2.4 Cultivation and media

Shake-flask growth experiments were performed in 500-mL conical shake flasks containing 100 mL of SM with urea as nitrogen source (2.3 g L⁻¹ urea, 6.6 g L⁻¹ K₂SO₄, 3 g L⁻¹ KH₂PO₄, 1 mL L⁻¹ trace elements solution (Verduyn *et al.* 1992) and 1 mL L⁻¹ vitamin solution [32] to prevent medium acidification. The initial pH of the medium was set to 6.0 by titration with 2 mol L⁻¹ KOH. Depending on the strains grown, different mixtures of carbon sources (glucose/xylose/fructose) were added and media were filter-sterilized (0.2 μm, Merck, Darmstadt, Germany). The temperature was set to 30 °C and the shaking speed to 200 rpm in an Innova incubator (New Brunswick Scientific, Edison, NJ). In each case, pre-culture shake-flasks were inoculated from frozen stocks. After 8-12 h of growth, exponentially growing cells from the initial shake-flasks were used to inoculate fresh cultures that, after 12-18 h of growth, were used as inoculum for the growth experiments, to a starting OD₆₆₀ of 0.4-0.5 in the case of shake-flask growth experiments and of 0.2-0.3 in the case of bioreactor cultivation.

Bioreactor cultures were grown on SM [32], supplemented with a glucose/xylose mixture (10 g L⁻¹ each for aerobic cultivation or 20 g L⁻¹/10 g L⁻¹ for anaerobic cultivation). Sterilization of the salt solution was performed by autoclaving at 121 °C for 20 min. Sugar solutions were sterilized separately by autoclaving at 110 °C for 20 min and added to the sterile salt media along with filter-sterilized vitamin solution. In the case of anaerobic cultivation, media were additionally supplemented with ergosterol (10 mg L⁻¹) and Tween 80 (420 mg L⁻¹). Sterile antifoam C (0.2 g L⁻¹; Sigma-Aldrich, St. Louis, MO) was added to all media used for bioreactor cultivation. Batch cultures were grown in 2-L bioreactors (Applikon, Delft, The Netherlands) with a 1-L working volume, stirred at 800 rpm. Culture pH was maintained at 5.0 by automatic titration with 2 mol L⁻¹ KOH. Temperature was maintained at 30 °C. Bioreactors were sparged at 0.5 L min⁻¹ with either pressurized air (aerobic cultivation) or nitrogen gas (<10 ppm oxygen, anaerobic cultivation). All reactors were equipped with Viton O-rings and

Norprene tubing to minimize oxygen diffusion. Evaporation in bioreactor cultures was minimized by cooling the offgas outlet to 4 °C.

5.2.5 Laboratory evolution

Laboratory evolution of strain IMX1046 was performed via serial shake-flask cultivation on SM [32]. Cultures were grown in 500-mL shake-flasks with 100 mL working volume. Growth conditions were the same as described above. Initially, the cultures were grown on a glucose/xylose concentration ratio of (1.0 g L⁻¹/20 g L⁻¹). After growth was observed, exponentially growing cells (0.05 mL of culture) were transferred to SM with a glucose/xylose concentration ratio of 2.0 g L⁻¹/20 g L⁻¹. During subsequent serial transfers, the glucose content was progressively increased as high growth rates were established at each sugar composition, reaching a final glucose/xylose ratio of 20 g L⁻¹/20 g L⁻¹. At that point three single colonies were isolated from two replicate evolution experiments (IMS0628-630 and IMS0634-636, respectively) by plating on SM with 10 g L⁻¹ glucose and 20 g L⁻¹ xylose.

5.2.6 Analytical methods

Off-gas analysis, biomass dry weight measurements, HPLC analysis of culture supernatants and correction for ethanol evaporation in bioreactor experiments were performed as previously described [30]. Determination of optical density was performed at 660 nm using a Jenway 7200 spectrophotometer (Cole-Palmer, Staffordshire, UK). Yields of products and biomass-specific sugar uptake rates in bioreactor batch cultures were determined as previously described [10, 30]. All values are represented as averages ± mean deviation of independent biological duplicate cultures.

5.2.7 *In silico* determination of sugar uptake

The Yeast v7.6 consensus metabolic model [42] was used for *in silico* prediction of relative xylose and glucose consumption rates in aerobic bioreactor batch cultures of strain IMS0629. The COBRA v2 toolbox [43] was used to read the model in MATLAB vR2017b (Mathworks, Natick, MA), supported by the SBML Toolbox v4.1 and the libSBML v5.12 [44]. The

Gurobi v6.5 linear programming solver (Gurobi Optimization Inc, Houston, TX) was installed and used according to the manual provided. The MATLAB script is provided in Additional File 2.

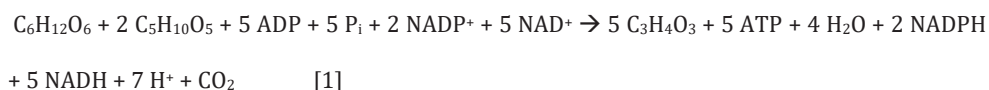
5.2.8 Genome sequencing

Genomic DNA of strains IMS0629 and IMS0634 was isolated from exponentially growing shake-flask cultures on SM (10 g L⁻¹ glucose/20 g L⁻¹ xylose) with a Qiagen Blood & Cell culture DNA kit (Qiagen, Germantown, MD), according to the manufacturer's specifications. Whole-genome sequencing was performed on an Illumina HiSeq PE150 sequencer (Novogene Company Limited, Hong Kong), as previously described [36]. Sequence data were mapped to the reference CEN.PK113-7D genome [45], to which the sequences of the *pTPI1-gndA-tCYC1* and *pTPI1-xylA-tCYC1* cassettes were manually added. Data processing and chromosome copy number analysis were carried as previously described [36].

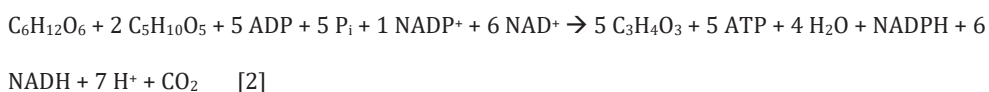
5.3 Results

5.3.1 Design of an *S. cerevisiae* strain with a forced, high stoichiometry of xylose and glucose co-consumption

Design of an *S. cerevisiae* strain whose growth depended on extensive co-consumption of xylose and glucose was based on the observation that inactivation of *PGI1* blocks entry of glucose-6-phosphate into glycolysis, while inactivation of *RPE1* prevents entry of ribulose-5-phosphate into the non-oxidative PPP (Figure 1). As a consequence, a *pgi1Δ rpe1Δ* strain is unable to grow on glucose. If conversion of xylose into xylulose-5-phosphate in such a strain is enabled by expression of a heterologous xylose isomerase and overexpression of the native xylulose kinase *Xks1* [28], co-consumption of xylose and glucose should enable growth (Figure 1). Overexpression of native genes encoding the enzymes of the non-oxidative PPP has previously been shown to stimulate the required conversion of xylulose-5-phosphate into the glycolytic intermediates fructose-6-phosphate and glyceraldehyde-3-phosphate (Figure 1) [28, 46]. The predicted stoichiometry for conversion of glucose and xylose into pyruvate in a yeast strain that combines these genetic modifications is summarized in Equation 1:



To prevent a potential excessive formation of NADPH [26, 27], the strain design further included replacement of the native *S. cerevisiae* NADP⁺-dependent 6-phosphogluconate dehydrogenases (Gnd1 and Gnd2) by the NAD⁺-dependent bacterial enzyme GndA [30], leading to the stoichiometry shown in Equation 2:



As indicated by Equation 2, this strain design forces co-consumption of 2 mol xylose and 1 mol glucose for the production of 5 mol pyruvate, with a concomitant formation of 1 mol NADPH, 6 mol NADH and 5 mol ATP. NADPH generated in this process can be reoxidized in biosynthetic reactions [47] or via an L-glutamate-2-oxoglutarate transhydrogenase cycle catalysed by Gdh1 and Gdh2 [26]. Actual *in vivo* stoichiometries of mixed-sugar consumption will depend on the relative contribution of precursors derived from glucose and xylose to biomass synthesis and on the biomass yield [48]. In aerobic cultures, the latter strongly depends on the mode of NADH reoxidation (mitochondrial respiration, alcoholic fermentation and/or glycerol production; Bakker *et al.* 2001). While quantitation of precise co-consumption stoichiometries will therefore require experimental analysis, this strain design clearly has the potential to force xylose and glucose co-consumption at much higher stoichiometries than previously reported [14, 19, 20, 23, 49-51].

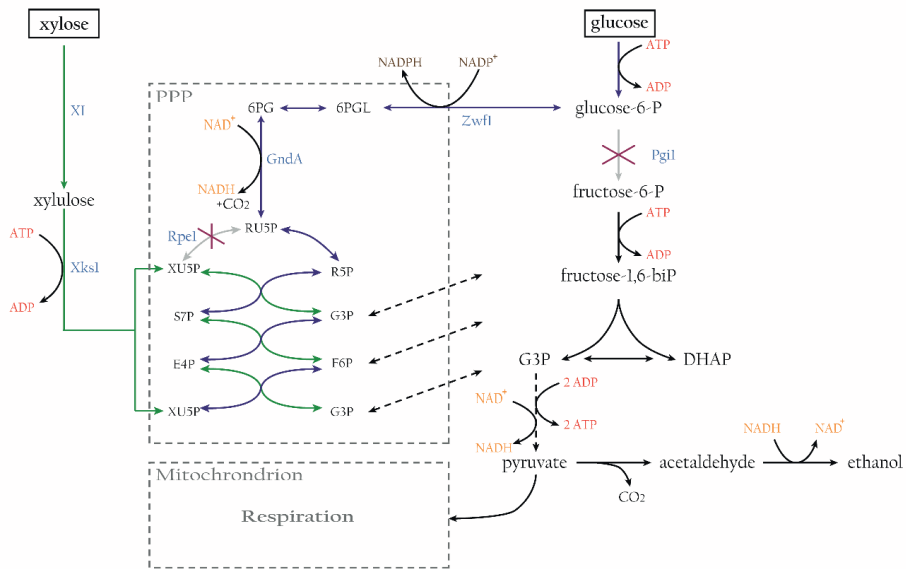


Figure 1. Schematic representation of central carbon metabolism in yeast strain engineered for forced co-consumption of glucose and xylose. In a *pgi1Δ rpe1Δ Saccharomyces cerevisiae* expressing a heterologous xylose isomerase (XI, Kuyper *et al.* 2003), the native 6-phosphogluconate dehydrogenases (Gnd1 and Gnd2) were replaced by a bacterial NAD⁺-dependent enzyme (GndA, Papapetridis *et al.* 2016). Additionally, xylulokinase (Xks1) and enzymes of the pentose phosphate pathway (PPP) were overexpressed. F6P fructose-6-phosphate; G3P glyceraldehyde-3-phosphate; DHAP dihydroxyacetone phosphate; 6PGL 6-phosphogluconolactone; 6PG 6-phosphogluconate; RU5P ribulose-5-phosphate; XU5P xylulose-5-phosphate; R5P ribose-5-phosphate; S7P sedoheptulose-7-phosphate; E4P erythrose-4-phosphate.

5.3.2 Construction, laboratory evolution and growth stoichiometry of glucose-xylose co-consuming *S. cerevisiae* strains

To implement the proposed strain design for forced co-consumption of xylose and glucose, multiple copies of a codon-optimized expression cassette for *Piromyces xylA* [29] were integrated into the genome of *S. cerevisiae* IMX705 (*gnd1Δ gnd2Δ gndA*; Papapetridis *et al.* 2016), along with overexpression cassettes for *S. cerevisiae* *XKS1* and for structural genes encoding PPP enzymes. Deletion of *RPE1* and *PGI1* in the resulting xylose-consuming strain IMX990, yielded strain IMX1046, which grew instantaneously in aerobic shake-flask cultures on SM with 1 g L⁻¹ glucose and 20 g L⁻¹ xylose as sole carbon sources. However, this strain did not grow at the same xylose concentration when the glucose concentration was increased to 10 g L⁻¹, indicating kinetic and/or regulatory constraints in glucose-xylose co-consumption at higher glucose concentrations.

To select for co-consumption of xylose at higher glucose concentrations, duplicate serial-transfer experiments were performed in aerobic shake-flask cultures on SM with 20 g L⁻¹ xylose. During serial transfer, the glucose concentration in the medium was gradually increased from 1 g L⁻¹ to 20 g L⁻¹ (Figure 2). Samples of the evolving cultures were regularly inoculated in SM containing either 20 g L⁻¹ glucose or 20 g L⁻¹ xylose as sole carbon source. Absence of growth on these single sugars showed that laboratory evolution did not result in an escape from their forced co-consumption. When, after 13 transfers, vigorous growth was observed on a mixture of 20 g L⁻¹ glucose and 20 g L⁻¹ xylose, three single-colony isolates were obtained from each laboratory evolution experiment by streaking on SM agar (10 g L⁻¹ glucose/20 g L⁻¹ xylose).

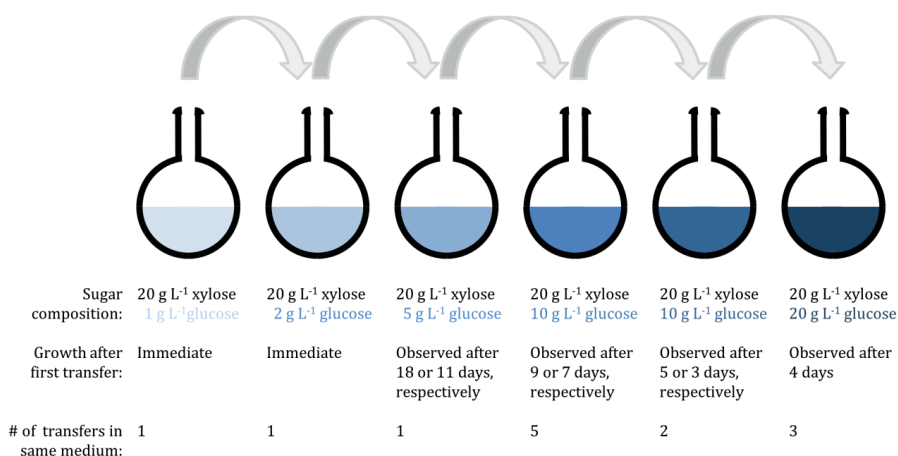


Figure 2. Laboratory evolution of *S. cerevisiae* IMX1046 (*pgi1Δ rpe1Δ gnd1Δ gnd2Δ gndA XylA XKS1↑ PPP↑*) for improved co-consumption of xylose at high glucose concentrations. Cultures were grown in shake flasks containing 100 mL SM (pH 6) supplemented with 20 g L⁻¹ xylose and progressively increasing glucose concentrations. In every transfer, 0.05 mL of an exponentially growing culture was used to inoculate the next shake flask.

Growth studies with the six evolved isolates in shake-flask cultures on SM with 10 g L⁻¹ glucose and 20 g L⁻¹ xylose (Additional File 3) identified isolate IMS0629 (Evolution Line 1) as the fastest growing isolate ($\mu = 0.21 \text{ h}^{-1}$). The physiology of this strain was further characterized in aerobic bioreactor batch cultures on SM containing 10 g L⁻¹ glucose and 20 g L⁻¹ xylose. After a 10 h lag phase (Figure 3, Additional File 4) exponential growth was observed at a specific growth rate of 0.18 h⁻¹. Biomass, ethanol and CO₂ were the main products, with additional minor formation of glycerol and acetate (Table 3, Figure 3, Additional File 4). During the exponential growth phase, xylose and glucose were co-consumed at a fixed molar ratio of 1.64 mol mol⁻¹ (Table 3, Figure 3). Growth ceased after glucose depletion, at which point xylose consumption rates drastically decreased and corresponded to a simultaneous low rate of xylitol formation (Figure 3, Additional File 4). As previously reported for XylA-expressing, xylose-fermenting *S. cerevisiae* strains [28, 29], no production of xylitol was observed during the exponential growth phase. The biomass and ethanol yields on total sugars consumed were 0.28 g biomass (g sugar)⁻¹ and 0.18 g ethanol (g sugar)⁻¹, respectively. Together with a respiratory quotient of 1.5, these

observations indicated a respiro-fermentative sugar dissimilation. In line with the inability of *pgi1Δ S. cerevisiae* to generate glucose-6-phosphate from ethanol and acetate, reconsumption of these fermentation products after glucose depletion was not coupled to growth (Figure 3, Additional File 4). However, their oxidation may have provided redox equivalents for the observed slow production of xylitol from xylose (Figure 3).

The quantitative data on biomass and product formation obtained from the bioreactor batch cultures enabled a comparison of the observed molar ratio of xylose and glucose consumption with a model-based prediction. To this end, the engineered metabolic network of strain IMX1046 was re-created *in silico*, using the Yeast v7.6 consensus metabolic model as a basis (Aung *et al.* 2013; Additional File 2). Consistent with the experimental observations on forced co-consumption, inactivation of either xylose or glucose uptake in the model network did not result in any feasible growth solutions. Using the experimentally determined average specific growth rates and oxygen consumption rates from the aerobic bioreactor batch cultures of strain IMS0629 as constraints on the model resulted in predicted xylose and glucose uptake rates of 2.68 and 1.93 mmol (g biomass)⁻¹ h⁻¹, respectively, corresponding to a molar ratio of the xylose and glucose consumption rates of 1.4. In view of the complexity of the model and the potential impact of differences in biomass composition, this number corresponded well with the experimentally measured value of 1.64 (Table 3).

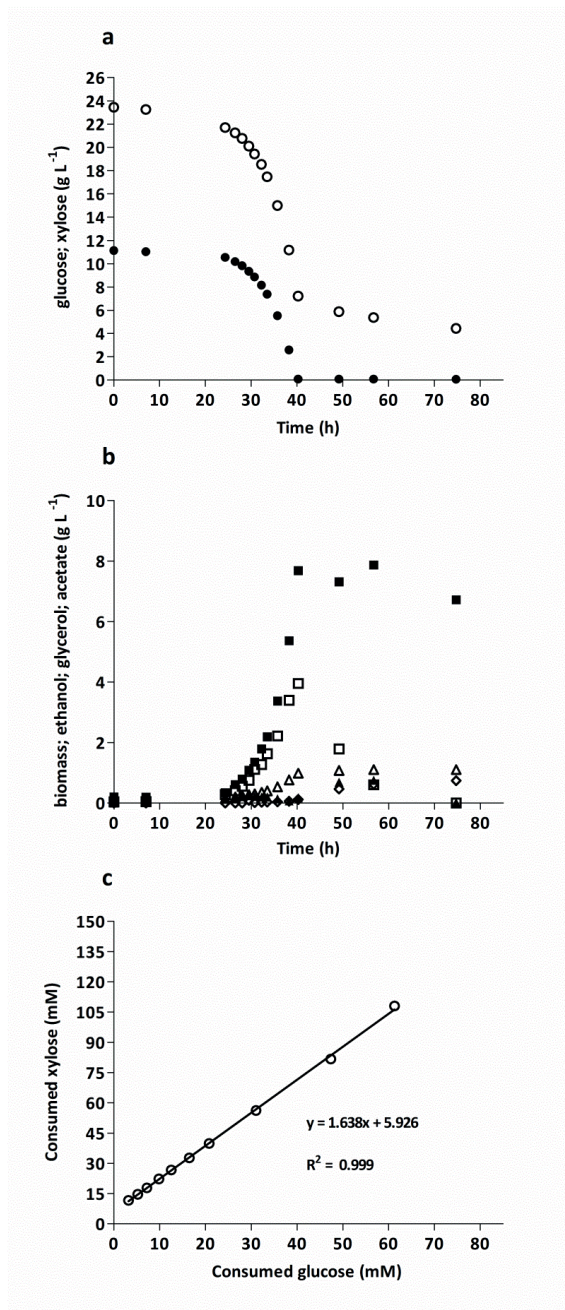


Figure 3. Sugar consumption, biomass and metabolite production profiles of the evolved *S. cerevisiae* strain IMS0629 (*pgi1Δ rpe1Δ gnd1Δ gnd2Δ gndA XylA XKS1↑ PPP↑*), grown on SM with 10 g L⁻¹ glucose and 20 g L⁻¹ xylose in aerobic bioreactor batch cultures (pH 5, 30 °C). Cultures were grown in duplicate, the data shown are from a single representative culture. **a**: ● glucose, ○ xylose; **b**: ■ biomass □ ethanol ▲ acetate △ glycerol ◇ xylitol; **c**: ratio of xylose and glucose consumption during exponential growth phase.

Table 3. Product yields, biomass specific sugar uptake and production rates in aerobic bioreactor batch cultures of evolved strain *S. cerevisiae* IMS0629 (*pgi1Δ rpe1Δ gnd1Δ gnd2Δ gndA XylA XKS1↑ PPPT*) on SM supplemented with 10 g L⁻¹ glucose and 20 g L⁻¹ xylose (pH 5, 30 °C). Biomass-specific rates, yields and ratios were calculated from samples taken during the mid-exponential growth phase and represent averages ± mean deviation of independent duplicate cultures. Ethanol yield was corrected for evaporation.

Growth rate (h ⁻¹)	0.18 ± 0.00
Glucose-xylose consumption ratio mol mol ⁻¹	1.64 ± 0.00
Spec. xylose uptake rate mmol (g biomass) ⁻¹ h ⁻¹	2.52 ± 0.00
Spec. glucose uptake rate mmol (g biomass) ⁻¹ h ⁻¹	1.54 ± 0.07
Spec. glycerol production rate mmol (g biomass) ⁻¹ h ⁻¹	0.23 ± 0.01
Spec. ethanol production rate mmol (g biomass) ⁻¹ h ⁻¹	2.25 ± 0.37
Spec. CO ₂ production rate mmol (g biomass) ⁻¹ h ⁻¹	10.43 ± 0.98
Spec. O ₂ uptake rate mmol (g biomass) ⁻¹ h ⁻¹	6.87 ± 0.56
Respiratory quotient	1.52 ± 0.03
Biomass yield g biomass (g sugars) ⁻¹	0.28 ± 0.00
Ethanol yield g (g sugars) ⁻¹	0.18 ± 0.00

5.3.3 Whole genome sequencing of evolved glucose-xylose co-consuming *S. cerevisiae*

To identify causal mutations for the improved growth of the evolved glucose-xylose co-consuming *S. cerevisiae* strains at high glucose concentrations, the genomes of strains IMS0629 and IMS0634 (fastest growing isolates from evolution line 1 and 2, respectively, Additional File 3) were sequenced and compared to that of their common parental strain [Genbank: PRJNA433919]. Despite the well documented role of *S. cerevisiae* hexose transporters in xylose uptake [18, 52-54], no mutations were found in the coding region of any of the 18 genes encoding these transporters (*HXT1-17* and *GAL2*), or in other known transporter genes. Both evolved strains harboured mutations in *HXK2* (Table 4). This gene encodes the major *S. cerevisiae* hexokinase which, in addition to its catalytic role, is involved in glucose repression [55, 56]. The mutation in IMS0629 caused a premature stop codon at position 309 of Hxk2. Both

strains also harboured mutations in *RSP5*, which encodes an E3-ubiquitin ligase linked to ubiquitination and endocytosis of membrane proteins [57]. In strain IMS0629, a substitution at position 686 caused a glycine to aspartic acid change at position 229 of Rsp5 (Table 4). Strain IMS0634 carried a 41 bp internal deletion in *RSP5*, which included the location of the mutation in strain IMS0629 and probably caused loss of function.

Compared to strain IMS0634, strain IMS0629 harboured 4 additional nucleotide changes in protein-coding regions (Table 4). A G-A change at position 896 of the transcriptional regulator gene *CYC8* introduced a stop codon at position 299 of the protein. Deletion of *CYC8* was previously shown to enhance xylose uptake in the presence of glucose, albeit at the expense of growth rate [58]. A G-T change at position 673 of the transcriptional regulator gene *GAL83* caused an amino acid change from aspartic acid to tyrosine at position 225 of the protein. Gal83 plays a vital role in the function of the Snf1-kinase complex of *S. cerevisiae*, which is involved in activation of glucose-repressed genes in the absence of the sugar [59-62].

Analysis of chromosomal copy number variations showed no chromosomal rearrangements in strain IMS0629 (Additional File 5). In contrast, strain IMS0634 carried a duplication of the right arm of chromosome 3, a duplication of the middle part of chromosome 8 and a duplication of chromosome 9 (Additional File 5). The duplications in chromosomes 8 and 9 in IMS0634 spanned the *GND1*, *GRE3* and *SGA1* loci at which the expressing cassettes for heterologous genes were integrated (Table 1). In the evolved strains IMS0629 and IMS0634, *xyIA* copy numbers had increased to ca. 27 and 20, respectively. This observation is consistent with previous research that showed a requirement for high copy numbers of *xyIA* expression cassettes to support fast xylose consumption [29, 63]. The duplication in of a segment of chromosome 8 in strain IMS0634 also spanned the locations of the low-to-moderate affinity hexose transporter genes *HXT1* and *HXT5* and the high-affinity hexose transporter gene *HXT4*.

Table 4. Mutations identified by whole-genome sequencing of glucose-xylose co-consuming *S. cerevisiae* strains evolved for fast growth at high glucose concentrations. Gene descriptions were taken from the Saccharomyces Genome Database (<https://www.yeastgenome.org/>, Accessed 14-12-2017).

Strain and gene	Nucleotide change	Amino acid change	Description
IMS0629 <i>CYC8</i>	G896A	W299 → Stop	General transcriptional co-repressor; acts together with Tup1; also acts as part of a transcriptional co-activator complex that recruits the SWI/SNF and SAGA complexes to promoters; can form the prion [OCT+]
<i>GAL83</i>	G673T	D225Y	One of three possible beta-subunits of the Snf1 kinase complex; allows nuclear localization of the Snf1 kinase complex in the presence of a non-fermentable carbon source
<i>RSP5</i>	G686A	G229D	NEDD4 family E3 ubiquitin ligase; regulates processes including: MVB sorting, the heat shock response, transcription, endocytosis and ribosome stability; ubiquitinates Sec23, Sna3, Ste4, Nfi1, Rpo21 and Sem1; autoubiquitinates; deubiquitinated by Ubp2; regulated by SUMO ligase Siz1, in turn regulates Siz1p
<i>HXK2</i>	C927G	Y309 → Stop	SUMO ligase activity; required for efficient Golgi-to-ER trafficking in COPI mutants
<i>RBH1</i>	C190A	Q64K	Hexokinase isoenzyme 2; phosphorylates glucose in cytosol; predominant hexokinase during growth on glucose; represses expression of <i>HXK1</i> , <i>GLK1</i>
<i>DCS1</i>	G636G	Y212 → Stop	Putative protein of unknown function; expression is cell-cycle regulated as shown by microarray analysis; potential regulatory target of Mbp1, which binds to the YJL181W promoter region; contains a PH-like domain
IMS0634 <i>RSP5</i>	Internal deletion (41 nucleotides)	Frameshift	Non-essential hydrolase involved in mRNA decapping; activates Xrn1; may function in a feedback mechanism to regulate deadenylation, contains pyrophosphatase activity and a HIT (histidine triad) motif; acts as inhibitor of neutral trehalase Nth1; required for growth on glycerol medium
<i>HXK2</i>	G1027C	D343H	NEDD4 family E3 ubiquitin ligase; regulates processes including: MVB sorting, the heat shock response, transcription, endocytosis and ribosome stability; ubiquitinates Sec23, Sna3, Ste4, Nfi1, Rpo21 and Sem1; autoubiquitinates; deubiquitinated by Ubp2; regulated by SUMO ligase Siz1, in turn regulates Siz1p
			SUMO ligase activity; required for efficient Golgi-to-ER trafficking in COPI mutants
			Hexokinase isoenzyme 2; phosphorylates glucose in cytosol; predominant hexokinase during growth on glucose; represses expression of <i>HXK1</i> , <i>GLK1</i>

5.3.4 Mutations in *HXK2*, *RSP5* and *GAL83* stimulate co-consumption of xylose and glucose in aerobic cultures of xylose-consuming *S. cerevisiae*

To investigate the impact of mutations in *HXK2*, *RSP5* and/or *GAL83* on mixed-sugar utilization by an *S. cerevisiae* strain without forced glucose-xylose co-consumption, they were introduced into an engineered, non-evolved xylose-consuming *S. cerevisiae* strain background (Table 1). Overexpression of *xyIA* was accomplished by transforming strains with the multi-copy *xyIA* expression vector pAKX002 [39]. In aerobic shake-flask cultures grown on 10 g L⁻¹ glucose and 10 g L⁻¹ xylose, the reference strain IMU079 (*XKS1*↑ *PPP*↑ pAKX002) displayed a pronounced biphasic growth profile and only a minor co-consumption of the two sugars (0.13 mol xylose (mol glucose)⁻¹; Table 5, Figure 4, Additional File 6). Co-consumption was strongly enhanced in the congenic *hvk2Δ* strain IMX1485, which showed a 3-fold higher molar ratio of xylose and glucose consumption (0.41 mol mol⁻¹). However, its specific growth rate before glucose depletion (0.28 h⁻¹) was 13% lower than that of the reference strain (Table 5). Strain IMX1487 (*rsp5Δ*), which showed a 20% lower specific growth rate than the reference strain, showed a slight improvement in co-consumption (Table 5). Deletion of *GAL83* (strain IMX1486) affected neither sugar co-consumption nor growth rate. In contrast, replacement of *GAL83* by *GAL83*^{G673T} (strain IMX1488) resulted in a 40% higher co-consumption of glucose and xylose than observed in the reference strain IMU079, without affecting growth rate (Table 5).

Since independently evolved glucose-xylose co-consuming strains both contained putative loss-of-function mutations in *HXK2* and *RSP5*, both genes were deleted in strain IMX1515 (*hvk2Δ rsp5Δ XKS1*↑ *PPP*↑ pAKX002). Similarly, deletion of *HXK2* and introduction of *GAL83*^{G673T} were combined in strain IMX1583 (*hvk2Δ gal83::GAL83*^{G673T} *XKS1*↑ *PPP*↑ pAKX002). Co-consumption ratios in the two strains (0.60 and 0.49 mol xylose (mol glucose)⁻¹, respectively) were 4- to 5-fold higher than in the reference strain IMU079 (Table 5, Figure 4, Additional File 6). However, strain IMX1515 exhibited a 40% lower specific growth rate (0.19 h⁻¹) than the reference strain, resulting in a 9 h extension of the fermentation experiments (Figure 4,

Additional File 6). In contrast, strain IMX1583 combined a high co-consumption ratio with the same specific growth rate as that of the reference strain.

Table 5. Specific growth rates (μ) and ratio of xylose and glucose consumption in aerobic shake-flask cultures of strains IMU079 (*XKS1*↑ PPP↑ pAKX002), IMX1485 (*hxx2*Δ *XKS1*↑ PPP↑ pAKX002), IMX1486 (*gal83*Δ *XKS1*↑ PPP↑ pAKX002), IMX1487 (*rsp5*Δ *XKS1*↑ PPP↑ pAKX002), IMX1488 (*gal83::GAL83^{G673T}* *XKS1*↑ PPP↑ pAKX002), IMX1515 (*hxx2*Δ *rsp5*Δ *XKS1*↑ PPP↑ pAKX002) and IMX1583 (*hxx2*Δ *gal83::GAL83^{G673T}* *XKS1*↑ PPP↑ pAKX002) grown on SM (urea as nitrogen source) with 10 g L⁻¹ glucose and 10 g L⁻¹ xylose (pH 6, 30 °C). Growth rates and ratios were calculated from samples taken during the mid-exponential growth phase and represent averages ± mean deviation of independent duplicate cultures.

Strain	Relevant Genotype	μ (h ⁻¹)	Xylose-Glucose consumption ratio (mol mol ⁻¹)
IMU079	<i>HXX2 RSP5 GAL83</i>	0.32 ± 0.01	0.13 ± 0.00
IMX1485	<i>hxx2</i> Δ	0.28 ± 0.00	0.41 ± 0.01
IMX1486	<i>gal83</i> Δ	0.31 ± 0.00	0.14 ± 0.01
IMX1487	<i>rsp5</i> Δ	0.26 ± 0.00	0.15 ± 0.00
IMX1488	<i>gal83::GAL83^{G673T}</i>	0.31 ± 0.00	0.18 ± 0.01
IMX1515	<i>hxx2</i> Δ <i>rsp5</i> Δ	0.19 ± 0.00	0.60 ± 0.00
IMX1583	<i>hxx2</i> Δ <i>gal83::GAL83^{G673T}</i>	0.31 ± 0.00	0.49 ± 0.00

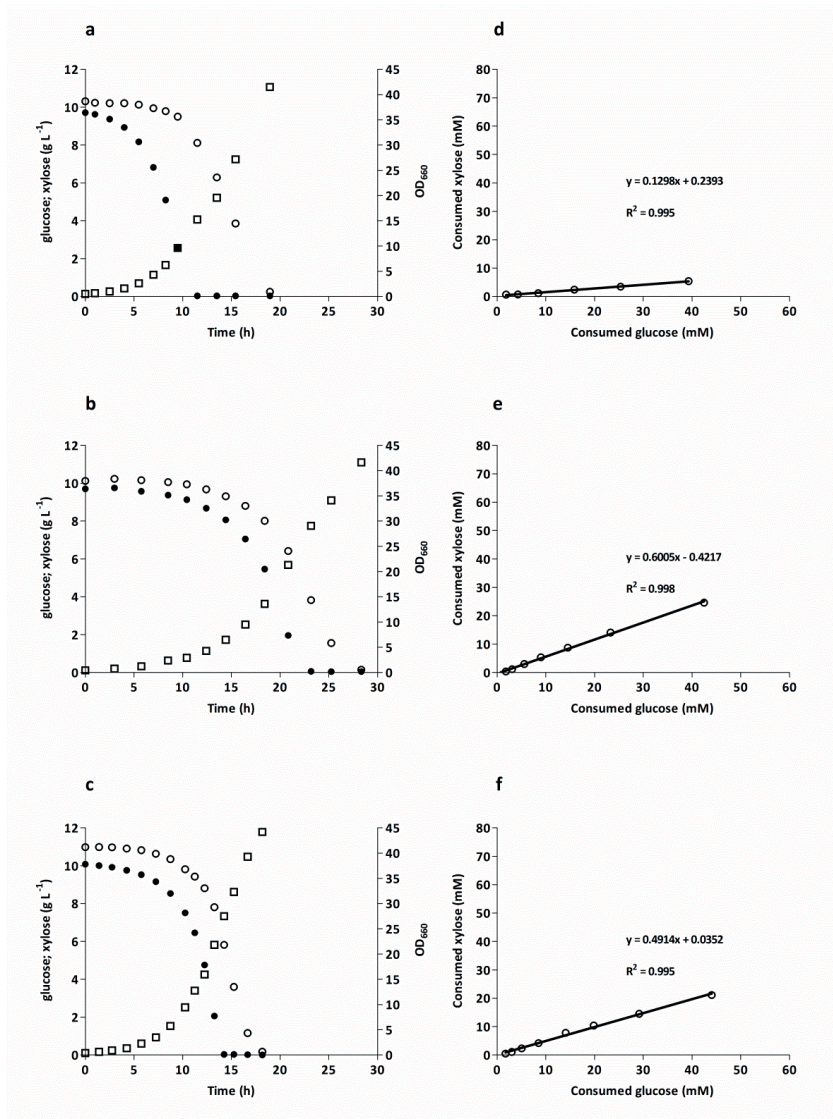


Figure 4. Consumption of glucose and xylose and growth of strains IMU079 (*XKS1*↑ PPP1 pAKX002; **a, d**), IMX1515 (*hxx2Δ rsp5Δ XKS1*↑ PPP1 pAKX002; **b, e**) and IMX1583 (*hxx2Δ gal83::GAL83^{G673T} XKS1*↑ PPP1 pAKX002; **c, f**) in batch cultures. The three strains were grown on SM (urea as nitrogen source) with 10 g L⁻¹ glucose and 10 g L⁻¹ xylose in aerobic shake-flask cultures (pH 6, 30 °C). **a, b, c**: ● glucose, ○ xylose, □ OD₆₆₀; **d, e, f**: ratio of xylose and glucose consumption during exponential growth phase.

5.3.5 Combined mutations in *HXK2* and *GAL83* significantly accelerate conversion of glucose-xylose mixtures by anaerobic cultures of xylose-consuming *S. cerevisiae*

To investigate the impact of the identified mutations under more industrially relevant conditions, anaerobic growth of the reference xylose-fermenting strain IMU079 (*XKS1*↑ *PPP*↑ *pAKX002*) in bioreactor batch experiments was compared with that of the two congenic double mutants IMX1515 (*hvk2Δ rsp5Δ*) and IMX1583 (*hvk2Δ gal83::GAL83^{G673T}*), that showed the highest glucose-xylose co-consumption in the aerobic shake-flask experiments. The anaerobic cultures were grown on 20 g L⁻¹ glucose and 10 g L⁻¹ xylose to simulate the relative concentrations of these sugars typically found in lignocellulosic hydrolysates [6].

In the anaerobic batch cultures, strains IMU079, IMX1515 and IMX1583 all produced CO₂, biomass, ethanol and glycerol as main products, with a minor production of acetate (Table 6, Figure 5, Additional File 7). The strains did not produce xylitol during exponential growth and low concentrations of xylitol in cultures of strain IMU079 (2.2 ± 0.1 mmol L⁻¹) were only observed at the end of fermentation. As observed in aerobic cultures (Figure 4), strain IMU079 showed a clear biphasic growth profile in the anaerobic bioreactors (Figure 5, Additional File 7), during which a fast glucose phase (ca. 16 h) was followed by a much slower and decelerating xylose consumption phase. During the glucose phase, this reference strain maintained a specific growth rate of 0.29 h⁻¹ and a glucose-xylose co-consumption ratio of 0.14 mol mol⁻¹ (Table 6). After a ca. 30 h lag phase (Figure 5, Additional File 7), strain IMX1515 exhibited an exponential growth rate of 0.07 ± 0.00 h⁻¹, with a high glucose-xylose co-consumption ratio (0.45 ± 0.03 mol mol⁻¹). Mainly as a result of its lag phase, strain IMX1515 took longer to consume all sugars than the reference strain IMU079, but its xylose-consumption phase was ca. 65% shorter (ca. 14 h and 43 h, respectively; Figure 5, Additional File 7).

In contrast to strain IMX1515, strain IMX1583 (*hvk2Δ gal83::GAL83^{G673T} XKS1*↑ *PPP*↑ *pAKX002*) did not exhibit a lag phase but immediately started exponential growth at 0.21 h⁻¹ (Figure 5). A comparison of biomass-specific uptake rates of xylose and glucose in the anaerobic batch experiments showed that strain IMX1583 maintained a 44% higher xylose uptake rate

than strain IMU079 before glucose exhaustion (Table 6). Moreover, both strains IMX1515 and IMX1583 did not show the pronounced decline of xylose consumption after glucose exhaustion that was observed in the reference strain (Figure 5, Additional File 7). As a result, the xylose consumption phase in anaerobic cultures of strain IMX1583 was 80% shorter than that strain IMU079 (ca. 9 h compared to 43 h), thereby reducing the time required for complete sugar conversion by over 24 h (Figure 5).

Table 6. Product yields, biomass specific rates and sugar uptake ratios in anaerobic bioreactor batch cultures of strains IMU079 (*XKS1*↑ PPP↑ pAKX002), IMX1515 (*hvk2Δ rsp5Δ XKS1*↑ PPP↑ pAKX002) and IMX1583 (*hvk2Δ gal83::GAL83^{G673T} XKS1*↑ PPP↑ pAKX002) grown on SM supplemented with 20 g L⁻¹ glucose and 10 g L⁻¹ xylose (pH 5, 30 °C). Rates, yields and ratios were calculated from samples taken during the mid-exponential growth phase and represent averages ± mean deviation of independent duplicate cultures. Ethanol yields were corrected for evaporation.

Strain	IMU079	IMX1515	IMX1583
Relevant genotype	<i>HVK2 RSP5 GAL83</i>	<i>hvk2Δ rsp5Δ</i>	<i>hvk2Δ gal83::GAL83^{G673T}</i>
μ (h⁻¹)	0.29 ± 0.01	0.07 ± 0.00	0.21 ± 0.00
Spec. xylose uptake rate mmol (g biomass)⁻¹ h⁻¹	2.22 ± 0.14	2.50 ± 0.12	3.19 ± 0.02
Spec. glucose uptake rate mmol (g biomass)⁻¹ h⁻¹	15.65 ± 0.52	5.58 ± 0.08	10.09 ± 0.08
Glucose-xylose consumption ratio (mol mol⁻¹)	0.14 ± 0.00	0.45 ± 0.03	0.32 ± 0.01
Biomass yield on sugars (g biomass g⁻¹)	0.09 ± 0.01	0.05 ± 0.00	0.09 ± 0.00
Ethanol yield on sugars (g g⁻¹)	0.37 ± 0.00	0.43 ± 0.00	0.38 ± 0.01
Glycerol yield on sugars (g g⁻¹)	0.10 ± 0.00	0.06 ± 0.00	0.08 ± 0.00
Ratio glycerol production on biomass production (mmol (g biomass)⁻¹)	11.5 ± 0.60	12.0 ± 0.50	9.9 ± 0.10
Xylitol production (mmol L⁻¹)	2.22 ± 0.06	0.90 ± 0.04	0.35 ± 0.04

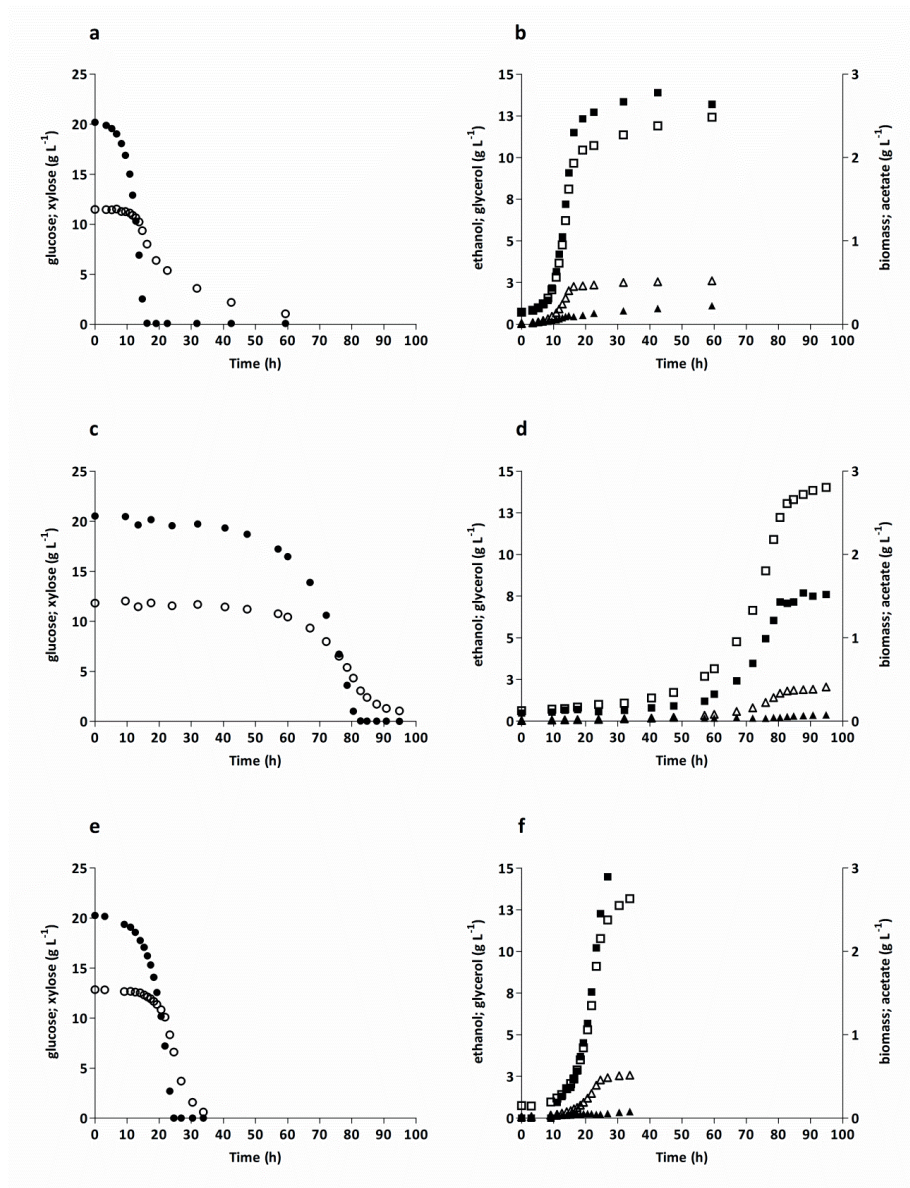


Figure 5. Sugar consumption, biomass and metabolite production profiles of *S. cerevisiae* strains IMU079 (*XKS1*↑ *PPP*↑ *pAKX002*; **a, b**), IMX1515 (*hvk2*Δ *rsp5*Δ *XKS1*↑ *PPP*↑ *pAKX002*; **c, d**) and IMX1583 (*hvk2*Δ *gal83::GAL83^{G673T}* *XKS1*↑ *PPP*↑ *pAKX002*; **e, f**), grown on SM with 20 g L⁻¹ glucose and 10 g L⁻¹ xylose in anaerobic bioreactor batch cultures (pH 5, 30 °C). Cultures were grown in duplicate, the data shown are from a single representative culture. **a, c, e:** ● glucose, ○ xylose; **b, d, f:** ■ biomass □ ethanol ▲ acetate Δ glycerol. Data on ethanol corrected for evaporation.

5.4 Discussion

5.4.1 Engineering *S. cerevisiae* for forced co-consumption of xylose and glucose

In previous studies, laboratory evolution of glucose-phosphorylation-negative, pentose-fermenting strains in the presence of glucose yielded valuable leads for improving utilization of glucose-xylose mixtures, including mutations in *HXT* genes that improved pentose uptake in the presence of glucose [18, 20, 58, 64]. The strategy described in this study not only enabled selection for xylose utilization in the presence of glucose, but also for simultaneous metabolism of the two sugars. The molar ratio of xylose and glucose co-consumption (1.64 mol xylose (mol glucose)⁻¹) by the evolved strain IMS0629 is the highest reported to date for batch cultures of *S. cerevisiae* [14, 19, 20, 23, 49-51].

Inactivation of *PGI1* played a key role in the presented strategy for forcing simultaneous utilization of xylose and glucose (Figure 1). The growth defect of *S. cerevisiae pgi1Δ* mutants on media that contain glucose as sole carbon source is related to their inability to reoxidize the NADPH that is generated when metabolism of glucose-6-phosphate is rerouted through the oxidative PPP [26, 65]. Since such a rerouting was a key element in our strain design (Figure 1), the NADPH yield from conversion of glucose-6-phosphate through the oxidative PPP was reduced from 2 to 1 mol mol⁻¹ by replacing Gnd1 and Gnd2 with the NAD⁺-linked bacterial 6-phosphogluconate dehydrogenase GndA [30]. Together with the co-consumption of xylose, via an engineered pathway that did not involve NAD(P)H generation (Figure 1), these modifications enabled the engineered strain IMX1046 to grow on mixtures of xylose and 1 g L⁻¹ glucose, without the fructose supplementation that is normally required for growth of *pgi1*-null mutants on glucose [24, 26]. The evolved strain IMS0629 consumed 8.6 mmol glucose (g biomass)⁻¹ in aerobic batch cultures (Table 3), which is close to the requirement of 9.3 mmol NADPH (g biomass)⁻¹ for aerobic growth on glucose of wild-type *S. cerevisiae* [47]. However, since glucose-6-phosphate is a key biosynthetic precursor, not all glucose consumed by the cultures can be converted through the oxidative PPP. Additional enzymes, such as NADP⁺-dependent

acetaldehyde dehydrogenase Ald6 [30, 66, 67] are therefore likely to have supplemented NADPH generation via the oxidative PPP in the 'forced co-consumption' strains.

The key objective of this study was to develop and test a strain platform that, via laboratory evolution and subsequent genome resequencing, can be used to identify mutations that support co-metabolism of xylose and glucose. However, the reported strategy for forced co-consumption of xylose and glucose may also be used in optimizing the yeast metabolic network for aerobic production of economically relevant compounds from lignocellulosic hydrolysates. In particular, imposing fixed stoichiometries of glycolytic and (non-oxidative) PPP reactions may offer interesting options for high-yield production of compounds whose synthesis requires a large net input of PPP intermediates and/or NADPH, such as aromatic compounds derived from the shikimate pathway and lipids [68-70].

5.4.2 Improvement of mixed-sugar fermentation in anaerobic cultures of xylose-fermenting *S. cerevisiae*

Mutations in *HXK2*, *RSP5* and *GAL83* were selected to investigate whether genetic changes that occurred during evolution of strain IMX1046 (*pgi1Δ rpe1Δ gnd1Δ gnd2Δ gndA XylA XKS1↑ PPP↑*) on glucose-xylose mixtures would also stimulate mixed-substrate utilization in a genetic background that does not impose forced co-utilization. To this end, these mutations were reverse engineered into a non-evolved strain (*XKS1↑ PPP↑*). During growth on glucose-xylose mixtures, the reference strain IMU079 (*XKS1↑ PPP↑ pAKX002*) displayed the typical biphasic growth profile seen in non-evolved, xylose-consuming strains that express a basic, functional xylose-isomerase (XI) based xylose fermentation pathway [28, 39]. Biphasic growth was especially pronounced in anaerobic cultures, in which the xylose consumption rate collapsed upon glucose depletion (Figure 5). Deletion of *HXK2*, either combined with the deletion of *RSP5* or with the introduction of a *GAL83^{G673T}* mutation, strongly improved mixed sugar fermentation kinetics, both by increased co-utilization and by faster conversion of xylose after glucose had been depleted (Figures 4 and 5). While analysis of the molecular mechanisms

by which the mutations in *HXK2*, *RSP5* and *GAL83* affected mixed substrate utilization is beyond the scope of this study, the scientific literature enables a first interpretation.

Hxk2, the major hexokinase in *S. cerevisiae*, plays an additional key role in transcriptional repression of a large set of yeast genes [71-73] by glucose. Deletion of *HXK2* has been shown to enhance co-consumption of combinations of natural substrates (glucose-galactose, glucose-sucrose and glucose-ethanol) in batch cultures [55]. During exponential growth on glucose in batch cultures, *hxk2Δ* mutants show increased transcription of the high-affinity hexose transporter genes *HXT2* and *HXT7* and decreased transcription of the low-affinity hexose transporter genes *HXT1* and *HXT3* [74]. The high-affinity Hxt transporters, which in wild-type strains are only expressed at low glucose concentrations [75], have a much lower K_m for xylose than their low-affinity counterparts [53, 54]. Several studies have demonstrated that overexpression of high-affinity hexose transporters stimulates xylose uptake [7, 18-21, 50, 76, 77]. The observed improved co-utilization of glucose and xylose upon inactivation of *HXK2* may therefore reflect an increased abundance of high-affinity hexose transporters in the yeast plasma membrane during growth on glucose-xylose mixtures. A recent *in silico* study also identified *HXK2* as potential target for improving xylose uptake rates in *S. cerevisiae* [78]. However, when this prediction was verified by deleting *HXK2* in a strain expressing a xylose reductase/xylytol dehydrogenase-based (XR/XDH) pathway, faster xylose uptake was accompanied by increased production of by-products and reduced ethanol productivity [78]. The absence of such negative effects in the present study is in line with previous reports that xylose-isomerase-based strains are less prone to by-product formation than XR/XDH-based strains (for reviews see Moysés *et al.* 2016; Jansen *et al.* 2017).

Rsp5, the only representative of the NEDD4 family of E3-ubiquitin ligases in *S. cerevisiae*, is involved in regulation of a multitude of cellular processes, including intracellular protein trafficking, regulation of the large subunit of RNA polymerase II, ribosome stability, regulation of fatty acid synthesis and stress response [57, 79-81]. This multitude of roles may explain the reduced growth rate of the *rsp5Δ* strains (Tables 5 and 6) in this study. Involvement of Rsp5 in

ubiquitination and subsequent endocytosis of the high-affinity hexose transporters Hxt6 and Hxt7 [82, 83] could explain the strong synergistic effect of the *hvk2Δ* and *rsp5Δ* deletions: while deletion of *HVK2* prevents glucose repression of the synthesis of these transporters, deletion of *RSP5* could prevent their ubiquitination and removal from the membrane. Removal of ubiquitination sites in the hexose transporters Hxt1 and Hxt36 was previously shown to enhance xylose uptake by *S. cerevisiae* [76]. Our results suggest that a similar modification of Hxt6 and Hxt7 could also be beneficial.

Gal83 is one of three possible β -subunits of the Snf1-kinase complex, which enables transcription of glucose-repressed genes at low glucose concentrations (for reviews see Gancedo 1998; Schüller 2003). At non-repressing glucose concentrations, Gal83 directs the Snf1-Gal83 complex to the cell nucleus [84], where it mediates transcriptional upregulation of genes involved in utilization of alternative carbon sources [61]. Targets of the Snf1-Gal83 complex include the *GAL* regulon [85, 86] and the high-affinity hexose transporter genes *HXT2* and *HXT4* [87]. The D225Y substitution, which stimulated glucose-xylose co-consumption in the present study, is located in the glycogen-binding domain (GBD) of Gal83 (residues 161-243 [88]). Other mutations in this domain have been shown to cause transcription of Snf1-Gal83 targets in the presence of glucose [88-90]. In contrast to deletion of the transcriptional regulator *CYC8* [58], which also stimulated co-utilization but caused severe reductions of the specific growth rate of engineered strains, the *GAL83^{G673T}* mutation did not have a strong impact on growth rate (Tables 5 and 6). The synergistic effect of the *hvk2Δ* and *GAL83^{G673T}* mutations may be related to the involvement of Hvk2 in deactivation of Snf1 in the presence of glucose, causing constitutive activity of the Snf1-Gal83 complex in *hvk2*-null mutants [91, 92].

The reverse engineered mutations in *HVK2* and *GAL83* or *RSP5* not only stimulated simultaneous utilization of xylose and glucose when both sugars were present, but also prevented the sharp decline in xylose uptake rates that occurred in the reference strain IMU079 (*XKS1↑ PPP↑ pAKX002*). In the reference strain, the biomass-specific rate of xylose consumption, probably mediated by low- or moderate-affinity Hxt transporters, declined to values below 0.5

mmol (g biomass)⁻¹ h⁻¹ after glucose depletion (Figure 5, Additional File 7). Under anaerobic conditions, this low rate of xylose fermentation would correspond to a biomass-specific rate of ATP production of 0.8 mmol (g biomass)⁻¹ h⁻¹. This value is lower than the estimated ATP requirement for cellular maintenance of *S. cerevisiae* (ca. 1 mmol ATP (g biomass)⁻¹ h⁻¹ [93]). Since protein synthesis is a highly ATP-intensive process [94], an inability of the reference strain to functionally express high-affinity hexose transporters upon glucose depletion may therefore reflect an energy shortage. A similar effect was observed during transitions between glucose and galactose growth in anaerobic *S. cerevisiae* cultures [95]. By already expressing functional high-affinity transporters before glucose was depleted, the *hvk2Δ rsp5Δ* and *hvk2Δ GAL83^{G673T}* may have enabled cells to avoid such a bioenergetic ‘valley of death’ upon the transition to xylose fermentation. In industrial processes using lignocellulosic feedstocks, this energetic challenge is likely to be even more stringent due to the presence of compounds such as acetic acid that increase maintenance energy requirements [17, 32, 96].

While reverse engineering of *HVK2*, *RSP5* and *GAL83* mutations demonstrated the relevance of the forced co-utilization strategy demonstrated in this study, they do not exhaust its possibilities. The IMS0629 strain can, for example, be used to select mutations that enable efficient co-utilization of glucose and xylose at different concentrations or in lignocellulosic hydrolysates that, in addition to fermentable sugars, contain inhibitors of yeast performance [8, 97, 98]. Alternatively, the strain design can be adapted to enable selection for co-metabolism of other sugars, for example by replacing the xylose pathway by a bacterial pathway for conversion of L-arabinose into xylulose-5-phosphate [99, 100].

5.5 Conclusions

Engineering of carbon and redox metabolism yielded an *S. cerevisiae* strain whose growth was strictly dependent on the simultaneous uptake and metabolism of xylose and glucose. Laboratory evolution improved growth of the resulting strains on mixtures of xylose and glucose at elevated glucose concentrations. Mutations in *HVK2*, *RSP5* and *GAL83* were

identified by genome sequencing of the evolved strains. Upon their combined introduction into an engineered xylose-fermenting yeast strain, these mutations strongly stimulated simultaneous utilization of xylose and glucose and, after depletion of glucose, fast conversion of the remaining xylose. The developed strain platform and modified versions thereof can be used for identification of further metabolic engineering targets for improving the performance of yeast strains in industrial processes based on lignocellulosic feedstocks.

5.6 Acknowledgements

We thank Jasmine Bracher and Oscar Martinez for construction of strain IMU079. We thank Jean-Marc Daran and Pilar de la Torre for advice on molecular biology, Marcel van den Broek for assistance with bioinformatics analyses and Erik de Hulster for advice on fermentations. We thank Laura Valk for stimulating discussions.

5.7 Additional Files

Additional File 1. Primers used in this study

Primer code	Sequence 5'-3'
5980	CGACCGAGTTGCTCTTG
5792	GTTTTAGAGCTAGAAATAGCAAGTTAAAATAAG
5979	TATTCAGCGCGGCAAGAGC
5978	ATTTTAACTTCTATTTCTAGCTCTAAAACCTTATGACGTATACGTTTAGGATCATTATCTTTCACCTGCGG
5941	GCTGGCCTTTTGCTCACATG
6005	GATCATTTATCTTTCACCTCGGAGAAG
9269	TGGGATGTTTCGGCGTTCGAAAACCTTCGGCAGTGAAGAATAAATGATCAITTGACACAAAACATGTTGTTTTAGAGCTAGAAATAGCAAGTTAAAATAAG
9401	TGGCCATGTTTCGGCGTTCGAAAACCTTCGGCAGTGAAGATAAATGATCTTTTTGTTCCAAAACATTACTCGTTTTTAGAGCTAGAAATAGCAAGTTAAAATAAGGCTAGTCCCGTTATCAAC
11270	GTTGATAAGGGAAGCTAGGCTTATTTTAACTTGCTATTTCTAGCTCTAAAACAGTAAGTACACTTTTATTAGGATCATTTATCTTTTCACTGGGAGAAGTTTCGAAACGGGAAACATGGGCA
11373	GTTGATAAGGGAAGCTAGGCTTATTTTAACTTGCTATTTCTAGCTCTAAAACCTTATATAAATGACTCTGCAGGATCATTTATCTTTTCACTGGGAGAAGTTTCGAAACGGGAAACATGGGCA
8956	GCCAGAGGTATAGACAPAGCCAGACCTACC2TAATTTGGTGCATCAAGTGTGCATGGCCCTTGACGGCATAACCGCTAGAG
8960	TGTATATGAGATAGTTGATT
8958	TGAGTACACTGTCGCAAGATTGGGACCTGTCATG6GTATAGG6TCTCGGAGATCGCTCCACTAGTCAGATGCCGGG
8961	TTTGATTTAGTGTTTGTGTG
8953	CCAAGCATACAATCACTATCTCATATACAAATGATGAAGGCCCGTCAA
8964	AGGGATCTGGAGACGCTATAGCCCATGACGAGGTCCAAATCTTTGGGACAGTGTACTCAGGGCAAAGGACAGATGAAG
8984	TGCTTTATCACACACAACACTAAATCAAAATGGTGACAGTGGTGCTT
8986	GTCACGGGTTCTCAGCAATTCGAGCTATTACCGATGATGGCTAGGGGTTAGAGTAATCTCGGCTAGAGATCTTCTGACTG

4870	GCCAGAGGTATAGACATAGCC
7369	AGCGATCTCGGAGACCGTATAG
3290	GTCACGGGTTCTCAGCAATTCC
3291	CTCTAACCGCTCAGCCATCATCG
4068	GCCTACGGTTCCCGAAAGTATGC
3274	TATTCACGTAGACGGATAGGTATAGC
3275	GTGCCATTGATGATCTGGGGAATG
3847	ACTATATGTGAAGGCATGGCTATGG
3276	GTTGAACATTTCTAGGCTGTGCGAATC
4691	CACCTTTCGAGAGCGCATG
3277	CTAGGGTCTCTCGCATAGTCTTAGATTG
3283	AGCTCTCAGGGATGTTATATGC
3288	TGCCGAACCTTTCCTCTATGAAGC
7133	TATAATAATTTCAATTCGGAACTTAGAATCTACTGTTTCCCAATTTGCTGGTAGGGCCCTTCGGGAGTTTATC
10460	ACTATATGTGAAGGCATGGCTATGGCAGGCAGACATTCGCCAGATCATCAATAGGCACCGCCGCTGTTAAAGATTAC
10461	GCCGTAGCTCCGCAAGTATGCCGTAGTTGAAGGCAATTTGCCGTCGGTTCAGGTCATATTCATAGGTGAGAAAGAGATGGAGAACTGATG
6285	AAGGGCAATGACCACTGATGCCAATAGTAGGCTGGCTATGCTATACCTTGCGCGGATAGCCCTGCGATCTTC
7548	GCATAGAACAATTCGCGGAAACCGGTATTAGGGGTGAGGTGAATAAGGAAAGTCAGGAAATCGGGCCCGCAGATTYAGCGAAGC
6280	GTGCCATTTGATGATCTGGGGAATGTCTGCCGTGCCATAGCCATGCCATTCACATATAGTCCGATACCCCTGGGATCTTTC
6273	GCCAGAGGTATAGACATAGCCAGACCTACCTAATTTGTCGCATCAGGTGCTATGGCCCTTCGCCGAGATTAGCGAAGC
6281	GTTGAACAATTTAGGCTGTGCAATCAATTTAGACACGGGCATCGTCTCTCGAAAGGTGGCGATACCCCTGGGATCTTTC
6270	ACTATATGTGAAGGCATGGCTATGGCAGGCAGACATTCGCCAGATCATCAATAGGCACCGCCGAGATTYAGCGAAGC

6282	CTAGGGCTCTCCGGCATACTCTTAGAATCTCGCTACGGCATAATACGATCCGTGAGCGTGCATACCCCTGGGATCTTTC
6271	CACCTTTCGAGGACGATGCCCGTGTCTAAATGATTCGACGCCCTAAGAATGTTCAACCCGGCAGATTAGCGAAGC
6284	AATCACTCTCATACAGGTTTCAACAATTTCTCCACGGGACCCACAGTGTAGATGGGTGGATACCCCTGGGATCTTTC
6272	AGCTCTCACGGATGCTATATGGCGTAGCGACAATCTAAGAACTATGGCGAGGACACGCTAGGCGCGAGATTAGCGAAGC
6283	ACCCATCTACGACTGTGGTCCCGTGGAGAAATGTATGAAACCCCTGTATGGAGAGTGTATTGGGATACCCCTGGGATCTTTC
6275	ACGAGATGAAGGCTCACCAGTGGACTTAGTATGATGCGCATCTGGAAGCTCCGGTCAATCCGCGCAGATTAACGGAAGC
6287	ATGACCGGAGCTTCCAGCATGCCATCATACTAAGTCCATCCGCTAGCCCTCATCTCTGTGCCATACCCCTGGGATCTTTC
6276	TTCTAGGCTTTGATGCCAAGTCCAGATATCTTCTGTTAGGACTCAATCGTGGCTGTGATCCGGCGCAGATTTAGCGAAGC
6288	GATCAGCAGCCACGATTTAGTCTAAGCGAAGATATCTGGACCTTGCATCAAAGCCTAGAAGCGATACCCCTGGGATCTTTC
6277	ATACTCCCTGCACAGATGAGTCAAGCTATTTGAACACCCGAGAACGGGCTGAACGATCATTTCCGGCAGATTAGCGAAGC
6289	GAATGATCGTTTACGGCGTTTCTGGGTGTTCAATAGCTTGACTCATCTGTGCAGGGAGTATGGGATACCCCTGGGATCTTTC
6274	GCCTACGGTTCCCGAAGTATGCTGATGTCTGGCTATAGCTATCCTATCCTGCTACGTGAATAGCGCCAGATTAGCGAAGC
5920	TATTCACGCTAGACGGATAGGTATAGCCAGACATCAGCAGCATACTTCGGGAACCGTGAAGCAGCTATAGCTTCAAATAATGTTTCTACTCC
9029	TATATTTGATGATAAATATCTAGGAAATACACTTCTGTATACCTTCTCGGCTTTTCTTTTATTTCCAGTGTCTTCCACATC
7135	ATATGACCTGAACCGAGCGGCAAAATGCTTCAAACCTACGGCATACTTGGGGAAGCTACGGCCATAGCTTCAAATAATGTTTCTACTCC
7222	CAGACGCAAACTTTGTTCATGTTGCCATTGACTATGGTGCAAATGGCTGACATGAGCGCTCCAGTGTCTCCACATC
11273	CCGTTAAAAACACAGGCCACG
11274	TGCCGTGTAACGTTCAAAG
3275	GTGCCATTGATGATCTGGGGAAATG
3276	GTTGAACAATTTAGGCTGTGCGAATC
5971	AGAGCGGCATGCAAGGAAC
6637	GGCTGCTTTAAGGATGATG
6640	CTAGATGTGTACGCCATTTC
7869	CTTTGGGCAATCCTTTGGAG
7870	CTTCATCAGCACCGTCAAAC
7871	GGTGATTTCCGGCTCTATTGC

7872	TGGGCTTCACCCCTTGTAAATC
7873	ACCCATGTGGTTGCTGATTC
7874	AAATCTGGGTGGCGAATTCC
7875	TTGATAAGCTAGCCGCTCC
7877	CAACCATATGCCTCGTATGG
7923	GAAGCAGCGTATTGCAAAGC
8969	TCAGAGAGCTGATCAGAAC
8987	ATCGTGGCACCAGCAACTC
8988	TTGGGCTGTGCTCGATGG
533	CATGGCATGTAATGGAAGCA
3354	AGCCATCTACGACTGTGGGTC
3837	GAATGATCGTTACGGCGG
3843	GATCAGCAGCCACGATTG
4173	GTTGAACATTCCTAGGCTGG
4184	ATGACGGGAGCTCCAGCATG
4692	AAGGGCCATGACCACCTG
5231	AATCACTCTCCATACAGGG
6632	AGGCTCGTAGTAGTGGAAAGC
6633	ATGGAGGCTATGGCTAGAGCTTTGG
7056	AGAGTGGTGGTTTCGTTAC
7298	TTGTTCAATGGATGGGGTTC
7479	GGACGTTCCGACATAGTATC
9010	CCTCTCCCTTCCAAAAGAAC
1814	CAAACTGGCCACTGAATTGC
1815	TCCAATTCTTGGCCGATGAC
5004	GTAGATTGCACCATCTCAAGAGCC
5007	GAGGATGCTAAAAGTCCCGTC
7868	CAACTTGGTTGGGAATGTC
7922	CGCAATTCCTTCGAGACTTC

Additional File 2. MATLAB script for modification of the Yeast v7.6 consensus metabolic model [42] according to the glucose-xylose forced co-consumption strategy. The COBRA v2 toolbox [43] was used to read the model in MATLAB vR2017b (Mathworks, Natick, MA).

```
function [model,solution,ratio] = coconsumption(model,mu,q02)
```

Adapting model to strategy

```
%remove GRE3, GND1/GND2, RPE1, PGI1 ad BNA5
removeList = [{'r_1093'},{'r_0889'},{'r_0984'},{'r_0467'},{'r_0670'}];
model_strat = changeRxnBounds(model,removeList,0,'b');
removed = ['The following reactions have been disabled in the stoichiometric model: ',
strjoin(removeList)]; disp(removed)
%add XI and gnda
disp('The following reactions have been added to the stoichiometric model: ')
model_strat = addReaction(model_strat,'r_5001',{'s_0578[c_03]','s_0580[c_03]'},[-1 1]);
model_strat = addReaction(model_strat,'r_5002',{'s_0340[c_03] + s_1198[c_03] <=> s_0456[c_03] +
s_0577[c_03] + s_1203[c_03]'});
%Unlimited boundaries for glucose and xylose uptake
model_strat = changeRxnBounds(model_strat, [{'r_1714'},{'r_1718'}],-1000, [{'l'},{'l'}]);
model_strat = changeRxnBounds(model_strat, [{'r_1714'},{'r_1718'}],1000, [{'u'},{'u'}]);
```

Add experimental data

```
%Add experimentally measured growth rate and O2 uptake rate
model_strat = changeRxnBounds(model_strat,'r_2111',mu,'u');
model_strat = changeRxnBounds(model_strat,'r_1992',q02,'b');
%Change objective function to growth
model_strat = changeObjective(model_strat,'r_2111');
```

Retrieve glucose and xylose uptake rates

```
solution = optimizeCbModel(model_strat);
glucose_rate = solution.x(findRxnIDs(model_strat,'r_1714'));
xylose_rate = solution.x(findRxnIDs(model_strat,'r_1718'));
rates = [glucose_rate; xylose_rate];
rates_disp = ['At a growth rate of ',num2str(mu), '/h and a qO2 of ',num2str(q02),'
mmol/gDW.h, the glucose- and xylose uptake rates are ',num2str(glucose_rate), ' and
',num2str(xylose_rate), ' mmol/gDW.h, respectively'];
ratio = xylose_rate/glucose_rate; ratio_disp = ['The ratio of xylose over glucose uptake is
',num2str(ratio)];
```

Check for requirement of co-consumption

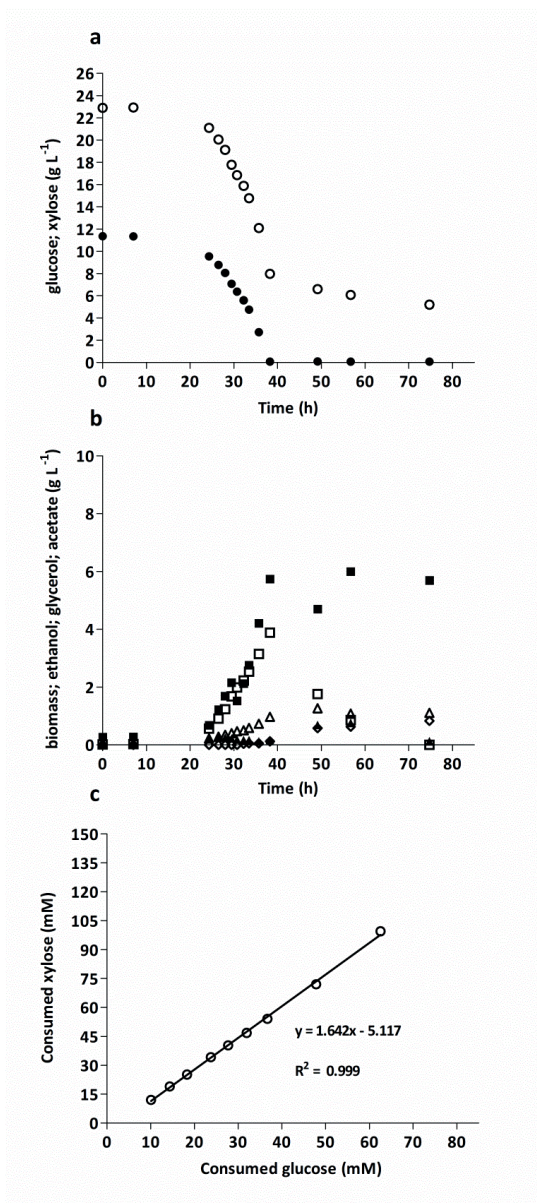
```
model_check = changeRxnBounds(model_strat,'r_1714',0,'b');
solution_check = optimizeCbModel(model_check); no_glucose = solution_check.origStat;
model_check = changeRxnBounds(model_strat,'r_1718',0,'b');
solution_check = optimizeCbModel(model_check); no_xylose = solution_check.origStat;
check1 = ['Without glucose, solving the model is ', no_glucose];
check2 = ['Without xylose, solving the model is ', no_xylose];
```

Displaying output

```
disp(rates_disp); disp(ratio_disp); disp(check1); disp(check2) end
```

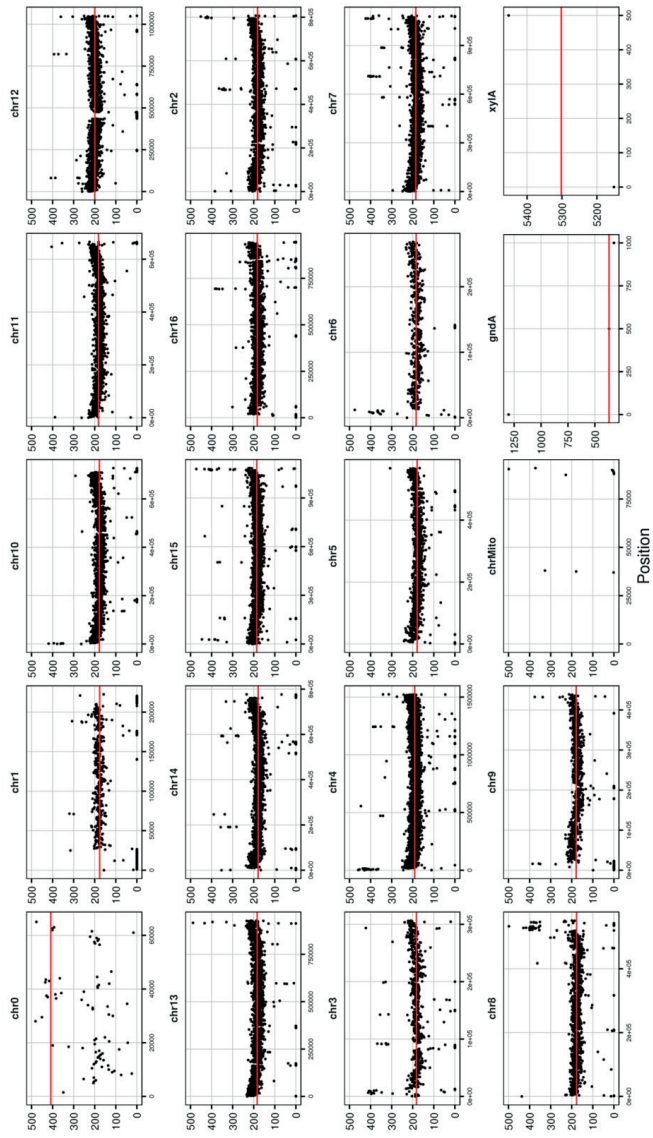
Additional File 3. Specific growth rates (μ) in aerobic shake-flask cultures of evolved strains grown on SM (parental IMX1046, *pgi1* Δ *rpe1* Δ *gnd1* Δ *gnd2* Δ *gndA* *XylA* *XKS1* \uparrow PPP \uparrow) with 10 g L⁻¹ glucose and 20 g L⁻¹ xylose (pH 6, 30 °C). Growth rates were calculated from samples taken during the mid-exponential growth phase and represent averages \pm mean deviation of independent duplicate cultures.

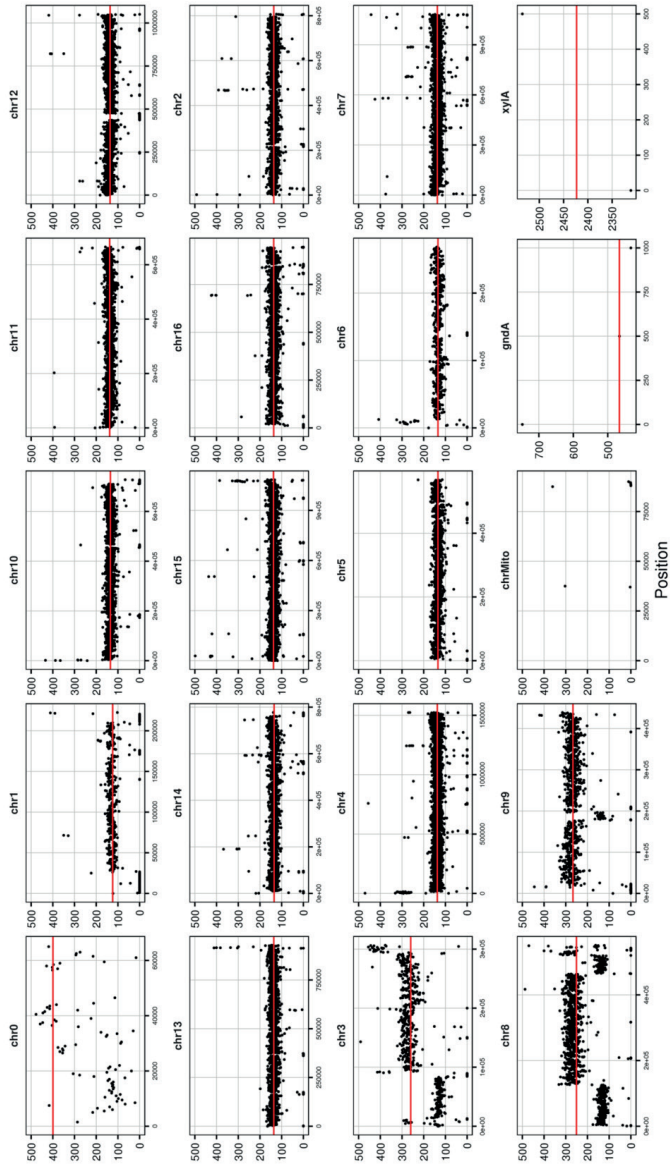
Strain		μ (h ⁻¹)
Evolution Line 1	IMS0628	0.18 \pm 0.00
	IMS0629	0.21 \pm 0.00
	IMS0630	0.19 \pm 0.01
Evolution Line 2	IMS0634	0.16 \pm 0.00
	IMS0635	0.14 \pm 0.01
	IMS0636	0.15 \pm 0.01



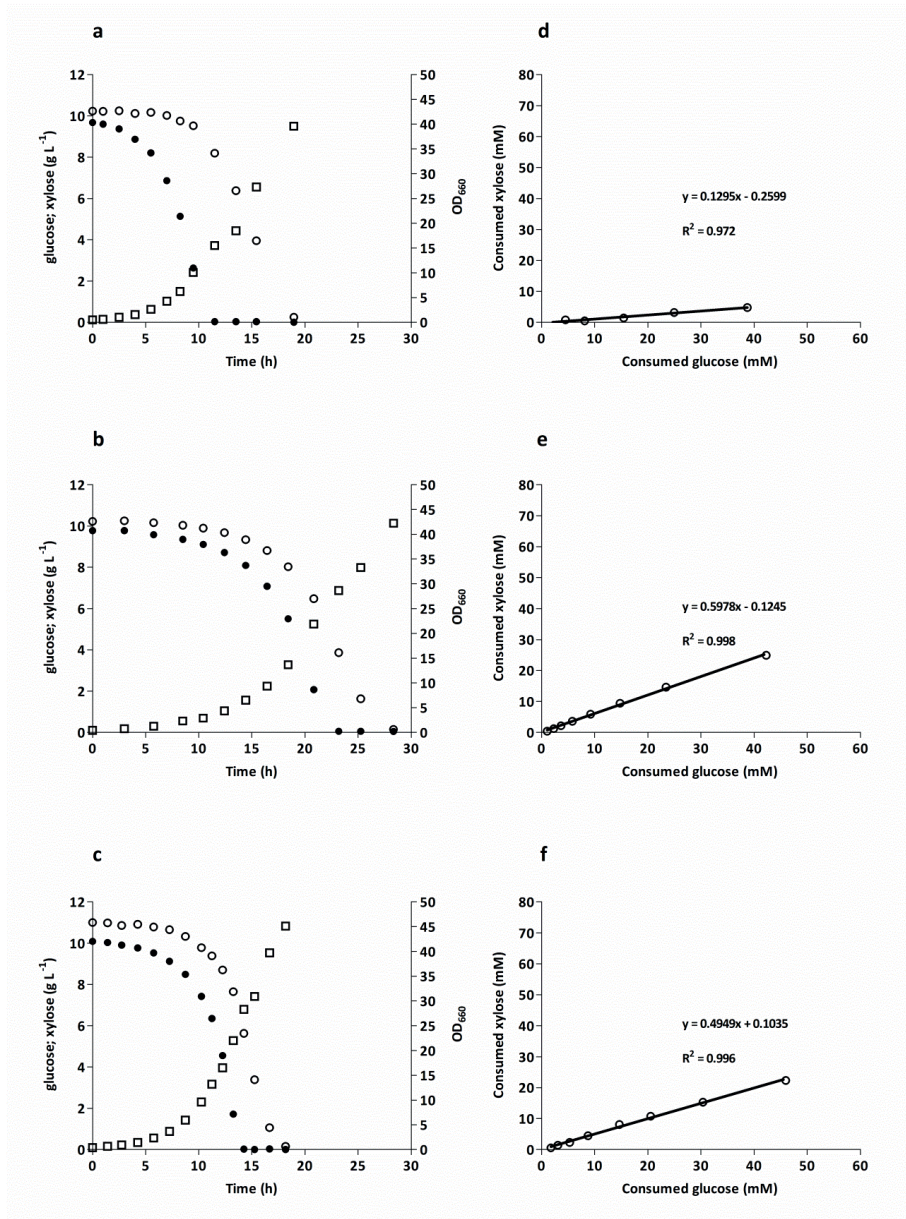
Additional File 4. Sugar consumption, biomass and metabolite production profiles of the evolved *S. cerevisiae* strain IMS0629 (*pgi1Δ rpe1Δ gnd1Δ gnd2Δ gndA XylA XKS1↑ PPP↑*), grown on SM with 10 g L⁻¹ glucose and 20 g L⁻¹ xylose in aerobic bioreactor batch cultures (pH 5, 30 °C). Cultures were grown in duplicate, the data shown are from a single representative culture. **a:** ● glucose, ○ xylose; **b:** ■ biomass □ ethanol ▲ acetate Δ glycerol ◇ xylitol; **c:** ratio of xylose and glucose consumption during exponential growth phase.

a

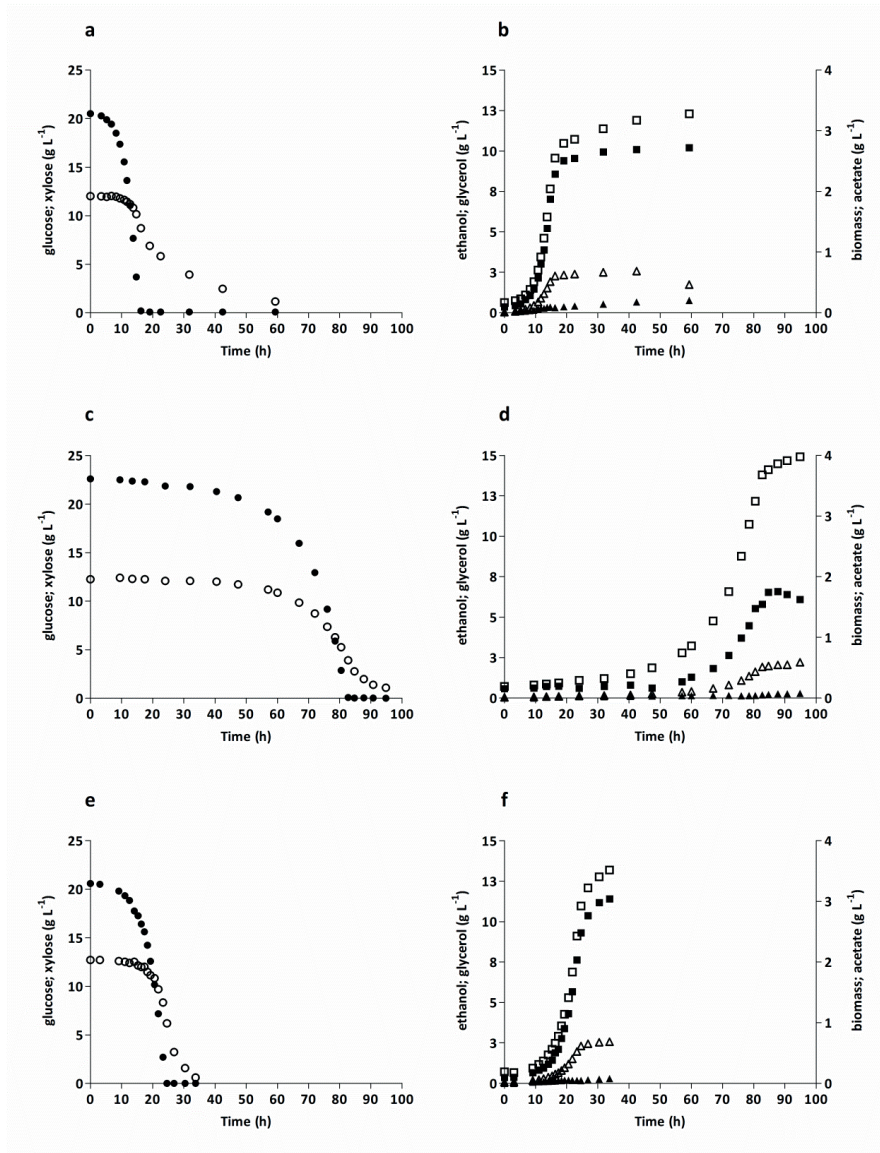


b

Additional File 5. Sequence coverage plots comparing the genome of IMS0629 (a) and IMS0634 (b) to a published genome of CEN.PK113-7D [45], generated using BWA to map the sequence reads from IMS0629 and IMS0634 to the CEN.PK113-7D reference. Further processed by SAMtools to extract the per base sequence depth and an in-house script to calculate the average coverage for 500 bp non-overlapping windows. R script was used to plot the 500 bp windows (black dots) and median coverage (red line).



Additional File 6. Consumption of glucose and xylose and growth of strains IMU079 (*XKS1*↑ PPP↑ pAKX002; a, d), IMX1515 (*hvk2Δ rsp5Δ XKS1*↑ PPP↑ pAKX002; b, e) and IMX1583 (*hvk2Δ gal83::GAL83^{G673T} XKS1*↑ PPP↑ pAKX002; c, f) in batch cultures. The three strains were grown on SM (urea as nitrogen source) with 10 g L⁻¹ glucose and 10 g L⁻¹ xylose in aerobic shake-flask cultures (pH 6, 30 °C). a, b, c: ● glucose, ○ xylose, □ OD₆₆₀; d, e, f: ratio of xylose and glucose consumption during exponential growth phase.



Additional File 7. Sugar consumption, biomass and metabolite production profiles of *S. cerevisiae* strains IMU079 (*XKS1*↑ *PPP*↑ *pAKX002*; a, b), IMX1515 (*hvk2Δ* *rsp5Δ* *XKS1*↑ *PPP*↑ *pAKX002*; c, d) and IMX1583 (*hvk2Δ* *gal83::GAL83^{G673T}* *XKS1*↑ *PPP*↑ *pAKX002*; e, f), grown on SM with 20 g L⁻¹ glucose and 10 g L⁻¹ xylose in anaerobic bioreactor batch cultures (pH 5, 30 °C). Cultures were grown in duplicate, the data shown are from a single representative culture. a: ● glucose, ○ xylose; b: ■ biomass □ ethanol ▲ acetate Δ glycerol. Data on ethanol corrected for evaporation.

5.8 References

1. Fulton LM, Lynd LR, Körner A, Greene N, Tonachel LR. The need for biofuels as part of a low carbon energy future. *Biofuels Bioprod Biorefin.* 2015;9:476-83.
2. Gombert AK, van Maris AJA. Improving conversion yield of fermentable sugars into fuel ethanol in 1st generation yeast-based production processes. *Curr Opin Biotechnol.* 2015;33:81-86.
3. Lopes ML, Paulillo SCdL, Godoy A, Cherubin RA, Lorenzi MS, Giometti FHC, Bernardino CD, Amorim Neto HBd, Amorim HVd. Ethanol production in Brazil: a bridge between science and industry. *Braz J Microbiol.* 2016;47:64-76.
4. Basso LC, Basso T, Nitsche Rocha S: *Ethanol production in Brazil: The Industrial process and its impact on yeast fermentation.* In *Biofuel Production - Recent Developments and Prospects.* Edited by Marco Aurelio dos Santos Bernardes: INTECH. 2011.
5. Lynd LR, Liang X, Biddy MJ, Allee A, Cai H, Foust T, Himmel ME, Laser MS, Wang M, Wyman CE. Cellulosic ethanol: status and innovation. *Cur Opin Biotechnol.* 2017;45:202-11.
6. Van Maris AJA, Abbott DA, Bellissimi E, van den Brink J, Kuyper M, Luttik MAH, Wisselink HW, Scheffers WA, van Dijken JP, Pronk JT. Alcoholic fermentation of carbon sources in biomass hydrolysates by *Saccharomyces cerevisiae*: current status. *Antonie van Leeuwenhoek.* 2006;90:391-418.
7. Jansen MLA, Bracher JM, Papapetridis I, Verhoeven MD, de Bruijn H, de Waal PP, van Maris AJA, Klaassen P, Pronk JT. *Saccharomyces cerevisiae* strains for second-generation ethanol production: from academic exploration to industrial implementation. *FEMS Yeast Res.* 2017;17:fox044-fox44.
8. Palmqvist E, Hahn-Hägerdal B. Fermentation of lignocellulosic hydrolysates. II: inhibitors and mechanisms of inhibition. *Bioresour Technol.* 2000;74:25-33.
9. Moysés D, Reis V, Almeida J, Moraes L, Torres F. Xylose fermentation by *Saccharomyces cerevisiae*: challenges and prospects. *Int J Mol Sci.* 2016;17:207.
10. Wisselink HW, Toirkens MJ, Wu Q, Pronk JT, van Maris AJA. Novel evolutionary engineering approach for accelerated utilization of glucose, xylose, and arabinose mixtures by engineered *Saccharomyces cerevisiae* strains. *App Environ Microbiol.* 2009;75:907-14.
11. Garcia Sanchez R, Karhumaa K, Fonseca C, Sánchez Nogué V, Almeida JR, Larsson CU, Bengtsson O, Bettiga M, Hahn-Hägerdal B, Gorwa-Grauslund MF. Improved xylose and arabinose utilization by an industrial recombinant *Saccharomyces cerevisiae* strain using evolutionary engineering. *Biotechnol Biofuels.* 2010;3:13.
12. Zhou H, Cheng J-s, Wang BL, Fink GR, Stephanopoulos G. Xylose isomerase overexpression along with engineering of the pentose phosphate pathway and evolutionary engineering enable rapid xylose utilization and ethanol production by *Saccharomyces cerevisiae*. *Metab Eng.* 2012;14:611-22.
13. Kuyper M, Toirkens MJ, Diderich JA, Winkler AA, van Dijken JP, Pronk JT. Evolutionary engineering of mixed-sugar utilization by a xylose-fermenting *Saccharomyces cerevisiae* strain. *FEMS Yeast Res.* 2005;5:925-34.
14. Shen Y, Chen X, Peng B, Chen L, Hou J, Bao X. An efficient xylose-fermenting recombinant *Saccharomyces cerevisiae* strain obtained through adaptive evolution and its global transcription profile. *App Microbiol Biotechnol.* 2012;96:1079-91.
15. Kim SR, Ha S-J, Wei N, Oh EJ, Jin Y-S. Simultaneous co-fermentation of mixed sugars: a promising strategy for producing cellulosic ethanol. *Trends Biotechnol.* 2012;30:274-82.
16. Ask M, Bettiga M, Duraiswamy VR, Olsson L. Pulsed addition of HMF and furfural to batch-grown xylose-utilizing *Saccharomyces cerevisiae* results in different physiological responses in glucose and xylose consumption phase. *Biotechnol Biofuels.* 2013;6:181-81.

17. Bellissimi E, van Dijken JP, Pronk JT, van Maris AJA. Effects of acetic acid on the kinetics of xylose fermentation by an engineered, xylose-isomerase-based *Saccharomyces cerevisiae* strain. *FEMS Yeast Res.* 2009;9:358-64.
18. Farwick A, Bruder S, Schadeweg V, Oreb M, Boles E. Engineering of yeast hexose transporters to transport D-xylose without inhibition by D-glucose. *Proc Natl Acad Sci USA.* 2014;111:5159-64.
19. Shin HY, Nijland JG, de Waal PP, de Jong RM, Klaassen P, Driessen AJM. An engineered cryptic Hxt11 sugar transporter facilitates glucose-xylose co-consumption in *Saccharomyces cerevisiae*. *Biotechnol Biofuels.* 2015;8:176.
20. Nijland JG, Shin HY, de Jong RM, de Waal PP, Klaassen P, Driessen AJM. Engineering of an endogenous hexose transporter into a specific D-xylose transporter facilitates glucose-xylose co-consumption in *Saccharomyces cerevisiae*. *Biotechnol Biofuels.* 2014;7:168.
21. Reznicek O, Facey SJ, de Waal PP, Teunissen AWRH, de Bont JAM, Nijland JG, Driessen AJM, Hauer B. Improved xylose uptake in *Saccharomyces cerevisiae* due to directed evolution of galactose permease Gal2 for sugar co-consumption. *J Appl Microbiol.* 2015;119:99-111.
22. Wei N, Oh EJ, Million G, Cate JHD, Jin Y-S. Simultaneous utilization of cellobiose, xylose, and acetic acid from lignocellulosic biomass for biofuel production by an engineered yeast platform. *ACS Synth Biol.* 2015;4:707-13.
23. Shen M-H, Song H, Li B-Z, Yuan Y-J. Deletion of D-ribulose-5-phosphate 3-epimerase (*RPE1*) induces simultaneous utilization of xylose and glucose in xylose-utilizing *Saccharomyces cerevisiae*. *Biotechnol Lett.* 2015;37:1031-36.
24. Aguilera A. Deletion of the phosphoglucose isomerase structural gene makes growth and sporulation glucose dependent in *Saccharomyces cerevisiae*. *Mol Gen Genet.* 1986;204:310-16.
25. Gawand P, Hyland P, Ekins A, Martin VJJ, Mahadevan R. Novel approach to engineer strains for simultaneous sugar utilization. *Metab Eng.* 2013;20:63-72.
26. Boles E, Lehnert W, Zimmermann FK. The role of the NAD-dependent glutamate dehydrogenase in restoring growth on glucose of a *Saccharomyces cerevisiae* phosphoglucose isomerase mutant. *Eur J Biochem.* 1993;217:469-77.
27. Dickinson JR, Sobanski MA, Hewlins MJE. In *Saccharomyces cerevisiae* deletion of phosphoglucose isomerase can be suppressed by increased activities of enzymes of the hexose monophosphate pathway. *Microbiology.* 1995;141:385-91.
28. Kuyper M, Hartog MMP, Toirkens MJ, Almering MJH, Winkler AA, van Dijken JP, Pronk JT. Metabolic engineering of a xylose-isomerase-expressing *Saccharomyces cerevisiae* strain for rapid anaerobic xylose fermentation. *FEMS Yeast Res.* 2005;5:399-409.
29. Verhoeven MD, Lee M, Kamoen L, van den Broek M, Janssen DB, Daran J-MG, van Maris AJA, Pronk JT. Mutations in *PMR1* stimulate xylose isomerase activity and anaerobic growth on xylose of engineered *Saccharomyces cerevisiae* by influencing manganese homeostasis. *Sci Rep.* 2017;7:46155.
30. Papapetridis I, van Dijk M, Dobbe APA, Metz B, Pronk JT, van Maris AJA. Improving ethanol yield in acetate-reducing *Saccharomyces cerevisiae* by cofactor engineering of 6-phosphogluconate dehydrogenase and deletion of *ALD6*. *Microb Cell Fact.* 2016;15:67.
31. Entian K-D, Kötter P. 25 yeast genetic strain and plasmid collections. In *Methods in Microbiology. Volume 36*. Edited by Stansfield I, Stark MJR: Academic Press; 2007: 629-66.
32. Verduyn C, Postma E, Scheffers WA, van Dijken JP. Effect of benzoic acid on metabolic fluxes in yeasts: A continuous-culture study on the regulation of respiration and alcoholic fermentation. *Yeast.* 1992;8:501-17.
33. Kuijpers NG, Solis-Escalante D, Bosman L, van den Broek M, Pronk JT, Daran J-MG, Daran-Lapujade P. A versatile, efficient strategy for assembly of multi-fragment expression vectors in *Saccharomyces cerevisiae* using 60 bp synthetic recombination sequences. *Microb Cell Fact.* 2013;12:47.

34. Mans R, van Rossum HM, Wijsman M, Backx A, Kuijpers NGA, van den Broek M, Daran-Lapujade P, Pronk JT, van Maris AJA, Daran J-MG. CRISPR/Cas9: a molecular Swiss army knife for simultaneous introduction of multiple genetic modifications in *Saccharomyces cerevisiae*. *FEMS Yeast Res.* 2015;15:fov004.
35. DiCarlo JE, Norville JE, Mali P, Rios X, Aach J, Church GM. Genome engineering in *Saccharomyces cerevisiae* using CRISPR-Cas systems. *Nucleic Acids Res.* 2013;41:4336-43.
36. Papapetridis I, Goudriaan M, Vázquez Vitali M, de Keijzer NA, van den Broek M, van Maris AJA, Pronk JT. Optimizing anaerobic growth rate and fermentation kinetics in *Saccharomyces cerevisiae* strains expressing Calvin-cycle enzymes for improved ethanol yield. *Biotechnol Biofuels.* 2018;11:17.
37. Van Rossum HM, Kozak BU, Niemeijer MS, Dykstra JC, Luttk MAH, Daran J-MG, van Maris AJA, Pronk JT. Requirements for carnitine shuttle-mediated translocation of mitochondrial acetyl moieties to the yeast cytosol. *mBio.* 2016;7.
38. Kuijpers NGA, Solis-Escalante D, Luttk MAH, Bisschops MMM, Boonekamp FJ, van den Broek M, Pronk JT, Daran J-MG, Daran-Lapujade P. Pathway swapping: toward modular engineering of essential cellular processes. *Proc Natl Acad Sci USA.* 2016;113:15060-65.
39. Kuyper M, Harhangi HR, Stave AK, Winkler AA, Jetten MSM, de Laat WTAM, den Ridder JJJ, Op den Camp HJM, van Dijken JP, Pronk JT. High-level functional expression of a fungal xylose isomerase: the key to efficient ethanolic fermentation of xylose by *Saccharomyces cerevisiae*? *FEMS Yeast Res.* 2003;4:69-78.
40. Gietz RD, Woods RA. Transformation of yeast by lithium acetate/single-stranded carrier DNA/polyethylene glycol method. *Methods Enzymol.* 2002;350:87-96.
41. Solis-Escalante D, Kuijpers NGA, Bongaerts N, Bolat I, Bosman L, Pronk JT, Daran J-MG, Daran-Lapujade P. *amdSYM*, a new dominant recyclable marker cassette for *Saccharomyces cerevisiae*. *FEMS Yeast Res.* 2013;13:126-39.
42. Aung HW, Henry SA, Walker LP. Revising the representation of fatty acid, glycerolipid, and glycerophospholipid metabolism in the consensus model of yeast metabolism. *Ind Biotechnol.* 2013;9:215-28.
43. Becker SA, Feist AM, Mo ML, Hannum G, Palsson BØ, Herrgard MJ. Quantitative prediction of cellular metabolism with constraint-based models: the COBRA Toolbox. *Nat Protoc.* 2007;2:727.
44. Hucka M, Finney A, Sauro HM, Bolouri H, Doyle JC, Kitano H, Arkin AP, Bornstein BJ, Bray D, Cornish-Bowden A, et al. The systems biology markup language (SBML): a medium for representation and exchange of biochemical network models. *Bioinformatics.* 2003;19:524-31.
45. Nijkamp JF, van den Broek M, Datema E, de Kok S, Bosman L, Luttk MA, Daran-Lapujade P, Vongsangnak W, Nielsen J, Heijne WHM, et al. De novo sequencing, assembly and analysis of the genome of the laboratory strain *Saccharomyces cerevisiae* CEN.PK113-7D, a model for modern industrial biotechnology. *Microb Cell Fact.* 2012;11:36-36.
46. Johansson B, Hahn-Hägerdal B. The non-oxidative pentose phosphate pathway controls the fermentation rate of xylulose but not of xylose in *Saccharomyces cerevisiae* TMB3001. *FEMS Yeast Res.* 2002;2:277-82.
47. Bruinenberg PM, Van Dijken JP, Scheffers WA. A theoretical analysis of NADPH production and consumption in yeasts. *Microbiology.* 1983;129:953-64.
48. Verduyn C, Postma E, Scheffers WA, van Dijken JP. Physiology of *Saccharomyces cerevisiae* in anaerobic glucose-limited chemostat cultures. *Microbiology.* 1990;136:395-403.
49. Katahira S, Ito M, Takema H, Fujita Y, Tanino T, Tanaka T, Fukuda H, Kondo A. Improvement of ethanol productivity during xylose and glucose co-fermentation by xylose-assimilating *S. cerevisiae* via expression of glucose transporter *Sut1*. *Enzyme Microb Technol.* 2008;43:115-19.

50. Gonçalves DL, Matsushika A, de Sales BB, Goshima T, Bon EPS, Stambuk BU. Xylose and xylose/glucose co-fermentation by recombinant *Saccharomyces cerevisiae* strains expressing individual hexose transporters. *Enzyme Microb Technol.* 2014;63:13-20.
51. Westman JO, Bonander N, Taherzadeh MJ, Franzén CJ. Improved sugar co-utilisation by encapsulation of a recombinant *Saccharomyces cerevisiae* strain in alginate-chitosan capsules. *Biotechnol Biofuels.* 2014;7:102.
52. Reifenberger E, Boles E, Ciriacy M. Kinetic characterization of individual hexose transporters of *Saccharomyces cerevisiae* and their relation to the triggering mechanisms of glucose repression. *Eur J Biochem.* 1997;245:324-33.
53. Hamacher T, Becker J, Gárdonyi M, Hahn-Hägerdal B, Boles E. Characterization of the xylose-transporting properties of yeast hexose transporters and their influence on xylose utilization. *Microbiology.* 2002;148:2783-88.
54. Lee W-J, Kim M-D, Ryu Y-W, Bisson L, Seo J-H. Kinetic studies on glucose and xylose transport in *Saccharomyces cerevisiae*. *App Microb Biotechnol.* 2002;60:186-91.
55. Raamsdonk LM, Diderich JA, Kuiper A, van Gaalen M, Kruckberg AL, Berden JA, van Dam K. Co-consumption of sugars or ethanol and glucose in a *Saccharomyces cerevisiae* strain deleted in the *HXX2* gene. *Yeast.* 2001;18:1023-33.
56. De Winde JH, Crauwels M, Hohmann S, Thevelein JM, Winderickx J. Differential requirement of the yeast sugar kinases for sugar sensing in establishing the catabolite-repressed state. *Eur J Biochem.* 1996;241:633-43.
57. Belgareh-Touzé N, Léon S, Erpapazoglou Z, Stawiecka-Mirota M, Urban-Grimal D, Haguenaer-Tsapis R. Versatile role of the yeast ubiquitin ligase Rsp5p in intracellular trafficking. *Biochem Soc Trans.* 2008;36:791.
58. Nijland JG, Shin HY, Boender LGM, de Waal PP, Klaassen P, Driessen AJM. Improved xylose metabolism by a *CYC8* mutant of *Saccharomyces cerevisiae*. *App Environ Microbiol.* 2017;83.
59. Vincent O, Carlson M. Sip4, a Snf1 kinase-dependent transcriptional activator, binds to the carbon source-responsive element of gluconeogenic genes. *EMBO J.* 1998;17:7002-08.
60. Rahner A, Schöler A, Martens E, Gollwitzer B, Schüller HJ. Dual influence of the yeast Cat1p (Snf1p) protein kinase on carbon source-dependent transcriptional activation of gluconeogenic genes by the regulatory gene *CAT8*. *Nucleic Acids Res.* 1996;24:2331-37.
61. Vincent O, Carlson M. Gal83 mediates the interaction of the Snf1 kinase complex with the transcription activator Sip4. *EMBO J.* 1999;18:6672-81.
62. Schmidt MC, McCartney RR. β -subunits of Snf1 kinase are required for kinase function and substrate definition. *EMBO J.* 2000;19:4936-43.
63. Alper H, Stephanopoulos G. Engineering for biofuels: exploiting innate microbial capacity or importing biosynthetic potential? *Nat Rev Microbiol.* 2009;7:715.
64. Wisselink HW, Van Maris AJA, Pronk JT. Polypeptides with permease activity. US Patent 9034608 B2. 2015.
65. Heux S, Cadiere A, Dequin S. Glucose utilization of strains lacking *PGI1* and expressing a transhydrogenase suggests differences in the pentose phosphate capacity among *Saccharomyces cerevisiae* strains. *FEMS Yeast Res.* 2008;8:217-24.
66. Grabowska D, Chelstowska A. The *ALD6* gene product is indispensable for providing NADPH in yeast cells lacking glucose-6-phosphate dehydrogenase activity. *J Biol Chem.* 2003;278:13984-88.
67. Celton M, Sanchez I, Goelzer A, Fromion V, Camarasa C, Dequin S. A comparative transcriptomic, fluxomic and metabolomic analysis of the response of *Saccharomyces cerevisiae* to increases in NADPH oxidation. *BMC Genomics.* 2012;13:317-17.
68. Gottardi M, Reifenrath M, Boles E, Tripp J. Pathway engineering for the production of heterologous aromatic chemicals and their derivatives in *Saccharomyces cerevisiae*: bioconversion from glucose. *FEMS Yeast Res.* 2017;17:fox035-fox35.
69. Klug L, Daum G. Yeast lipid metabolism at a glance. *FEMS Yeast Res.* 2014;14:369-88.

70. Tehlivets O, Scheuringer K, Kohlwein SD. Fatty acid synthesis and elongation in yeast. *Biochimica et Biophysica Acta (BBA) - Mol and Cell Biol Lipids*. 2007;1771:255-70.
71. Entian K-D. Genetic and biochemical evidence for hexokinase PII as a key enzyme involved in carbon catabolite repression in yeast. *Mol Gen Genet*. 1980;178:633-37.
72. Entian KD, Fröhlich K-U. *Saccharomyces cerevisiae* mutants provide evidence of hexokinase PII as a bifunctional enzyme with catalytic and regulatory domains for triggering catabolite repression. *J Bacteriol*. 1984;158:29-35.
73. Peláez R, Herrero P, Moreno F. Functional domains of yeast hexokinase 2. *Biochem J*. 2010;432:181-90.
74. Petit T, Diderich JA, Kruckeberg AL, Gancedo C, Van Dam K. Hexokinase regulates kinetics of glucose transport and expression of genes encoding hexose transporters in *Saccharomyces cerevisiae*. *J Bacteriol*. 2000;182:6815-18.
75. Diderich JA, Schepper M, van Hoek P, Luttik MAH, van Dijken JP, Pronk JT, Klaassen P, Boelens HFM, de Mattos MJT, van Dam K, Kruckeberg AL. Glucose uptake kinetics and transcription of *HXT* Genes in chemostat cultures of *Saccharomyces cerevisiae*. *J Biol Chem*. 1999;274:15350-59.
76. Nijland JG, Vos E, Shin HY, de Waal PP, Klaassen P, Driessen AJM. Improving pentose fermentation by preventing ubiquitination of hexose transporters in *Saccharomyces cerevisiae*. *Biotechnol Biofuels*. 2016;9:158.
77. Subtil T, Boles E. Competition between pentoses and glucose during uptake and catabolism in recombinant *Saccharomyces cerevisiae*. *Biotechnol Biofuels*. 2012;5:14-14.
78. Miskovic L, Alff-Tuomala S, Soh KC, Barth D, Salusjärvi L, Pitkänen J-P, Ruohonen L, Penttilä M, Hatzimanikatis V. A design-build-test cycle using modeling and experiments reveals interdependencies between upper glycolysis and xylose uptake in recombinant *S. cerevisiae* and improves predictive capabilities of large-scale kinetic models. *Biotechnol Biofuels*. 2017;10:166.
79. Shcherbik N, Pestov DG. The ubiquitin ligase Rsp5 is required for ribosome stability in *Saccharomyces cerevisiae*. *RNA*. 2011;17:1422-28.
80. Huibregtse JM, Yang JC, Beaudenon SL. The large subunit of RNA polymerase II is a substrate of the Rsp5 ubiquitin-protein ligase. *Proc Natl Acad Sci USA*. 1997;94:3656-61.
81. Kaliszewski P, Zoladek T. The role of Rsp5 ubiquitin ligase in regulation of diverse processes in yeast cells. *Acta Biochim Pol*. 2008;55:649-62.
82. Haguenaer-Tsapis R, André B: Membrane trafficking of yeast transporters: mechanisms and physiological control of downregulation. In *Molecular Mechanisms Controlling Transmembrane Transport*. Berlin, Heidelberg: Springer Berlin Heidelberg; 2004: 273-323.
83. Krampe S, Stamm O, Hollenberg CP, Boles E. Catabolite inactivation of the high-affinity hexose transporters Hxt6 and Hxt7 of *Saccharomyces cerevisiae* occurs in the vacuole after internalization by endocytosis. *FEBS Lett*. 1998;441:343-47.
84. Vincent O, Townley R, Kuchin S, Carlson M. Subcellular localization of the Snf1 kinase is regulated by specific β subunits and a novel glucose signaling mechanism. *Genes Dev*. 2001;15:1104-14.
85. Erickson JR, Johnston M. Genetic and molecular characterization of Gal83: Its interaction and similarities with other genes involved in glucose repression in *Saccharomyces cerevisiae*. *Genetics*. 1993;135:655-64.
86. Matsumoto K, Toh-e A, Oshima Y. Isolation and characterization of dominant mutations resistant to carbon catabolite repression of galactokinase synthesis in *Saccharomyces cerevisiae*. *Mol Cell Biol*. 1981;1:83-93.
87. Özcan S, Johnston M. Function and regulation of yeast hexose transporters. *Microbiol Mol Biol Rev*. 1999;63:554-69.
88. Momcilovic M, Iram SH, Liu Y, Carlson M. Roles of the glycogen-binding domain and Snf4 in glucose inhibition of *SNF1* protein kinase. *J Biol Chem*. 2008;283:19521-29.

89. Wiatrowski HA, van Denderen BJW, Berkey CD, Kemp BE, Stapleton D, Carlson M. Mutations in the Gal83 glycogen-binding domain activate the Snf1/Gal83 kinase pathway by a glycogen-independent mechanism. *Mol Cell Biol.* 2004;24:352-61.
90. Mangat S, Chandrashekarappa D, McCartney RR, Elbing K, Schmidt MC. Differential roles of the glycogen-binding domains of β subunits in regulation of the Snf1 kinase complex. *Eukar Cell.* 2010;9:173-83.
91. Schüller H-J. Transcriptional control of nonfermentative metabolism in the yeast *Saccharomyces cerevisiae*. *Curr Genet.* 2003;43:139-60.
92. Gancedo JM. Yeast carbon catabolite repression. *Microbiol Mol Biol Rev.* 1998;62:334-61.
93. Boender LGM, de Hulster EAF, van Maris AJA, Daran-Lapujade P, Pronk JT. Quantitative physiology of *Saccharomyces cerevisiae* at near-zero specific growth rates. *App Environ Microbiol.* 2009;75:5607-14.
94. Canelas AB, Harrison N, Fazio A, Zhang J, Pitkänen J-P, van den Brink J, Bakker BM, Bogner L, Bouwman J, Castrillo JI, et al. Integrated multilaboratory systems biology reveals differences in protein metabolism between two reference yeast strains. *Nat Commun.* 2010;1:145.
95. Van den Brink J, Akeroyd M, van der Hoeven R, Pronk JT, de Winde JH, Daran-Lapujade P. Energetic limits to metabolic flexibility: responses of *Saccharomyces cerevisiae* to glucose-galactose transitions. *Microbiology.* 2009;155:1340-50.
96. Abbott DA, Knijnenburg TA, De Poorter LMI, Reinders MJT, Pronk JT, van Maris AJA. Generic and specific transcriptional responses to different weak organic acids in anaerobic chemostat cultures of *Saccharomyces cerevisiae*. *FEMS Yeast Res.* 2007;7:819-33.
97. Klinke HB, Ahring BK, Schmidt AS, Thomsen AB. Characterization of degradation products from alkaline wet oxidation of wheat straw. *Bioresour Technol.* 2002;82:15-26.
98. Almeida JRM, Modig T, Petersson A, Hähn-Hägerdal B, Lidén G, Gorwa-Grauslund MF. Increased tolerance and conversion of inhibitors in lignocellulosic hydrolysates by *Saccharomyces cerevisiae*. *J Chem Technol Biotechnol.* 2007;82:340-49.
99. Becker J, Boles E. A modified *Saccharomyces cerevisiae* strain that consumes l-arabinose and produces ethanol. *App Environ Microbiol.* 2003;69:4144-50.
100. Wisselink HW, Toirkens MJ, del Rosario Franco Berriel M, Winkler AA, van Dijken JP, Pronk JT, van Maris AJA. Engineering of *Saccharomyces cerevisiae* for efficient anaerobic alcoholic fermentation of l-arabinose. *Appl Environ Microbiol.* 2007;73:4881-91.

Outlook

Ethanol, produced by the yeast *Saccharomyces cerevisiae*, is the largest-volume product of industrial biotechnology. Improvements in the yield of ethanol on carbohydrate feedstocks can not only improve the economics of ethanol production, but also help to further reduce the carbon footprint of the production of ethanol as a renewable liquid transport fuel. This thesis describes optimization of redox engineering strategies that enable significant increases in the ethanol yield in anaerobic *Saccharomyces cerevisiae* cultures. These strategies are based on the replacement of the role of glycerol formation in redox cofactor balancing during anaerobic growth by the reduction of acetic acid or CO₂ to ethanol. In designing these strategies, it was an explicit criterion that, in principle, their implementation in industry should not require major changes in unit operations of industrial processes, but could instead be based on readily available substrates. In **Chapter 2**, efficient CO₂ reduction to ethanol in fast-growing, glucose-fermenting yeast strains was enabled by multi-copy expression of a bacterial gene encoding ribulose-1,5-bisphosphate carboxylase, expression of a spinach phosphoribulokinase gene from the anaerobically inducible *DAN1* promoter, deletion of the yeast Gpd2 glycerol-phosphate dehydrogenase gene, combined with overexpression of the *Escherichia coli* chaperones GroEL/GroES together with the structural genes of the yeast non-oxidative pentose-phosphate pathway. Rapid implementation of these extensive modifications was made possible by the use of CRISPR/Cas9-mediated genome editing in combination with *in vivo* assembly of DNA fragments by the native yeast homologous recombination machinery. This approach enabled simultaneous assembly and genomic integration of up to 14 DNA fragments in a single transformation experiment. These results show the enormous potential of genome editing techniques to strongly accelerate construction of microbial strains with industrially-relevant phenotypes. Transfer of the optimized CO₂-reduction pathway to industrial yeast strains should facilitate increased ethanol yields in real-life industrial processes. An alternative approach for improving ethanol yields is described in **Chapters 3 and 4**. Instead of using CO₂ as electron

acceptor, this strategy is based on reduction of acetic acid to ethanol. The optimized acetic acid reduction pathways described in **Chapters 3 and 4** were based on changes of the cofactor specificities of 6-phosphogluconate dehydrogenase and glycerol-3-phosphate dehydrogenase, as well as deletion of the NADP⁺-dependent acetaldehyde dehydrogenase Ald6. These modification strategies can be combined to generate osmotolerant yeast strains with increased ethanol yields and medium detoxification capacities. Low concentrations of acetic acid can be found in at least some feedstocks for first-generation ethanol production (e.g. corn mash), while much higher concentrations of acetic acid are found in the hydrolysates of lignocellulosic plant biomass that are used for second-generation bioethanol production processes. CO₂ is abundantly present in all bioethanol fermentation processes. The availability of two complementary strategies for improving bioethanol yield increases flexibility in industrial designs and in implementation of engineered yeast strains for improved ethanol yields.

Even though the modification strategies described in **Chapters 2,3 and 4** have the potential to increase ethanol yield on feedstock, the time required for full conversion of carbohydrate feedstocks remains a key parameter for optimization, especially in second-generation processes. The laboratory evolution strategy developed in **Chapter 5** can identify key mutations for increasing pentose utilization rates in *S. cerevisiae* in a variety of feedstocks and can be adapted to different process conditions.

The economics of bioethanol production can greatly benefit from further results to accelerate and intensify ethanol production. Despite many decades of research, many possibilities remain to further improve bioethanol production by *S. cerevisiae* by metabolic engineering. Under-utilized carbon compounds such as uronic acids, which are currently not converted into ethanol, could be unlocked as additional substrates for ethanol production by further metabolic engineering of *S. cerevisiae*. Alternatively, the optimized pathways developed for *S. cerevisiae* could be transferred to other industrially relevant yeasts with increased robustness to process conditions such as low pH and high temperature values. It should however be noted that successful ethanol production does not only depend on yeast strain

performance. Especially in second-generation bioethanol production, the upstream pretreatment of the lignocellulosic biomass requires extreme conditions and external addition of expensive hydrolytic enzyme cocktails. Development of yeast strains which can produce hydrolytic enzymes during the fermentation process (so-called 'consolidated bioprocessing') is intensively studied and offers the prospect of reducing operational costs. Beyond yeast, the construction and improvement of ethanol-producing thermophilic and cellulolytic bacteria for consolidated bioprocessing may transform industrial ethanol production from first- as well as second-generation feedstocks.

Acknowledgements

This dissertation is the result of a journey that started more than 10 years ago, when, after the Greek state university entrance examinations were finished, I had to select a BSc programme. In multiple occasions during this journey I had to choose between branching paths that would have led to completely different outcomes. Thinking back, I am glad for every choice I made and I would not have had it any other way. I have met a lot of people along the way that helped me and without them none of it would have been possible. It is likely that some names may slip my mind while writing this. If this happens, please forgive me.

First and foremost, I would like to thank my parents. Through their personal sacrifices they provided me with everything I needed in order to go forward not just with my career but also with my life. I am grateful that they raised me to be a thinker and a grown-up individual that is able to deal with life's decisions and their outcomes. I also want to thank the rest of my family and especially my brother and sister, who have always been there for me whenever I needed help, advice, or just someone to talk to.

To Jack and Ton, thank you for trusting in me and giving me a great project to work on. I still remember how happy I was after the skype call during which Ton described the project, as it was a perfect fit for me and a great opportunity to broaden my knowledge. I enjoyed my 4 years working at IMB a lot and could not have asked for better supervisors, not only in terms of daily work but also of guidance! Your enthusiasm and eagerness to answer any questions I had and help with all the challenges I encountered during my research is a huge part of why I was able to finish my PhD project.

I want to thank my teachers back in the School of Biology in Aristotle University for showing me that genetic engineering and using microbes to make stuff is cool, especially Rea and Nikoletta for teaching me how to isolate DNA and run PCRs back in 2009. Special thanks to Alexander Triantafyllidis for entrusting me with a great BSc project and for, along with

Konstantinos Triantafyllidis, providing me with reference letters that enabled the scholarship that financed my MSc studies in the Netherlands.

I will forever be grateful to Leo de Graaff, who not only welcomed me at his lab for my MSc end project, but also recommended me to DSM for my industrial internship and to Ton and Jack for my PhD. You had a tremendously positive impact on my life. Special thanks to Laura, Jasper and Juan at SSB for the supervision and advice during my time there. A big thank you to Sybe, who accepted me as a fermentation intern at DSM despite me knowing nothing about fermentation at the time. My time working with you taught me a lot! Also thank you for your suggestion to do a PhD instead of opening a snail farm in Greece as I was considering at the time! Also special thanks to Erik and all the fermentation technicians and colleagues at DSM, who taught me how to assemble bioreactors and how to run fermentations!

A very big thank you to Paul Kleiborn for a great collaboration and teaching me a lot about how the puzzle of intellectual property works. I will always remember you. Sander, thank you for the great collaboration! I enjoyed all our meetings a lot and working with you taught me a lot on how to think out-of-the-box!

To Paul Klaassen, Hans, Paul de Waal, Mickel and all other colleagues that were part of my project, thank you for the great collaboration! I am very grateful for your enthusiasm and you going out of your way to help me not only with my project, but also with making my next steps!

Starting a PhD project can be quite intimidating. I would like to thank all the IMB people that welcomed me in the group when I joined in 2014 and made it a smooth transition for me. Special thanks to Robert, Harmen, Niels, Daniel, Dani, Stefan, Tim, Barbara, Nick, Matthijs, Angel and Susan for answering the many questions I had when I started and helping me acclimate with the multiple techniques we use in IMB. Mark, thank you for helping me with the statistical analysis in chapter 2. Roderick, Xavier, Arthur and Ewout, thank you for helping me translate my summary to Dutch, my initial plan to google translate it would have probably been quite

embarrassing. Also, thanks to all current IMB colleagues that make this group a very nice environment to be in!

Special thanks to Jean-Marc and Pascale, who were always happy to take time off their schedules to assist with anything that I needed. Also, a very special thanks to the Ethanolics team for all the great discussions and especially Maarten who I directly teamed up with in the last chapter of this dissertation. I will always remember the planning phase of that project and how enjoyable those discussions were!

Finishing my PhD project would not have been possible without Marcel, Erik, Marijke and Pilar that were always there when I needed their help and were happy to answer any questions that I had. Special thanks to Apilena, Jannie and Astrid for always being eager to help with everything regarding the preparation of my experiments. Also, thanks to Tracey for always helping me with administrative things during the duration and the finishing up of my project!

Marlous and Maaïke, thank you for being my project teammates and for helping me design and run fermentations. I am sure that you will both do great in your own PhD projects!

During my project I was lucky to supervise a team of very enthusiastic BSc and MSc students. To Arthur Dobbe, Teun, Donna, Maaïke, Nikita, Julius, Sanne and Maria, thank you for the amazing contributions to my project and for tolerating me as your supervisor! I learnt a lot from each one of you and I hope I was a good influence as well.

A very big thank you to Arthur and Hannes for being my paranymphs and helping me with proofreading and arranging all the craziness that comes with wrapping a PhD project up.

To Jasmine, meeting you was the best thing that happened to me in Delft. Thank you for making me a better person. Thank you for showing me many aspects of the world and life that I was not aware of. Thank you for sharing your journey with me and letting me share mine with you. Your light makes my life brighter every day.

Curriculum vitae

Ioannis Papapetridis was born on August 24, 1988 in Thessaloniki, Greece. After finishing his high school studies in his home town of Katerini in 2006, he enrolled in the BSc Biology programme of Aristotle University of Thessaloniki in Greece. Ioannis performed his BSc end project at the Department of Genetics, Development and Molecular Biology under the supervision of dr. Rea Aleksandri and dr. Alexander Triantafyllidis. The research topic was the analysis of population distribution of the Greek brown hare (*Lepus europaeus*) in mainland and island Greece using mitochondrial DNA sequencing. After finishing his army service, Ioannis received a full scholarship for his MSc studies, during which he followed the MSc Biotechnology programme of Wageningen University in the Netherlands. For his MSc end project Ioannis joined the group of dr. ir. Leo de Graaff in the Laboratory of Systems and Synthetic Biology of Wageningen University, where he worked on the development of molecular toolbox techniques for *Aspergillus niger* transformations under the supervision of Laura van der Straat. Ioannis performed his industrial internship on characterization of protein production in *Aspergillus niger* fermentations at Royal DSM, a Netherlands-based biotechnology company. After completion of his MSc studies (2013, with honours), Ioannis started a PhD project at the Industrial Microbiology group of TU Delft, under the supervision of Prof. dr. ir. Antonius J.A. van Maris and Prof. dr. Jack T. Pronk. The project goal was the optimization of ethanol production in *Saccharomyces cerevisiae* fermentations by redox engineering of metabolism, and the results are discussed in this dissertation.

List of publications

1. Jansen MLA, Bracher JM, **Papapetridis I**, Verhoeven MD, de Bruijn H, de Waal PP, van Maris AJA, Klaassen P, Pronk JT. 2017. *Saccharomyces cerevisiae* strains for second-generation ethanol production: from academic exploration to industrial implementation, *FEMS Yeast Research* 17(5):fox044
2. **Papapetridis I**, van Dijk M, Dobbe APA, Metz B, Pronk JT, van Maris AJA. 2016. Improving ethanol yield in acetate-reducing *Saccharomyces cerevisiae* by cofactor engineering of 6-phosphogluconate dehydrogenase and deletion of *ALD6*. *Microbial Cell Factories* 15:67
3. **Papapetridis I**, van Dijk M, van Maris AJA, Pronk JT. 2017. Metabolic engineering strategies for optimizing acetate reduction, ethanol yield and osmotolerance in *Saccharomyces cerevisiae*. *Biotechnology for Biofuels* 10:107
4. **Papapetridis I**, Goudriaan M, Vitali MM, de Keijzer NA, van den Broek M, van Maris AJA, Pronk JT. 2018. Optimizing anaerobic growth rate and fermentation kinetics in *Saccharomyces cerevisiae* strains expressing Calvin-cycle enzymes for improved ethanol yield. *Biotechnology for Biofuels* 11:17
5. **Papapetridis I**, **Verhoeven MD**, Wiersma SJ, Goudriaan M, van Maris AJA, Pronk JT. 2018. Laboratory evolution for forced glucose-xylose co-consumption enables identification of mutations that improve mixed-sugar fermentation by xylose-fermenting *Saccharomyces cerevisiae*. Submitted for publication.